R-13-52

A seismic evaluation of SFR

Analysis of the Silo structure for earthquake load

Ginko Georgiev, Reinertsen Sverige AB

December 2013

Svensk Kärnbränslehantering AB
Swedish Nuclear Fuel
and Waste Management Co

Box 250, SE-101 24 Stockholm
Phone +46 8 459 84 00

ISSN 1402-3091
SKB R-13-52
ID 1372637

A seismic evaluation of SFR

Analysis of the Silo structure for earthquake load

Ginko Georgiev, Reinertsen Sverige AB

December 2013

This report concerns a study which was conducted for SKB. The conclusions and viewpoints presented in the report are those of the author. SKB may draw modified conclusions, based on additional literature sources and/or expert opinions.

Data in SKB's database can be changed for different reasons. Minor changes in SKB's database will not necessarily result in a revised report. Data revisions may also be presented as supplements, available at www.skb.se.

A pdf version of this document can be downloaded from www.skb.se

Abstract

This report aims to present an estimation of the SFR Silo structure capacity to withstand the load effects that arise in the event of an earthquake.

The earthquake loads are classified according to their probability level. The level indicates the possibility of a seismic event with a certain magnitude, to occur within a certain period of time and within a certain distance, and is called annual exceeding frequency. The SFR Silo was analyzed for earthquake loads with annual exceeding frequency of 10^{-5}, 10^{-6} and 10^{-7}, derived for use in the nuclear power industry in Sweden and defined in SKI (1992).

The earthquake load used here is defined for a point at the ground level. This introduces additional safety in the analysis as the Silo structure lies significantly underground. The assumption for pure elastic behaviour and use of responce spectrum analysis also add to the conservatism in the analysis.

Other loads acting on the Silo structure that were considered are the dead weight of the structure, the waste and the surrounding bentonite. The long term effect of creep and shrinkage on the concrete was also considered. The swelling pressure from the bentonite, temperature loads and water pressure were not considered in the analysis.

The possible deterioration of the concrete material in the Silo was not accounted for in the analysed cases. The reinforcement, on the other hand, was considered to be severely corroded and therefore ineffective. The loss of the concrete cover, which is an indirect consequence of the corrosion of the reinforcement, was considered in the analysis. The structural integrity of the Silo was considered to rely entirely on the concrete strength. The capacity of the SFR Silo structure to withstand the load from earthquake was assessed from the global stability of structure, maximum stresses in the concrete material and forces that arise in the casting joint between the outer wall and the bottom plate.

The results from the analyses and capacity checks show, that the SFR Silo structure will maintain its integrity under the loading from an earthquake with an annual exceeding frequency 10^{-5}, but not 10^{-6}. The more intense ground motions, with probability levels 10^{-6} and 10^{-7}, showed excessive cracking in the whole structure thus the structural integrity cannot be guaranteed for these events.

Sammanfattning

Rapportens syfte är att uppskatta SFR Silons förmåga att motstå lasteffekten av jordbävning.

Jordbävningslasten är klassificerad enligt dess sannolikhetsnivå. Nivån indikerar sannolikheten för en seismisk händelse med viss magnitud och avstånd att uppstå under bestämd tidsperiod, också kallad för årlig överskridandefrekvens. SFR Silon har analyserats för jordbävningar med årlig överskridandefrekvens 10^{-5}, 10^{-6} and 10^{-7}, framtagna för kärnkraftsindustrin i Sverige och definierat i SKI (1992).

Jordbävningslasten är definierad, genom responsspektran, för en punkt på marknivån. Detta adderar ytterligare säkerhet i analysen, eftersom Silon är grundlagd betydligt lägre nivå än marknivån, vilket innebär lägre seismisk lasteffekt. Antaganden för helt elastiskt respons och analys med responsspektrum metodiken bidrar också till säkerheten i analysen.

Övriga laster som verkar på Silon och som har inkluderats i analysen är egenvikten av konstruktionen, avfallet, samt bentoniten. Krypning och krympning i betongen har också beaktats. Yttre trycket från bentonitens svällning, temperaturändringar samt vattentrycket har inte medräknats i analysen.

Hänsyn till betongens åldring och försämring med tiden har inte tagits i de analyserade fallen. Armeringen, däremot, har antagits vara fullkomligt korroderad och verkningslös. Spjälkning av det täckande betongskiktet, vilket är direkt konsekvens av armeringens korrosion, har beaktats i analysen. Silons strukturella integritetet är helt beroende av betongens hållfasthets egenskaper.

SFR Silons kapacitetet att motstå jordbävningslasten har utvärderats för globalstabiliteten av konstruktionen, maximala spänningar i betongmaterialet, samt krafterna som uppstår i gjutfogen mellan ytterväggen och bottenplattan.

Resultaten från analysen och kapacitetskontrollen visar, att SFR Silon behåller sin strukturella integritet under belastning från jordbävning med årlig överskridandefrekvens på 10^{-5} men inte 10^{-6}. De mer kraftfulla jordbävningarna med sannolikhetsnivåer på 10^{-6} och 10^{-7} visar uppsprickning i stora delar av konstruktionen och därmed kan Silons integritet inte garanteras för dessa fall.

Contents

1 Introduction 7
1.1 Background 7
1.2 Scope of the work 7
1.3 Objective 7

2 Initial conditions and assumptions for the analysis 9
2.1 Existing drawings and reports 9
2.2 Standards and regulations 9
2.3 Geometry 9
2.3.1 Overview 9
2.3.2 Joint between the bottom slab and the silo wall 10
2.4 Material 11
2.4.1 Concrete 11
2.4.2 Bentonite 12
2.5 Load and loading combination 12
2.5.1 Permanent loads 12
2.5.2 Earthquake 12
2.5.3 Creep and shrinkage 14
2.5.4 Other loads 14
2.5.5 Load combination 14
2.6 Loss of concrete cover due to corrosion of the reinforcement 14
2.7 Detail of the joint between the bottom slab and the silo wall 15
2.8 Conditions and criteria for the structural integrity 15
2.9 Modeling consideration and analysis method 16

3 Finite element model 19
3.1 Overview 19
3.2 Elements 19
3.3 Material properties 20
3.4 Boundary conditions 20
3.4.1 Case 1 and 2 20
3.4.2 Hinged connection between the bottom slab and the outer wall 20
3.5 Loads and masses 21
3.5.1 Permanent loads and added mass by the waste 21
3.5.2 Earthquake load 22
3.5.3 Creep and shrinkage 22
3.6 Element groups 22
3.7 Results 23
3.8 Simplified model 23

4 Analysis 25
4.1 Overview 25
4.2 Analysis assumptions and parameters 25
4.2.1 Damping 25
4.2.2 Number of eigenmodes 25
4.2.3 Hydro dynamic effects on the structure 25
4.3 Response spectrum analysis criteria 25
4.3.1 Effective mass ratio 25

5 Results and capacity control 27
5.1 Summary of the results 27
5.2 Overall stability of the silo structure 28
5.3 Verification of the capacity of the silo 29
5.3.1 Case 1 30
5.3.2 Case 2 34
5.3.3 Results for a reduced cross section thickness of the outer wall 36

5.3.4 Shear capacity of the casting joint 38
5.3.5 Displacements of the silo 39
5.4 Influence of the choice of standard on the capacity verification 39
6 Conclusions 41
References 43
Appendix A FE-model in ADINA 45
Appendix B Results from the FE-model 75

1 Introduction

1.1 Background

Svensk Kärnbränslehantering AB, SKB, owns and runs the facility for final repository of radioactive operational waste, SFR, since 1987. The repository is situated 50 m below the bottom of the Baltic Sea and currently stores operational waste from the Swedish nuclear power plants as well as toxic waste from the healthcare industry and other industries, see the facility layout in Figure 1-1.

The effects of an earthquake on the SFR facility, the possibility for a collapse and the associated environmental consequences, have been analyzed in previous safety assessments (SKB 2008). In the reviewing comments, made by the Swedish Radiation Safety Authority, it was required that the safety analysis was complemented with a more detailed study, with accent to the structural integrity of the facility (SSM 2009).

SKB have commissioned Reinertsen Sverige AB to perform the analysis of the earthquake effect on the SFR facility. The main interest, identified under a preparatory phase, is in the Silo structure, see Figure 1-1. The objective is to present estimation of the structural capacity to withstand the earthquake loading. The final results will then be used to complement the safety assessment of the SFR facility.

1.2 Scope of the work

The current report presents the assumptions, numerical model, analysis parameters and capacity control for the Silo structure in the SFR facility. A brief description of the structure, a detailed presentation of the Finite Element model (FE-model) and the performed analysis is also given. The results are summarized in the report and presented in full in the appendices.

1.3 Objective

The objective of the report is to give an estimation of the SFR Silos ability to withstand earthquake loads. There was no predefined load that the structure was required to withstand, so the aim have been to find the critical load instead – the load level for which the integrity of the structure is compromised. The estimation of the capacity is nevertheless restricted by the assumptions and simplifications that were made in the modeling and analysis phases.

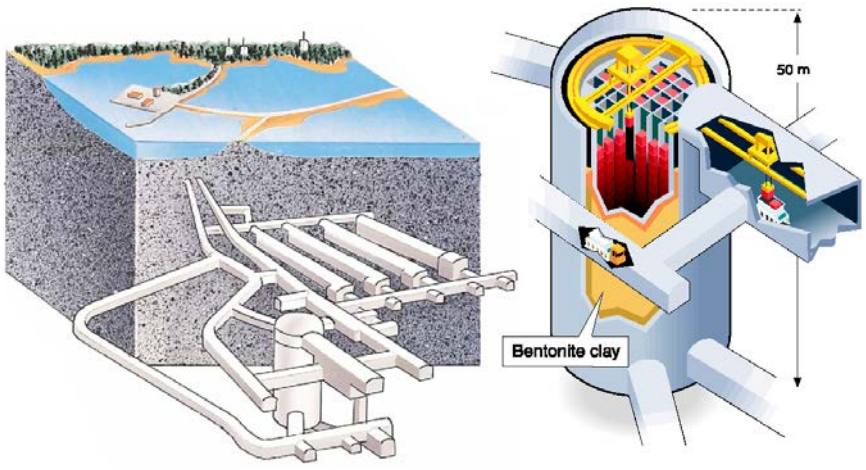

Figure 1-1. *Layout of the SFR-facility and detailed section of the Silo structure. The pictures are taken from presentation material from SKB.*

2 Initial conditions and assumptions for the analysis

2.1 Existing drawings and reports

The information used for the modeling of the structure of the Silo comes mainly from existing drawings and reports on different subject matters, related to the Silo.

- The geometry of the Silo is based on the following drawings:
  - 1-1010006 SFR. Forsmark. Silo 1. Sektion D-D. Huvudritning.
  - 1-1010007 SFR. Forsmark. Silo 1. Sektion E-E. Huvudritning.
  - 1-1010008 SFR. Forsmark. Silo 1. Sektion 1-1. Huvudritning.
  - 1-1010008 SFR. Forsmark. Silo 1. Sektion 1-1. Bottenplatta +369.75, Armering.
- The material parameters for the bentonite are based on SKB reports (references follow with the material description in section).

2.2 Standards and regulations

The following standards and regulations were used in the analysis:

- BBK 94/04 (Boverket 2004) for the material properties of the concrete;
- BKR/BBK (Boverket 2004) for the analysis of the structural capacity as well as general load combination.

The BBK 04 (Boverket 2004) was the valid building standard for concrete buildings at the time the project was started. At the current moment it is replaced by Eurocode 2 (CEN 2004). It is nevertheless BBK 04 that is used as a valid standard in this particular report. The differences between the two standards that concern the calculations in the report are minimal. They are pointed out where relevant and also are also summarized in Section 5.4.

The seismic load and the parameters concerning the structural behavior are obtained from the following documents:

- SKI 92:3 (SKI 1992). Contains the load spectra for earthquakes as well as the parameters for the derivation of the spectra.
- ASCE 4-98 (ASCE 2000). Used as guidelines the choice of parameters regarding the materials (ex. damping) as well as choice for analysis method.

2.3 Geometry

2.3.1 Overview

The geometry of the Silo is based on the drawings specified in Section 2.1. It is basically a cylinder with a height of 53 m and diameter of 27.6 m with 0.8 m thick outer walls, see Figure 2-1. The inside is divided into rectangular prism cells (shafts) by perpendicular vertical concrete walls, each cell base being 2.55×2.55 m in size. The silo rests on a compacted sand-bentonite foundation bed. The cylinder is built in a rock cavern excavated for that purpose. The space between the Silos outer wall and the rock is filled with granulated bentonite.

In the analysis it is assumed that the cells are filled with waste material and the Silo structure is sealed.

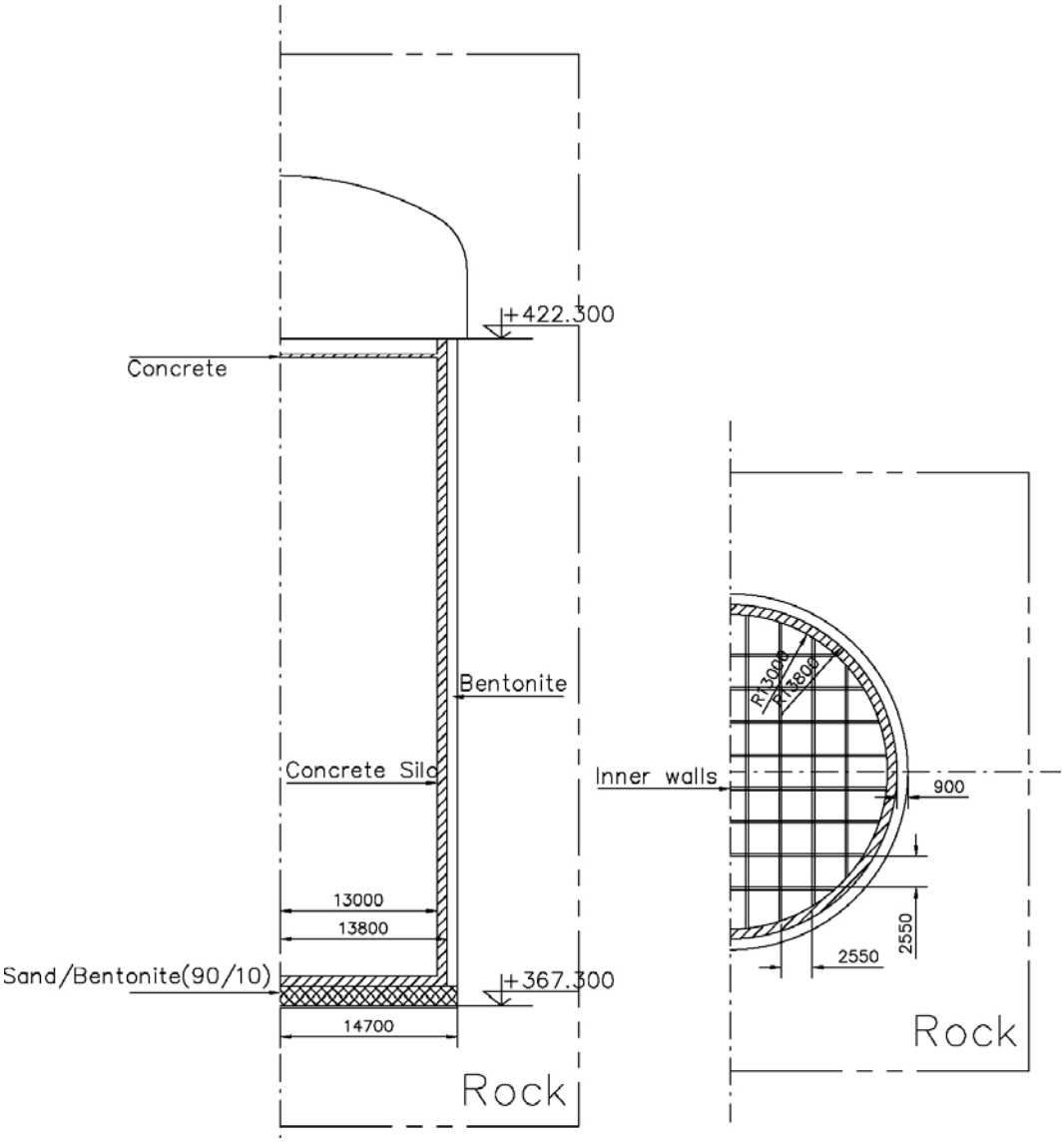

Figure 2-1. *Geometry of the Silo structure.*

2.3.2 Joint between the bottom slab and the silo wall

The bottom slab was cast separately from the outer and inner walls, which is also normally the case for this type of structure. The section between the walls and the bottom slab is a casting joint in the structure. The function of the joint is secured through reinforcement bars from the bottom slab extending up into the outer wall as well as shear keys in the radial direction along the silo wall.

Usually, the casting joint will be supplied with an additional membrane in order to secure the water-tightness of the whole structure. This, however, cannot be seen in the present detail, Figure 2-2. As mentioned in the preconditions, the reinforcement is considered to be ineffective. The same can be assumed also for a possible existing membrane.

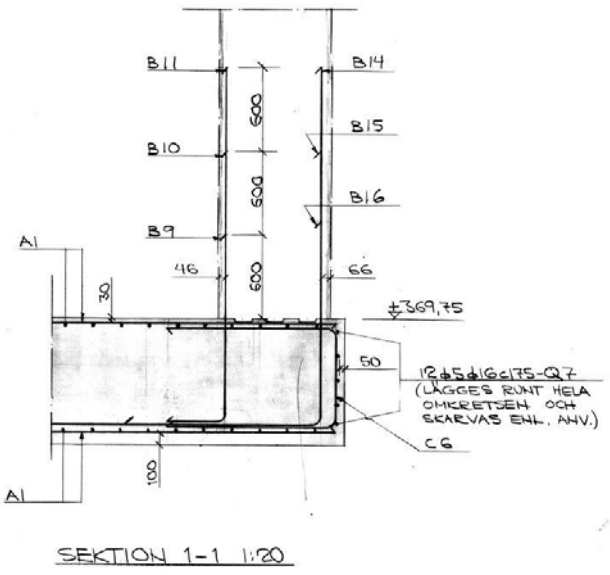

Figure 2-2. *Detail for the joint between the silo outer wall and the slab.*

2.4 Material

2.4.1 Concrete

The concrete material used for the Silo is K40, according to the drawings listed in Section 2.1.The concrete class is in accordance with the standard that was in effect at the time of the construction. The values used in the analysis are listed below.

- Concrete K40
  - Young's modulus: E = 32 GPa BBK 04 (Boverket 2004). $E_{dyn} = 1.0 \cdot 32 = 32.0$ GPa.
  - Poisson's ratio: $\upsilon = 0.2$.
  - Density : $\rho = 2{,}400$ kg/m^3.
  - Tensile strength: $f_{ctk} = 1.95$ MPa.
  - Compression strentgth: $f_{cck} = 28.5$ MPa.

Since the structure will be loaded with dynamic loads, the Young's modulus can be multiplied by a factor of 1.2 in accordance with BBK 04 (Boverket 2004) and BKR (Boverket 2003). This is however not used here as it is not supported in ASCE (2000) or Eurocode 1992 (CEN 2004).

Design values for the capacity controls in Chapter 5 in the report– only the case for accidental loading is relevant:

$$f_{ctk} = 1.95MPa \rightarrow f_t = \frac{f_{ctk}}{\gamma_m \cdot \gamma_n} = \frac{1.95}{1.2 \cdot 1.0} = 1.625MPa$$

$$f_{cck} = 28.5MPa \rightarrow f_c = \frac{f_{cck}}{\gamma_m \cdot \gamma_n} = \frac{28.5}{1.2 \cdot 1.0} = 23.75\,MPa$$

- Long term effects on the concrete
  - Shrinkage: $\varepsilon_{sh} = 0.25 \cdot 10^{-3}$
  - Creep: creep factor $\varphi = 2$

The eventual deterioration of the concrete material is not taken into account in the analysis and its parameters are assumed to correspond to those at the time of the construction. The reinforcement, on the other hand, is considered to be ineffective (corroded and having lost its initial mechanical after properties), see Section 2.6. This assumption and its influence on the numerical model is further discussed in the preconditions for the structural integrity specified in Section 2.8.

2.4.2 Bentonite

Bentonite is used as a fill material between the rock and the silo walls as well as in combination with sand (sand/bentonite 90/10 ratio) for the foundation bed of the silo. The material properties are derived from Fälth B (2011, personal communication), Börgesson et al. (2010) and Pusch (2003).

- Bentonite filling
  - Young's modulus: E = 6 MPa (Fälth B 2011, personal communication, Börgesson et al. 2010).
  - Poisson's ratio: $\upsilon = 0.2$.
  - Density: $\rho = 1{,}650$ kg/m^3.
- Sand/bentonite (in ratio 90/10) for the silo foundation bed.
  - Young's modulus: E = 150 MPa (Pusch 2003).
  - Poisson's ratio: $\upsilon = 0.4$.
  - Density: $\rho = 2{,}100$ kg/m^3 (Pusch 2003).

2.5 Load and loading combination

2.5.1 Permanent loads

The weight of the Silo, the sand/bentonite foundation bed and the waste in the Silo are included in the permanent load. The estimated mass of the waste material is 44,000 t = $44{,}000 \cdot 10^3$ kg (Pusch 2003).

Along with the waste material in each cell is poured concrete in order to seal it. This does introduce additional stiffness to the structure, which here is not accounted for.

2.5.2 Earthquake

2.5.2.1 Response spectrum load

The seismic load is represented by an acceleration response spectrum. It essentially specifies the level of the seismic force acting on a structure based on the structure's natural frequency and damping. Such spectra are derived for use in the nuclear power industry in Sweden, as the local seismic conditions were taken into consideration (SKI 1992). The load is defined as frequency-acceleration dependency as well as synthetic time history for the ground motion. This spectrum takes into account an envelope of earthquake motions, and hence, differs from that of a "real" earthquake. However, this approximation also means that it is conservative compared to the real earthquake.

The earthquake loading response spectra are classified in accordance to their annual exceeding frequency, that is to say, the probability level of an earthquake with a certain magnitude to occur in a period of time. The annual exceeding frequencies of the predefined spectra are 10^{-5}, 10^{-6} and 10^{-7}. The earthquake loading response spectra are classified in accordance to their *annual exceeding frequency*, that is to say, the probability level of an earthquake with a certain magnitude to occur in a period of time. The annual exceeding frequencies of the predefined spectra are 10^{-5}, 10^{-6} and 10^{-7}. The response spectra cover also earthquakes with a range of magnitudes that can occur at varying distances from the analyzed structure. In the matrix with occurrence frequencies in the seismic hazard model, SKI (1992) are presented earthquakes with certain seismic moment within a varying range. The probability of an earthquake, on the scale of those included in the study, occurring within the boundaries or in the vicinity of the facility, is extremely low. The particular case where the seismic fault occurs locally – directly at or adjacent to the Silo structure, is therefore not included in the study.

The connection between the load spectra and earthquake magnitude is not discussed in this report and is presented in details in SKI (1992).

The response spectra described above are originally intended to be used for design of structures above the ground level. The amplification of the acceleration that takes place in the top layer nearest to the ground surface is therefore included. The frequency-acceleration relation changes (the acceleration amplitude decreases) with the depth of the studied level. Therefore, it can be safely assumed that a response spectrum valid for the ground surface would have the same or higher accelerations at any particular frequency compared to an arbitrary point below the surface.

2.5.2.2 Load parameters

The loads are defined as ground response spectra in SKI (1992). The Silo structure is tested for earthquakes with annual exceeding frequencies of 10^{-5}, 10^{-6} and 10^{-7}, where the lower probability stands for a more powerful earthquake. The damping in the structure is assumed to be 4%, a typical choice for a concrete structure ASCE 4-98 (ASCE 2000). The presence of the bentonite between the silo and the rock would contribute to an even higher damping in the system, making this assumption conservative.

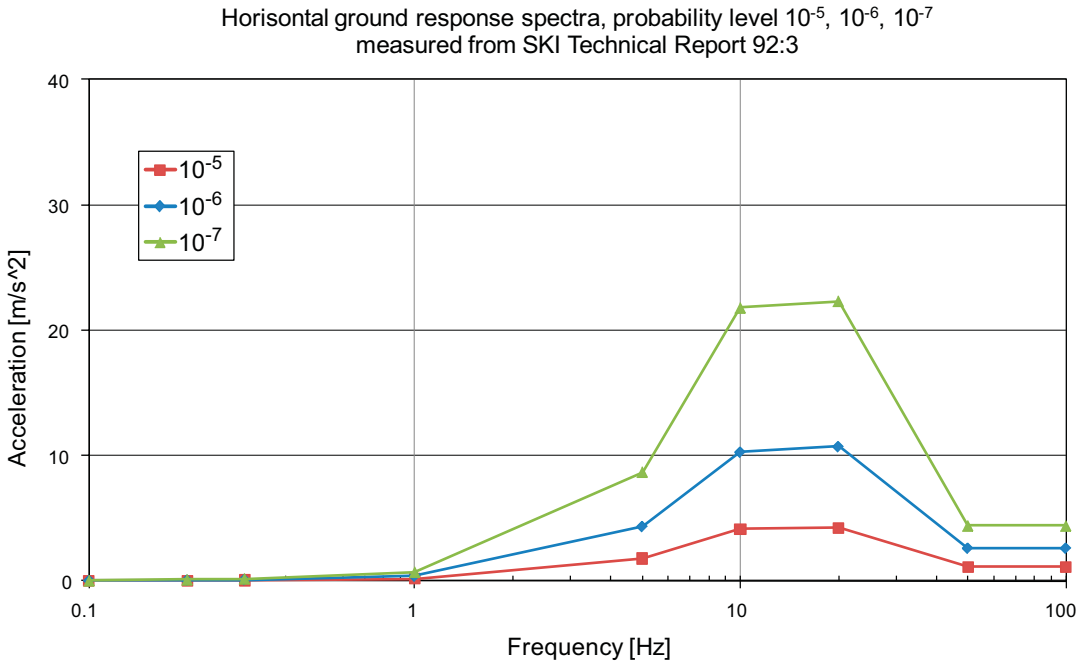

Figure 2-3. *Horizontal ground response spectra. All curves have 4% damping.*

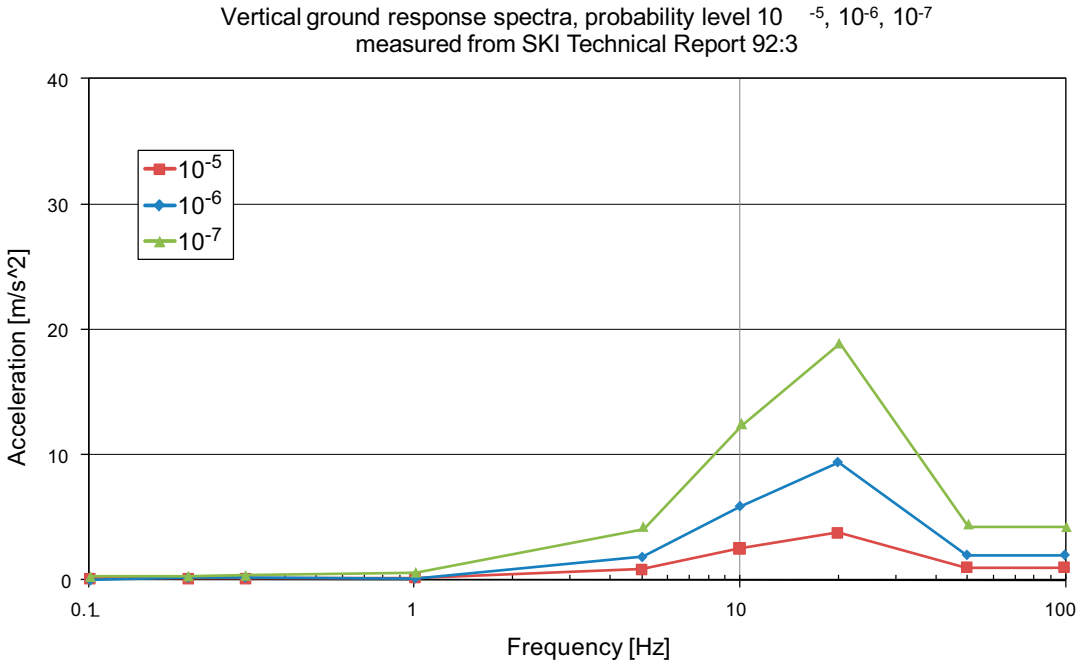

Figure 2-4. *Vertical ground response spectra. All curves have 4% damping.*

2.5.3 Creep and shrinkage

The larger part of the shrinkage of the concrete takes place immediately after the concrete is cast. The strains that are imposed on the structure are considered with a "final" shrinkage of $0.25 \cdot 10^{-3}$, in accordance with BBK 04 (Boverket 2004).

The effect of long term loading on the structure is considered with a creep value of the concrete material. The creep factor is chosen to j = 2 in accordance with BBK 04 (Boverket 2004).

The implementation of the creep and shrinkage in the numerical model is presented in Section 3.5.3.

2.5.4 Other loads

In the preliminary study were identified several potential loads that might be of significance for the capacity evaluation of the Silo structure. With the exception of the ones mentioned above, the following were also found to be of interest:

- Temperature.
- Water pressure.
- Swelling pressure (of the potentially liquefied bentonite filling).

It can be argued that these loads, and particularly the water pressure, will have certain dynamic and static effects on the overall structural behavior and locally for the casting joint between the outer wall and the slab. None of these were though considered here since the effect of the respective load was either found to be trivial to the overall stability of the structure or the load itself irrelevant (Notes from telephone meeting, Reinertsen-SKB, 24/3 2011).

2.5.5 Load combination

The only relevant combination for the analysis is the one including earthquake load, classified generally as "accidental". The combination rule for the section forces is done in accordance with standard praxis; a relevant reference is also ASCE 4-98 (ASCE 2000).

All permanent loads are included in a single load case.

The response of the structure in the three directions – X, Y and Z is combined with a SRSS method, as shown below. The response of the earthquake is added to the permanent loads with the sign that maximizes its effect on the final result:

$$\left.\begin{aligned} S_{DL} &= S_{SW} + S_{creep+shrinkage} \\ S_{SSE} &= \sqrt{S_X^2 + S_Y^2 + S_Z^2} \end{aligned}\right\} \rightarrow S = S_D \pm S_{SSE}$$ where S is an arbitrary section force.

2.6 Loss of concrete cover due to corrosion of the reinforcement

The reinforcement is said to have corroded and lost its mechanical properties. The process of corrosion of the rebars affects also the surrounding concrete. The expansion of the volume of the bars introduces additional stresses to the concrete which leads to the development of cracks and eventually the loss of the concrete cover.

The concrete cover is initially set to 50 mm for the outer cylinder wall. Considering the two layers of reinforcement and part of the concrete behind the reinforcement that will fall away, a total reduction of 300 mm seem to be a reasonable assumption (Notes from review meeting, Reinertsen-SKB, 6/3 2013).

Both cases with full cross section and reduced cross section are analyzed.

In the case with the reduced section the mass of the separated concrete cover does not contribute to the gravity load in the walls. The mass is however still considered as part of the wall in the dynamic analysis. This is done in order to introduce further safety in the analysis – the reduced weight means less pressure in the joint and at the same time the active mass for the seismic load is not changed.

2.7 Detail of the joint between the bottom slab and the silo wall

The joint between the silo wall and the slab is a weak point in the structure. Due to the compatibility of the deformations between the wall and the slab there are significant stresses that occur locally along the joint perimeter. At the same time there is no guaranteed bond between the concrete elements since the slab and the wall were cast separately. As the reinforcement is considered to be corroded and ineffective, the capacity for the joint depends to entirely on the compression provided by the external loads and in particular the self-weight of the concrete structure.

With none existent reinforcement it can be argued that the structure will not be able to resist bending moments that occur at the joint, thus forming a hinge. This is further discussed in the modeling and result presentation in Section 5.3. Eventually, both cases with moment resisting (rigid) joint and a hinged joint are studied.

2.8 Conditions and criteria for the structural integrity

It was stated in Section 2.4.1, that the reinforcement is considered to be completely ineffective and not taken into account in either the analysis or the capacity checks. The concrete structure, on the other hand, is considered to be entirely or partially intact (reduction of the thickness of the outer wall due to loss of the concrete cover is accounted for in a separate analysis).

The main criterion that the structure has to fulfill is that the overall integrity of the Silos outer shell should not be compromised (partial or total collapse of the outer wall of the silo). Since the reinforcement is considered not effective, both the compression and tensile internal forces have to be handled by the concrete material. The potential tension is certainly critical and most likely the reason for a collapse, since the tensile strength of the concrete is more than ten times lower than in compression.

The criterion, used here to define failure of the concrete silo, is that the stresses in the structure should not exceed the maximum allowed tension or compression (the tensile and compressive strengths as defined in Section 2.4.1). In practice, this means that no cracks in the concrete should occur. The allowed tensile stress is further reduced in accordance with BBK 04 (Boverket 2004) since the capacity in an ultimate limit state relies on the uncracked concrete section.

$$\sigma_t = \frac{f_{ct}}{\zeta} = \frac{1.625}{2} = 0.8125 MPa$$

Such reduction is not present in Eurocode 2 (CEN 2004) and therefore can be seen as an additional safety factor in the analysis. On the other hand, it can be argued that the allowed stress can be reduced further due to the uncertainties of the considered time span. This is however not considered further in this report.

For the outer wall of the silo are presented the maximum vertical and the hoop stresses as well as the maximum principal stresses that occur on the inside/outside edge of the wall. Special attention is paid to the joint between the outer wall and the bottom slab as it is considered a weak point due to the concentration of stresses along the joint.

The inner walls of the silo structure are considered secondary to the overall structural integrity since they are not part of the outer shell. Nevertheless the resulting principal stresses for the inner walls are presented.

Besides the stress levels, which present the structural integrity on local level, the global stability of the silo has to be secured. It is considered to be satisfactory to show that there is no separation that can occur between the bottom slab of the silo and the sand-bentonite foundation bed, that is to say no tension between the two occurs.

These are the summarized criteria:

- Overall stability of the structure
  - No tension between the bottom slab and the sand-bentonite bed.
- Silo wall
  - $\sigma_{P1}<\sigma_t$ (the principal stresses are within the limit for the material capacity).
- Inner wall
  - $\sigma_{P1}<\sigma_t$ (the principal stresses are within the limit for the material capacity).
- Joint between the slab and the outer wall:
  - $\sigma_{zz}< 0$ (compression in the joint from the vertical stresses).
  - $\sigma_{22}<\sigma_t$ (the hoop stresses are within the limit for the material capacity).

When a hinged joint is considered, the resultant force instead of the stresses in the joint is verified:
- $F_z< 0$ (the resultant from the vertical stresses force in the joint is compression).

2.9 Modeling consideration and analysis method

The model of the silo is done with some considerations and simplifications that generally do not influence the results.

- The concrete walls are represented by their midsurface. The thickness of the wall is a property of the midsurface. The bentonite is on the other hand modeled as “volume”.
- The bottom slab and the sand/bentonite foundation bed are “glued” together. No sliding can occur.
- The bentonite filling is on one side glued to the silos outer wall and on the other side fixed to the rock, see the boundary conditions in Section 3.4.
- The masses in the model are calculated through the material assigned to each element. The mass of the waste, which is smeared on the inner walls, requires a modified material for the inner walls, see also Section 3.5.1.
- The additional stiffness provided by the concreted cells is not accounted for in the model. The assumption is considered to be conservative.

The analysis is done in case studies (scenarios), which based on the already safely assumed loading (see Section 2.5.2.1) presents the model boundaries in two different ways:

- Case 1a, 1b. The Silo stands on the sand/bentonite bed foundation with no bentonite filling between rock and silo wall, thus allowing unrestrained movements for the silo structure above the bottom slab. Case 1a denotes a rigid joint between the slab and the outer walls and 1b – hinged joint.
- Case 2a, 2b. The Bentonite filling between the rock and silo wall is included in the model, presenting elastic restrain for the movements of the silos outer wall. Case 2a denotes a rigid joint between the slab and the outer walls and 2b – hinged joint.

The two cases are run with the full cross section of the silo wall (0.8 m) as well as a reduced wall cross section (0.5 m). In the latter case, the density of the material is modified so that the total mass remains the same for the dynamic analysis where the seismic load effect is evaluated. For the static analysis the weight of the separated concrete is not considered as a load and does not contribute to the pressure in the outer wall and the joint.

The cases are also shown in Figure 2-5. The rock boundary is represented by an infinite rigid support on the bottom surface of the sand/bentonite foundation bed as well as the outer surface of the bentonite filling.

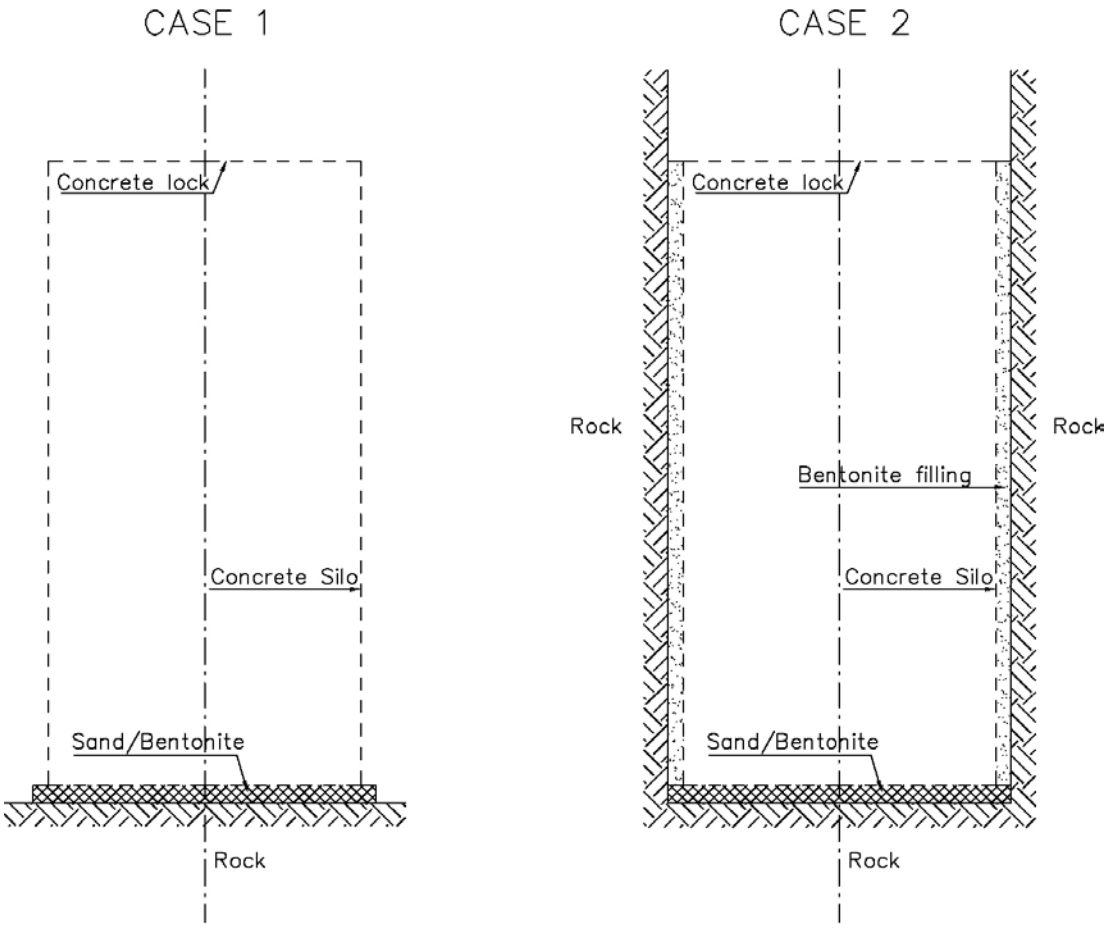

Figure 2-5. *Case 1 and 2 – boundaries.*

3 Finite element model

3.1 Overview

The finite element model is made in the program ADINA (2010).

The Silo structure and the bentonite surrounding it are modeled with a 3D structure, using shell elements for the concrete silo and 3D solid elements for the bentonite. The elements are given properties so that they correctly represent the stiffness and the mass of the real structure.

The concrete walls of the Silo are represented by shell elements, defined on the midsurface of the actual walls.

The model and the consequent analysis use a linear elastic assumption for the material properties.

The boundary conditions are presented in Section 3.4.

The implementation loads, described in Section 2.5, as well as further consideration of the mass and the self-weight in the FE-model is presented in Section 3.5.

3.2 Elements

The elements used in the FE-model are as follows:

- 4-node, shell element (silo structure).
- 8-node solid element (bentonite).

The shell elements have specifically been assigned integration according to Newton-Cotes, meaning that the integration points are located so that the obtained stresses can be used with no further extrapolation (ADINA 2010).

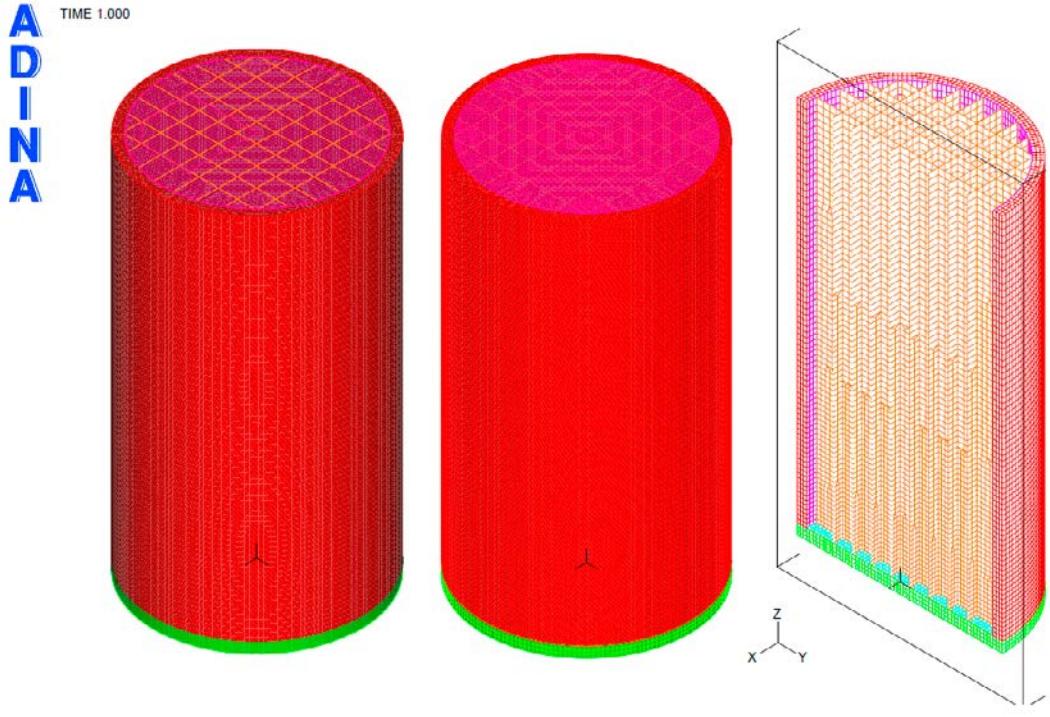

Figure 3-1. *Finite element model. Geometry overview (left), full element mesh (center) and section through the center of the model (right).*

3.3 Material properties

The materials used in the model are isotropic linear elastic materials, see also Section 2.4. The materials listed below are used in the FE-model:

Table 3-1. Materials in the FE-model.

Description (Material N)	E [GPa]	ν [–]	ρ [kg/m^3]
Concrete, Silo (1)	32.0	0.2	2,400
Concrete, Inner walls (5)	32.0	0.2	13,470*
Sand/Bentonite (3)	0.150	0.4	2,100
Bentonite filling (4)	0.006	0.2	0**

* see Section 3.5.1.

** the bentonite filling is modeled with zero mass.

3.4 Boundary conditions

The boundary conditions are predetermined by the surrounding rock, which constitutes an infinite stiff region. In the model where the bentonite filling is not considered, the only interface with the rock is the sand/bentonite foundation bed.

3.4.1 Case 1 and 2

The bentonite surrounding the Silo is considered to be fully restrained along the outer surface. For case 1 that is only the bottom surface of the sand/bentonite foundation bed, while for case 2 the outer surface of the bentonite filling is also included, see Figure 3-2.

3.4.2 Hinged connection between the bottom slab and the outer wall

The translation degrees of freedom along the edge of the silo wall are constraint with the bottom slab in order to model the hinged joint. This modification is optional and its purpose is described in Section 5.3.1.

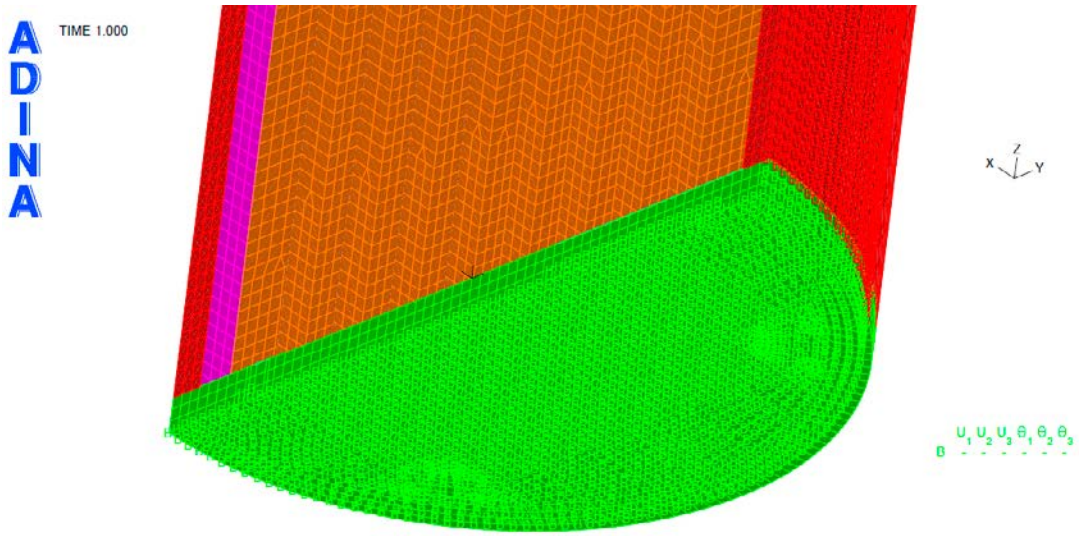

Figure 3-2. *Boundary conditions – Case 2.*

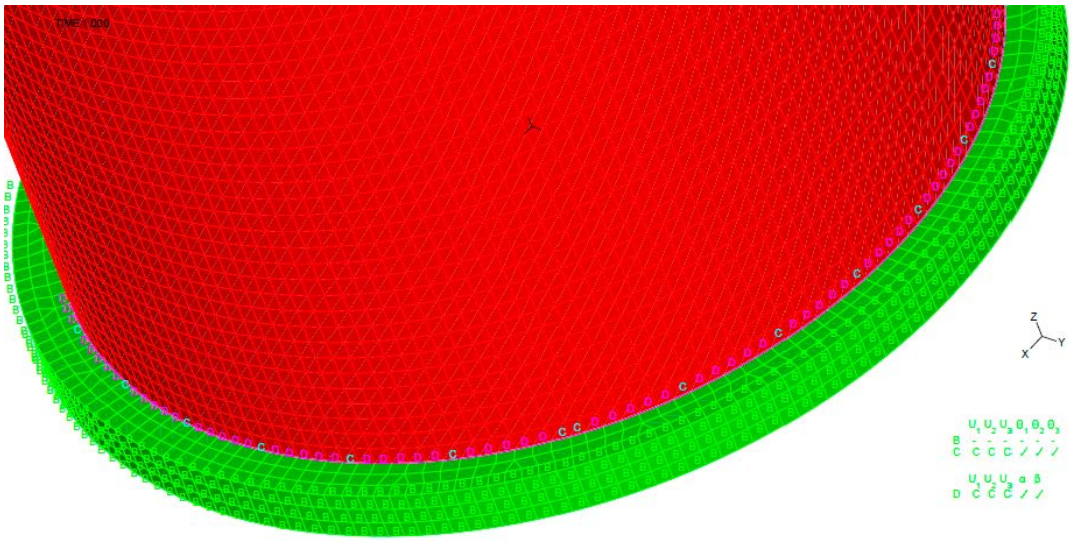

Figure 3-3. *Boundary conditions – Constraints between the silo wall and the bottom slab.*

3.5 Loads and masses

3.5.1 Permanent loads and added mass by the waste

The concrete structure of the silo, outer walls, inner walls, top cover and bottom slab, as well as the bentonite foundation bed are considered as permanent loads. The bentonite filling is modeled with zero mass as it is considered to act only as an elastic medium around the structure. These loads are calculated automatically in the model through the element geometry and the assigned material properties (thickness of the shell element, density of the assigned material).

In a dynamic analysis the mass is an important parameter. Hence, the mass of the waste has to be taken into account in the FE-model. Here, the waste is considered in the mass of the inner walls, that is to say, the waste mass is "smeared" out on the walls. This is a simple and effective technique for applying additional distributed mass in the FE-model. It is done by using a fictitious material with a modified density in which the waste mass is calculated:

The estimated waste is 44,000 t = 44,000 · 10^3 kg (Pusch 2003).

$$A_{inner_walls} = 4 \cdot \sum_{i=1..4} L_i \cdot H_{silo} = 375 \cdot 53.0 = 19{,}875\ m^2$$

$$q_{inner_wall} = \frac{M_{waste}}{A_{inner_walls}} = \frac{44{,}000 \cdot 10^3}{19{,}875} = 2{,}214\ kg/m^2$$

$$\rho_{concrete_inner_wall} = \rho_{btg} + \frac{q_{inner_wall}}{t_{inner_wall}} = 2{,}400 + \frac{2{,}214}{0.2} = 13{,}470\ kg/m^3$$

The assumption for the smeared mass of the waste on the inner walls is however valid only for the dynamic analysis (earthquake consideration). In the ordinary static case the waste acts as a vertical load that does not "hang" on the inner walls, but rather acts directly on the bottom slab.

Since the load case that introduces the mass of the model as weight is applied to the whole model, a compensating vertical load is applied on the walls, so that for the static case the weight of the waste is neutralized. The static vertical weight is then considered with a distributed load directly on the bottom slab.

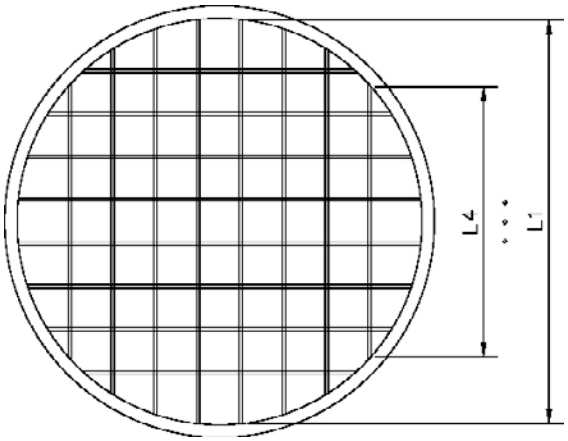

Figure 3-4. *Inner walls – "smeared mass".*

3.5.2 Earthquake load

The earthquake load is defined by the spectra presented in Section 2.5.2.

The load in the FE-model is introduced through the calculated eigenmodes in combination with a response spectrum.

3.5.3 Creep and shrinkage

The final shrinkage is assumed to be $0.25 \cdot 10^{-3}$ see also Section 2.4.1. It is implemented in the numerical model as a temperature difference, applied simultaneously on the whole structure. The temperature elongation constant for concrete is $\alpha = 1.0 \cdot 10^{-5}$, and the temperature difference is calculated as follows:

$$\varepsilon_{sh} = 0.25 \cdot 10^{-3} \rightarrow \frac{\Delta l}{l} = \varepsilon_{sh} = \alpha \Delta T$$

$$\Delta T = \frac{\varepsilon_{sh}}{\alpha} = -\frac{0.25 \cdot 10^{-3}}{1 \cdot 10^{-5}} = -25^{\circ}C$$

The concrete creep is considered with a creep factor $\varphi = 2$ BBK 04 (Boverket 2004) which reduces the effect of the long-term shrinkage:

$$\frac{EA}{1+\varphi} \cdot \Delta T = EA \cdot \frac{1}{1+2} \cdot \left(-25^{\circ}C\right) = -8.3^{\circ}C$$

3.6 Element groups

The element groups in the ADINA model are summarized in the table below.

Table 3-2. Element groups.

Element group	Type	Description
EG2	3D solid elements	Sand/bentonite foundation bed
EG3	3D solid elements	Bentonite filling
EG4	Shell elements	Silo, outer wall
EG5	Shell elements	Silo, bottom slab
EG6	Shell elements	Silo, inner wall
EG7	Shell elements	Silo, top cover.

3.7 Results

The results for element group 4 (outer walls) as well as the lower part of the inner walls are found to be relevant for the capacity control.

The results are presented and discussed in Chapter 5.

3.8 Simplified model

In order to verify the behavior of the finite element model of the silo structure as well as to easily check the overall stability of the silo, a simplified model for the foundation is used. The sand/bentonite bed is replaced by a generalized spring-set (translation and rotation springs) positioned in the center of the silos bottom slab. The slab is then connected to the spring through rigid links.

The properties of the spring are calculated in accordance with ASCE 4-98 (ASCE 2000). The calculation is presented in Appendix A4.

Table 3-3. Spring and dampnings constants.

Direction	Spring constant	Dampning
Translation – X,Y	$2.876 \cdot 10^{10}$ N/m	$5.034 \cdot 10^{8}$ Ns/m
Translation – Z	$3.795 \cdot 10^{10}$ N/m	$9.802 \cdot 10^{8}$ Ns/m
Torsion	$5.782 \cdot 10^{12}$ N/rad	$5.895 \cdot 10^{10}$ Nsm
Rotation – X, Y	$4.818 \cdot 10^{12}$ N/rad	–

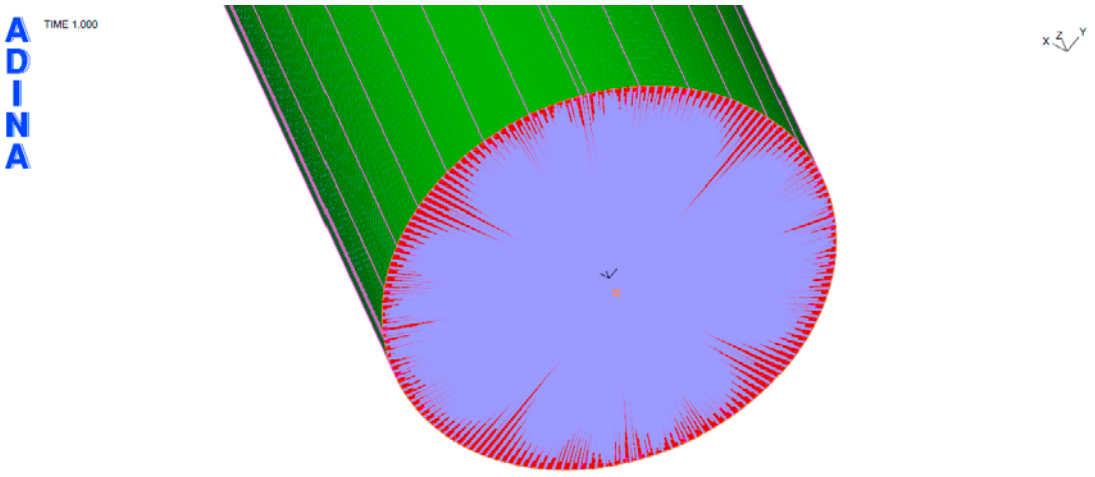

Figure 3-5. *Boundary condition for the simplified model. The bottom slab is connected with rigid links to the spring-set at the center of the foundation bed.*

4 Analysis

4.1 Overview

The dynamic analysis for the earthquake loads was performed using the response spectrum analysis with mode superposition method. It produces the response, in terms of deformations and section forces, to a response spectrum loading, see also Section 2.5.2. The analysis is done for the different directions of the earthquake motions (x, y and z) in order to assure that all the significant modes are excited.

In the response spectrum analysis the pre-calculated eigenmodes of the structure are used to estimate the potential load from the earthquake on the structure. For the frequency of each eigenmode corresponds certain maximum acceleration in the load spectra. The acceleration, together with the excited mass and the form that characterize an eigenmode, can be applied to the structure as a regular static load. The response of the structure is then the sum of the load effects of all eigenmodes. The eigenmodes, where the larger part of the structural mass vibrates, have larger impact on the dynamic response of the structure.

The mode superposition method is an approximate solution when only a limited number of modes are considered. As a guideline, the approximation is considered satisfactory when 90% of the modal mass is excited in the analyses (common praxis).

Modal damping of 4% was used, as described in Section 4.2.

The analysis was performed using the well-established finite element program ADINA. Linear elastic material models and small deformations were assumed in the analysis.

4.2 Analysis assumptions and parameters

4.2.1 Damping

The damping ratio, i.e. percentage of critical damping, is an approximation of the overall energy dissipation in the system during a cyclic response. In a modal superposition analysis, modal damping is used.

The damping value is conservatively chosen to 4% of critical damping in accordance with the recommendations in ASCE 4-98 (ASCE 2000) for a low-ductile structure.

4.2.2 Number of eigenmodes

The number of used eigenmodes in the analysis is limited to the first 20 modes. This parameter is justified with the check for the effective mass ratio, see Section 4.3.1.

4.2.3 Hydro dynamic effects on the structure

Any effect from the dynamic response of the surrounding bentonite besides the purely elastic behavior is not considered in the analysis.

4.3 Response spectrum analysis criteria

4.3.1 Effective mass ratio

The eigenfrequencies and the effective mass ratio is presented for each model and case below. It is found that the first mode of the structure appears at a rather low frequency (just above 1 Hz for case 1).The complete list of the calculated eigenmodes of the structure as well as the modal participation factors are presented in Appendix A.

All of the used models produce a satisfactory effective mass ratio with the first 20 eigenmodes, see Table 4-1.

The two eigenmodes that contribute most in its respective direction (X, Y and Z) are here referred to as primary and secondary. They have consequently the most significant effect to the section forces and stress development in the structure under the dynamic loading.

The eigenmodes that are left out are contributing only marginally to the critical stresses in the structure. A sensitivity test for case 1 with the first 200 eigenmodes (effective mass ratio X, Y = 98.47%, Z = 97.78%) showed practically no deviation from the results with only 20 modes (effective mass ratio X, Y = 98.37%, Z = 97.76%).

Table 4-1. Eigenmodes, Case 1 and 2.

Model	Primary global eigenmode [Hz]	Secondary global eigenmode [Hz]	Mass participation factor for 20 modes X, Y [%]	Z [%]
Case 1 (simple model)	1.141	5.534	99.68	99.67
Case 1	1.206	5.095	98.37	97.76
Case 1 – hinged	1.205	5.095	98.38	97.75
Case 2	2.876	5.682	98.36	95.74
Case 2 – hinged	2.876	5.679	98.36	95.74

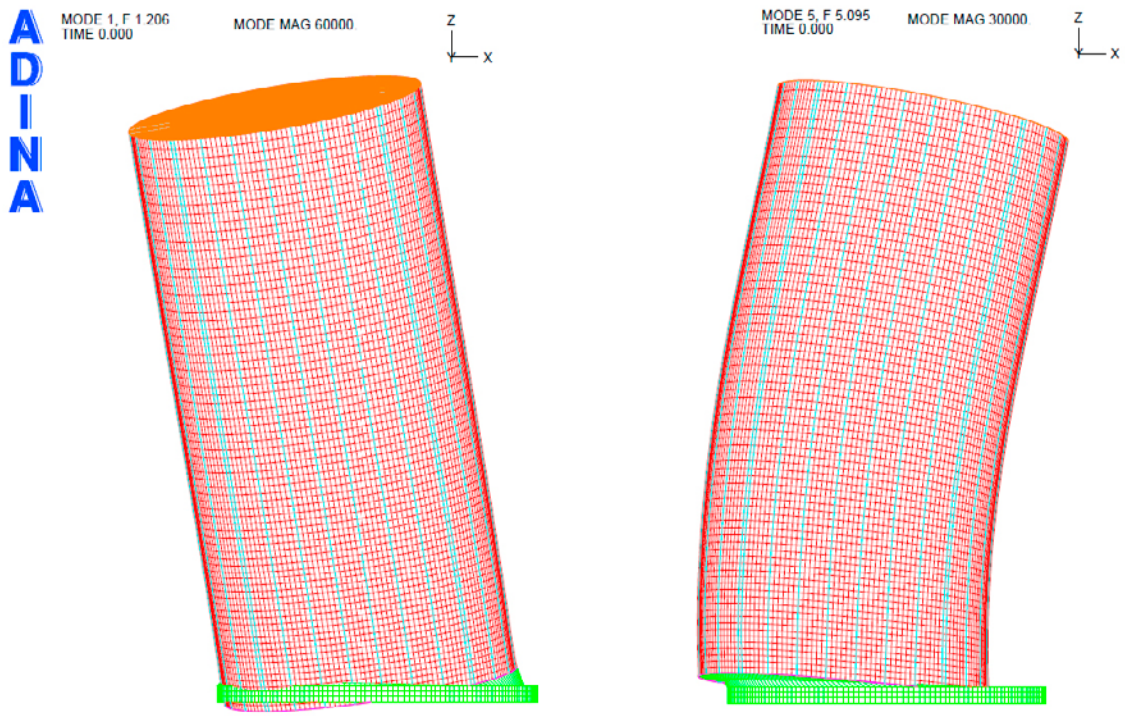

Figure 4.1. *Case 1. Fundamental eigenmodes f_1=1.206 Hz, f_5=5.095 Hz. The deformation magnitude is adjusted so that the eigenform of the silo structure is more pronounced.*

5 Results and capacity control

5.1 Summary of the results

The results are summarized in Table 5-1, Table 5-2 and Table 5-3, where with "Ok" is noted that the structure has maintained the condition for its structural integrity (the principal tensile stresses are lower than the concrete tensile strength). The results show that the Silo structure can withstand an earthquake that is classified with an annual occurrence probability of 10^{-5}.

The criterion for the structural integrity was presented in Section 2.8. The condition for fully compressed joint could not be fulfilled for any of the models as tensile stresses occur with the application of the permanent loads. The analyses were performed also by allowing a "hinge" to occur in the joint between the outer wall and the bottom slab, see Section 5.3.1. The assumption was made on the basis that the forming of a hinge does not compromise the structural integrity. With this modification, the stresses in the outer silo wall remain below the concrete tensile strength.

The stresses in the inner walls are however clearly higher and exceed the modified tensile strength. A case for the importance of the inner walls is also made in results discussion in Section 5.3.1

Table 5-1. Summary of the results, Silo outer wall.

	Case 1		Case 2	
Earthquake	**Restrained silo wall**	**Hinged silo wall**	**Restrained silo wall**	**Hinged silo wall**
10^{-5}	Ok*	Ok	Ok	Ok
10^{-6}	Fail!	Fail!	Fail!	Fail!
10^{-7}	Fail!	Fail!	Fail!	Fail!

* Max principal tension stress exceeds the tensile strength of the concrete in localized regions. Vertical stress in the joint region does not exceed the limits.

Table 5-2. Summary of the results, Silo inner walls.

	Case 1		Case 2	
Earthquake	**Restrained silo wall**	**Hinged silo wall**	**Restrained silo wall**	**Hinged silo wall**
10^{-5}	Fail!	Fail*	Fail*	Fail*
10^{-6}	Fail!	Fail!	Fail!	Fail!
10^{-7}	Fail!	Fail!	Fail!	Fail!

* Max principal tension stress exceeds the tensile strength of the concrete in localized regions/singular points.

Table 5-3. Summary of the results, reduced cross section.

	Case 1		Case 2	
Earthquake	**Restrained silo wall**	**Hinged silo wall**	**Restrained silo wall**	**Hinged silo wall**
10^{-5}	N/A	Ok	N/A	Ok
10^{-6}		Fail!		Fail!
10^{-7}		Fail!		Fail!

* Max principal tension stress exceeds the tensile strength of the concrete in localized regions.

5.2 Overall stability of the silo structure

The stability verification of the silo is narrowed down to a simple check if uplift in the bottom slab is possible under the seismic loading. No uplift takes place as long as the eccentricity of the resultant vertical reaction is within the area of D/4 in the center of the plate, see also Figure 5-1:

$$e = \frac{R_z}{R_m} \le \frac{1}{2}\frac{D}{4} \; where \; \left| \begin{array}{l} R_m = \sqrt{R_{mx}^2 + R_{my}^2} \\ \frac{1}{2}\frac{D}{4} = \frac{27.6m}{8} = 3.45m \end{array} \right.$$

The stability of the silo is verified with the simplified model presented in Section 3.8 so that the reaction forces are easily calculated. The results for all relevant cases are presented in Table 5-4 and Table 5-5. The results indicate that for the cases 10^{-5} and 10^{-6} there is no uplift while for the 10^{-7} case there is risk for uplift. This is not further investigated as the capacity checks for the structure itself are critical.

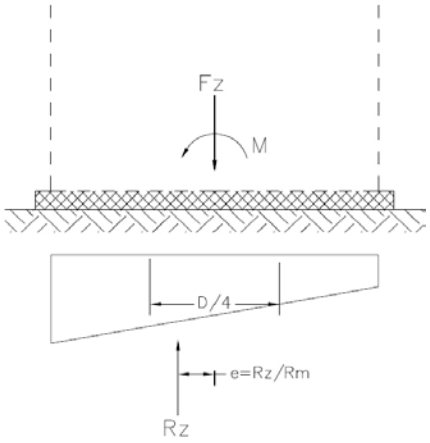

Figure 5-1. *Eccentricity for the resultant reaction.*

Table 5-4. Reaction forces, simple model.

Load case / Load combination	R_X [MN]	R_Y [MN]	R_Z [MN]	R_{mX} [MNm]	R_{mY} [MNm]	R_{mZ} [MNm]
Static load	0.0	0.0	–637.3	0.0	0.0	0.0
Earthquake 10^{-5}	29.6	29.6	29.9	337.2	337.2	0.0
Earthquake 10^{-6}	75.7	75.7	71.5	830.1	830.1	0.0
Earthquake 10^{-7}	152.6	152.6	150.4	1,620.0	1,620.0	0.0
Static load + Earthquake 10^{-5}	29.6	29.6	–607.4	337.2	337.2	0.0
Static load + Earthquake 10^{-6}	75.7	75.7	–565.8	830.1	830.1	0.0
Static load + Earthquake 10^{-7}	152.6	152.6	–486.9	1,620.1	1,620.0	0.0

Table 5-5. Verification, eccentricity of the resultant vertical reaction.

Model	R_z [MN]	R_m $(R_{mx}^2 + R_{mx}^2)^{0.5}$ [MNm]	$e = R_m/R_z$ [m]	|e|<D/8 = 3.45m
Static load + Earthquake 10^{-5}	–607.4	476.9	0.8	Ok
Static load + Earthquake 10^{-6}	–565.8	1,174.0	2.1	Ok
Static load + Earthquake 10^{-7}	–486.9	2,291.1	4.7	Ej Ok!

5.3 Verification of the capacity of the silo

In this section are presented and discussed the results that were found to be of significance to the structural integrity of the silo. The principal, vertical and hoop stresses are presented in full in Sections B1 and B4. The plots are adjusted so that the dark red areas mark the sections where the stresses in the concrete are higher than the modified reduced tensile strength $\sigma_t = 0.8125$ MPa. The stresses and forces along the joint between the slab and the outer wall are presented in diagrams.

The cases where a reduced cross section is studied are presented separately in Section 5.3.3.

As pointed out in Section 2.7 the joint between the slab and the silo outer wall is a weak point in the structure. When the joint is fully compressed, it can be considered rigid and that it effectively manages the compatibility for the rotation between the wall and the slab. Since the reinforcement considered ineffective, the joint is unable to effectively transfer any tensile stresses when they occur. When the load increases, tensile stresses are initiated on the outside edge of the wall and since they cannot be resisted the rotation of the wall is no longer restrained by the slab – the joint becomes a hinged joint, see Figure 5-3. As long as the resultant force in the joint is compression force the structure will not collapse, but rather adjust its static system.

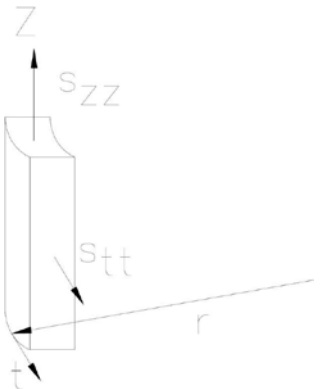

Figure 5-2. *Stresses in the silo outer wall: σ_{zz} – vertical stresses σ_{tt} – tangential (hoop) stress.*

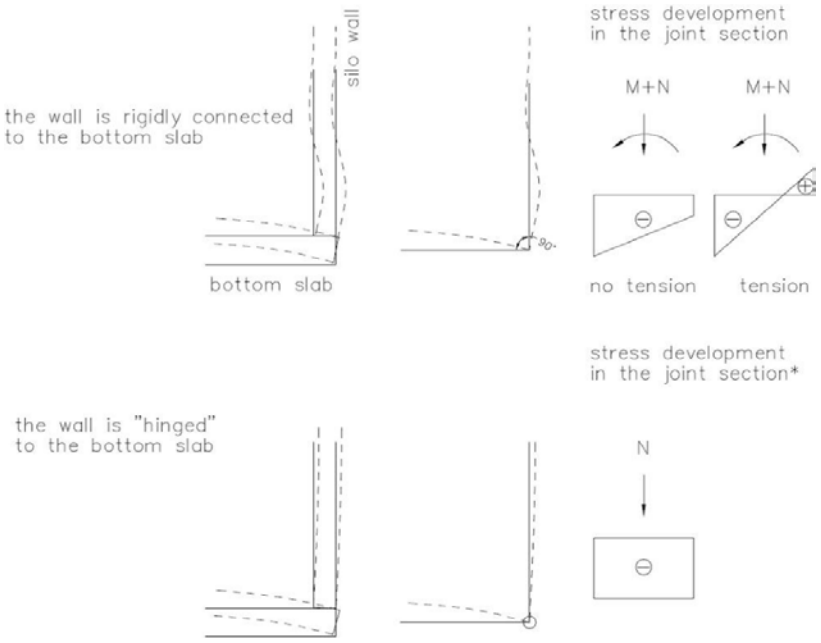

Figure 5-3. *Static system – the outer wall rigidly connected to the bottom slab (90° angle remains constant under the deformation) and hinged joint between the wall and the slab (free rotation, the translation between the wall and slab remains restrained).*

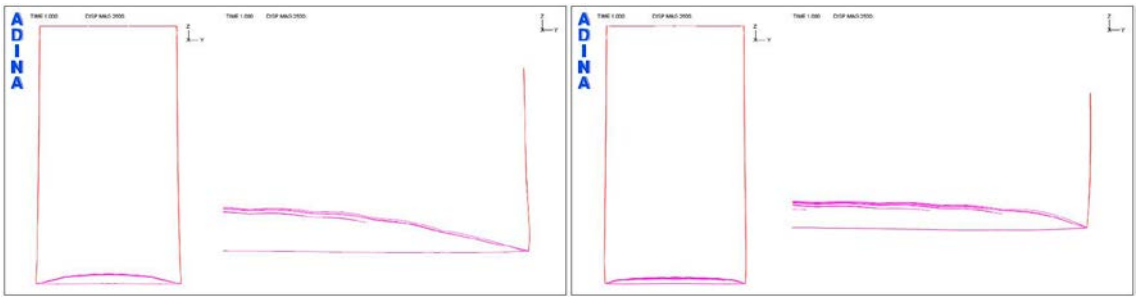

Figure 5-4. *Deformations in the cases with rigid (left) and hinged connection (right)between the silo outer wall and the slab in the FE-model.*

5.3.1 Case 1

The stresses in the outer wall are low and the vertical stress is negative (compression) with the exception of the outside edge of the joint section where tensile stresses occur (Figures 5-5 to 5-7). The tension appears with the application of the permanent loads, with the seismic load yet to be considered. The appearance of even low vertical tensile stress in the joint section is a reason to correct the joint connection in the model and change from rigid to hinged, as described above. This also means that any further results from case 1a with rigid joint are rather irrelevant.

The silo is further studied with a hinge forming along the joint between the slab and the outer wall, case 1b. For the 10^{-5} load case the principal stresses are within the limits of the modified tensile strength (σ_t = 0.8125 MPa), but still has its highest value at the joint section (Figure 5-8). This is mainly due to the hoop stresses that occur in this zone. It is important that no tension appears along the joint section.

For the 10^{-6} case both the vertical and the hoop stresses are under the limit, the principal stresses however exceed the modified tensile strength in large areas (Figure 5-9). The resultant force in the joint casting joint is tension, meaning that it is possible that there is separation between the two elements at certain points along the joint (Figure 5-10).

The stresses that develop in the inner walls are much higher than in the outer wall. For the 10^{-5} case the limit is exceeded in localized zones in direct proximity to the outer wall (Figure 5-11). The major contribution to the principal stresses comes from the shear stresses in the inner walls.

The tensile stresses are high from the permanent loads and even exceed the modified tensile strength at certain points (Figure 5-12). The stress development in the inner walls is closely connected to the elastic bed foundation on which the silo is resting. In the simplified model, where a rigid bottom slab is assumed, the inner walls are practically stress-free from the permanent loads. The seismic loading alone does not introduce large stresses and the stress level remains under the limit for the 10^{-5} case (see Appendix B2).

It can be argued whether the development of shear cracks in the inner walls can successively lead to collapse in the structure. In Figure 5-12 is shown the principal tensile stresses in the inner-wall where the peak stress occurs and the area where the stresses are exceeded is amplified. It is clear that the critical areas are localized in small zones at the corner of the inner wall. The potential development of shear cracks in this zone alone cannot be the single cause for collapse of the structure. It is important to point out, that the inner walls have a compression vertical stress over the whole area as the casting joint between the slab and the walls.

At this particular stage it is considered safe to assume that the structure will most likely maintain its overall stability but the effect cannot be ruled out as insignificant for the structural behavior.

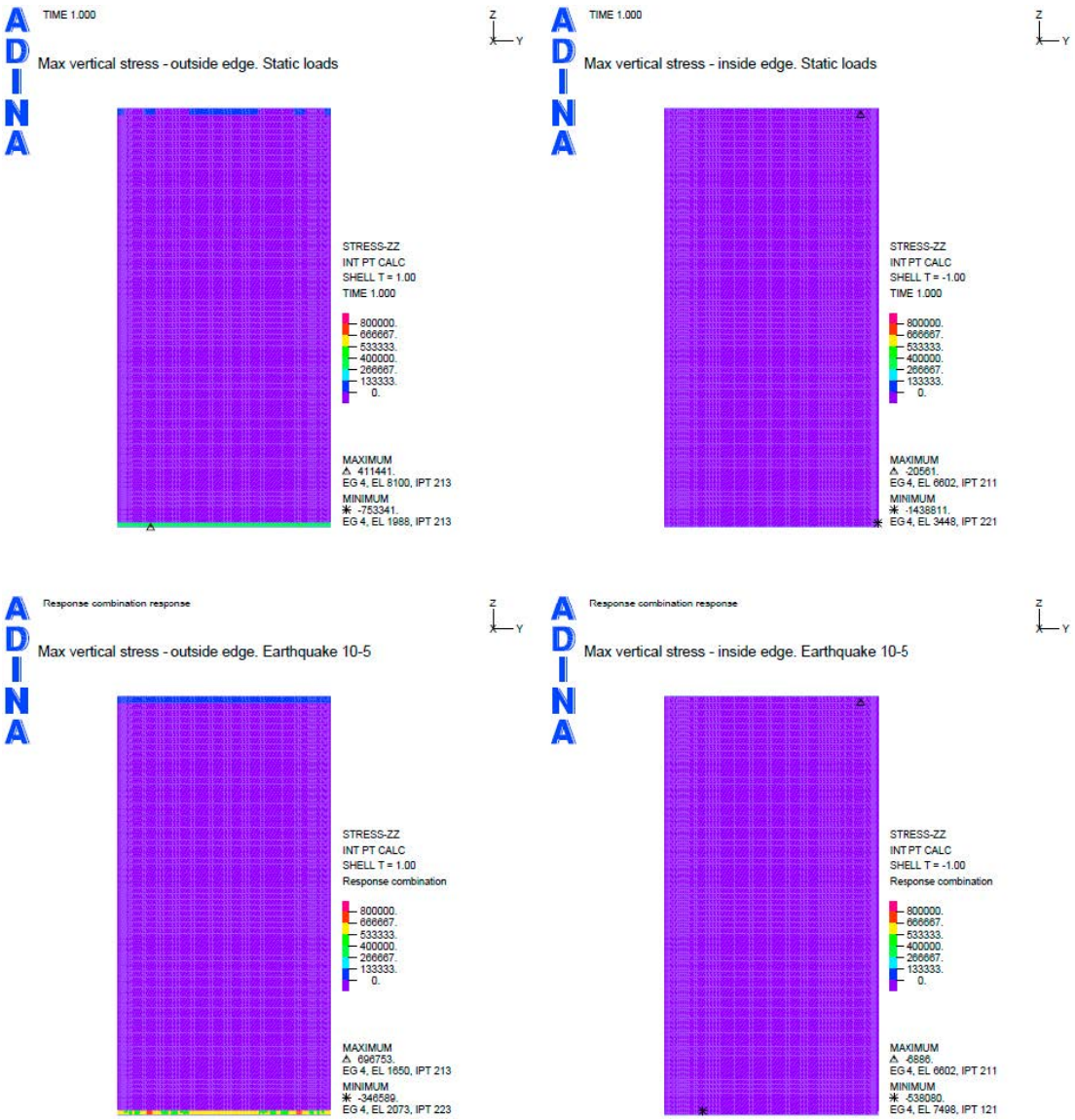

Figure 5-5. *Case 1a. Vertical stresses for the static load and 10^{-5}earthquake.*

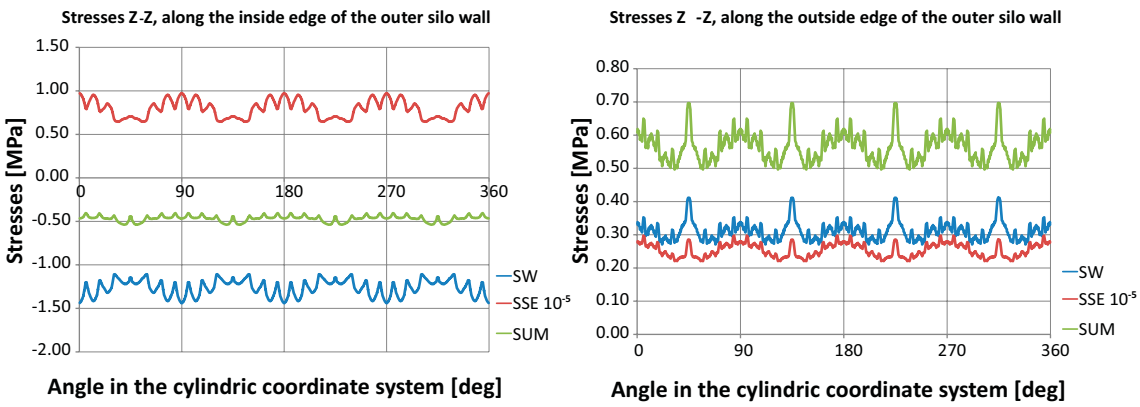

Figure 5-6. *Case 1a. Vertical stresses for the 10^{-5} earthquake along the joint between the slab and the wall. Contributions from the permanent loads (SW) earthquake (SSE 10^{-5}) and the total (SUM).*

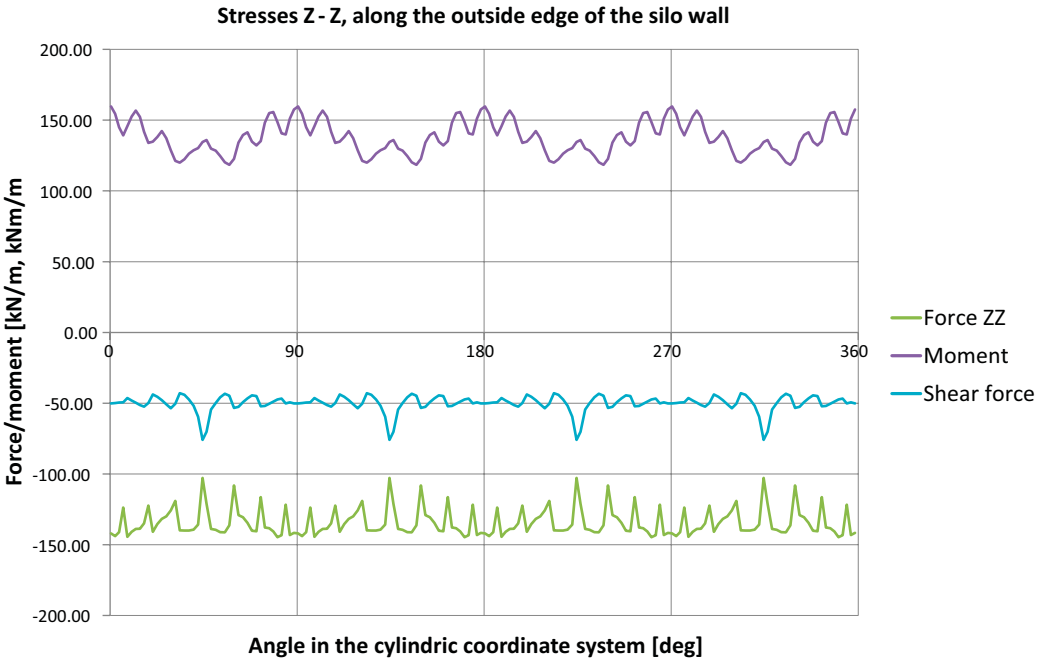

Figure 5-7. *Case 1a. Forces for the 10^{-5} earthquake along the joint between the slab and the wall.*

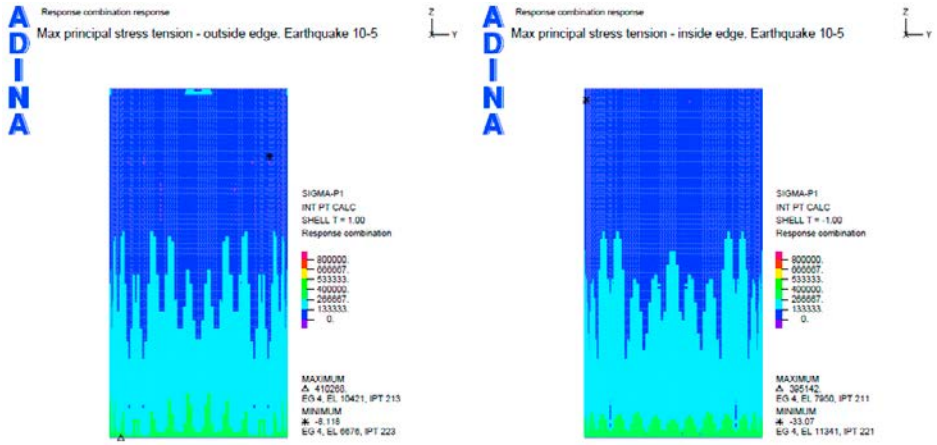

Figure 5-8. *Case 1b. Principal tension stresses and vertical stresses for the 10^{-5}earthquake.*

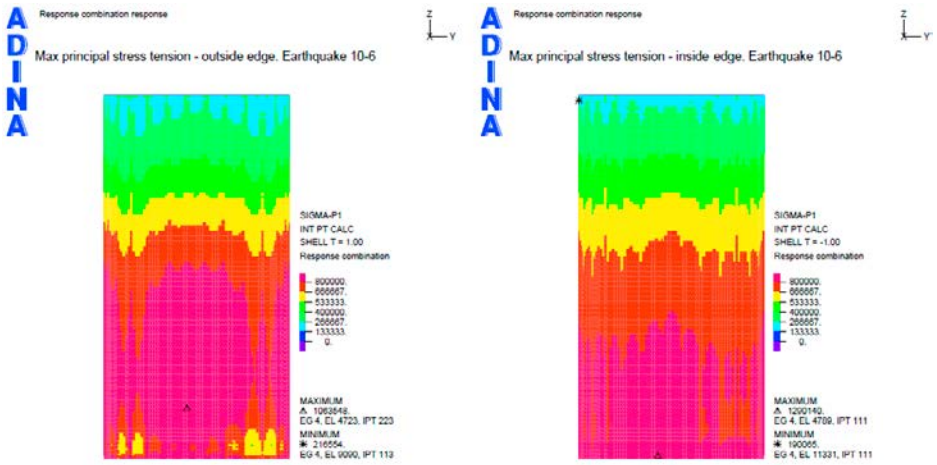

Figure 5-9. *Case 1b. Principal tension stresses and vertical stresses for the 10^{-6}earthquake.*

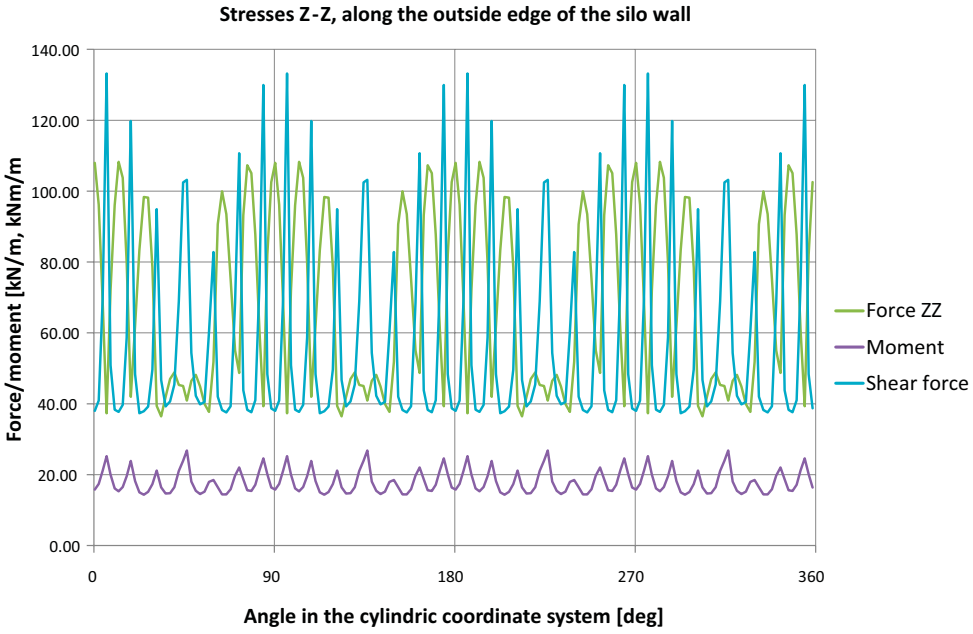

Figure 5-10. *Case 1b. Forces for the 10^{-6} earthquake along the joint between the slab and the wall.*

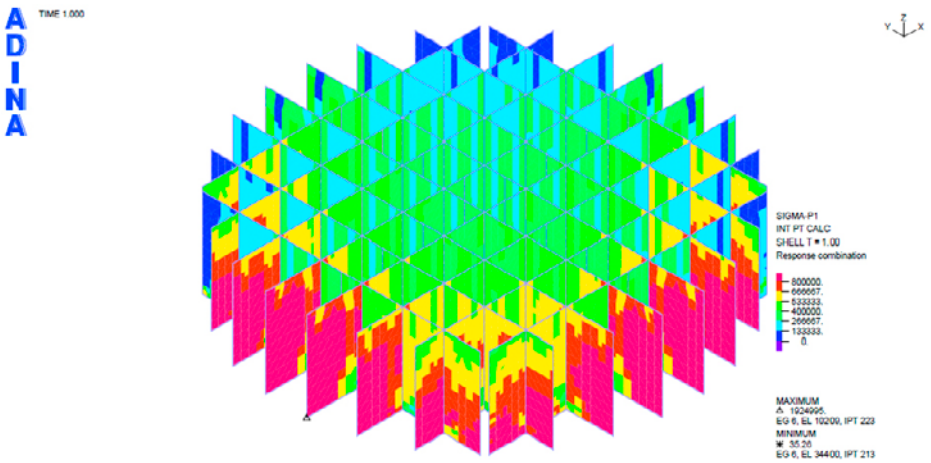

Figure 5-11. *Case 1b. Principal tensile stresses for the 10^{-5}earthquake for the bottom part of the inner walls.*

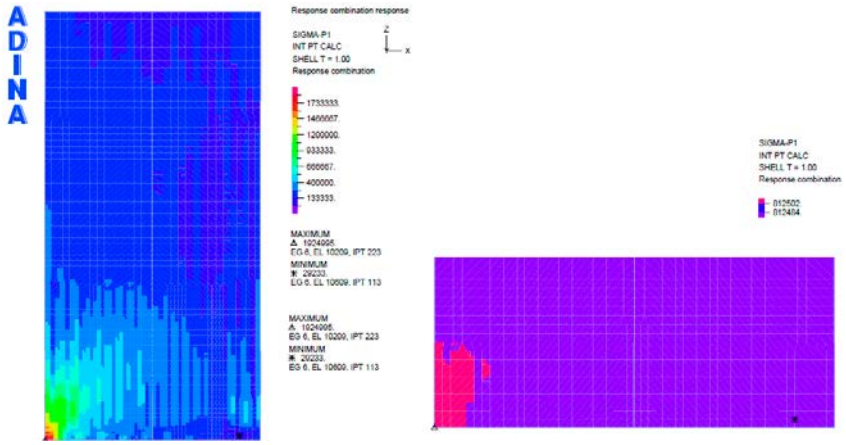

Figure 5-12. *Case 1. Principal tensile stresses in the inner walls for the 10^{-5}earthquake.*

5.3.2 Case 2

Case 2 was expected to produce lower stresses compared to case 1 due to the elastic support provided by the bentonite filling. The results, in terms of the magnitude of the obtained stresses, for case 2 confirm the picture presented in case 1. The stresses are relatively low for the 10^{-5} and exceed the limit tensile strength in for the 10^{-6} and 10^{-7} loading, see Figure 5-13.

There is no practical difference between case 1 and case 2 in how the structure behaves or the critical areas under the adjusted boundary condition (elastic support from the bentonite on the side of the walls). Like in case 1, tensile stresses along the outer perimeter of the casting joint appear in case 2 with the application of the permanent loads. Therefore only the results for case 2b with a hinged joint are presented.

The stress levels are slightly lower than in the previous case. The stresses from 10^{-5} earthquake load case are within limits. There is significant compression force along the perimeter of the joint (Figure 5-14, 5-15).

The stresses in the 10^{-6} and 10^{-7} cases are above the limits set in the preconditions. The 10^{-6} is a borderline case where the principal tensile stresses exceed the modified strength in local regions away from the casting joint (Figure 5-16). At the same time the resultant vertical force in the joint is a compression force (Figure 5-17).

The inner walls also present similar stress picture where the modified tensile strength is exceeded in localized zones adjacent to the outer walls (Figure 5-18). The same argument for the importance on the overall stability and the influence on the structural behavior can be made here as is in case 1b.

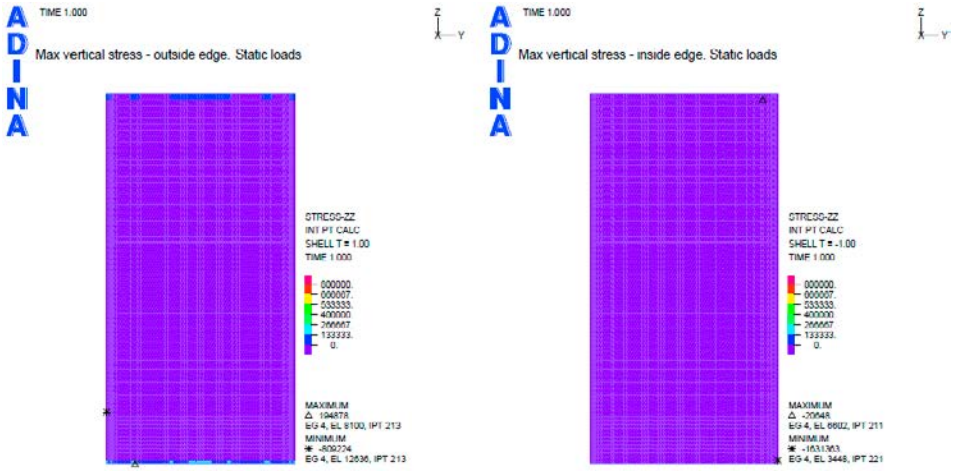

Figure 5-13. *Case 2. Vertical stresses for the load case with permanent loads only.*

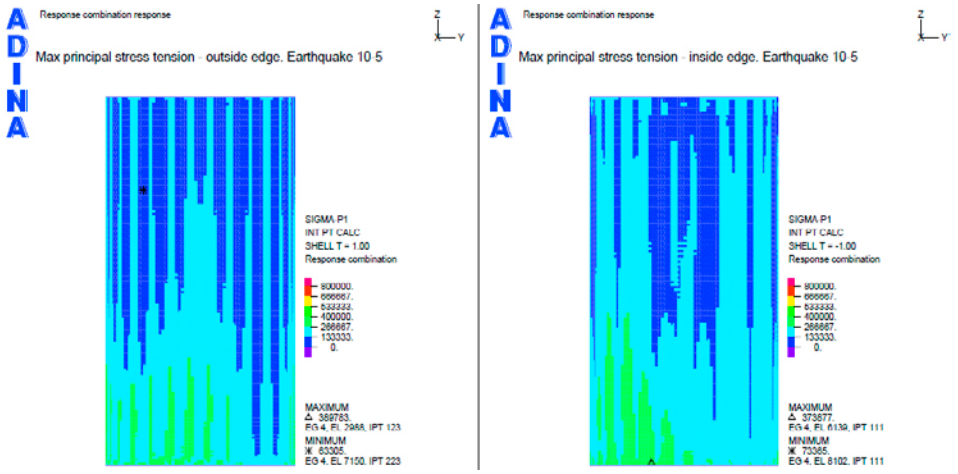

Figure 5-14. *Case 2b. Principal tensile stresses and vertical stresses for the 10^{-5} earthquakes.*

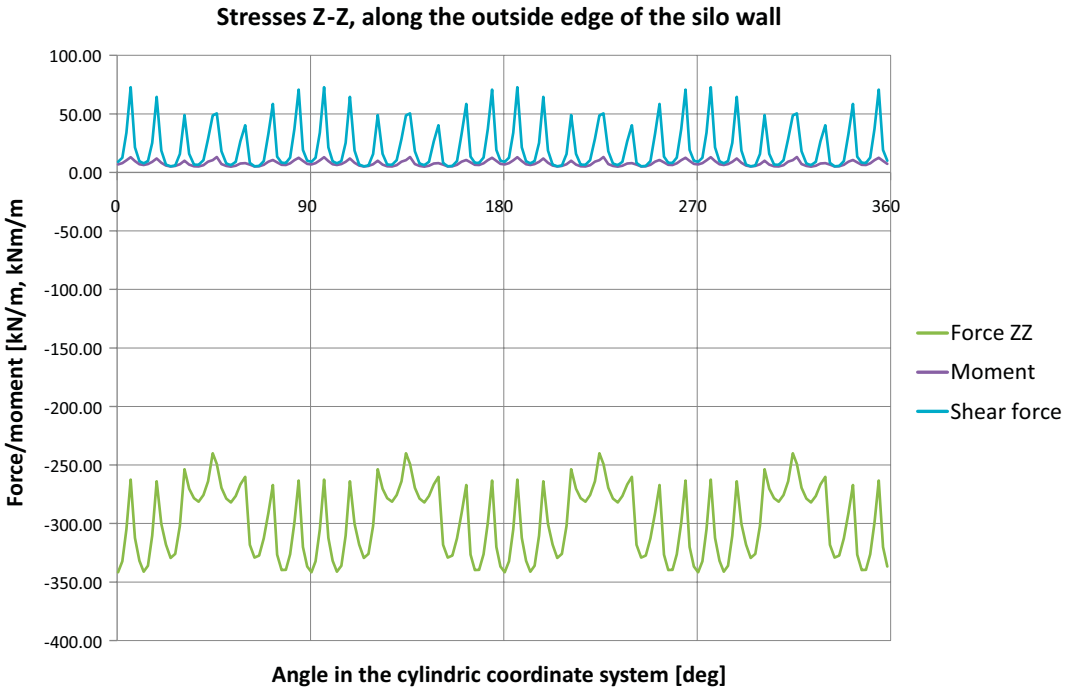

Figure 5-15. *Case 2b. Forces for the 10^{-5} earthquake along the joint between the slab and the wall.*

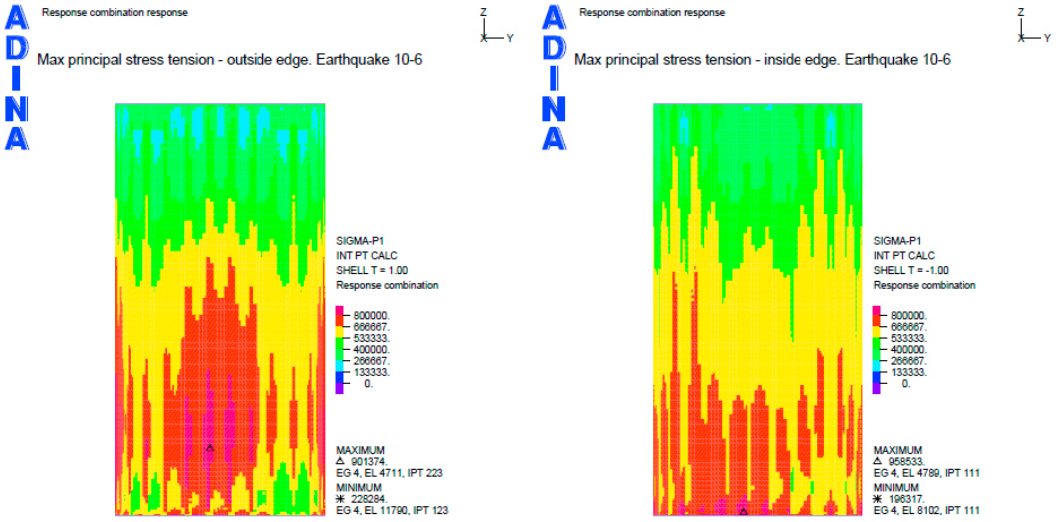

Figure 5-16. *Case 2b. Principal tensile stresses and vertical stresses for the 10^{-6} earthquake.*

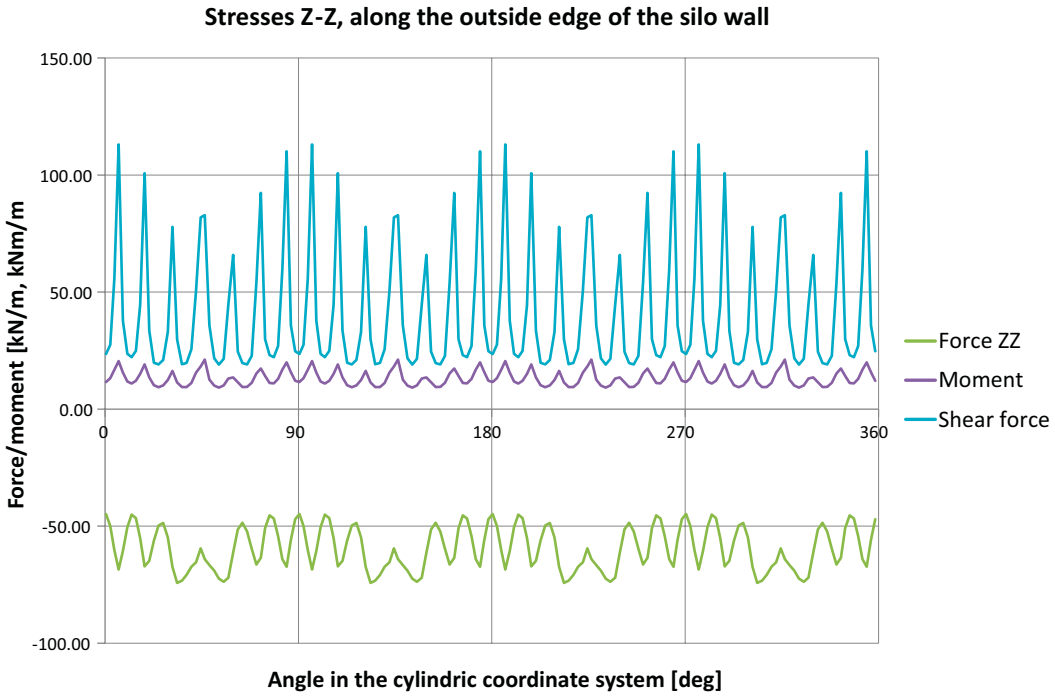

Figure 5-17. *Case 2b. Forces for the 10^{-6} earthquake along the joint between the slab and the wall.*

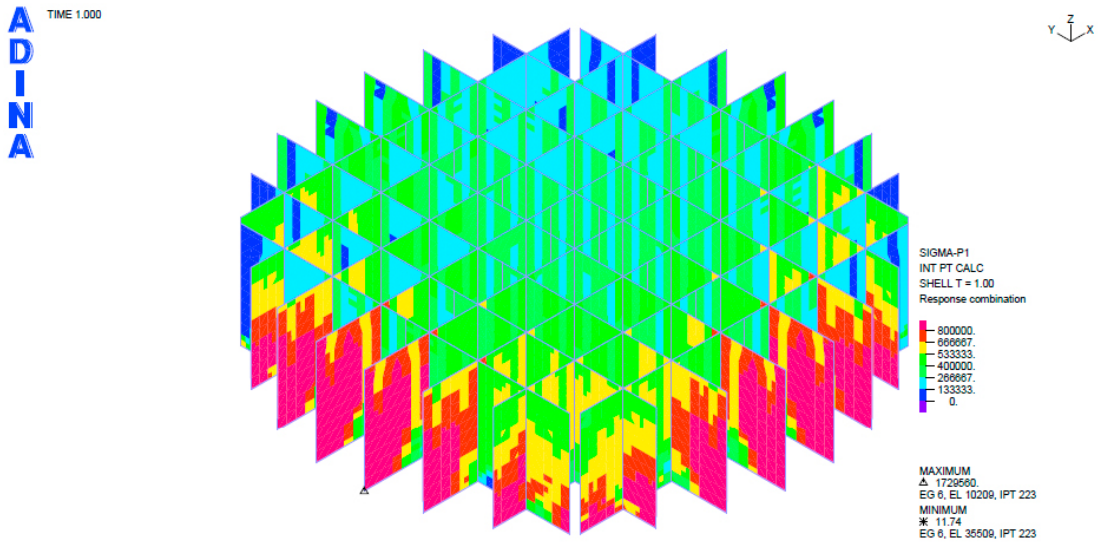

Figure 5-18. *Case 2b. Principal tensile stresses in the inner walls for the 10^{-5} earthquake.*

5.3.3 Results for a reduced cross section thickness of the outer wall

The reduced cross section for the outer wall does not significantly influence the dynamic behavior of the structure. The results are presented briefly here and in full in Appendices B5 and B8.

Only models with hinged joint are studied. This is due to what has been shown earlier for the full cross section studies, but also since a reduced cross section can hardly be justified an assumption for a rigid joint.

The results for the study can show that a potential reduction of the effective cross section does not lead to a stress increase in the structure. In fact, the stresses at the peak points are slightly lower (Figures 5-19 to 5-22).

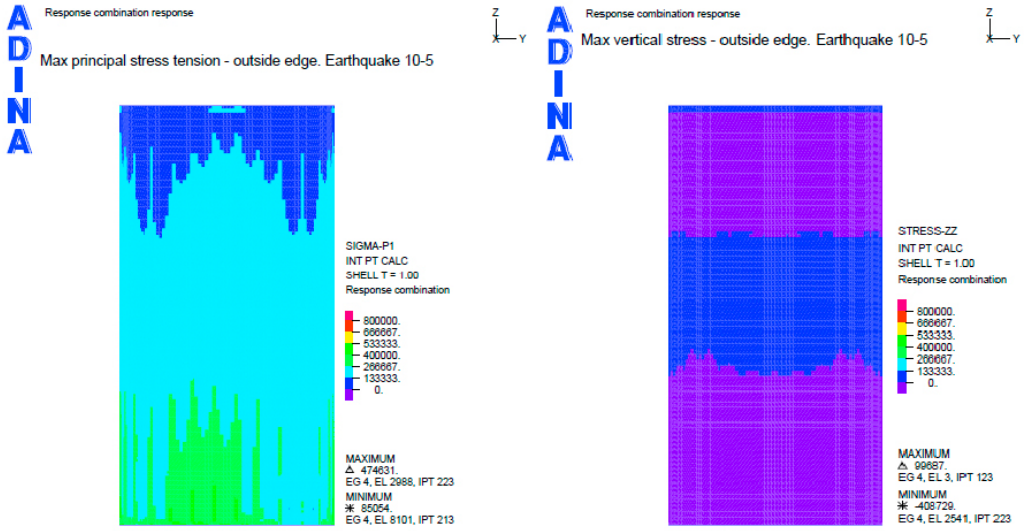

Figure 5-19. *Case 1b (reduced thickness). Principal tensile stresses and vertical stresses in the walls for the 10^{-5} earthquake.*

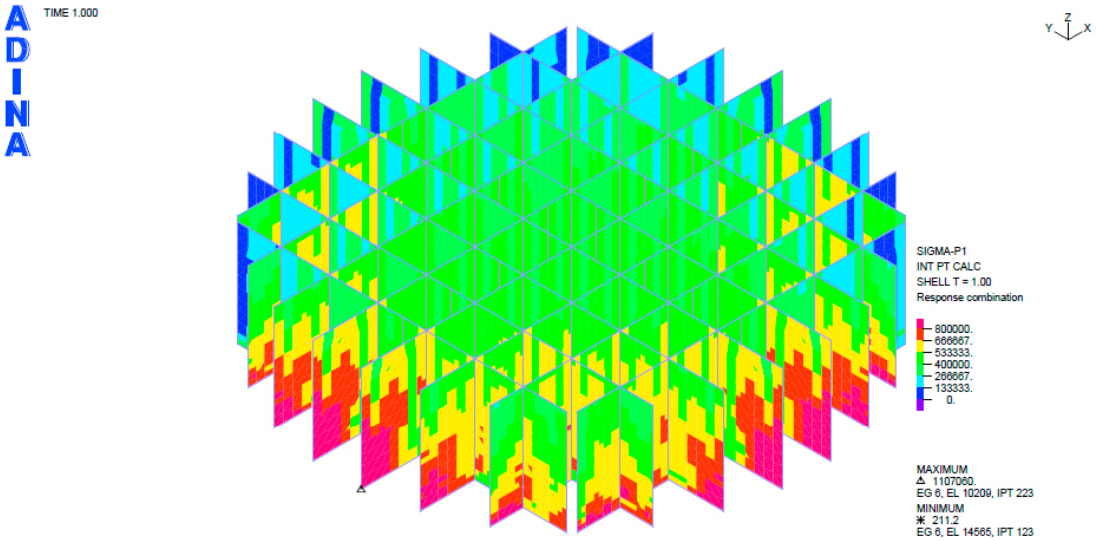

Figure 5-20. *Case 1b (reduced thickness). Principal tensile stresses in the inner walls for the 10^{-5} earthquake.*

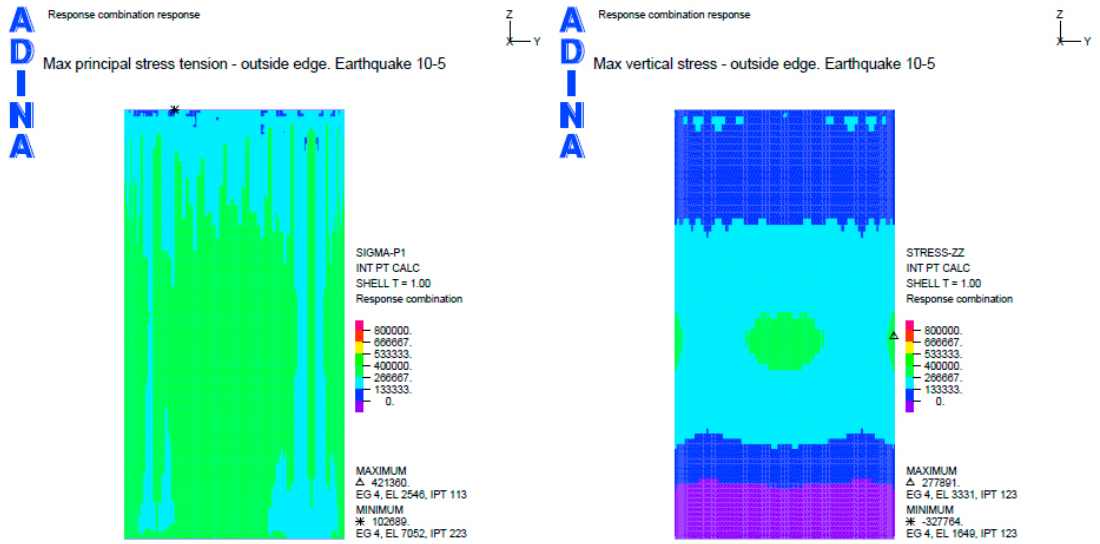

Figure 5-21. *Case 2b (reduced thickness). Principal tensile stresses and vertical stresses in the walls for the 10^{-5} earthquake.*

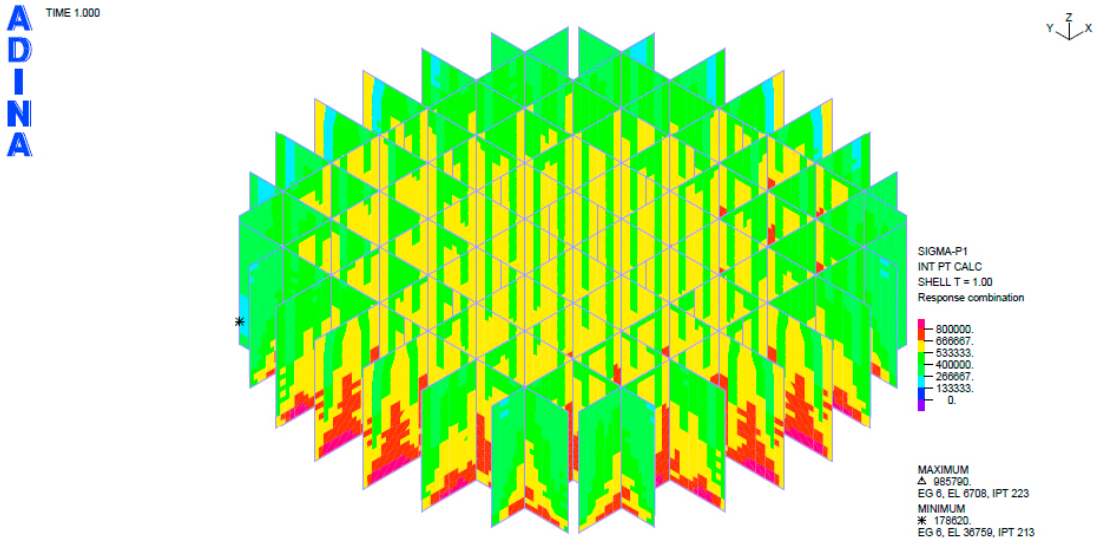

Figure 5-22. *Case 2b (reduced thickness). Principal tensile stresses in the inner walls for the 10^{-5} earthquake.*

5.3.4 Shear capacity of the casting joint

Based on the obtained forces in the joint is made an easy check on the shear force capacity in the casting joint, see the full calculation in Appendix B.9. The total horizontal shear force normal to the wall is checked against the joint capacity, provided by only the pressure in the joint.

The resultant vertical forces in the joint for the cases 10^{-6} and 10^{-7} cannot be proven to be in compression and therefore have no shear capacity.

Table 5-6. Verification, shear capacity for the casting joint.

Model	F_z [kN/m]	F_v [kN/m]	F_{max} [MN]	Check
Case 1 – simple				
Static load + Earthquake 10^{-5}	–550	100	768	Ok
Static load + Earthquake 10^{-6}	tension	–	–	–
Static load + Earthquake 10^{-7}	tension	–	–	–
Case 1b				
Static load + Earthquake 10^{-5}	–200	80	333	Ok
Static load + Earthquake 10^{-6}	tension	–	–	–
Static load + Earthquake 10^{-7}	tension	–	–	–
Case 2b				
Static load + Earthquake 10^{-5}	–240	50	400	Ok
Static load + Earthquake 10^{-6}	–50	80	83	Ok
Static load + Earthquake 10^{-7}	tension	–	–	–

5.3.5 Displacements of the silo

The maximum displacements appear at the top of the Silo. They are presented in Table 5-7. for the earthquakes with different probability, only case 1 is considered. In the displacements are included the permanent loads and the earthquake contribution

Table 5-7. Displacements of the silo.

Load case/Earthquake probability	X [mm]	Y [mm]	Z [mm]
Permanent loads	1.4	1.4	10.8
10^{-5}	6.2	6.2	12.4
10^{-6}	13.6	13.6	14.8
10^{-7}	25.6	25.6	1.9

5.4 Influence of the choice of standard on the capacity verification

The valid standard for design of concrete structures in Sweden at the start of the project was BBK 04 (Boverket 2004) and it was natural to adopt it in the report. Since the current valid standard for concrete structures is Eurocode 2 (CEN 2004), it was found proper to summarize the difference between the two that are essential to the report.

The two codes differ in certain aspects of the methodology of determination of the capacities, for example the partial coefficients for the limit states and the material coefficients. In the analyzed case was considered an accidental load combination for which the combined load effects are not multiplied by partial coefficients in both codes. The material coefficient for the accidental limit state are or is the same – $\gamma_{MC} = 1.2$.

Other differences are also mentioned in the preconditions, Sections 2.4.1, 2.6 and 2.8, regarding the dynamic properties of the material and the reduction of the concrete tensile strength. The dynamic factor on the Young's modulus of 1.2 is disregarded as it complies with Eurocode 2 (CEN 2004).

The reduction of the tensile strength is not supported in Eurocode 2 (CEN 2004). The assumption in BBK 04 (Boverket 2004) is conservative, thus motivated.

The use of BBK 04 (Boverket 2004) instead of Eurocode 2 (CEN 2004) for the analysis and capacity verification does not influence the final conclusions.

6 Conclusions

The Silo structure is analyzed with three response spectra which represent earthquakes with different intensity. The probability level, or the annual exceeding frequency, is 10^{-5}, 10^{-6} and 10^{-7}, where the lower probability equals more powerful load effect. The analyses were performed in a numerical model where the boundary conditions and structural properties were varied in order to present extreme cases for the dynamic response of the structure.

The results presented herein show that the Silo structure will be able to maintain its structural integrity under the loading from an earthquake with annual exceeding frequency of 10^{-5}. The stresses in the outer wall obtained for the studied cases, where the structure was subjected to the earthquake loading, remained within the pre-defined limits of the concrete material used in the structure. The resultant force in casting joint, between the outer wall and bottom slab, is in compression.

The modified tensile strength was exceeded for certain parts of the inner walls. This is due to large shear stresses that occur in close proximity to the outer wall and occur in localized zones. Nevertheless, the overall stability of the silo is considered to be secured.

The more powerful earthquakes, with probability levels 10^{-6} and 10^{-7}, showed extensive cracking in the outer wall as well as tension in the casting joint between the slab and outer wall. The inner walls showed also stresses significantly above the tensile limit strength.

The performed analyses are based on certain simplifications. The earthquake load used here is defined for a point at the ground level. This introduces additional safety in the analysis as the Silo structure lies significantly under the ground level. The assumptions for pure elastic behavior and use of response spectrum analysis disregarding the positive effect of the sealed cells in the silo, also add to the safety in the analyses.

The presence or effect of groundwater on the structural response or capacity is not considered in the analysis as a precondition.

References

SKB's (Svensk Kärnbränslehantering AB) publications can be found at www.skb.se/publications.

ADINA, 2010. ADINA command reference manual, Volume I: ADINA model definition. Report ARD 10-2, ADINA R & D, Inc., Watertown, MA.

ASCE, 2000. ASCE 4-98: Seismic analysis of safety-related nuclear structures and commentary. New York: American Society of Civil Engineers.

Boverket, 2003. Regelsamling för konstruktion: Boverkets konstruktionsregler, BKR, byggnadsverkslagen och byggnadsverksförordningen. Karlskrona: Boverket. (In Swedish.)

Boverket, 2004. Boverkets handbok om betongkonstruktioner: BBK04. Karlskrona: Boverket. (In Swedish.)

Börgesson L, Dueck A, Johanesson L-E, 2010. Material model for shear of the buffer – evaluation of laboratory test results. SKB TR-10-31, Svensk Kärnbränslehantering AB.

CEN, 2004. EN 1992-1-1:2004: Eurocode 2: Design of concrete structures – Part 1-1: General rules and rules for buildings. Brussels: European Committee for Standardization.

Pusch R, 2003. Design, construction and performance of the clay-based isolation of the SFR silo. SKB R-03-30, Svensk Kärnbränslehantering AB.

SKB, 2008. Safety analysis SFR 1. Long term safety. SKB R-08-130, Svensk Kärnbränslehantering AB.

SKI, 1992. Project Seismic Safety. Characterization of seismic ground motions for probabilistic safety analyses of nuclear facilities in Sweden. Summary report. SKI Technical Report 92:3, Statens kärnkraftinspektion (Swedish Nuclear Power Inspectorate).

SSM, 2009. Granskning av SFR-1 SAR.08. SSM dnr 20008/961, Strålsäkerhetsmyndigheten (Swedish Radiation Safety Authority. (In Swedish).

Appendix A

FE-model in ADINA

A1 Input files

Indata.in (Case 2B)

```
* SKB - SFR-PROJEKT, FEM-BERÄKNINGAR JORBÄVNINGSANALYS SILO SFR FEB-JUN 2013

* GINKO GEORGIEV, REINERTSEN SVERIGE AB


DATABASE NEW SAVE=NO PROMPT=NO
FEPROGRAM ADINA
CONTROL FILEVERSION=V89
*
FEPROGRAM PROGRAM=ADINA
*
CONTROL PLOTUNIT=PERCENT VERBOSE=YES ERRORLIM=0 LOGLIMIT=0 UNDO=5,
    PROMPTDE=UNKNOWN AUTOREPA=YES DRAWMATT=YES DRAWTEXT=EXACT,
    DRAWLINE=EXACT DRAWFILL=EXACT AUTOMREB=YES ZONECOPY=NO,
    SWEEPCOI=YES SESSIONS=YES DYNAMICT=YES UPDATETH=YES AUTOREGE=NO,
    ERRORACT=CONTINUE FILEVERS=V89 INITFCHE=NO SIGDIGIT=6,
    AUTOZONE=YES PSFILEVE=V0



FILEECHO OPTION=FILE F=loggfil.ut
FILELOG OPTION=FILE F=loggfil.ut


************************* INDATA GEOMETRI ************************************

READ F='modell/geometry.in'

************************* INDATA MATERIAL ************************************

READ F='modell/material.in'

************************* SUBDIVISION*****************************************

READ F='modell/subdivide.in'

************************* INDATA ELEMEN& MESH ********************************

READ F='modell/mesh.in'


************************* INDATA RANDVILLKOR *********************************

READ F='modell/boundary.in'

************************* INDATA ANALYS***************************************

READ F='modell/master_MPF.in'

ADINA OPTIMIZE=SOLVER FILE='mpf.dat'  FIXBOUND=YES MIDNODE=NO OVERWRIT=YES

*******************************************************************************

************************* INDATA LAST*****************************************

READ F='modell/load.in'

READ F='modell/master_stat.in'

MATERIAL ELASTIC NAME=4 E=0.01 NU=0.0 DENSITY=0.01 ALPHA=1.0E-5

ADINA OPTIMIZE=SOLVER FILE='stat.dat'  FIXBOUND=YES MIDNODE=NO OVERWRIT=YES

*******************************************************************************
```

```
**************************Geometri*******************************

********************** Silo bottenplatta ************

COORDINATES POINT SYSTEM=0
1000  -20.0 -20.0 0.0 0
@

LINE EXTRUDED NAME=1000 POINT=1000 DX=1 DY=0 DZ=0.0 SYSTEM=0 PCOINCID=YES

SURFACE EXTRUDED NAME=1000 LINE=1000 DX=0 DY=1 DZ=0.0 SYSTEM=0 PCOINCID=YES

LOADDXF F='modell/geometry/plan.dxf'

SURFACE PATCH NAME=1052 EDGE1=1124 EDGE2=1125 EDGE3=1126 EDGE4=0

SURFACE PATCH NAME=1065 EDGE1=1185 EDGE2=1147 EDGE3=1184 EDGE4=1175

SURFACE PATCH NAME=1066 EDGE1=1184 EDGE2=1143 EDGE3=1183 EDGE4=1174

SURFACE PATCH NAME=1067 EDGE1=1183 EDGE2=1135 EDGE3=1182 EDGE4=1173

SURFACE PATCH NAME=1068 EDGE1=1182 EDGE2=1176 EDGE3=1172 EDGE4=0

SURFACE PATCH NAME=1069 EDGE1=1126 EDGE2=1181 EDGE3=1171 EDGE4=1176

SURFACE PATCH NAME=1070 EDGE1=1181 EDGE2=1177 EDGE3=1170 EDGE4=0

SURFACE PATCH NAME=1071 EDGE1=1123 EDGE2=1178 EDGE3=1169 EDGE4=1177

SURFACE PATCH NAME=1072 EDGE1=1120 EDGE2=1179 EDGE3=1168 EDGE4=1178

SURFACE PATCH NAME=1073 EDGE1=1117 EDGE2=1180 EDGE3=1167 EDGE4=1179

SURFACE PATCH NAME=1074 EDGE1=1166 EDGE2=1175 EDGE3=1156 EDGE4=1165

SURFACE PATCH NAME=1075 EDGE1=1156 EDGE2=1174 EDGE3=1155 EDGE4=1164

SURFACE PATCH NAME=1076 EDGE1=1155 EDGE2=1173 EDGE3=1154 EDGE4=1163

SURFACE PATCH NAME=1077 EDGE1=1154 EDGE2=1172 EDGE3=1153 EDGE4=1162

SURFACE PATCH NAME=1078 EDGE1=1153 EDGE2=1171 EDGE3=1152 EDGE4=1161

SURFACE PATCH NAME=1079 EDGE1=1152 EDGE2=1170 EDGE3=1151 EDGE4=1160

SURFACE PATCH NAME=1080 EDGE1=1151 EDGE2=1169 EDGE3=1150 EDGE4=1159

SURFACE PATCH NAME=1081 EDGE1=1150 EDGE2=1168 EDGE3=1149 EDGE4=1158

SURFACE PATCH NAME=1082 EDGE1=1149 EDGE2=1167 EDGE3=1148 EDGE4=1157

TRANSFORMATI ROTATION NAME=11 MODE=AXIS SYSTEM=0 AXIS=ZL  ANGLE=-90

SURFACE TRANSFORMED NAME=1083 PARENT=0 TRANSFOR=11 PCOINCID=YES PTOLERAN=1.0E-05 COUPLED=YES NCOPY=3 MESH=NO
EGROUP=0 NCOINCID=NO NTOLERAN=1.00000000000000E-05
@CLEAR
1065
TO
1082
@


********************** Silo ytterväggar/bentonite fyllning ************

COORDINATES POINT SYSTEM=0
2000  -20.0 -20.0 0.0 0
@

LINE EXTRUDED NAME=2000 POINT=2000 DX=1 DY=0 DZ=0.0 SYSTEM=0 PCOINCID=YES

SURFACE EXTRUDED NAME=2000 LINE=2000 DX=0 DY=1 DZ=0.0 SYSTEM=0 PCOINCID=YES

VOLUME EXTRUDED NAME=2001 SURFACE=0 DX=0  DY=0 DZ=53 SYSTEM=0 PCOINCID=YES PTOLERAN=1.0E-05 NDIV=1 OPTION=VECTOR

@CLEAR
1074
to
1082
1110
to
1136
@

COORDINATES POINT SYSTEM=0
3000  -20.0 -20.0 0.0 0
@

********************** Silo innerväggar ************

LINE EXTRUDED NAME=3000 POINT=1000 DX=1 DY=0 DZ=0.0 SYSTEM=0 PCOINCID=YES

SURFACE EXTRUDED NAME=3000 LINE=3000 DX=0 DY=1 DZ=0.0 SYSTEM=0 PCOINCID=YES

LOADDXF F='modell/geometry/plan_innerv.dxf'


********************** Silo sand/bentonite bädd ************
```

```
COORDINATES POINT SYSTEM=0
4000  -20.0 -20.0 0.0 0
@

LINE EXTRUDED NAME=4000 POINT=4000 DX=1 DY=0 DZ=0.0 SYSTEM=0 PCOINCID=YES

SURFACE EXTRUDED NAME=4000 LINE=4000 DX=0 DY=1 DZ=0.0 SYSTEM=0 PCOINCID=YES

VOLUME EXTRUDED NAME=4001 SURFACE=0 DX=0 DY=0 DZ=-1.5 SYSTEM=0 PCOINCID=YES PTOLERAN=1.0E-05 NDIV=1 OPTION=VECTOR
@CLEAR
1001
to
1136
@


********** Silo topplock ***********

COORDINATES POINT SYSTEM=0
5000  -20.0 -20.0 0.0 0
@

LINE EXTRUDED NAME=5000 POINT=5000 DX=1 DY=0 DZ=0.0 SYSTEM=0 PCOINCID=YES

SURFACE EXTRUDED NAME=5000 LINE=5000 DX=0 DY=1 DZ=0.0 SYSTEM=0 PCOINCID=YES


TRANSFORMATI TRANSLATION NAME=21 MODE=SYSTEM SYSTEM=0  DX=0 DY=0 DZ=53

SURFACE TRANSFORMED NAME=5001 PARENT=0 TRANSFOR=21 PCOINCID=YES PTOLERAN=1.0E-05 COUPLED=YES NCOPY=1
@CLEAR
1001
to
1073
1083
to
1109
@


FIXBOUNDARY SURFACES FIXITY=ALL
4005  'ALL'
4009  'ALL'
4013  'ALL'
4017  'ALL'
4021  'ALL'
4024  'ALL'
4027  'ALL'
4030  'ALL'
4034  'ALL'
4037  'ALL'
4040  'ALL'
4043  'ALL'
4047  'ALL'
4050  'ALL'
4053  'ALL'
4056  'ALL'
4061  'ALL'
4065  'ALL'
4069  'ALL'
4073  'ALL'
4077  'ALL'
4080  'ALL'
4083  'ALL'
4086  'ALL'
4090  'ALL'
4093  'ALL'
4096  'ALL'
4099  'ALL'
4102  'ALL'
4104  'ALL'
4106  'ALL'
4108  'ALL'
4113  'ALL'
4117  'ALL'
4121  'ALL'
4124  'ALL'
4128  'ALL'
4131  'ALL'
4134  'ALL'
4136  'ALL'
4140  'ALL'
4143  'ALL'
4146  'ALL'
4148  'ALL'
4152  'ALL'
4155  'ALL'
4158  'ALL'
4160  'ALL'
4164  'ALL'
4168  'ALL'
4172  'ALL'
4175  'ALL'
4178  'ALL'
4181  'ALL'
4184  'ALL'
4187  'ALL'
4190  'ALL'
4193  'ALL'
4196  'ALL'
4199  'ALL'
```

4201 'ALL'
4203 'ALL'
4205 'ALL'
4207 'ALL'
4211 'ALL'
4214 'ALL'
4217 'ALL'
4220 'ALL'
4223 'ALL'
4226 'ALL'
4229 'ALL'
4232 'ALL'
4235 'ALL'
4239 'ALL'
4242 'ALL'
4245 'ALL'
4248 'ALL'
4251 'ALL'
4254 'ALL'
4257 'ALL'
4260 'ALL'
4263 'ALL'
4268 'ALL'
4273 'ALL'
4278 'ALL'
4282 'ALL'
4286 'ALL'
4290 'ALL'
4294 'ALL'
4298 'ALL'
4302 'ALL'
4305 'ALL'
4308 'ALL'
4311 'ALL'
4315 'ALL'
4319 'ALL'
4323 'ALL'
4326 'ALL'
4329 'ALL'
4332 'ALL'
4336 'ALL'
4340 'ALL'
4344 'ALL'
4348 'ALL'
4352 'ALL'
4356 'ALL'
4360 'ALL'
4364 'ALL'
4368 'ALL'
4372 'ALL'
4376 'ALL'
4380 'ALL'
4383 'ALL'
4386 'ALL'
4389 'ALL'
4392 'ALL'
4395 'ALL'
4398 'ALL'
4401 'ALL'
4404 'ALL'
4407 'ALL'
4410 'ALL'
4413 'ALL'
4416 'ALL'
4419 'ALL'
4422 'ALL'
4425 'ALL'
4428 'ALL'
4431 'ALL'
4434 'ALL'
4437 'ALL'
4440 'ALL'
4443 'ALL'
4446 'ALL'
4449 'ALL'
4452 'ALL'
@

FIXBOUNDARY SURFACES FIXITY=ALL

2004 'ALL'
2008 'ALL'
2012 'ALL'
2016 'ALL'
2020 'ALL'
2024 'ALL'
2028 'ALL'
2032 'ALL'
2036 'ALL'
2041 'ALL'
2046 'ALL'
2051 'ALL'
2055 'ALL'
2059 'ALL'
2063 'ALL'
2067 'ALL'
2071 'ALL'
2075 'ALL'
2079 'ALL'
2083 'ALL'
2087 'ALL'

```
2091  'ALL'
2095  'ALL'
2099  'ALL'
2103  'ALL'
2107  'ALL'
2111  'ALL'
2115  'ALL'
2119  'ALL'
2123  'ALL'
2127  'ALL'
2131  'ALL'
2135  'ALL'
2139  'ALL'
2143  'ALL'
2147  'ALL'
4238  'ALL'
4241  'ALL'
4244  'ALL'
4247  'ALL'
4250  'ALL'
4253  'ALL'
4256  'ALL'
4259  'ALL'
4262  'ALL'
4371  'ALL'
4375  'ALL'
4379  'ALL'
4382  'ALL'
4385  'ALL'
4388  'ALL'
4391  'ALL'
4394  'ALL'
4397  'ALL'
4400  'ALL'
4403  'ALL'
4406  'ALL'
4409  'ALL'
4412  'ALL'
4415  'ALL'
4418  'ALL'
4421  'ALL'
4424  'ALL'
4427  'ALL'
4430  'ALL'
4433  'ALL'
4436  'ALL'
4439  'ALL'
4442  'ALL'
4445  'ALL'
4448  'ALL'
4451  'ALL'
@


*************************** Material Prop.****************************
MATERIAL ELASTIC NAME=1 E=32.0E+09 NU=0.20 DENSITY=2400 ALPHA=1.0E-5 MDESCRIP='Silo'
*
MATERIAL ELASTIC NAME=3 E=150.0E+06 NU=0.40 DENSITY=2100 ALPHA=1.0E-5 MDESCRIP='Bentonite- botten platta'
*
MATERIAL ELASTIC NAME=4 E=6.0E+06 NU=0.25 DENSITY=0.1650 ALPHA=1.0E-5 MDESCRIP='Bentonite_vaggar'
*
MATERIAL ELASTIC NAME=5 E=38.40E+09 NU=0.20 DENSITY=13470 ALPHA=1.0E-5 MDESCRIP='Silo mellan vaggar'



************************Element Group***********************************
****Element GROUP=4          Rock
****Element GROUP=5          Bentonite bottom plate, Body
****Element Group=3          Bentonite fill around silo walls, Body
****Element Group=4          Silo walls, Shell element
****Element Group=5          Silon bottm, Shell element
****Element Group=6          Silo inside walls, Shell elements.
****Element Group=7          Silo slab, Shell elements.
*******************************************************************************


READ F='modell/mesh_bentonite.in'


READ F='modell/mesh_silo_LED.in'
*

************************Element Group***********************************
****Element Group=2          Bentonite bottom plate, Body
****Element Group=3          Bentonite fill around silo walls, Body
****Element Group=4          Silo walls, Shell element
****Element Group=5          Silon bottm, Shell element
****Element Group=6          Silo inside walls, Shell elements.
****Element Group=7          Silo slab, Shell elements.
*******************************************************************************
***Element group for Bentonite
*******************************************************************************
EGROUP THREEDSOLID NAME=2 DISPLACE=DEFAULT STRAINS=DEFAULT MATERIAL=3,
    RSINT=DEFAULT TINT=DEFAULT RESULTS=STRESSES DEGEN=DEFAUL,
    FORMULAT=0 STRESSRE=GLOBAL INITIALS=NONE FRACTUR=NO,
    CMASS=DEFAULT STRAIN-F=0 UL-FORMU=DEFAULT LVUS1=0 LVUS2=0 SED=NO,
    RUPTURE=ADINA INCOMPAT=DEFAULT TIME-OFF=0.00000000000000,
    POROUS=NO WTMC=1.00000000000000 OPTION=NONE DESCRIPT='NONE',
    PRINT=DEFAULT  SAVE=NO  TBIRTH=0.00000000000000,
    TDEATH=0.00000000000000 TMC-MATE=1 RUPTURE-=0 EM=NO JOULE=NO,
```

```
    BOLT-NUM=0 BOLT-PLA=0 BOLT-LOA=0.00000000000000,
    BOLT-TOL=0.00000000000000

EGROUP THREEDSOLID NAME=3 DISPLACE=DEFAULT STRAINS=DEFAULT MATERIAL=4,
    RSINT=DEFAULT TINT=DEFAULT RESULTS=STRESSES DEGEN=DEFAUL,
    FORMULAT=0 STRESSRE=GLOBAL INITIALS=NONE FRACTUR=NO,
    CMASS=DEFAULT STRAIN-F=0 UL-FORMU=DEFAULT LVUS1=0 LVUS2=0 SED=NO,
    RUPTURE=ADINA INCOMPAT=DEFAULT TIME-OFF=0.00000000000000,
    POROUS=NO WTMC=1.00000000000000 OPTION=NONE DESCRIPT='NONE',
    PRINT=DEFAULT  SAVE=NO  TBIRTH=0.00000000000000,
    TDEATH=0.00000000000000 TMC-MATE=1 RUPTURE-=0 EM=NO JOULE=NO,
    BOLT-NUM=0 BOLT-PLA=0 BOLT-LOA=0.00000000000000,
    BOLT-TOL=0.00000000000000



GVOLUME NODES=8 PATTERN=0 NCOINCID=BOUNDARIES NCFACE=123456 NCEDGE=,
'123456789ABC' NCVERTEX=12345678 NCTOLERA=1.000000000000000E-05,
    SUBSTRUC=0 GROUP=3 MESHING=MAPPED PREFSHAP=AUTOMATIC,
    DEGENERA=YES COLLAPSE=NO MIDNODES=CURVED METHOD=DELAUNAY,
    BOUNDARY=ADVFRONT
@CLEAR
2001
to
2036
@


GVOLUME NODES=8 PATTERN=0 NCOINCID=BOUNDARIES NCFACE=123456 NCEDGE=,
'123456789ABC' NCVERTEX=12345678 NCTOLERA=1.000000000000000E-05,
    SUBSTRUC=0 GROUP=2 MESHING=MAPPED PREFSHAP=AUTOMATIC,
    DEGENERA=YES COLLAPSE=NO MIDNODES=CURVED METHOD=DELAUNAY,
    BOUNDARY=ADVFRONT
@CLEAR
4001
to
4012
4014
to
4019
4021
to
4044
4046
to
4051
4053
to
4067
4069
4071
to
4091
4095
4096
4097
4101
to
4136
@


GVOLUME NODES=8 PATTERN=0 NCOINCID=BOUNDARIES NCFACE=123456 NCEDGE=,
'123456789ABC' NCVERTEX=12345678 NCTOLERA=1.000000000000000E-05,
    SUBSTRUC=0 GROUP=2 MESHING=MAPPED PREFSHAP=AUTOMATIC,
    DEGENERA=NO COLLAPSE=NO MIDNODES=CURVED METHOD=DELAUNAY,
    BOUNDARY=ADVFRONT
@CLEAR
4013
4020
4045
4052
4068
4070
 4092 to 4094
 4098 to 4100
@

************************Element Group**********************************
****Element GROUP=4          Rock
****Element GROUP=5          Bentonite bottom plate, Body
****Element Group=3          Bentonite fill around silo walls, Body
****Element Group=4          Silo walls, Shell element
****Element Group=5          Silon bottm, Shell element
****Element Group=6          Silo inside walls, Shell elements.
****Element Group=7          Silo slab, Shell elements.
************************************************************************

*****************************Outer silo walls***********************

EGROUP SHELL NAME=4 DISPLACE=DEFAULT MATERIAL=1 DESCRIPT='Silo outer walls' THICKNES=0.8 SECTIONRESULT=1 SAVE=YES TINT=3
TINT-TYPE=NEWTON-COTES


****************************** Silo bottom slab ***********************

EGROUP SHELL NAME=5 DISPLACE=DEFAULT MATERIAL=1 RINT=DEFAULT SINT=DEFAULT TINT=2 SECTIONRESULT=1 STRESSRE=GLOBAL
DESCRIPT='Bottom slab' THICKNES=0.90 SAVE=NO TINT=3 TINT-TYPE=NEWTON-COTES

****************************** Interior walls ***************************
```

```
EGROUP SHELL NAME=6 DISPLACE=DEFAULT MATERIAL=5 RINT=DEFAULT SINT=DEFAULT TINT=2 SECTIONRESULT=1 STRESSRE=GLOBAL
DESCRIPT='Interior walls' THICKNES=0.20  SAVE=NO TINT=3 TINT-TYPE=NEWTON-COTES

****************************** Top lock ***************************

EGROUP SHELL NAME=7 DISPLACE=DEFAULT MATERIAL=1 RINT=DEFAULT SINT=DEFAULT TINT=2 SECTIONRESULT=1 STRESSRE=GLOBAL
DESCRIPT='Silo top-lock' THICKNES=0.30  SAVE=NO TINT=3 TINT-TYPE=NEWTON-COTES
*****************************************************************Silo walls*****************************************************************



GSURFACE NODES=4 PATTERN=AUTOMATIC NCOINCID=ALL GROUP=5
@CLEAR
1001
to
1073
1083
to
1109
@

GSURFACE NODES=4 PATTERN=AUTOMATIC NCOINCID=ALL GROUP=6
@CLEAR
3001
to
3152
@
GSURFACE NODES=4 PATTERN=AUTOMATIC NCOINCID=ALL GROUP=7
@CLEAR
5001
to
5109
@

GSURFACE NODES=4 PATTERN=AUTOMATIC NCOINCID=ALL GROUP=4
@CLEAR
2002
2006
2010
2014
2018
2022
2026
2030
2034
2039
2044
2049
2053
2057
2061
2065
2069
2073
2077
2081
2085
2089
2093
2097
2101
2105
2109
2113
2117
2121
2125
2129
2133
2137
2141
2145
@

SUBDIVIDE MODEL MODE=LENGTH SIZE=0.50000000000000 NDIV=1,
    PROGRESS=GEOMETRIC MINCUR=1


SUBDIVIDE LINE NAME=2000 MODE=DIVISIONS NDIV=75,
    RATIO=1.6000000000000 PROGRESS=GEOM CBIAS=NO
2000 to 2005
2010 to 2011
2015 to 2016
2020 to 2021
2025 to 2026
2030 to 2031
2035 to 2036
2040 to 2041
2045 to 2046
2050 to 2051
2055 to 2058
2063 to 2066
2071 to 2072
2076 to 2077
2081 to 2082
2086 to 2087
2091 to 2092
2096 to 2097
2101 to 2102
2106 to 2107
2111 to 2112
```

2116 to 2117
2121 to 2122
2126 to 2127
2131 to 2132
2136 to 2137
2141 to 2142
2146 to 2147
2151 to 2152
2156 to 2157
2161 to 2162
2166 to 2167
2171 to 2172

3002
3004
3006
3009
3012
3015
3018
3020
3023
3026
3029
3031
3034
3036
3039
3042
3045
3047
3050
3052
3055
3058
3060
3063
3067
3073
3077
3085
3089
3097
3107
3109
3111
3113
3116
3119
3124
3126
3129
3132
3135
3139
3141
3144
3147
3150
3154
3156
3159
3162
3166
3170
3176
3180
3188
3192
3200
3210
3212
3214
3216
3219
3222
3227
3229
3232
3235
3238
3242
3244
3247
3250
3253
3257
3259
3262
3265
3269
3273
3279
3283
3291
3295
3303
3313
3315
3317
3319

3322
3325
3330
3332
3335
3338
3341
3345
3347
3350
3353
3356
3360
3362
3365
3368
3375
3384
3395
3412

SUBDIVIDE LINE NAME=2000 MODE=DIVISIONS NDIV=75,
RATIO=0.625 PROGRESS=GEOM CBIAS=NO
3004
3020
3023
3026
3029
3036
3039
3042
3045
3052
3055
3058
3067
3077
3089
3107
3111
3126
3129
3132
3135
3141
3144
3147
3150
3156
3159
3162
3170
3180
3192
3210
3214
3229
3232
3235
3238
3244
3247
3250
3253
3259
3262
3265
3273
3283
3295
3313
3317
3332
3335
3338
3341
3347
3350
3353
3356
3362
3365
3368
3375
3384
3395
3412

SUBDIVIDE LINE NAME=2000 MODE=LENGTH SIZE=1.0000000000000

3003
3007
3010
3013
3016
3019
3022
3025
3028

3306
3308
3310
3312
3316
3320
3323
3326
3328
3331
3334
3337
3340
3343
3346
3349
3352
3355
3358
3361
3364
3367
3370
3372
3374
3377
3379
3381
3383
3386
3388
3390
3392
3394
3397
3399
3401
3403
3405
3407
3409
3411
*5001 to 5340

************************** Loads **************************
LOAD TEMPERATURE NAME=1 MAGNITUD=-8.33000000000000

LOAD MASS-PROPORTIONAL NAME=1 MAGNITUD=10   AX=0 AY=0 AZ=-1.0 INTERPRE=BODY-FORCE

LOAD PRESSURE NAME=1 MAGNITUD=22.14e3

LOAD PRESSURE NAME=2 MAGNITUD=-780e3

*

APPLY-LOAD
@CLEAR
1 'MASS-PROPORTIONAL' 1 'MODEL' 0 0 1 0.00 0 -1 0 0 0 'NO' 0 0 1 0 'MID'
*2 'TEMPERATURE' 1 'NODE-SET' 4 0 1
*3 'TEMPERATURE' 1 'NODE-SET' 5 0 1
*4 'TEMPERATURE' 1 'NODE-SET' 6 0 1
*5 'TEMPERATURE' 1 'NODE-SET' 7 0 1

*STATIC CORRECTION
101 'PRESSURE' 1 'SURFACE' 3001 0 1 0 13 -1
0
102 'PRESSURE' 1 'SURFACE' 3002 0 1 0 13 -1
0
103 'PRESSURE' 1 'SURFACE' 3003 0 1 0 13 -1
0
104 'PRESSURE' 1 'SURFACE' 3004 0 1 0 13 -1
0
105 'PRESSURE' 1 'SURFACE' 3005 0 1 0 13 -1
0
106 'PRESSURE' 1 'SURFACE' 3006 0 1 0 13 -1
0
107 'PRESSURE' 1 'SURFACE' 3007 0 1 0 13 -1
0
108 'PRESSURE' 1 'SURFACE' 3008 0 1 0 13 -1
0
109 'PRESSURE' 1 'SURFACE' 3009 0 1 0 13 -1
0
110 'PRESSURE' 1 'SURFACE' 3010 0 1 0 13 -1
0
111 'PRESSURE' 1 'SURFACE' 3011 0 1 0 13 -1
0
112 'PRESSURE' 1 'SURFACE' 3012 0 1 0 13 -1
0
113 'PRESSURE' 1 'SURFACE' 3013 0 1 0 13 -1
0
114 'PRESSURE' 1 'SURFACE' 3014 0 1 0 13 -1
0
115 'PRESSURE' 1 'SURFACE' 3015 0 1 0 13 -1
0
116 'PRESSURE' 1 'SURFACE' 3016 0 1 0 13 -1
0
117 'PRESSURE' 1 'SURFACE' 3017 0 1 0 13 -1
0
118 'PRESSURE' 1 'SURFACE' 3018 0 1 0 13 -1
0

119	'PRESSURE'	1	'SURFACE'	3019	0	1	0	13	-1
120	'PRESSURE'	1	'SURFACE'	3020	0	1	0	13	-1
121	'PRESSURE'	1	'SURFACE'	3021	0	1	0	13	-1
122	'PRESSURE'	1	'SURFACE'	3022	0	1	0	13	-1
123	'PRESSURE'	1	'SURFACE'	3023	0	1	0	13	-1
124	'PRESSURE'	1	'SURFACE'	3024	0	1	0	13	-1
125	'PRESSURE'	1	'SURFACE'	3025	0	1	0	13	-1
126	'PRESSURE'	1	'SURFACE'	3026	0	1	0	13	-1
127	'PRESSURE'	1	'SURFACE'	3027	0	1	0	13	-1
128	'PRESSURE'	1	'SURFACE'	3028	0	1	0	13	-1
129	'PRESSURE'	1	'SURFACE'	3029	0	1	0	13	-1
130	'PRESSURE'	1	'SURFACE'	3030	0	1	0	13	-1
131	'PRESSURE'	1	'SURFACE'	3031	0	1	0	13	-1
132	'PRESSURE'	1	'SURFACE'	3032	0	1	0	13	-1
133	'PRESSURE'	1	'SURFACE'	3033	0	1	0	13	-1
134	'PRESSURE'	1	'SURFACE'	3034	0	1	0	13	-1
135	'PRESSURE'	1	'SURFACE'	3035	0	1	0	13	-1
136	'PRESSURE'	1	'SURFACE'	3036	0	1	0	13	-1
137	'PRESSURE'	1	'SURFACE'	3037	0	1	0	13	-1
138	'PRESSURE'	1	'SURFACE'	3038	0	1	0	13	-1
139	'PRESSURE'	1	'SURFACE'	3039	0	1	0	13	-1
140	'PRESSURE'	1	'SURFACE'	3040	0	1	0	13	-1
141	'PRESSURE'	1	'SURFACE'	3041	0	1	0	13	-1
142	'PRESSURE'	1	'SURFACE'	3042	0	1	0	13	-1
143	'PRESSURE'	1	'SURFACE'	3043	0	1	0	13	-1
144	'PRESSURE'	1	'SURFACE'	3044	0	1	0	13	-1
145	'PRESSURE'	1	'SURFACE'	3045	0	1	0	13	-1
146	'PRESSURE'	1	'SURFACE'	3046	0	1	0	13	-1
147	'PRESSURE'	1	'SURFACE'	3047	0	1	0	13	-1
148	'PRESSURE'	1	'SURFACE'	3048	0	1	0	13	-1
149	'PRESSURE'	1	'SURFACE'	3049	0	1	0	13	-1
150	'PRESSURE'	1	'SURFACE'	3050	0	1	0	13	-1
151	'PRESSURE'	1	'SURFACE'	3051	0	1	0	13	-1
152	'PRESSURE'	1	'SURFACE'	3052	0	1	0	13	-1
153	'PRESSURE'	1	'SURFACE'	3053	0	1	0	13	-1
154	'PRESSURE'	1	'SURFACE'	3054	0	1	0	13	-1
155	'PRESSURE'	1	'SURFACE'	3055	0	1	0	13	-1
156	'PRESSURE'	1	'SURFACE'	3056	0	1	0	13	-1
157	'PRESSURE'	1	'SURFACE'	3057	0	1	0	13	-1
158	'PRESSURE'	1	'SURFACE'	3058	0	1	0	13	-1
159	'PRESSURE'	1	'SURFACE'	3059	0	1	0	13	-1
160	'PRESSURE'	1	'SURFACE'	3060	0	1	0	13	-1
161	'PRESSURE'	1	'SURFACE'	3061	0	1	0	13	-1
162	'PRESSURE'	1	'SURFACE'	3062	0	1	0	13	-1
163	'PRESSURE'	1	'SURFACE'	3063	0	1	0	13	-1
164	'PRESSURE'	1	'SURFACE'	3064	0	1	0	13	-1
165	'PRESSURE'	1	'SURFACE'	3065	0	1	0	13	-1
166	'PRESSURE'	1	'SURFACE'	3066	0	1	0	13	-1
167	'PRESSURE'	1	'SURFACE'	3067	0	1	0	13	-1
168	'PRESSURE'	1	'SURFACE'	3068	0	1	0	13	-1

169	'PRESSURE'	1	'SURFACE'	3069	0	1	0	13	-1
0									
170	'PRESSURE'	1	'SURFACE'	3070	0	1	0	13	-1
0									
171	'PRESSURE'	1	'SURFACE'	3071	0	1	0	13	-1
0									
172	'PRESSURE'	1	'SURFACE'	3072	0	1	0	13	-1
0									
173	'PRESSURE'	1	'SURFACE'	3073	0	1	0	13	-1
0									
174	'PRESSURE'	1	'SURFACE'	3074	0	1	0	13	-1
0									
175	'PRESSURE'	1	'SURFACE'	3075	0	1	0	13	-1
0									
176	'PRESSURE'	1	'SURFACE'	3076	0	1	0	13	-1
0									
177	'PRESSURE'	1	'SURFACE'	3077	0	1	0	13	-1
0									
178	'PRESSURE'	1	'SURFACE'	3078	0	1	0	13	-1
0									
179	'PRESSURE'	1	'SURFACE'	3079	0	1	0	13	-1
0									
180	'PRESSURE'	1	'SURFACE'	3080	0	1	0	13	-1
0									
181	'PRESSURE'	1	'SURFACE'	3081	0	1	0	13	-1
0									
182	'PRESSURE'	1	'SURFACE'	3082	0	1	0	13	-1
0									
183	'PRESSURE'	1	'SURFACE'	3083	0	1	0	13	-1
0									
184	'PRESSURE'	1	'SURFACE'	3084	0	1	0	13	-1
0									
185	'PRESSURE'	1	'SURFACE'	3085	0	1	0	13	-1
0									
186	'PRESSURE'	1	'SURFACE'	3086	0	1	0	13	-1
0									
187	'PRESSURE'	1	'SURFACE'	3087	0	1	0	13	-1
0									
188	'PRESSURE'	1	'SURFACE'	3088	0	1	0	13	-1
0									
189	'PRESSURE'	1	'SURFACE'	3089	0	1	0	13	-1
0									
190	'PRESSURE'	1	'SURFACE'	3090	0	1	0	13	-1
0									
191	'PRESSURE'	1	'SURFACE'	3091	0	1	0	13	-1
0									
192	'PRESSURE'	1	'SURFACE'	3092	0	1	0	13	-1
0									
193	'PRESSURE'	1	'SURFACE'	3093	0	1	0	13	-1
0									
194	'PRESSURE'	1	'SURFACE'	3094	0	1	0	13	-1
0									
195	'PRESSURE'	1	'SURFACE'	3095	0	1	0	13	-1
0									
196	'PRESSURE'	1	'SURFACE'	3096	0	1	0	13	-1
0									
197	'PRESSURE'	1	'SURFACE'	3097	0	1	0	13	-1
0									
198	'PRESSURE'	1	'SURFACE'	3098	0	1	0	13	-1
0									
199	'PRESSURE'	1	'SURFACE'	3099	0	1	0	13	-1
0									
200	'PRESSURE'	1	'SURFACE'	3100	0	1	0	13	-1
0									
201	'PRESSURE'	1	'SURFACE'	3101	0	1	0	13	-1
0									
202	'PRESSURE'	1	'SURFACE'	3102	0	1	0	13	-1
0									
203	'PRESSURE'	1	'SURFACE'	3103	0	1	0	13	-1
0									
204	'PRESSURE'	1	'SURFACE'	3104	0	1	0	13	-1
0									
205	'PRESSURE'	1	'SURFACE'	3105	0	1	0	13	-1
0									
206	'PRESSURE'	1	'SURFACE'	3106	0	1	0	13	-1
0									
207	'PRESSURE'	1	'SURFACE'	3107	0	1	0	13	-1
0									
208	'PRESSURE'	1	'SURFACE'	3108	0	1	0	13	-1
0									
209	'PRESSURE'	1	'SURFACE'	3109	0	1	0	13	-1
0									
210	'PRESSURE'	1	'SURFACE'	3110	0	1	0	13	-1
0									
211	'PRESSURE'	1	'SURFACE'	3111	0	1	0	13	-1
0									
212	'PRESSURE'	1	'SURFACE'	3112	0	1	0	13	-1
0									
213	'PRESSURE'	1	'SURFACE'	3113	0	1	0	13	-1
0									
214	'PRESSURE'	1	'SURFACE'	3114	0	1	0	13	-1
0									
215	'PRESSURE'	1	'SURFACE'	3115	0	1	0	13	-1
0									
216	'PRESSURE'	1	'SURFACE'	3116	0	1	0	13	-1
0									
217	'PRESSURE'	1	'SURFACE'	3117	0	1	0	13	-1
0									
218	'PRESSURE'	1	'SURFACE'	3118	0	1	0	13	-1
0									

```
219             'PRESSURE'   1           'SURFACE'   3119    0    1    0    13    -1
                0
220             'PRESSURE'   1           'SURFACE'   3120    0    1    0    13    -1
                0
221             'PRESSURE'   1           'SURFACE'   3121    0    1    0    13    -1
                0
222             'PRESSURE'   1           'SURFACE'   3122    0    1    0    13    -1
                0
223             'PRESSURE'   1           'SURFACE'   3123    0    1    0    13    -1
                0
224             'PRESSURE'   1           'SURFACE'   3124    0    1    0    13    -1
                0
225             'PRESSURE'   1           'SURFACE'   3125    0    1    0    13    -1
                0
226             'PRESSURE'   1           'SURFACE'   3126    0    1    0    13    -1
                0
227             'PRESSURE'   1           'SURFACE'   3127    0    1    0    13    -1
                0
228             'PRESSURE'   1           'SURFACE'   3128    0    1    0    13    -1
                0
229             'PRESSURE'   1           'SURFACE'   3129    0    1    0    13    -1
                0
230             'PRESSURE'   1           'SURFACE'   3130    0    1    0    13    -1
                0
231             'PRESSURE'   1           'SURFACE'   3131    0    1    0    13    -1
                0
232             'PRESSURE'   1           'SURFACE'   3132    0    1    0    13    -1
                0
233             'PRESSURE'   1           'SURFACE'   3133    0    1    0    13    -1
                0
234             'PRESSURE'   1           'SURFACE'   3134    0    1    0    13    -1
                0
235             'PRESSURE'   1           'SURFACE'   3135    0    1    0    13    -1
                0
236             'PRESSURE'   1           'SURFACE'   3136    0    1    0    13    -1
                0
237             'PRESSURE'   1           'SURFACE'   3137    0    1    0    13    -1
                0
238             'PRESSURE'   1           'SURFACE'   3138    0    1    0    13    -1
                0
239             'PRESSURE'   1           'SURFACE'   3139    0    1    0    13    -1
                0
240             'PRESSURE'   1           'SURFACE'   3140    0    1    0    13    -1
                0
241             'PRESSURE'   1           'SURFACE'   3141    0    1    0    13    -1
                0
242             'PRESSURE'   1           'SURFACE'   3142    0    1    0    13    -1
                0
243             'PRESSURE'   1           'SURFACE'   3143    0    1    0    13    -1
                0
244             'PRESSURE'   1           'SURFACE'   3144    0    1    0    13    -1
                0
245             'PRESSURE'   1           'SURFACE'   3145    0    1    0    13    -1
                0
246             'PRESSURE'   1           'SURFACE'   3146    0    1    0    13    -1
                0
247             'PRESSURE'   1           'SURFACE'   3147    0    1    0    13    -1
                0
248             'PRESSURE'   1           'SURFACE'   3148    0    1    0    13    -1
                0
249             'PRESSURE'   1           'SURFACE'   3149    0    1    0    13    -1
                0
250             'PRESSURE'   1           'SURFACE'   3150    0    1    0    13    -1
                0
251             'PRESSURE'   1           'SURFACE'   3151    0    1    0    13    -1
                0
252             'PRESSURE'   1           'SURFACE'   3152    0    1    0    13    -1
                0

301   'PRESSURE'             2           'SURFACE'   1001    0    1    0    13    -1
                0
step 1 to
373   'PRESSURE'             2           'SURFACE'   1073    0    1    0    13    -1
                0

383   'PRESSURE'             2           'SURFACE'   1083    0    1    0    13    -1
                0
step 1 to
409   'PRESSURE'             2           'SURFACE'   1109    0    1    0    13    -1
                0


1001   'TEMPERATURE' 1  'SURFACE' 1001 0 1 1 0 -1 0 0 0  'NO' 0.00000000000000 0.00000000000000 1 0  'MID'
step 1 to
1136   'TEMPERATURE' 1  'SURFACE' 1136 0 1 1 0 -1 0 0 0  'NO' 0.00000000000000 0.00000000000000 1 0  'MID'

2001   'TEMPERATURE' 1  'SURFACE' 2001 0 1 1 0 -1 0 0 0  'NO' 0.00000000000000 0.00000000000000 1 0  'MID'
step 1 to
2148   'TEMPERATURE' 1  'SURFACE' 2148 0 1 1 0 -1 0 0 0  'NO' 0.00000000000000 0.00000000000000 1 0  'MID'

3001   'TEMPERATURE' 1  'SURFACE' 3001 0 1 1 0 -1 0 0 0  'NO' 0.00000000000000 0.00000000000000 1 0  'MID'
step 1 to
3152   'TEMPERATURE' 1  'SURFACE' 3152 0 1 1 0 -1 0 0 0  'NO' 0.00000000000000 0.00000000000000 1 0  'MID'

5001   'TEMPERATURE' 1  'SURFACE' 5001 0 1 1 0 -1 0 0 0  'NO' 0.00000000000000 0.00000000000000 1 0  'MID'
step 1 to
5100   'TEMPERATURE' 1  'SURFACE' 5100 0 1 1 0 -1 0 0 0  'NO' 0.00000000000000 0.00000000000000 1 0  'MID'

@
```

********** Master MPF **********

```
ANALYSIS MODAL-PARTICIPATION-FACTORS EXCITATI=GROUND-MOTION NMODES=20,
    STATIC=NO CORRECTI=NO FREQUENC=YES DUSIZE=0.00000000000000

MASTER ANALYSIS=MODAL-PARTICIPATION-FACTORS MODEX=EXECUTE IDOF=000000 CMASS=YES

ANALYSIS MODAL-PARTICIPATION-FACTORS EXCITATI=GROUND-MOTION NMODES=20 STATIC=NO CORRECTI=NO FREQUENC=YES

FREQUENCIES METHOD=LANCZOS-ITERATION NEIGEN=20 NMODE=0

PORTHOLE VOLUME=MINIMUM SAVEDEFAULT=NO DISPLACEMENTS=YES VELOCTIES=YES ACCELERATIONS=YES
```

********** Master Static **********

```
MASTER ANALYSIS=STATIC MODEX=EXECUTE TSTART=0.00000000000000 IDOF=0,
    OVALIZAT=NONE FLUIDPOT=AUTOMATIC CYCLICPA=1 IPOSIT=STOP,
    REACTION=YES INITIALS=NO FSINTERA=NO IRINT=DEFAULT CMASS=YES,
    SHELLNDO=AUTOMATIC AUTOMATI=OFF SOLVER=SPARSE,
    CONTACT-=CONSTRAINT-FUNCTION TRELEASE=0.00000000000000,
    RESTART-=NO FRACTURE=NO LOAD-CAS=NO LOAD-PEN=NO SINGULAR=YES,
    STIFFNES=0.0001000000000000000 MAP-OUTP=NONE MAP-FORM=NO,
    NODAL-DE='' POROUS-C=NO ADAPTIVE=0 ZOOM-LAB=1 AXIS-CYC=0,
    PERIODIC=NO VECTOR-S=GEOMETRY EPSI-FIR=NO STABILIZ=NO,
    STABFACT=1.00000000000000E-10 RESULTS=PORTHOLE FEFCORR=NO,
    BOLTSTEP=1 EXTEND-S=YES CONVERT-=NO DEGEN=YES TMC-MODE=NO,
    ENSIGHT-=NO IRSTEPS=1 INITIALT=NO TEMP-INT=NO ESINTERA=NO,
    OP2GEOM=NO INSITU-D=NO OP2ERCS=ELEMENT
```

A2 Element groups

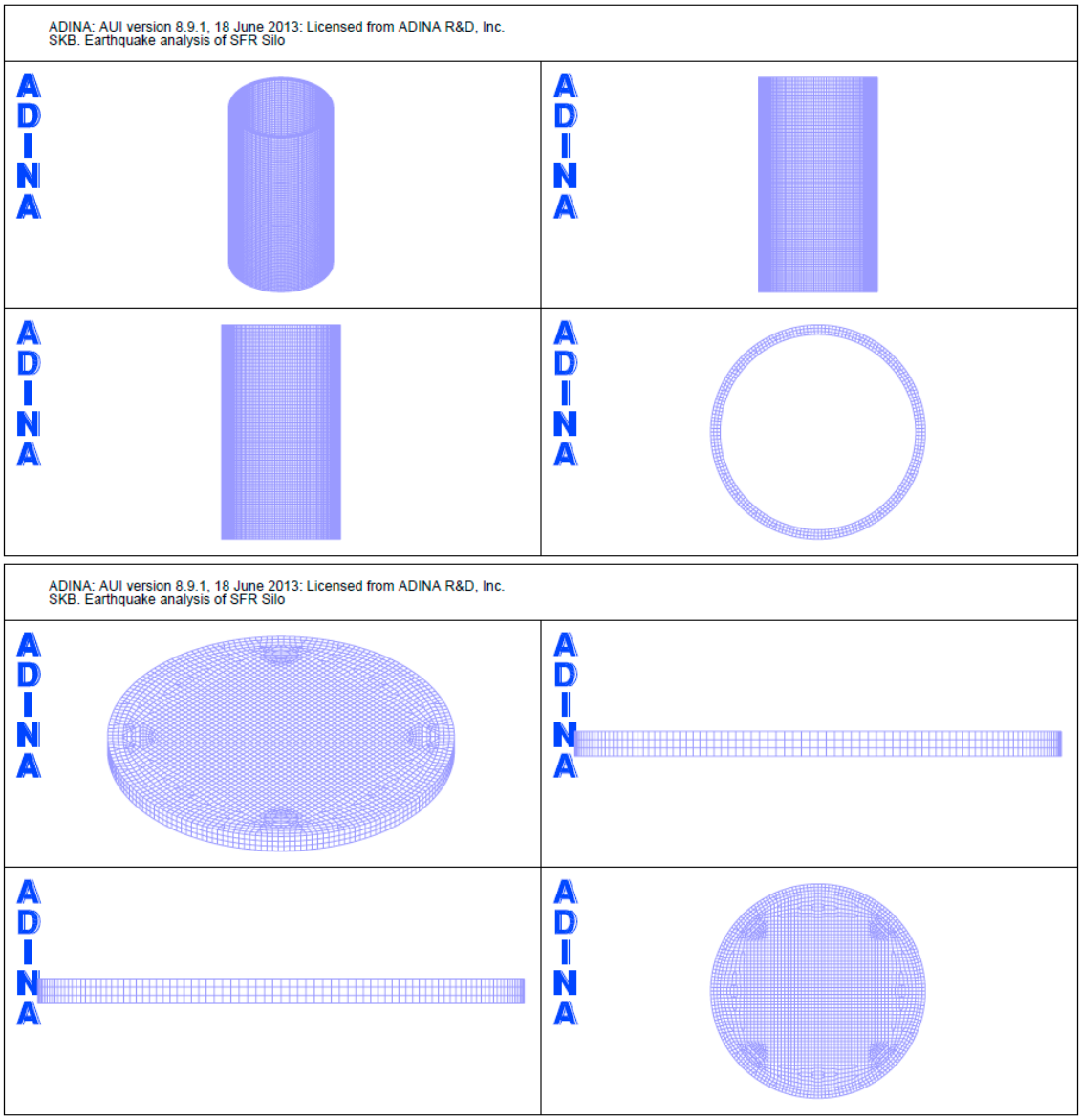

Figure A-1. *Elements groups 2 and 3.*

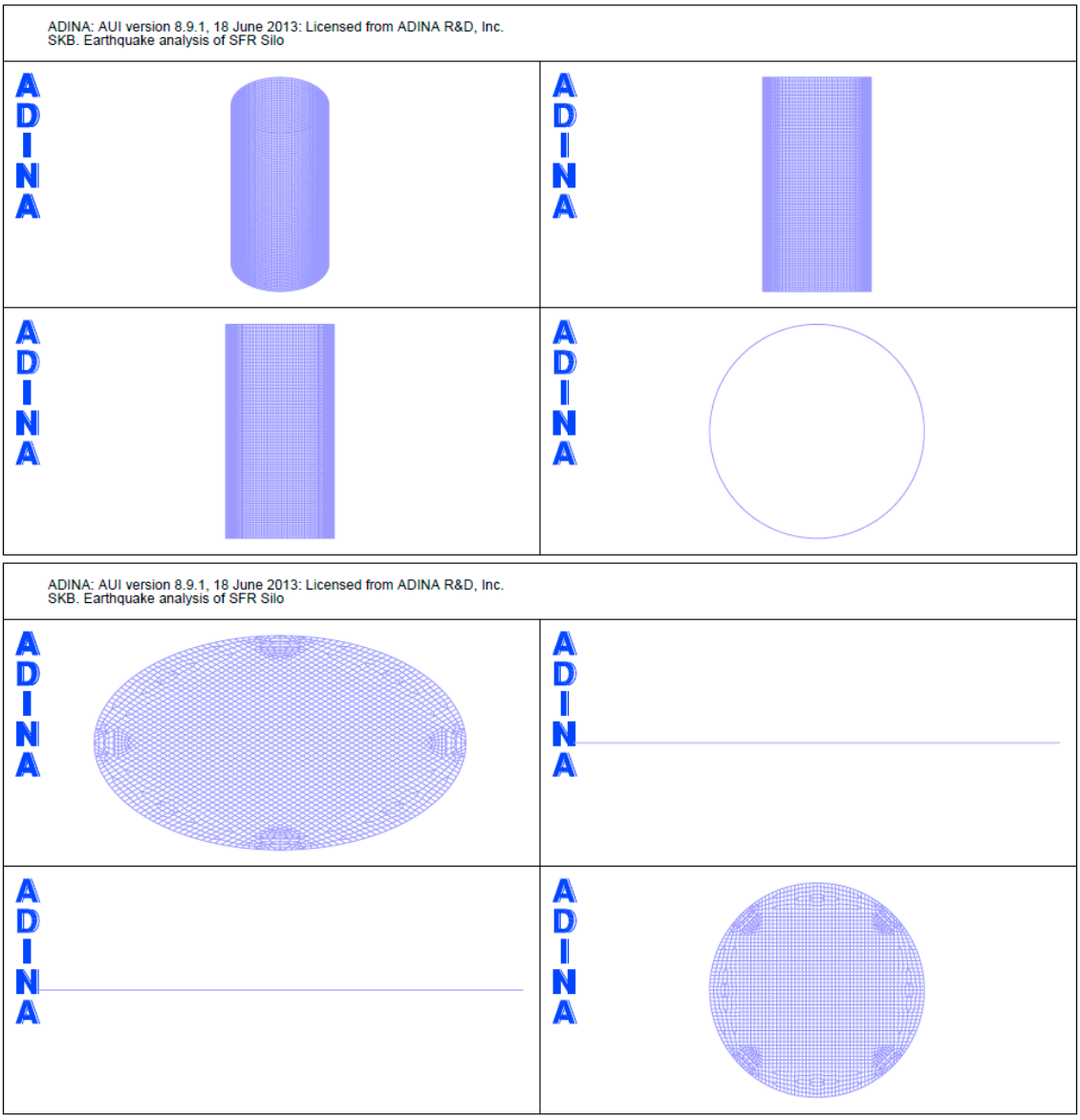

Figure A-2. *Elements groups 4 and 5.*

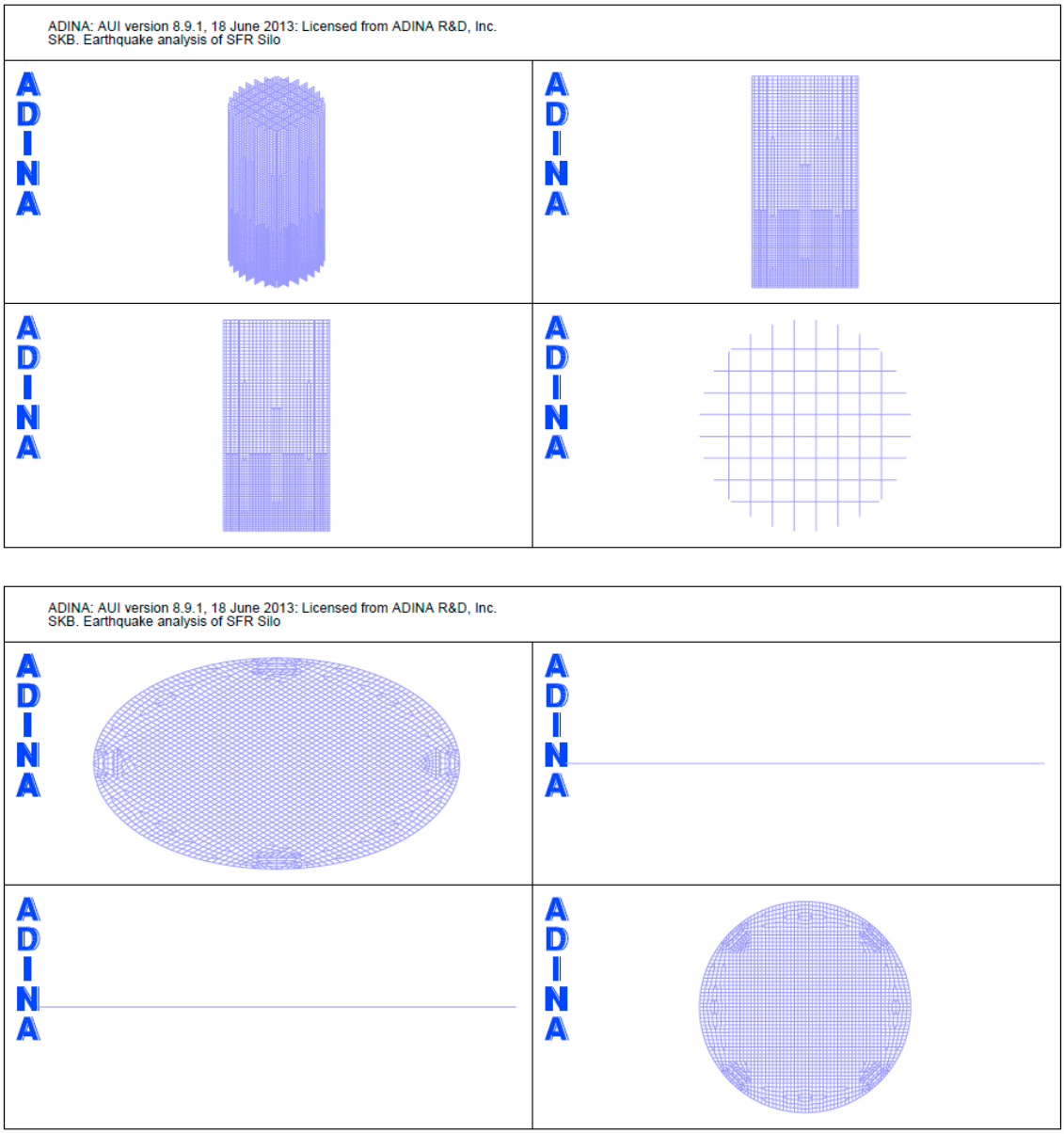

Figure A-3. *Elements groups 6 and 7.*

A3 Eigenmodes and mode participation factors

A3.1 Case 1 –simple model

MODE	FREQUENCY	ACCUM MODAL MASS(X)	ACCUM MODAL MASS(Y)	MASS(Z)
1	1.14130E+00	4.79850E+07	3.06578E+05	2.43381E-12
2	1.14130E+00	4.82916E+07	4.82916E+07	3.07685E-12
3	3.64596E+00	4.82916E+07	4.82916E+07	6.35583E+07
4	3.88253E+00	4.82916E+07	4.82916E+07	6.35583E+07
5	5.48243E+00	4.82916E+07	4.82916E+07	6.35583E+07
6	5.53427E+00	5.83770E+07	5.28783E+07	6.35583E+07
7	5.53427E+00	6.29637E+07	6.29637E+07	6.35583E+07
8	8.95147E+00	6.29637E+07	6.29637E+07	6.35583E+07
9	1.04194E+01	6.29638E+07	6.29710E+07	6.35583E+07
10	1.04194E+01	6.29711E+07	6.29711E+07	6.35583E+07
11	1.11189E+01	6.29711E+07	6.29711E+07	6.35583E+07
12	1.18189E+01	6.29711E+07	6.29711E+07	6.35583E+07
13	1.21980E+01	6.29711E+07	6.29711E+07	6.35583E+07
14	1.32578E+01	6.34075E+07	6.31948E+07	6.35583E+07
15	1.32578E+01	6.36312E+07	6.36312E+07	6.35583E+07
16	1.53265E+01	6.36316E+07	6.36334E+07	6.35583E+07
17	1.53265E+01	6.36338E+07	6.36338E+07	6.35583E+07
18	1.61723E+01	6.36338E+07	6.36338E+07	6.35583E+07
19	1.67383E+01	6.36338E+07	6.36338E+07	6.35583E+07
20	1.67697E+01	6.36338E+07	6.36338E+07	6.35583E+07

ADINA: AUI version 8.9.1, 4 June 2013: *** NO HEADING DEFINED ***
Licensed from ADINA R&D, Inc.
Listing of ground motion modal participation factor information:

MODE	FREQUENCY	ACCUM PERCENT MASS(X)	ACCUM PERCENT MASS(Y)	ACCUM PERCENT MASS(Z)
1	1.14130E+00	75.25163 %	0.48079 %	0.00000 %
2	1.14130E+00	75.73242 %	75.73242 %	0.00000 %
3	3.64596E+00	75.73242 %	75.73242 %	99.67407 %
4	3.88253E+00	75.73242 %	75.73242 %	99.67407 %
5	5.48243E+00	75.73242 %	75.73242 %	99.67407 %
6	5.53427E+00	91.54855 %	82.92543 %	99.67407 %
7	5.53427E+00	98.74156 %	98.74156 %	99.67407 %
8	8.95147E+00	98.74156 %	98.74156 %	99.67407 %
9	1.04194E+01	98.74173 %	98.75312 %	99.67407 %
10	1.04194E+01	98.75328 %	98.75328 %	99.67407 %
11	1.11189E+01	98.75328 %	98.75328 %	99.67407 %
12	1.18189E+01	98.75328 %	98.75328 %	99.67407 %
13	1.21980E+01	98.75328 %	98.75328 %	99.67407 %
14	1.32578E+01	99.43769 %	99.10406 %	99.67407 %
15	1.32578E+01	99.78847 %	99.78847 %	99.67407 %
16	1.53265E+01	99.78908 %	99.79191 %	99.67407 %
17	1.53265E+01	99.79252 %	99.79252 %	99.67407 %
18	1.61723E+01	99.79252 %	99.79252 %	99.67407 %
19	1.67383E+01	99.79252 %	99.79252 %	99.67407 %
20	1.67697E+01	99.79256 %	99.79256 %	99.67407 %

*** End of list.

A3.2 Case 1a – rigid casting joint

ADINA: AUI version 8.9.1, 4 June 2013: *** NO HEADING DEFINED ***
Licensed from ADINA R&D, Inc.
Listing of ground motion modal participation factor information:

MODE	FREQUENCY	MODAL PART FACTOR(X)	MODAL PART FACTOR(Y)	MODAL PART FACTOR(Z)
1	1.20590E+00	-5.16079E+03	-4.60669E+03	9.64795E-07
2	1.20590E+00	-4.60669E+03	5.16079E+03	2.15630E-06
3	2.76614E+00	6.06741E-05	7.86316E-05	3.68683E-04
4	4.74292E+00	1.04019E-05	4.37220E-04	-6.34523E-03
5	5.09450E+00	-3.27501E+03	-2.37694E+03	-3.56941E-05
6	5.09450E+00	-2.37694E+03	3.27501E+03	4.69654E-05
7	5.64745E+00	6.77280E-07	-3.28373E-05	7.94397E+03
8	8.69773E+00	-4.54229E-04	-4.70859E-04	1.25880E-04
9	1.02278E+01	-6.64721E+00	4.71556E+01	-8.08856E-04
10	1.02279E+01	4.71563E+01	6.64746E+00	9.03409E-04
11	1.03650E+01	5.30117E-03	-3.98549E-03	-1.58238E-03
12	1.15391E+01	2.43558E-05	-3.72847E-04	-1.00413E-04
13	1.17367E+01	-1.54214E-04	-6.14893E-05	2.58205E-04
14	1.28037E+01	-6.53193E+02	-4.10217E+02	2.69773E-05
15	1.28037E+01	-4.10217E+02	6.53193E+02	1.34988E-04
16	1.49248E+01	8.75264E+00	-2.11794E+01	-1.66416E-03
17	1.49248E+01	-2.11808E+01	-8.75262E+00	1.02987E-03
18	1.55659E+01	-6.38208E-04	-4.94318E-04	-2.20149E-04
19	1.61679E+01	-1.52061E-03	1.06163E-03	-2.37625E-03
20	1.66028E+01	-1.07691E+01	1.06828E+01	-7.26345E-04

ADINA: AUI version 8.9.1, 4 June 2013: *** NO HEADING DEFINED ***
Licensed from ADINA R&D, Inc.
Listing of ground motion modal participation factor information:

MODE	FREQUENCY	MODAL MASS(X)	MODAL MASS(Y)	MODAL MASS(Z)
1	1.20590E+00	2.66338E+07	2.12216E+07	9.30829E-13
2	1.20590E+00	2.12216E+07	2.66338E+07	4.64965E-12
3	2.76614E+00	3.68134E-09	6.18293E-09	1.35927E-07
4	4.74292E+00	1.08199E-10	1.91161E-07	4.02619E-05
5	5.09450E+00	1.07257E+07	5.64982E+06	1.27407E-09
6	5.09450E+00	5.64982E+06	1.07257E+07	2.20575E-09
7	5.64745E+00	4.58709E-13	1.07829E-09	6.31067E+07
8	8.69773E+00	2.06324E-07	2.21708E-07	1.58458E-08
9	1.02278E+01	4.41854E+01	2.22365E+03	6.54249E-07
10	1.02279E+01	2.22372E+03	4.41888E+01	8.16149E-07
11	1.03650E+01	2.81024E-05	1.58841E-05	2.50394E-06
12	1.15391E+01	5.93206E-10	1.39015E-07	1.00828E-08
13	1.17367E+01	2.37819E-08	3.78094E-09	6.66698E-08
14	1.28037E+01	4.26661E+05	1.68278E+05	7.27773E-10
15	1.28037E+01	1.68278E+05	4.26661E+05	1.82217E-08
16	1.49248E+01	7.66087E+01	4.48567E+02	2.76944E-06
17	1.49248E+01	4.48628E+02	7.66084E+01	1.06064E-06
18	1.55659E+01	4.07309E-07	2.44350E-07	4.84657E-08
19	1.61679E+01	2.31226E-06	1.12707E-06	5.64655E-06
20	1.66028E+01	1.15973E+02	1.14122E+02	5.27577E-07

ADINA: AUI version 8.9.1, 4 June 2013: *** NO HEADING DEFINED ***
Licensed from ADINA R&D, Inc.
Listing of ground motion modal participation factor information:

MODE	FREQUENCY	PERCENT MASS(X)	PERCENT MASS(Y)	PERCENT MASS(Z)
1	1.20590E+00	40.41287 %	32.20066 %	0.00000 %
2	1.20590E+00	32.20066 %	40.41287 %	0.00000 %
3	2.76614E+00	0.00000 %	0.00000 %	0.00000 %
4	4.74292E+00	0.00000 %	0.00000 %	0.00000 %
5	5.09450E+00	16.27470 %	8.57279 %	0.00000 %
6	5.09450E+00	8.57279 %	16.27470 %	0.00000 %
7	5.64745E+00	0.00000 %	0.00000 %	95.75527 %
8	8.69773E+00	0.00000 %	0.00000 %	0.00000 %
9	1.02278E+01	0.00007 %	0.00337 %	0.00000 %
10	1.02279E+01	0.00337 %	0.00007 %	0.00000 %
11	1.03650E+01	0.00000 %	0.00000 %	0.00000 %
12	1.15391E+01	0.00000 %	0.00000 %	0.00000 %
13	1.17367E+01	0.00000 %	0.00000 %	0.00000 %
14	1.28037E+01	0.64740 %	0.25534 %	0.00000 %
15	1.28037E+01	0.25534 %	0.64740 %	0.00000 %
16	1.49248E+01	0.00012 %	0.00068 %	0.00000 %
17	1.49248E+01	0.00068 %	0.00012 %	0.00000 %
18	1.55659E+01	0.00000 %	0.00000 %	0.00000 %
19	1.61679E+01	0.00000 %	0.00000 %	0.00000 %
20	1.66028E+01	0.00018 %	0.00017 %	0.00000 %

ADINA: AUI version 8.9.1, 4 June 2013: *** NO HEADING DEFINED ***
Licensed from ADINA R&D, Inc.
Listing of ground motion modal participation factor information:

MODE	FREQUENCY	ACCUM MODAL MASS(X)	ACCUM MODAL MASS(Y)	MASS(Z)
1	1.20590E+00	2.66338E+07	2.12216E+07	9.30829E-13
2	1.20590E+00	4.78553E+07	4.78553E+07	5.58048E-12
3	2.76614E+00	4.78553E+07	4.78553E+07	1.35933E-07
4	4.74292E+00	4.78553E+07	4.78553E+07	4.03979E-05
5	5.09450E+00	5.85810E+07	5.35052E+07	4.03991E-05
6	5.09450E+00	6.42309E+07	6.42309E+07	4.04014E-05
7	5.64745E+00	6.42309E+07	6.42309E+07	6.31067E+07
8	8.69773E+00	6.42309E+07	6.42309E+07	6.31067E+07
9	1.02278E+01	6.42309E+07	6.42331E+07	6.31067E+07
10	1.02279E+01	6.42331E+07	6.42331E+07	6.31067E+07
11	1.03650E+01	6.42331E+07	6.42331E+07	6.31067E+07
12	1.15391E+01	6.42331E+07	6.42331E+07	6.31067E+07
13	1.17367E+01	6.42331E+07	6.42331E+07	6.31067E+07
14	1.28037E+01	6.46598E+07	6.44014E+07	6.31067E+07
15	1.28037E+01	6.48281E+07	6.48281E+07	6.31067E+07
16	1.49248E+01	6.48281E+07	6.48285E+07	6.31067E+07
17	1.49248E+01	6.48286E+07	6.48286E+07	6.31067E+07
18	1.55659E+01	6.48286E+07	6.48286E+07	6.31067E+07
19	1.61679E+01	6.48286E+07	6.48286E+07	6.31067E+07
20	1.66028E+01	6.48287E+07	6.48287E+07	6.31067E+07

ADINA: AUI version 8.9.1, 4 June 2013: *** NO HEADING DEFINED ***
Licensed from ADINA R&D, Inc.
Listing of ground motion modal participation factor information:

MODE	FREQUENCY	ACCUM PERCENT MASS(X)	ACCUM PERCENT MASS(Y)	ACCUM PERCENT MASS(Z)
1	1.20590E+00	40.41287 %	32.20066 %	0.00000 %
2	1.20590E+00	72.61353 %	72.61353 %	0.00000 %
3	2.76614E+00	72.61353 %	72.61353 %	0.00000 %
4	4.74292E+00	72.61353 %	72.61353 %	0.00000 %
5	5.09450E+00	88.88824 %	81.18632 %	0.00000 %
6	5.09450E+00	97.46103 %	97.46103 %	0.00000 %
7	5.64745E+00	97.46103 %	97.46103 %	95.75527 %
8	8.69773E+00	97.46103 %	97.46103 %	95.75527 %
9	1.02278E+01	97.46109 %	97.46440 %	95.75527 %
10	1.02279E+01	97.46447 %	97.46447 %	95.75527 %
11	1.03650E+01	97.46447 %	97.46447 %	95.75527 %
12	1.15391E+01	97.46447 %	97.46447 %	95.75527 %
13	1.17367E+01	97.46447 %	97.46447 %	95.75527 %
14	1.28037E+01	98.11186 %	97.71980 %	95.75527 %
15	1.28037E+01	98.36720 %	98.36720 %	95.75527 %
16	1.49248E+01	98.36732 %	98.36788 %	95.75527 %
17	1.49248E+01	98.36800 %	98.36800 %	95.75527 %
18	1.55659E+01	98.36800 %	98.36800 %	95.75527 %
19	1.61679E+01	98.36800 %	98.36800 %	95.75527 %
20	1.66028E+01	98.36817 %	98.36817 %	95.75527 %

*** End of list.

.

A3.3 Case 1b – hinged casting joint

ADINA: AUI version 8.9.1, 4 June 2013: *** NO HEADING DEFINED ***
Licensed from ADINA R&D, Inc.
Listing of ground motion modal participation factor information:

MODE	FREQUENCY	MODAL PART FACTOR(X)	MODAL PART FACTOR(Y)	MODAL PART FACTOR(Z)
1	1.20474E+00	-5.14139E+03	-4.62570E+03	9.45196E-07
2	1.20474E+00	-4.62570E+03	5.14139E+03	2.15714E-06
3	2.76613E+00	6.06409E-05	7.85667E-05	3.86992E-04
4	4.74185E+00	1.26348E-05	4.38078E-04	-6.38639E-03
5	5.09054E+00	-3.26062E+03	-2.40191E+03	-3.58422E-05
6	5.09054E+00	-2.40191E+03	3.26062E+03	4.69204E-05
7	5.64207E+00	8.29472E-07	-3.29057E-05	7.94390E+03
8	8.69366E+00	-4.51115E-04	-4.67932E-04	1.26818E-04
9	1.02253E+01	-6.56688E+00	4.67081E+01	-8.05826E-04
10	1.02253E+01	4.67089E+01	6.56713E+00	9.00760E-04
11	1.03572E+01	5.43129E-03	-4.08795E-03	-1.57167E-03
12	1.15353E+01	-2.06452E-05	3.75051E-04	8.10824E-05
13	1.17334E+01	-1.53006E-04	-6.17040E-05	2.57866E-04
14	1.28013E+01	-6.50676E+02	-4.12568E+02	2.63393E-05
15	1.28013E+01	-4.12568E+02	6.50676E+02	1.34852E-04
16	1.49167E+01	8.44456E+00	-2.04454E+01	-1.65880E-03
17	1.49167E+01	-2.04469E+01	-8.44454E+00	1.02715E-03
18	1.55602E+01	-6.19020E-04	-4.80853E-04	-2.30286E-04
19	1.61496E+01	-1.48920E-03	1.03612E-03	-2.36387E-03
20	1.65994E+01	9.04369E-03	8.63999E-03	9.65516E-04

ADINA: AUI version 8.9.1, 4 June 2013: *** NO HEADING DEFINED ***
Licensed from ADINA R&D, Inc.
Listing of ground motion modal participation factor information:

MODE	FREQUENCY	MODAL MASS(X)	MODAL MASS(Y)	MODAL MASS(Z)
1	1.20474E+00	2.64339E+07	2.13971E+07	8.93395E-13
2	1.20474E+00	2.13971E+07	2.64339E+07	4.65325E-12
3	2.76613E+00	3.67732E-09	6.17273E-09	1.49763E-07
4	4.74185E+00	1.59639E-10	1.91912E-07	4.07860E-05
5	5.09054E+00	1.06317E+07	5.76917E+06	1.28467E-09
6	5.09054E+00	5.76917E+06	1.06317E+07	2.20152E-09
7	5.64207E+00	6.88024E-13	1.08278E-09	6.31055E+07
8	8.69366E+00	2.03505E-07	2.18961E-07	1.60828E-08
9	1.02253E+01	4.31239E+01	2.18165E+03	6.49355E-07
10	1.02253E+01	2.18172E+03	4.31272E+01	8.11369E-07
11	1.03572E+01	2.94989E-05	1.67113E-05	2.47014E-06
12	1.15353E+01	4.26223E-10	1.40663E-07	6.57436E-09
13	1.17334E+01	2.34107E-08	3.80739E-09	6.64946E-08
14	1.28013E+01	4.23379E+05	1.70212E+05	6.93760E-10
15	1.28013E+01	1.70212E+05	4.23379E+05	1.81850E-08
16	1.49167E+01	7.13106E+01	4.18015E+02	2.75163E-06
17	1.49167E+01	4.18074E+02	7.13103E+01	1.05504E-06
18	1.55602E+01	3.83185E-07	2.31220E-07	5.30316E-08
19	1.61496E+01	2.21770E-06	1.07354E-06	5.58787E-06
20	1.65994E+01	8.17884E-05	7.46495E-05	9.32221E-07

ADINA: AUI version 8.9.1, 4 June 2013: *** NO HEADING DEFINED ***
Licensed from ADINA R&D, Inc.
Listing of ground motion modal participation factor information:

MODE	FREQUENCY	PERCENT MASS(X)	PERCENT MASS(Y)	PERCENT MASS(Z)
1	1.20474E+00	40.10968 %	32.46700 %	0.00000 %
2	1.20474E+00	32.46700 %	40.10968 %	0.00000 %
3	2.76613E+00	0.00000 %	0.00000 %	0.00000 %
4	4.74185E+00	0.00000 %	0.00000 %	0.00000 %
5	5.09054E+00	16.13203 %	8.75388 %	0.00000 %
6	5.09054E+00	8.75388 %	16.13203 %	0.00000 %
7	5.64207E+00	0.00000 %	0.00000 %	95.75348 %
8	8.69366E+00	0.00000 %	0.00000 %	0.00000 %
9	1.02253E+01	0.00007 %	0.00331 %	0.00000 %
10	1.02253E+01	0.00331 %	0.00007 %	0.00000 %
11	1.03572E+01	0.00000 %	0.00000 %	0.00000 %
12	1.15353E+01	0.00000 %	0.00000 %	0.00000 %
13	1.17334E+01	0.00000 %	0.00000 %	0.00000 %
14	1.28013E+01	0.64242 %	0.25827 %	0.00000 %
15	1.28013E+01	0.25827 %	0.64242 %	0.00000 %
16	1.49167E+01	0.00011 %	0.00063 %	0.00000 %
17	1.49167E+01	0.00063 %	0.00011 %	0.00000 %
18	1.55602E+01	0.00000 %	0.00000 %	0.00000 %
19	1.61496E+01	0.00000 %	0.00000 %	0.00000 %
20	1.65994E+01	0.00000 %	0.00000 %	0.00000 %

ADINA: AUI version 8.9.1, 4 June 2013: *** NO HEADING DEFINED ***
Licensed from ADINA R&D, Inc.
Listing of ground motion modal participation factor information:

		ACCUM	ACCUM	ACCUM

MODE	MODAL FREQUENCY	MODAL MASS(X)	MODAL MASS(Y)	MASS(Z)
1	1.20474E+00	2.64339E+07	2.13971E+07	8.93395E-13
2	1.20474E+00	4.78310E+07	4.78310E+07	5.54665E-12
3	2.76613E+00	4.78310E+07	4.78310E+07	1.49768E-07
4	4.74185E+00	4.78310E+07	4.78310E+07	4.09357E-05
5	5.09054E+00	5.84627E+07	5.36002E+07	4.09370E-05
6	5.09054E+00	6.42319E+07	6.42319E+07	4.09392E-05
7	5.64207E+00	6.42319E+07	6.42319E+07	6.31055E+07
8	8.69366E+00	6.42319E+07	6.42319E+07	6.31055E+07
9	1.02253E+01	6.42319E+07	6.42341E+07	6.31055E+07
10	1.02253E+01	6.42341E+07	6.42341E+07	6.31055E+07
11	1.03572E+01	6.42341E+07	6.42341E+07	6.31055E+07
12	1.15353E+01	6.42341E+07	6.42341E+07	6.31055E+07
13	1.17334E+01	6.42341E+07	6.42341E+07	6.31055E+07
14	1.28013E+01	6.46575E+07	6.44043E+07	6.31055E+07
15	1.28013E+01	6.48277E+07	6.48277E+07	6.31055E+07
16	1.49167E+01	6.48278E+07	6.48281E+07	6.31055E+07
17	1.49167E+01	6.48282E+07	6.48282E+07	6.31055E+07
18	1.55602E+01	6.48282E+07	6.48282E+07	6.31055E+07
19	1.61496E+01	6.48282E+07	6.48282E+07	6.31055E+07
20	1.65994E+01	6.48282E+07	6.48282E+07	6.31055E+07

ADINA: AUI version 8.9.1, 4 June 2013: *** NO HEADING DEFINED ***
Licensed from ADINA R&D, Inc.
Listing of ground motion modal participation factor information:

MODE	FREQUENCY	ACCUM PERCENT MASS(X)	ACCUM PERCENT MASS(Y)	ACCUM PERCENT MASS(Z)
1	1.20474E+00	40.10968 %	32.46700 %	0.00000 %
2	1.20474E+00	72.57668 %	72.57668 %	0.00000 %
3	2.76613E+00	72.57668 %	72.57668 %	0.00000 %
4	4.74185E+00	72.57668 %	72.57668 %	0.00000 %
5	5.09054E+00	88.70870 %	81.33056 %	0.00000 %
6	5.09054E+00	97.46258 %	97.46258 %	0.00000 %
7	5.64207E+00	97.46258 %	97.46258 %	95.75348 %
8	8.69366E+00	97.46258 %	97.46258 %	95.75348 %
9	1.02253E+01	97.46265 %	97.46589 %	95.75348 %
10	1.02253E+01	97.46596 %	97.46596 %	95.75348 %
11	1.03572E+01	97.46596 %	97.46596 %	95.75348 %
12	1.15353E+01	97.46596 %	97.46596 %	95.75348 %
13	1.17334E+01	97.46596 %	97.46596 %	95.75348 %
14	1.28013E+01	98.10838 %	97.72423 %	95.75348 %
15	1.28013E+01	98.36665 %	98.36665 %	95.75348 %
16	1.49167E+01	98.36676 %	98.36728 %	95.75348 %
17	1.49167E+01	98.36739 %	98.36739 %	95.75348 %
18	1.55602E+01	98.36739 %	98.36739 %	95.75348 %
19	1.61496E+01	98.36739 %	98.36739 %	95.75348 %
20	1.65994E+01	98.36739 %	98.36739 %	95.75348 %

*** End of list.

A3.4 Case 2a – rigid casting joint

ADINA: AUI version 8.9.1, 4 June 2013: *** NO HEADING DEFINED ***
Licensed from ADINA R&D, Inc.
Listing of ground motion modal participation factor information:

MODE	FREQUENCY	MODAL PART FACTOR(X)	MODAL PART FACTOR(Y)	MODAL PART FACTOR(Z)
1	2.87607E+00	5.31060E+03	-4.42537E+03	4.89748E-05
2	2.87607E+00	4.42537E+03	5.31060E+03	-1.55234E-05
3	3.76136E+00	4.55660E-04	6.98447E-04	4.40356E-04
4	5.68163E+00	-3.65420E+03	-1.75071E+03	-4.90808E-05
5	5.68163E+00	-1.75071E+03	3.65420E+03	4.30297E-04
6	5.71127E+00	-1.10322E-02	9.32116E-03	-2.62093E-02
7	5.94390E+00	3.37990E-05	-1.62975E-04	7.94350E+03
8	9.29830E+00	1.01557E-03	8.58740E-04	-9.98668E-05
9	1.05483E+01	-1.33858E+01	1.71450E+02	-9.08063E-04
10	1.05483E+01	1.71451E+02	1.33847E+01	1.14059E-03
11	1.08290E+01	8.62188E-03	-6.54632E-03	-1.92978E-03
12	1.17325E+01	-1.05391E-03	-5.47571E-04	1.29938E-04
13	1.19904E+01	3.88901E-04	-5.69814E-05	-3.19142E-04
14	1.30187E+01	-6.58906E+02	-3.98297E+02	4.13223E-05
15	1.30187E+01	3.98297E+02	-6.58906E+02	-1.82267E-04
16	1.51443E+01	-8.65899E+00	2.21417E+01	1.88235E-03
17	1.51443E+01	-2.21432E+01	-8.65959E+00	1.21281E-03
18	1.58850E+01	-1.76521E-04	-4.17958E-05	-2.19843E-04
19	1.64427E+01	9.62813E-04	-7.30660E-04	2.64401E-03
20	1.67875E+01	2.23361E-04	-6.70069E-04	1.28104E-03

ADINA: AUI version 8.9.1, 4 June 2013: *** NO HEADING DEFINED ***
Licensed from ADINA R&D, Inc.
Listing of ground motion modal participation factor information:

MODE	FREQUENCY	MODAL MASS(X)	MODAL MASS(Y)	MODAL MASS(Z)
1	2.87607E+00	2.82025E+07	1.95839E+07	2.39853E-09
2	2.87607E+00	1.95839E+07	2.82025E+07	2.40975E-10
3	3.76136E+00	2.07626E-07	4.87828E-07	1.93913E-07
4	5.68163E+00	1.33532E+07	3.06498E+06	2.40893E-09
5	5.68163E+00	3.06498E+06	1.33532E+07	1.85156E-07
6	5.71127E+00	1.21710E-04	8.68840E-05	6.86928E-04
7	5.94390E+00	1.14238E-09	2.65610E-08	6.30992E+07
8	9.29830E+00	1.03138E-06	7.37435E-07	9.97338E-09
9	1.05483E+01	1.79178E+02	2.93952E+04	8.24578E-07
10	1.05483E+01	2.93954E+04	1.79151E+02	1.30094E-06
11	1.08290E+01	7.43368E-05	4.28543E-05	3.72404E-06
12	1.17325E+01	1.11073E-06	2.99834E-07	1.68838E-08
13	1.19904E+01	1.51244E-07	3.24688E-09	1.01852E-07
14	1.30187E+01	4.34157E+05	1.58640E+05	1.70754E-09
15	1.30187E+01	1.58640E+05	4.34157E+05	3.32214E-08
16	1.51443E+01	7.49782E+01	4.90256E+02	3.54325E-06
17	1.51443E+01	4.90322E+02	7.49884E+01	1.47091E-06
18	1.58850E+01	3.11597E-08	1.74689E-09	4.83310E-08
19	1.64427E+01	9.27010E-07	5.33864E-07	6.99080E-06
20	1.67875E+01	4.98902E-08	4.48993E-07	1.64106E-06

ADINA: AUI version 8.9.1, 4 June 2013: *** NO HEADING DEFINED ***
Licensed from ADINA R&D, Inc.
Listing of ground motion modal participation factor information:

MODE	FREQUENCY	PERCENT MASS(X)	PERCENT MASS(Y)	PERCENT MASS(Z)
1	2.87607E+00	42.79258 %	29.71529 %	0.00000 %
2	2.87607E+00	29.71529 %	42.79258 %	0.00000 %
3	3.76136E+00	0.00000 %	0.00000 %	0.00000 %
4	5.68163E+00	20.26119 %	4.65059 %	0.00000 %
5	5.68163E+00	4.65059 %	20.26119 %	0.00000 %
6	5.71127E+00	0.00000 %	0.00000 %	0.00000 %
7	5.94390E+00	0.00000 %	0.00000 %	95.74250 %
8	9.29830E+00	0.00000 %	0.00000 %	0.00000 %
9	1.05483E+01	0.00027 %	0.04460 %	0.00000 %
10	1.05483E+01	0.04460 %	0.00027 %	0.00000 %
11	1.08290E+01	0.00000 %	0.00000 %	0.00000 %
12	1.17325E+01	0.00000 %	0.00000 %	0.00000 %
13	1.19904E+01	0.00000 %	0.00000 %	0.00000 %
14	1.30187E+01	0.65876 %	0.24071 %	0.00000 %
15	1.30187E+01	0.24071 %	0.65876 %	0.00000 %
16	1.51443E+01	0.00011 %	0.00074 %	0.00000 %
17	1.51443E+01	0.00074 %	0.00011 %	0.00000 %
18	1.58850E+01	0.00000 %	0.00000 %	0.00000 %
19	1.64427E+01	0.00000 %	0.00000 %	0.00000 %
20	1.67875E+01	0.00000 %	0.00000 %	0.00000 %

ADINA: AUI version 8.9.1, 4 June 2013: *** NO HEADING DEFINED ***
Licensed from ADINA R&D, Inc.
Listing of ground motion modal participation factor information:

MODE	FREQUENCY	ACCUM MODAL MASS(X)	ACCUM MODAL MASS(Y)	ACCUM MODAL MASS(Z)

1	2.87607E+00	2.82025E+07	1.95839E+07	2.39853E-09
2	2.87607E+00	4.77864E+07	4.77864E+07	2.63950E-09
3	3.76136E+00	4.77864E+07	4.77864E+07	1.96553E-07
4	5.68163E+00	6.11396E+07	5.08514E+07	1.98962E-07
5	5.68163E+00	6.42046E+07	6.42046E+07	3.84117E-07
6	5.71127E+00	6.42046E+07	6.42046E+07	6.87312E-04
7	5.94390E+00	6.42046E+07	6.42046E+07	6.30992E+07
8	9.29830E+00	6.42046E+07	6.42046E+07	6.30992E+07
9	1.05483E+01	6.42047E+07	6.42340E+07	6.30992E+07
10	1.05483E+01	6.42341E+07	6.42341E+07	6.30992E+07
11	1.08290E+01	6.42341E+07	6.42341E+07	6.30992E+07
12	1.17325E+01	6.42341E+07	6.42341E+07	6.30992E+07
13	1.19904E+01	6.42341E+07	6.42341E+07	6.30992E+07
14	1.30187E+01	6.46683E+07	6.43928E+07	6.30992E+07
15	1.30187E+01	6.48269E+07	6.48269E+07	6.30992E+07
16	1.51443E+01	6.48270E+07	6.48274E+07	6.30992E+07
17	1.51443E+01	6.48275E+07	6.48275E+07	6.30992E+07
18	1.58850E+01	6.48275E+07	6.48275E+07	6.30992E+07
19	1.64427E+01	6.48275E+07	6.48275E+07	6.30992E+07
20	1.67875E+01	6.48275E+07	6.48275E+07	6.30992E+07

ADINA: AUI version 8.9.1, 4 June 2013: *** NO HEADING DEFINED ***
Licensed from ADINA R&D, Inc.
Listing of ground motion modal participation factor information:

MODE	FREQUENCY	ACCUM PERCENT MASS(X)	ACCUM PERCENT MASS(Y)	ACCUM PERCENT MASS(Z)
1	2.87607E+00	42.79258 %	29.71529 %	0.00000 %
2	2.87607E+00	72.50787 %	72.50787 %	0.00000 %
3	3.76136E+00	72.50787 %	72.50787 %	0.00000 %
4	5.68163E+00	92.76906 %	77.15845 %	0.00000 %
5	5.68163E+00	97.41965 %	97.41965 %	0.00000 %
6	5.71127E+00	97.41965 %	97.41965 %	0.00000 %
7	5.94390E+00	97.41965 %	97.41965 %	95.74250 %
8	9.29830E+00	97.41965 %	97.41965 %	95.74250 %
9	1.05483E+01	97.41992 %	97.46425 %	95.74250 %
10	1.05483E+01	97.46452 %	97.46452 %	95.74250 %
11	1.08290E+01	97.46452 %	97.46452 %	95.74250 %
12	1.17325E+01	97.46452 %	97.46452 %	95.74250 %
13	1.19904E+01	97.46452 %	97.46452 %	95.74250 %
14	1.30187E+01	98.12328 %	97.70523 %	95.74250 %
15	1.30187E+01	98.36399 %	98.36399 %	95.74250 %
16	1.51443E+01	98.36410 %	98.36473 %	95.74250 %
17	1.51443E+01	98.36485 %	98.36485 %	95.74250 %
18	1.58850E+01	98.36485 %	98.36485 %	95.74250 %
19	1.64427E+01	98.36485 %	98.36485 %	95.74250 %
20	1.67875E+01	98.36485 %	98.36485 %	95.74250 %

*** End of list.

.

A3.5 Case 2b – hinged casting joint

ADINA: AUI version 8.9.1, 4 June 2013: *** NO HEADING DEFINED ***
Licensed from ADINA R&D, Inc.
Listing of ground motion modal participation factor information:

MODE	FREQUENCY	MODAL PART FACTOR(X)	MODAL PART FACTOR(Y)	MODAL PART FACTOR(Z)
1	2.87558E+00	5.31021E+03	-4.42325E+03	4.89934E-05
2	2.87558E+00	4.42325E+03	5.31021E+03	-1.55292E-05
3	3.76134E+00	4.55614E-04	6.98308E-04	4.63685E-04
4	5.67870E+00	-3.61470E+03	-1.83734E+03	-5.91177E-05
5	5.67870E+00	-1.83734E+03	3.61470E+03	4.31639E-04
6	5.71040E+00	-1.02723E-02	8.67740E-03	-2.66961E-02
7	5.93903E+00	3.45229E-05	-1.64337E-04	7.94343E+03
8	9.29466E+00	1.01082E-03	8.54574E-04	-1.02440E-04
9	1.05458E+01	-1.32775E+01	1.71112E+02	-9.04959E-04
10	1.05458E+01	1.71112E+02	1.32765E+01	1.13786E-03
11	1.08218E+01	8.72445E-03	-6.62723E-03	-1.92013E-03
12	1.17288E+01	1.05130E-03	5.46356E-04	-1.10815E-04
13	1.19872E+01	3.87583E-04	-5.67511E-05	-3.18834E-04
14	1.30167E+01	-6.56486E+02	-4.00915E+02	4.03671E-05
15	1.30167E+01	4.00915E+02	-6.56486E+02	-1.82024E-04
16	1.51365E+01	8.41234E+00	-2.15252E+01	-1.87700E-03
17	1.51365E+01	-2.15267E+01	-8.41293E+00	1.21008E-03
18	1.58796E+01	1.64641E-04	3.43888E-05	2.29944E-04
19	1.64254E+01	-9.54698E-04	7.22241E-04	-2.63281E-03
20	1.67788E+01	-2.93839E-04	6.30403E-04	-1.27065E-03

ADINA: AUI version 8.9.1, 4 June 2013: *** NO HEADING DEFINED ***
Licensed from ADINA R&D, Inc.
Listing of ground motion modal participation factor information:

MODE	FREQUENCY	MODAL MASS(X)	MODAL MASS(Y)	MODAL MASS(Z)
1	2.87558E+00	2.81984E+07	1.95652E+07	2.40036E-09
2	2.87558E+00	1.95652E+07	2.81984E+07	2.41155E-10
3	3.76134E+00	2.07584E-07	4.87634E-07	2.15003E-07
4	5.67870E+00	1.30661E+07	3.37583E+06	3.49490E-09
5	5.67870E+00	3.37583E+06	1.30661E+07	1.86313E-07
6	5.71040E+00	1.05521E-04	7.52973E-05	7.12682E-04
7	5.93903E+00	1.19183E-09	2.70067E-08	6.30980E+07
8	9.29466E+00	1.02176E-06	7.30297E-07	1.04939E-08
9	1.05458E+01	1.76291E+02	2.92792E+04	8.18951E-07
10	1.05458E+01	2.92793E+04	1.76264E+02	1.29473E-06
11	1.08218E+01	7.61160E-05	4.39202E-05	3.68689E-06
12	1.17288E+01	1.10522E-06	2.98505E-07	1.22800E-08
13	1.19872E+01	1.50221E-07	3.22068E-09	1.01655E-07
14	1.30167E+01	4.30974E+05	1.60733E+05	1.62950E-09
15	1.30167E+01	1.60733E+05	4.30974E+05	3.31328E-08
16	1.51365E+01	7.07674E+01	4.63335E+02	3.52312E-06
17	1.51365E+01	4.63400E+02	7.07773E+01	1.46429E-06
18	1.58796E+01	2.71068E-08	1.18259E-09	5.28743E-08
19	1.64254E+01	9.11448E-07	5.21632E-07	6.93170E-06
20	1.67788E+01	8.63412E-08	3.97408E-07	1.61456E-06

ADINA: AUI version 8.9.1, 4 June 2013: *** NO HEADING DEFINED ***
Licensed from ADINA R&D, Inc.
Listing of ground motion modal participation factor information:

MODE	FREQUENCY	PERCENT MASS(X)	PERCENT MASS(Y)	PERCENT MASS(Z)
1	2.87558E+00	42.78627 %	29.68687 %	0.00000 %
2	2.87558E+00	29.68687 %	42.78627 %	0.00000 %
3	3.76134E+00	0.00000 %	0.00000 %	0.00000 %
4	5.67870E+00	19.82556 %	5.12225 %	0.00000 %
5	5.67870E+00	5.12225 %	19.82556 %	0.00000 %
6	5.71040E+00	0.00000 %	0.00000 %	0.00000 %
7	5.93903E+00	0.00000 %	0.00000 %	95.74070 %
8	9.29466E+00	0.00000 %	0.00000 %	0.00000 %
9	1.05458E+01	0.00027 %	0.04443 %	0.00000 %
10	1.05458E+01	0.04443 %	0.00027 %	0.00000 %
11	1.08218E+01	0.00000 %	0.00000 %	0.00000 %
12	1.17288E+01	0.00000 %	0.00000 %	0.00000 %
13	1.19872E+01	0.00000 %	0.00000 %	0.00000 %
14	1.30167E+01	0.65393 %	0.24389 %	0.00000 %
15	1.30167E+01	0.24389 %	0.65393 %	0.00000 %
16	1.51365E+01	0.00011 %	0.00070 %	0.00000 %
17	1.51365E+01	0.00070 %	0.00011 %	0.00000 %
18	1.58796E+01	0.00000 %	0.00000 %	0.00000 %
19	1.64254E+01	0.00000 %	0.00000 %	0.00000 %
20	1.67788E+01	0.00000 %	0.00000 %	0.00000 %

ADINA: AUI version 8.9.1, 4 June 2013: *** NO HEADING DEFINED ***
Licensed from ADINA R&D, Inc.
Listing of ground motion modal participation factor information:

MODE	FREQUENCY	ACCUM MODAL MASS(X)	ACCUM MODAL MASS(Y)	ACCUM MODAL MASS(Z)

1	2.87558E+00	2.81984E+07	1.95652E+07	2.40036E-09
2	2.87558E+00	4.77635E+07	4.77635E+07	2.64151E-09
3	3.76134E+00	4.77635E+07	4.77635E+07	2.17645E-07
4	5.67870E+00	6.08296E+07	5.11394E+07	2.21140E-07
5	5.67870E+00	6.42054E+07	6.42054E+07	4.07452E-07
6	5.71040E+00	6.42054E+07	6.42054E+07	7.13089E-04
7	5.93903E+00	6.42054E+07	6.42054E+07	6.30980E+07
8	9.29466E+00	6.42054E+07	6.42054E+07	6.30980E+07
9	1.05458E+01	6.42056E+07	6.42347E+07	6.30980E+07
10	1.05458E+01	6.42349E+07	6.42349E+07	6.30980E+07
11	1.08218E+01	6.42349E+07	6.42349E+07	6.30980E+07
12	1.17288E+01	6.42349E+07	6.42349E+07	6.30980E+07
13	1.19872E+01	6.42349E+07	6.42349E+07	6.30980E+07
14	1.30167E+01	6.46658E+07	6.43956E+07	6.30980E+07
15	1.30167E+01	6.48266E+07	6.48266E+07	6.30980E+07
16	1.51365E+01	6.48267E+07	6.48270E+07	6.30980E+07
17	1.51365E+01	6.48271E+07	6.48271E+07	6.30980E+07
18	1.58796E+01	6.48271E+07	6.48271E+07	6.30980E+07
19	1.64254E+01	6.48271E+07	6.48271E+07	6.30980E+07
20	1.67788E+01	6.48271E+07	6.48271E+07	6.30980E+07

ADINA: AUI version 8.9.1, 4 June 2013: *** NO HEADING DEFINED ***
Licensed from ADINA R&D, Inc.
Listing of ground motion modal participation factor information:

MODE	FREQUENCY	ACCUM PERCENT MASS(X)	ACCUM PERCENT MASS(Y)	ACCUM PERCENT MASS(Z)
1	2.87558E+00	42.78627 %	29.68687 %	0.00000 %
2	2.87558E+00	72.47314 %	72.47314 %	0.00000 %
3	3.76134E+00	72.47314 %	72.47314 %	0.00000 %
4	5.67870E+00	92.29870 %	77.59540 %	0.00000 %
5	5.67870E+00	97.42095 %	97.42095 %	0.00000 %
6	5.71040E+00	97.42095 %	97.42095 %	0.00000 %
7	5.93903E+00	97.42095 %	97.42095 %	95.74070 %
8	9.29466E+00	97.42095 %	97.42095 %	95.74070 %
9	1.05458E+01	97.42122 %	97.46538 %	95.74070 %
10	1.05458E+01	97.46565 %	97.46565 %	95.74070 %
11	1.08218E+01	97.46565 %	97.46565 %	95.74070 %
12	1.17288E+01	97.46565 %	97.46565 %	95.74070 %
13	1.19872E+01	97.46565 %	97.46565 %	95.74070 %
14	1.30167E+01	98.11958 %	97.70953 %	95.74070 %
15	1.30167E+01	98.36346 %	98.36346 %	95.74070 %
16	1.51365E+01	98.36357 %	98.36417 %	95.74070 %
17	1.51365E+01	98.36427 %	98.36427 %	95.74070 %
18	1.58796E+01	98.36427 %	98.36427 %	95.74070 %
19	1.64254E+01	98.36427 %	98.36427 %	95.74070 %
20	1.67788E+01	98.36427 %	98.36427 %	95.74070 %

*** End of list.

A4 Spring-set for the simple model

For the simple model the foundation bed is presented through a set of springs and dashpots that replace the elastic bed modeled with finite elements.

The equivalent spring constants are calculated in accordance with ASCE 4-98 (ASCE 2000). The formulas for the equivalent spring are presumably based on only one layer with large enough depth so that it can be considered as homogenious domain . This is however not the case for the silo since the layer of sand/bentonite between the silo and the rock is only 1.5 m thick, Naturally the foundation is stiffer compared to one that lies on infinitely deep lager av sand/bentonite.

The modulus of elasticity is modified so that it correctly represents the stiffness of the foundation. A scale factor is used, based on the calculated settlement from the weight of the empty silo. According to Pusch (2003), the settlement is 4 mm.

The adjusted properties showed very good correspondence with the models where the foundation is actually modeled with finite elements.

Equivelent spring constants:

Input data and properties

Scale factor $k := 3.3$

Soil properties; $E_{bentonite} := k \cdot 150\,MPa = 495 \cdot MPa$ $\nu := 0.4$

$$G_{bentonite} := \frac{E_{bentonite}}{2(1+\nu)} = 412.5 \cdot MPa$$

$$\rho_{bentonite} := 2000 \frac{kg}{m^3}$$

Bottom slab radius: $R_{base} := \frac{d_1}{2} = 13.8\,m$

Total mass of the structure: $M_{tot} = 6.7 \times 10^4 \cdot tonne$

Mass moment of inertia about the rocking axis : $I_0 := \frac{1}{3} \cdot M_{tot} \cdot L_c^{\,2} = 6.392 \times 10^{10}\, m^2 \cdot kg$

Evaluation of the foundations spring properties:

Equivalent spring constants:

Horisontal translation:
$$k_x := \frac{32\cdot(1-\nu)\cdot G_{bentonite}\cdot R_{base}}{7-8\cdot\nu} = 2.876\times 10^{10}\cdot\frac{N}{m}$$

Vertical translation:
$$k_z := \frac{4G_{bentonite}\cdot R_{base}}{1-\nu} = 3.795\times 10^{10}\cdot\frac{N}{m}$$

Rocking motion:
$$k_\psi := \frac{8G_{bentonite}\cdot R_{base}^{3}}{3\cdot(1-\nu)} = 4.818\times 10^{12}\cdot\frac{N\cdot m}{rad}$$

Torsion motion:
$$k_t := \frac{16\cdot G_{bentonite}\cdot R_{base}^{3}}{3} = 5.782\times 10^{12}\cdot N\cdot\frac{m}{rad}$$

Check for the scale factor with an equivelent spring from the calculated settlement from an empty silo, Pusch (2003):

Weight of an empty silo:
$$F_{silo} := 16000\ \text{tonne}\cdot g = 156.906\cdot MN$$

Equivelent spring:
$$k_{z_PUSCH} := \frac{F_{silo}}{4\,mm} = 3.923\times 10^{10}\cdot\frac{N}{m}$$

Ratio between the two springs:
$$\frac{k_z}{k_{z_PUSCH}} = 0.967$$

Appendix B

Results from the FE-model

B1 Orientation

The results of all of the analyzed cases are presented in color plots for the stresses in the outer walls and the inner walls. Additional diagrams for the variation of the stresses and forces along the casting joints are also presented for the relevant cases.

- Outer walls:
  - Maximum principal tensile stress (outside edge/inside edge).
  - Maximum vertical stress (outside edge/inside edge).
  - Maximum hoop stress (outside edge/inside edge).
- Inner walls:
  - Maximum principal tensile stress.
- Joint between the outer wall and the bottom slab.
  - Stresses, contribution from the load cases-inside edge.
  - Stresses, contribution from the load cases-outside edge.
  - Vertical force, contribution from the load cases.
  - Forces in the joint section.

B2 Case 1 – simple model

Static (permanent loads)

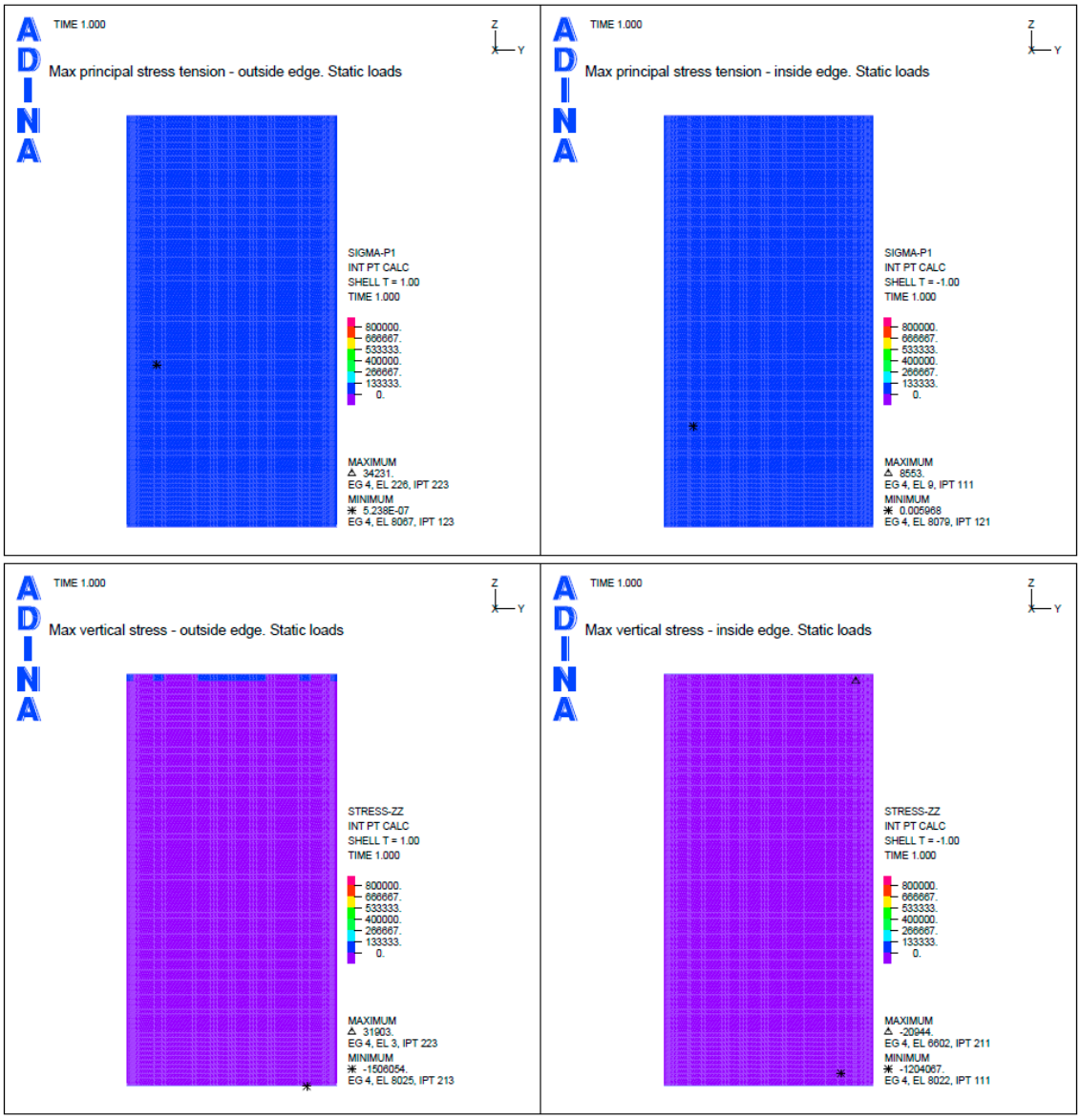

Figure B-1. *Case 1 – simple. Static load cases (permanent loads). Max principal tensile stresses and max vertical stresses.*

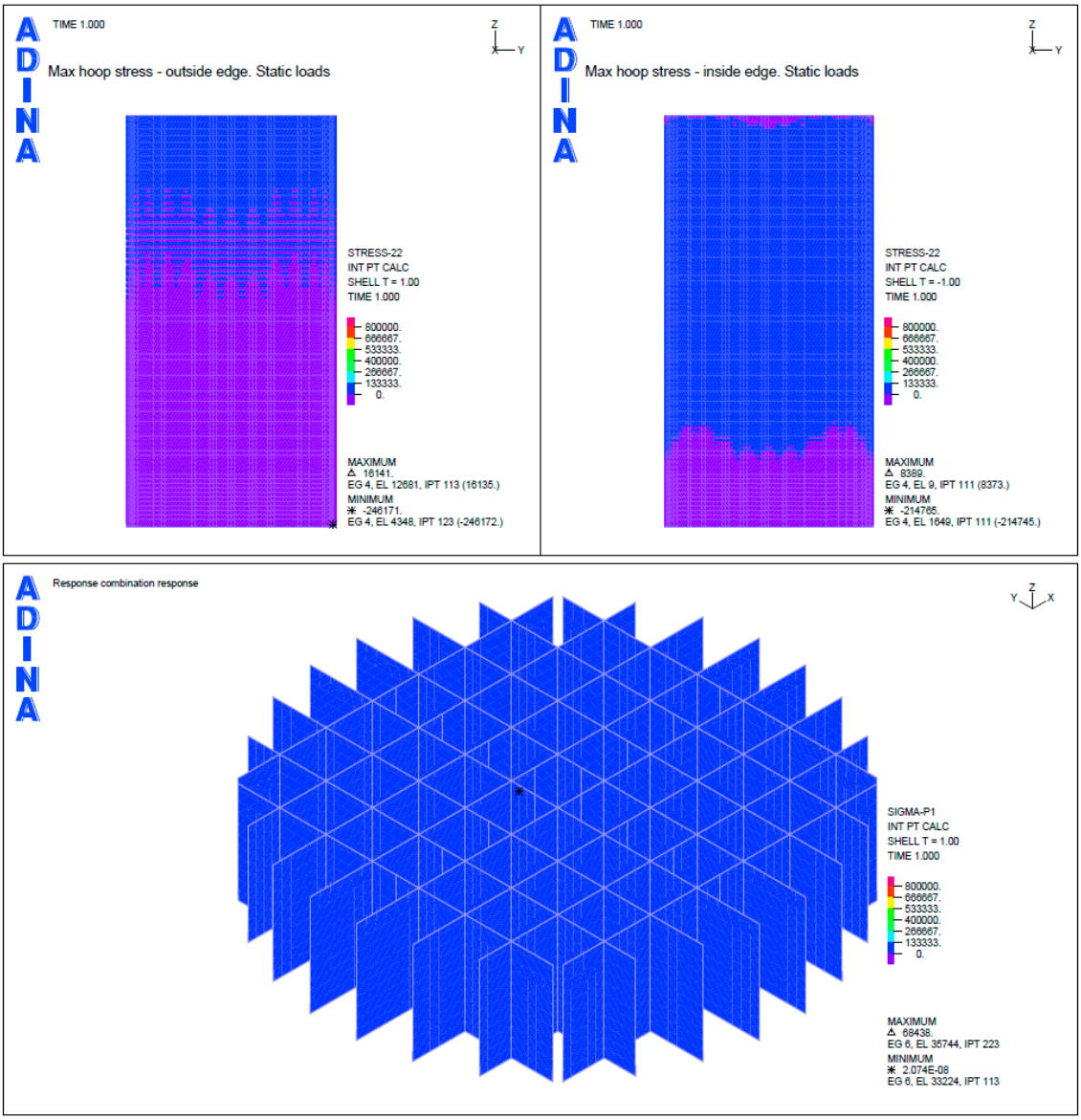

Figure B-2. *Case 1 – simple. Static load cases (permanent loads). Max hoop stresses and max principal tensile stresses for the inner wall.*

SSE 10^{-5} case

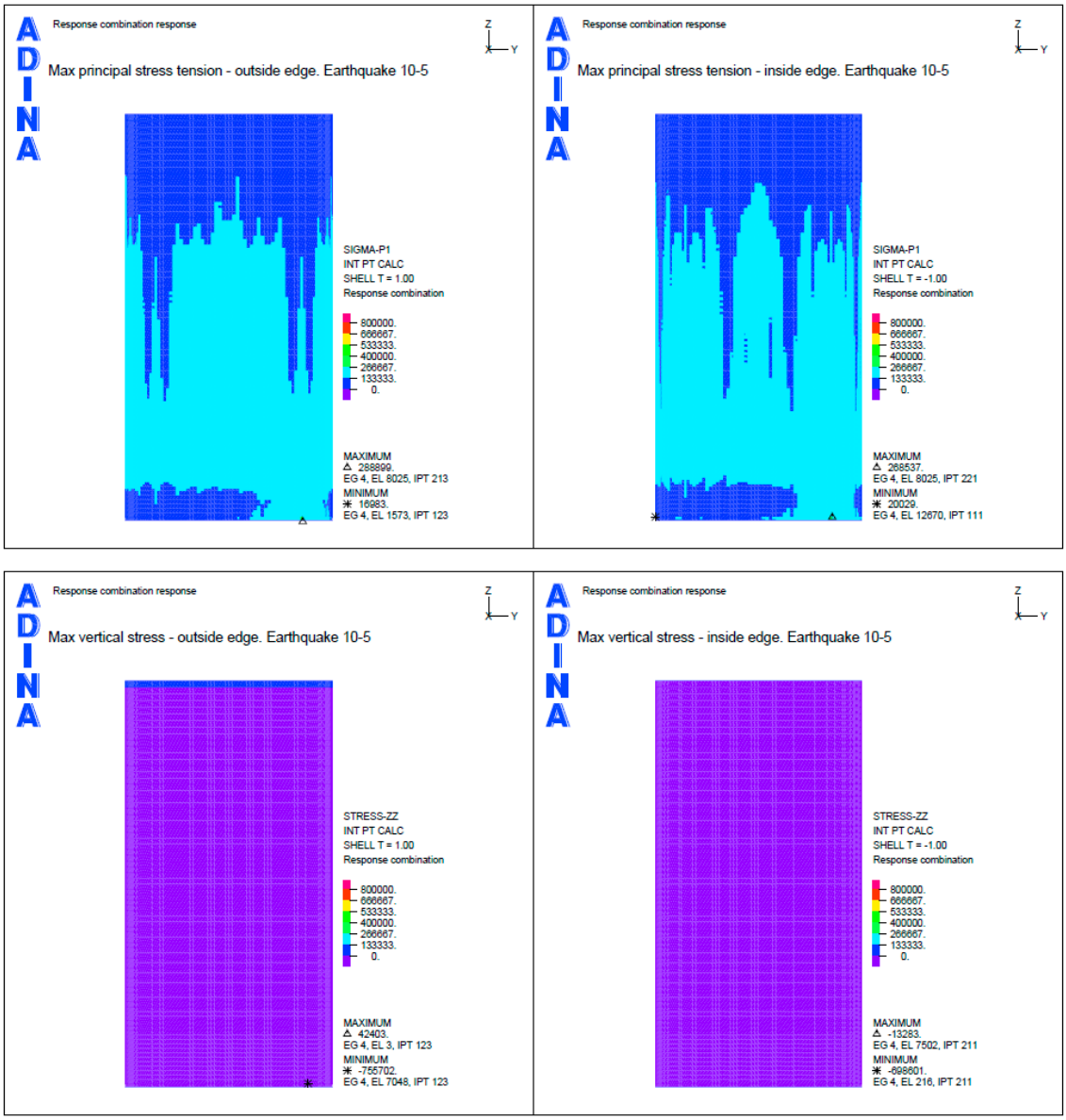

Figure B-3. *Case 1 – simple. Earthquake load combination with SSE 10^{-5}. Max principal tensile stresses and max vertical stresses.*

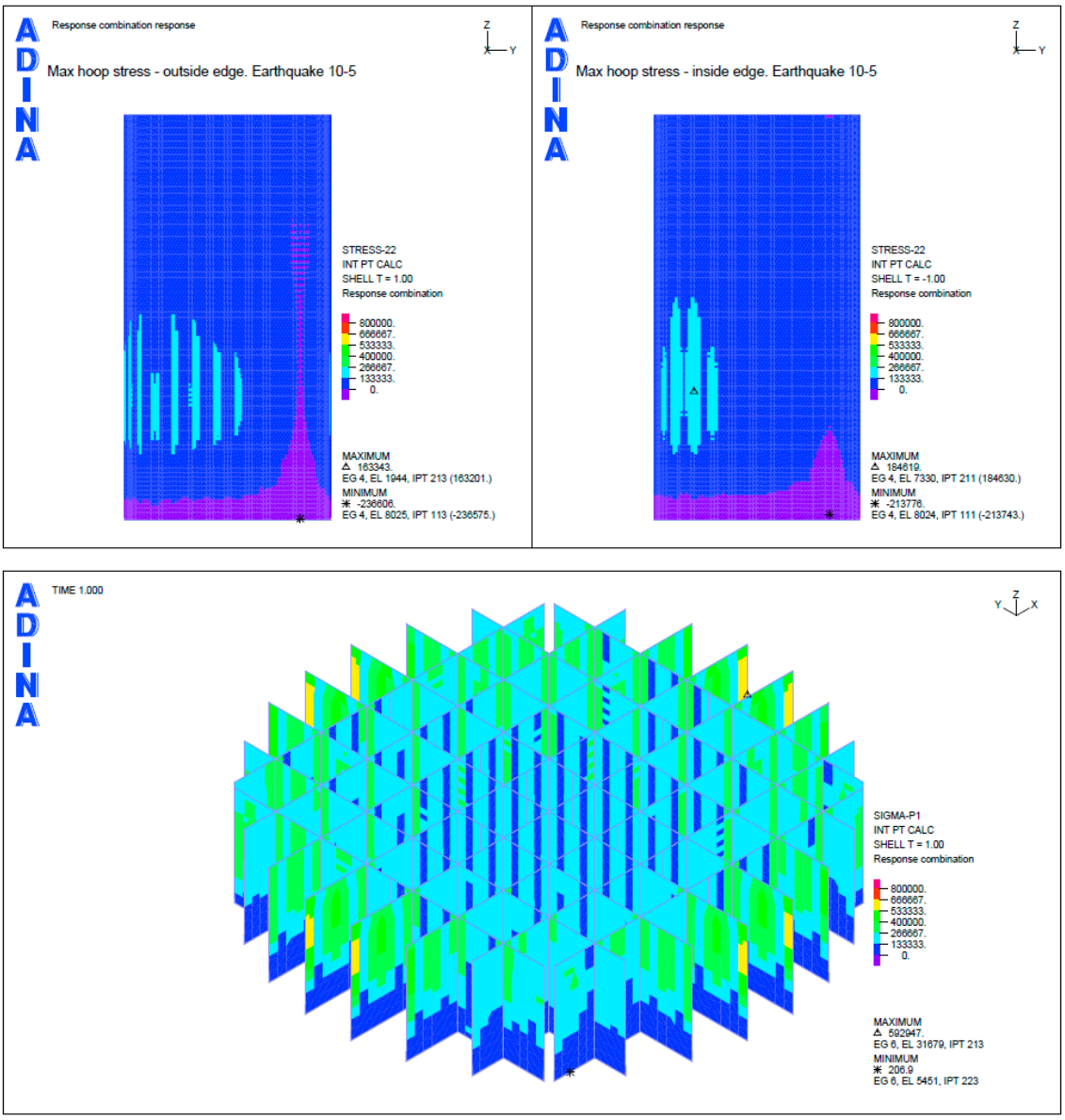

Figure B-4. *Case 1 – simple. Earthquake load combination with SSE 10^{-5}. Max hoop stresses and max principal tensile stresses for the inner wall.*

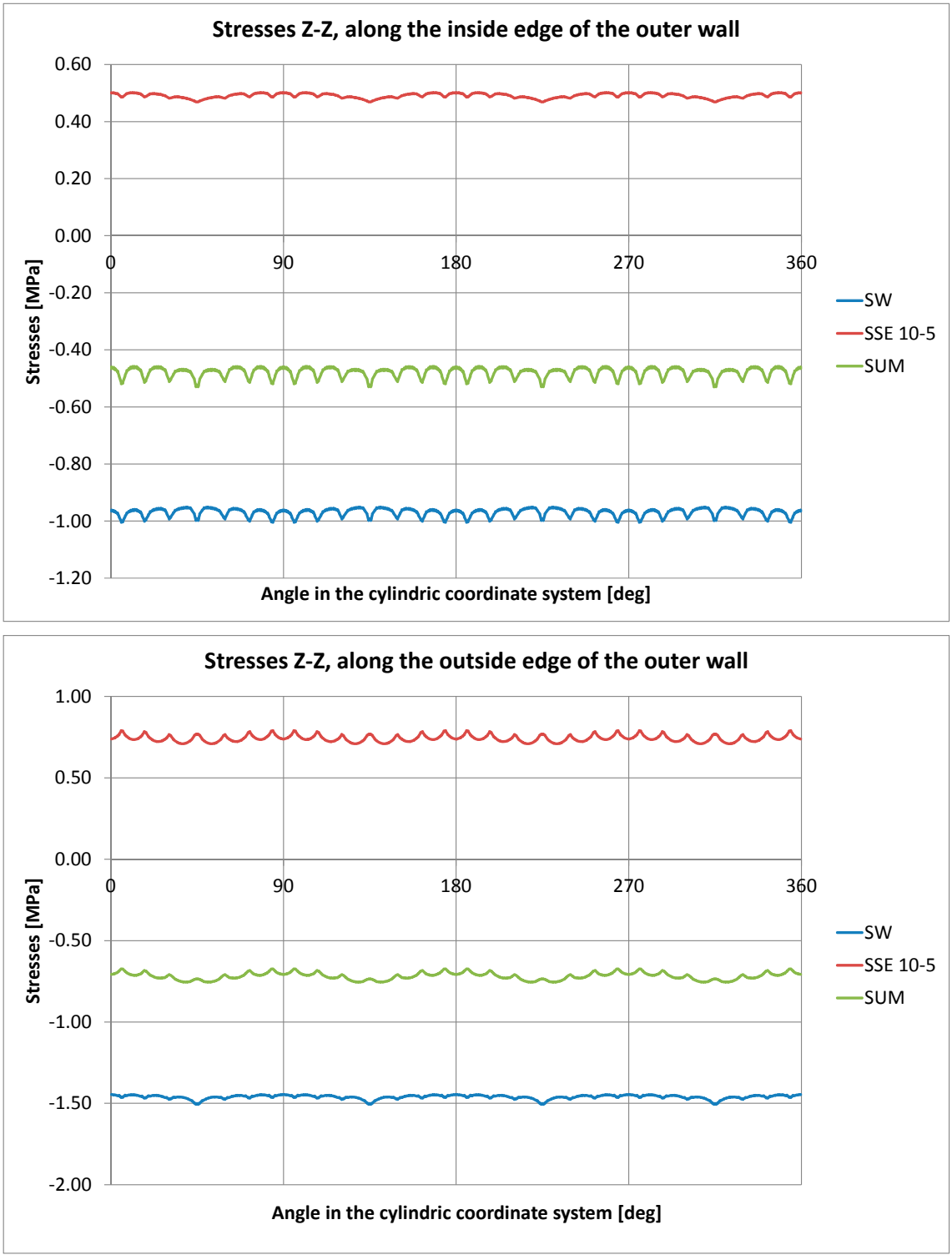

Figure B-5. *Case 1 – simple. Earthquake load combination with SSE 10^{-5}. Vertical stress along the casting joint.*

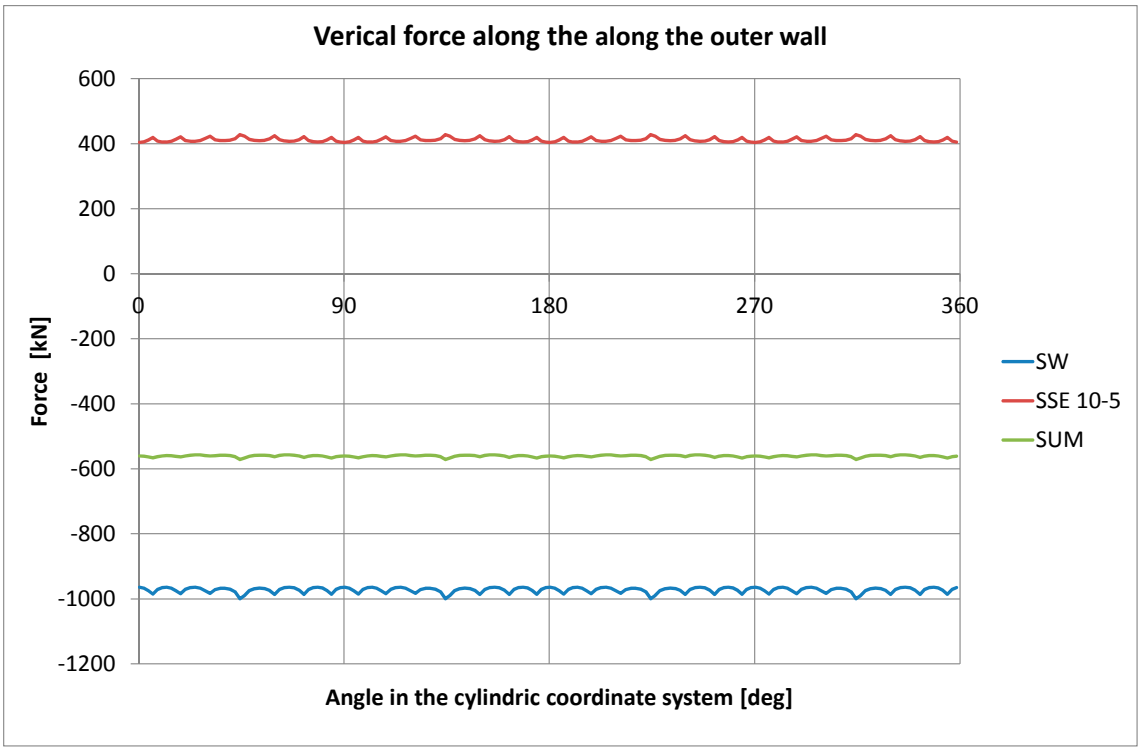

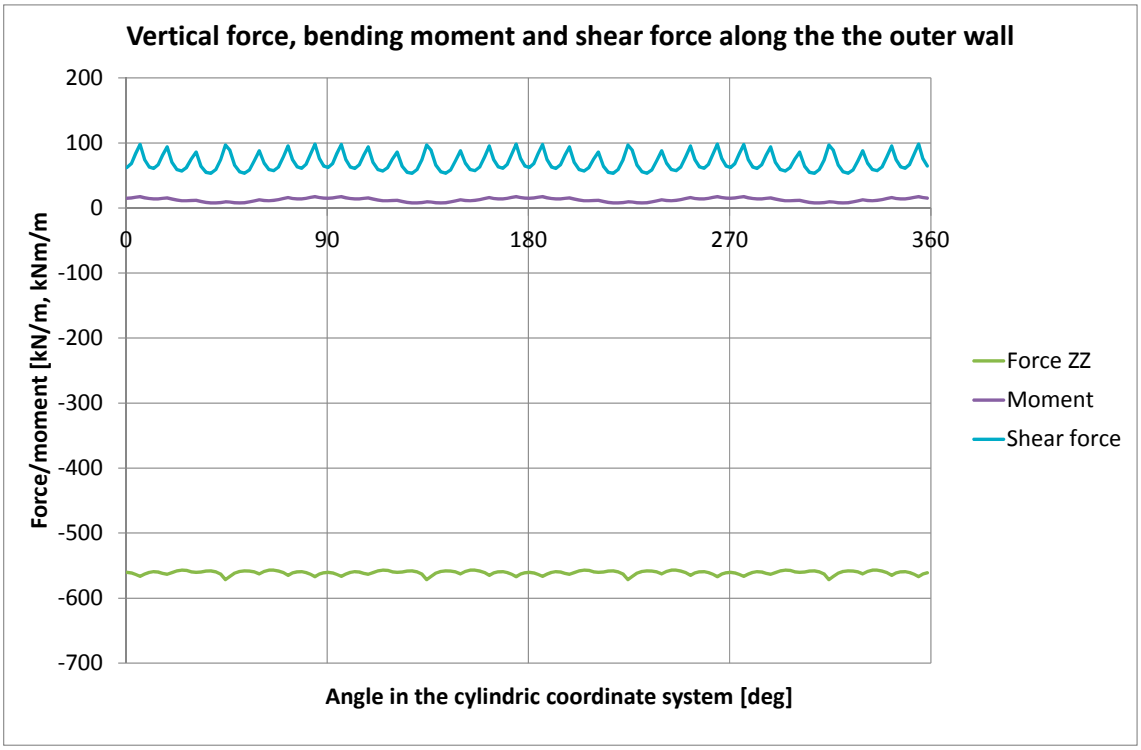

Figure B-6. *Case 1 – simple. Earthquake load combination with SSE 10^{-5}. Forces along the casting joint.*

SSE 10^{-6} case

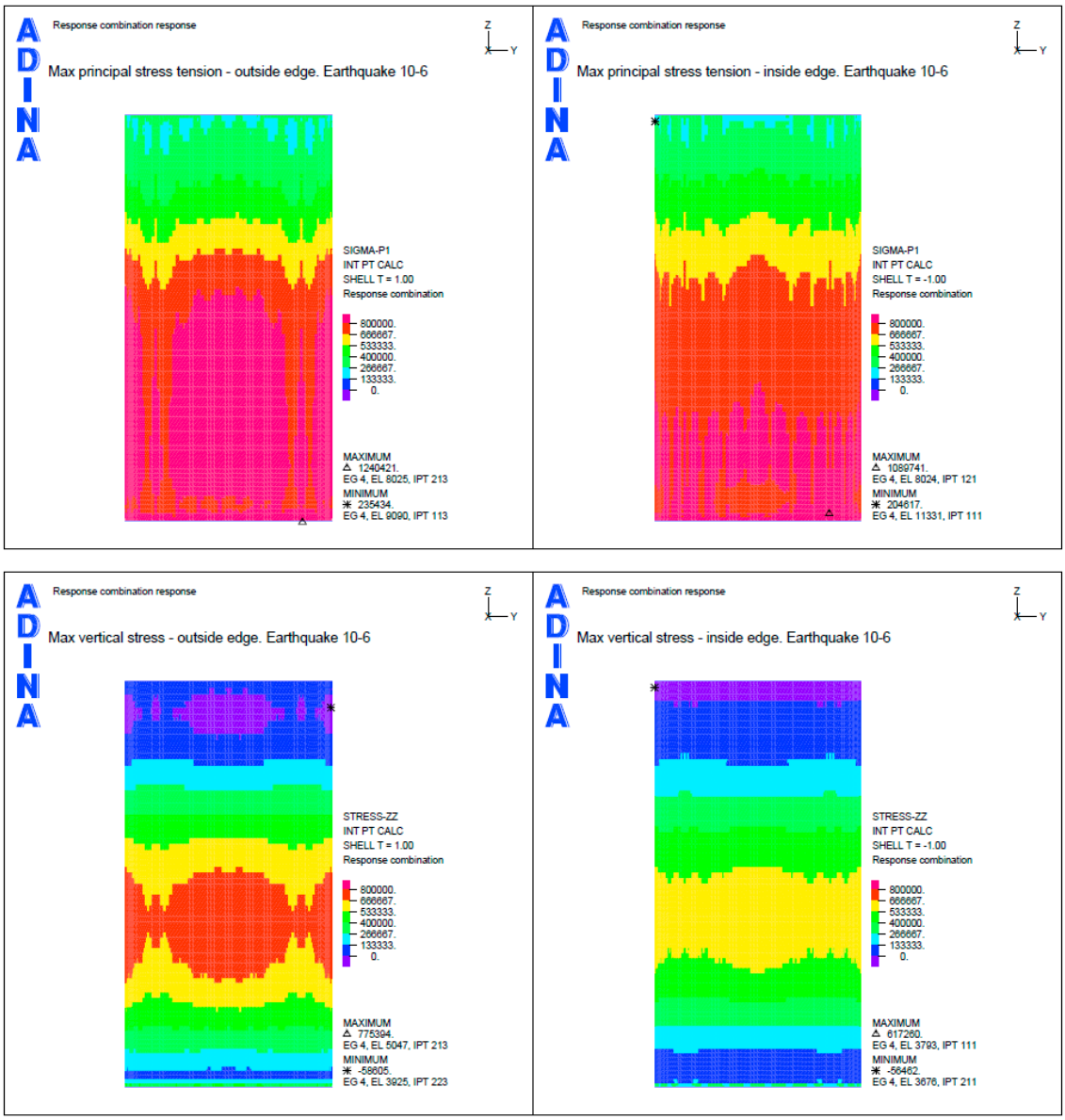

Figure B-7. *Case 1 – simple. Earthquake load combination with SSE 10^{-6}. Max principal tensile stresses and max vertical stresses.*

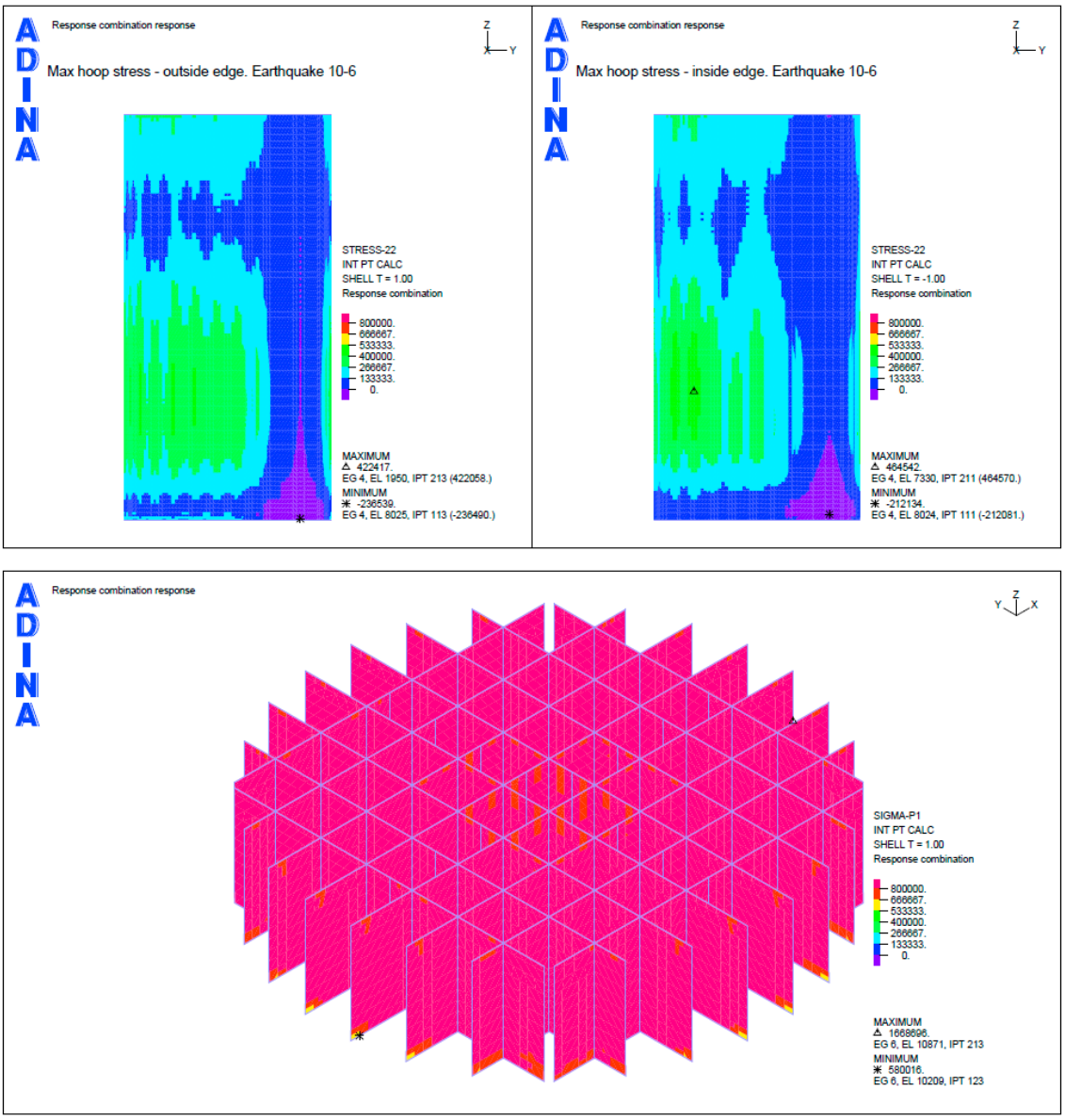

Figure B-8. *Case 1 – simple. Earthquake load combination with SSE 10^{-6}. Max hoop stresses and max principal tensile stresses for the inner wall.*

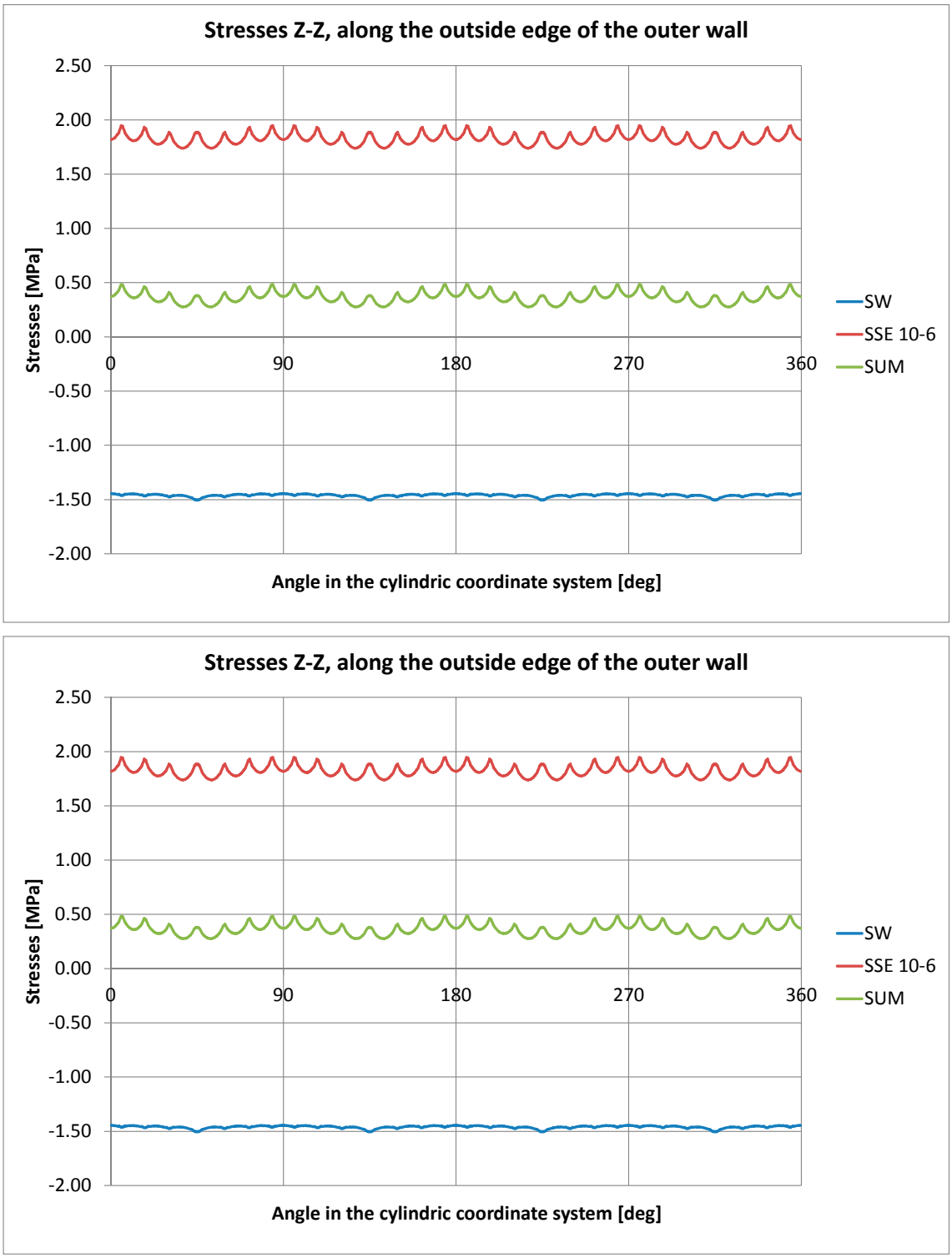

Figure B-9. *Case 1 – simple. Earthquake load combination with SSE 10^{-6}. Vertical stress along the casting joint.*

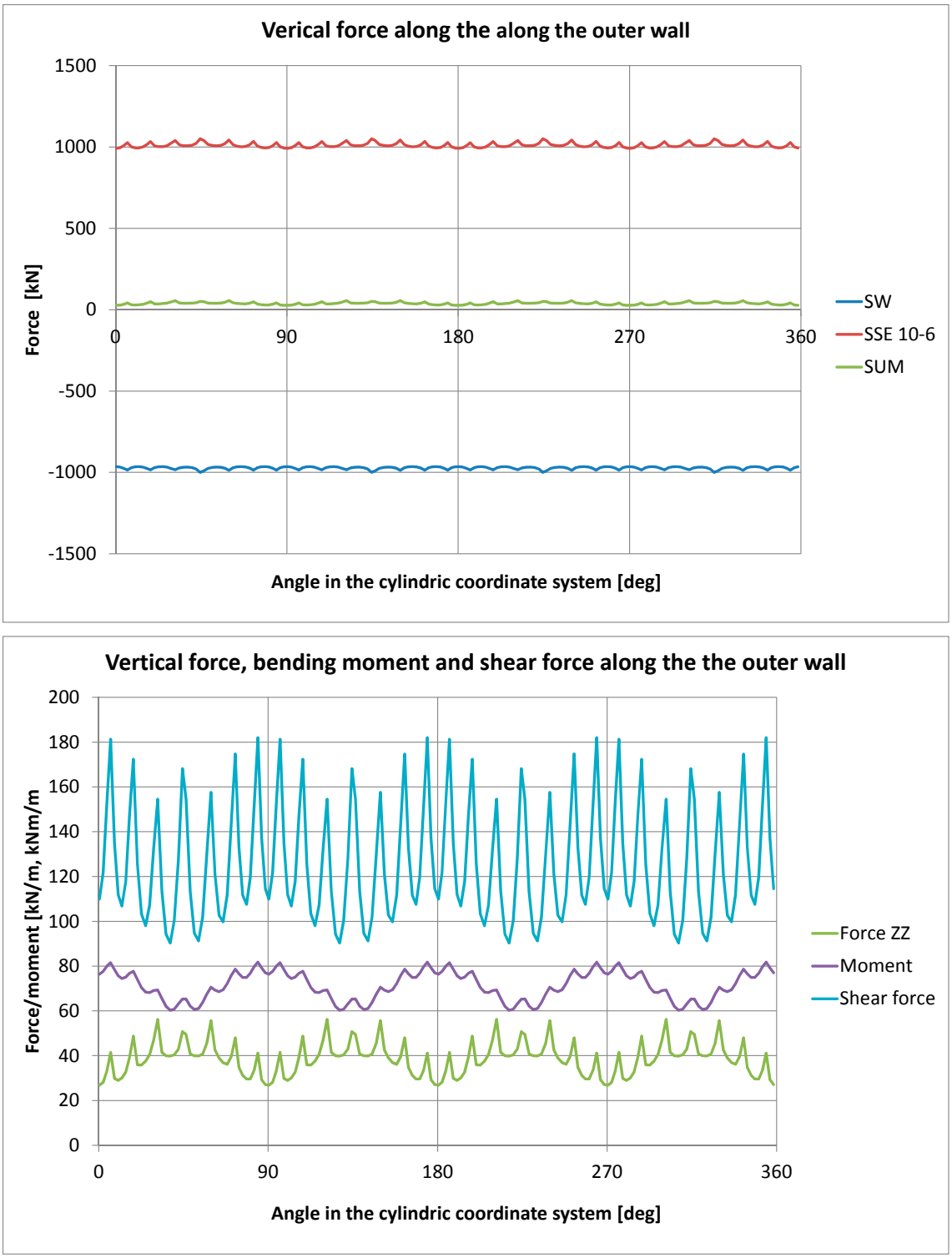

Figure B-10. *Case 1 – simple. Earthquake load combination with SSE 10^{-6}. Forces along the casting joint.*

SSE 10^{-7} case

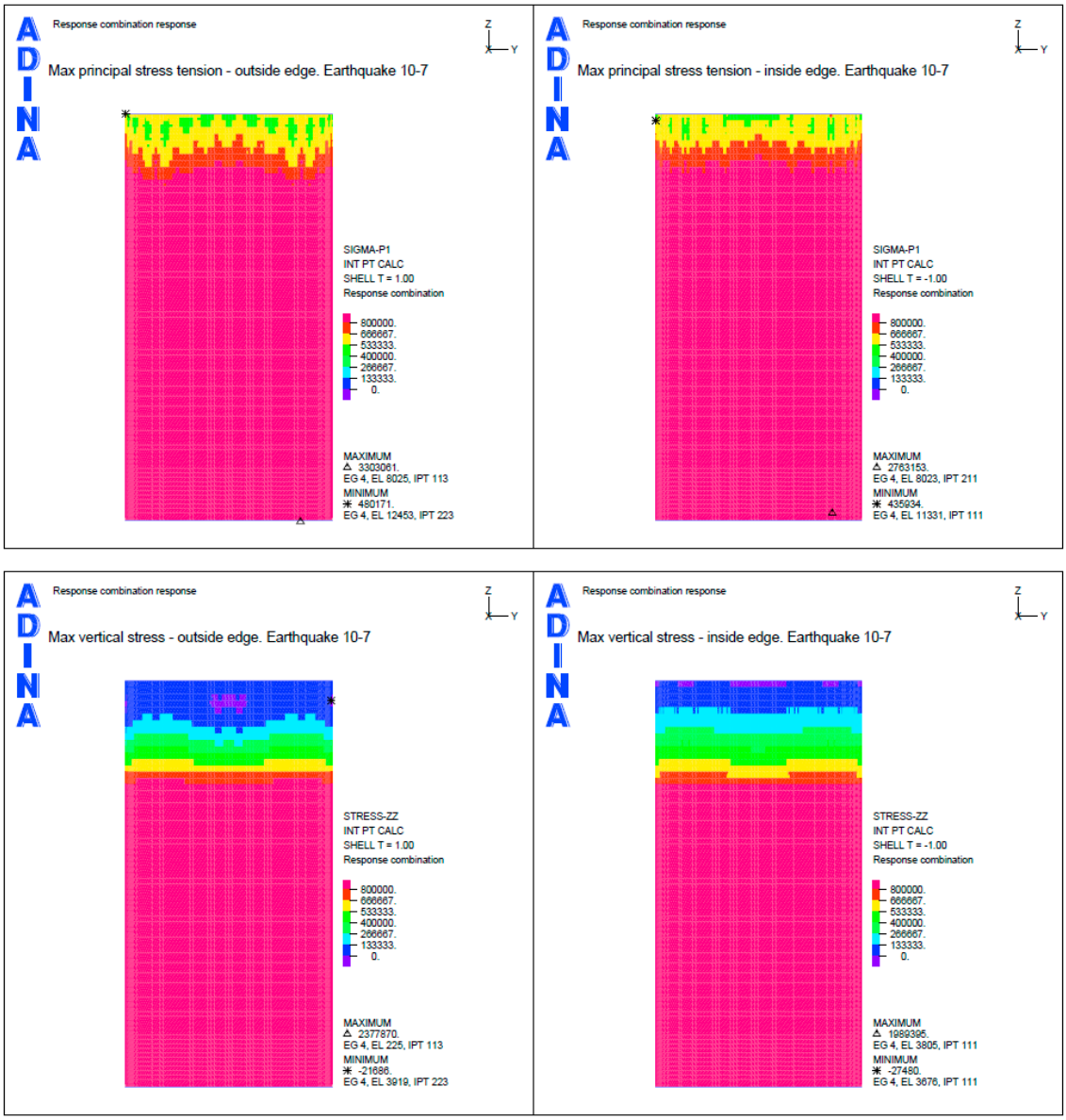

Figure B-11. *Case 1 – simple. Earthquake load combination with SSE 10^{-7}. Max principal tensile stresses and max vertical stresses.*

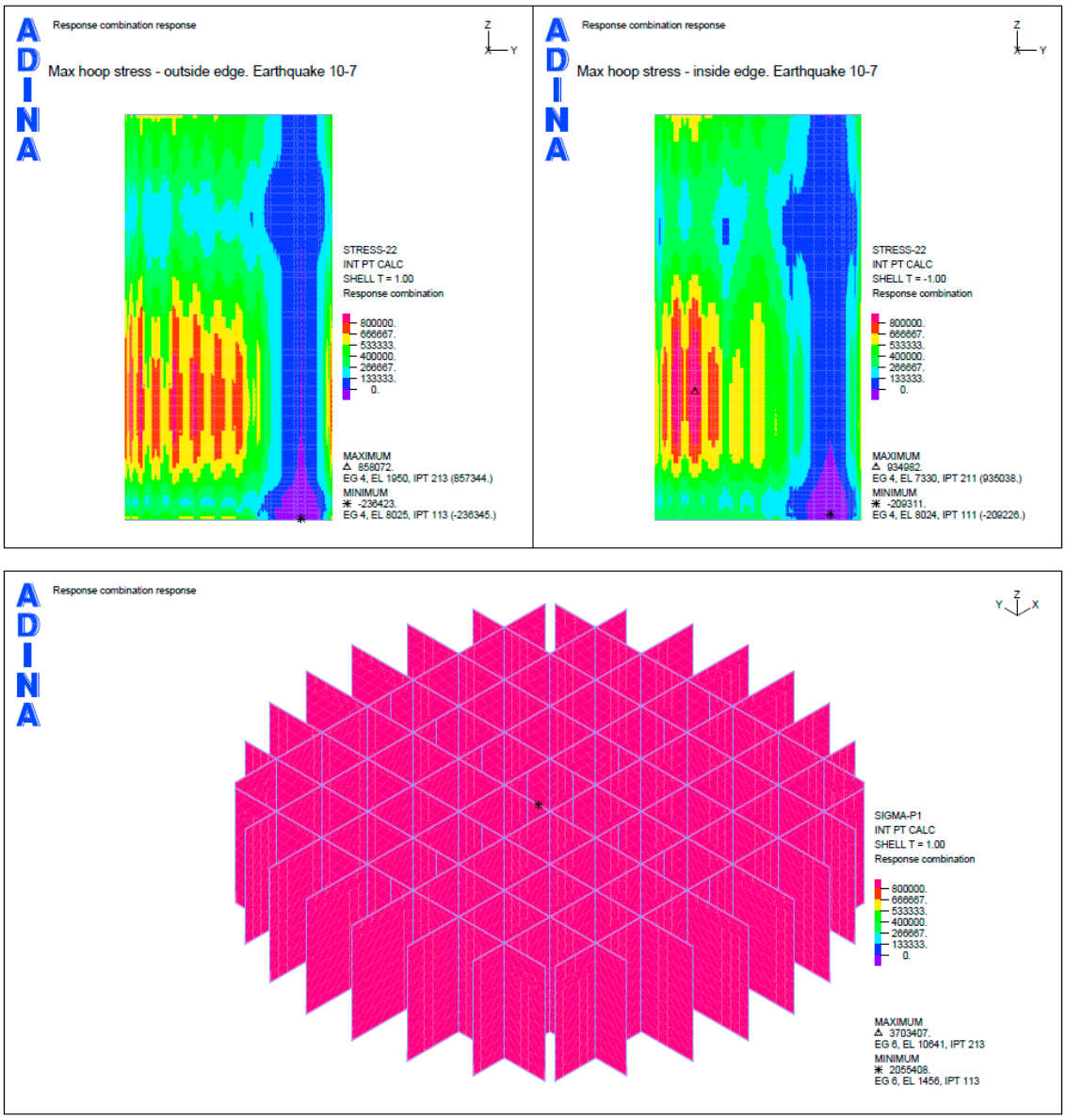

Figure B-12. *Case 1 – simple. Earthquake load combination with SSE 10^{-7}. Max hoop stresses and max principal tensile stresses for the inner wall.*

B3 Case 1a – rigid connection between wall and slab

Static load cases (permanent loads)

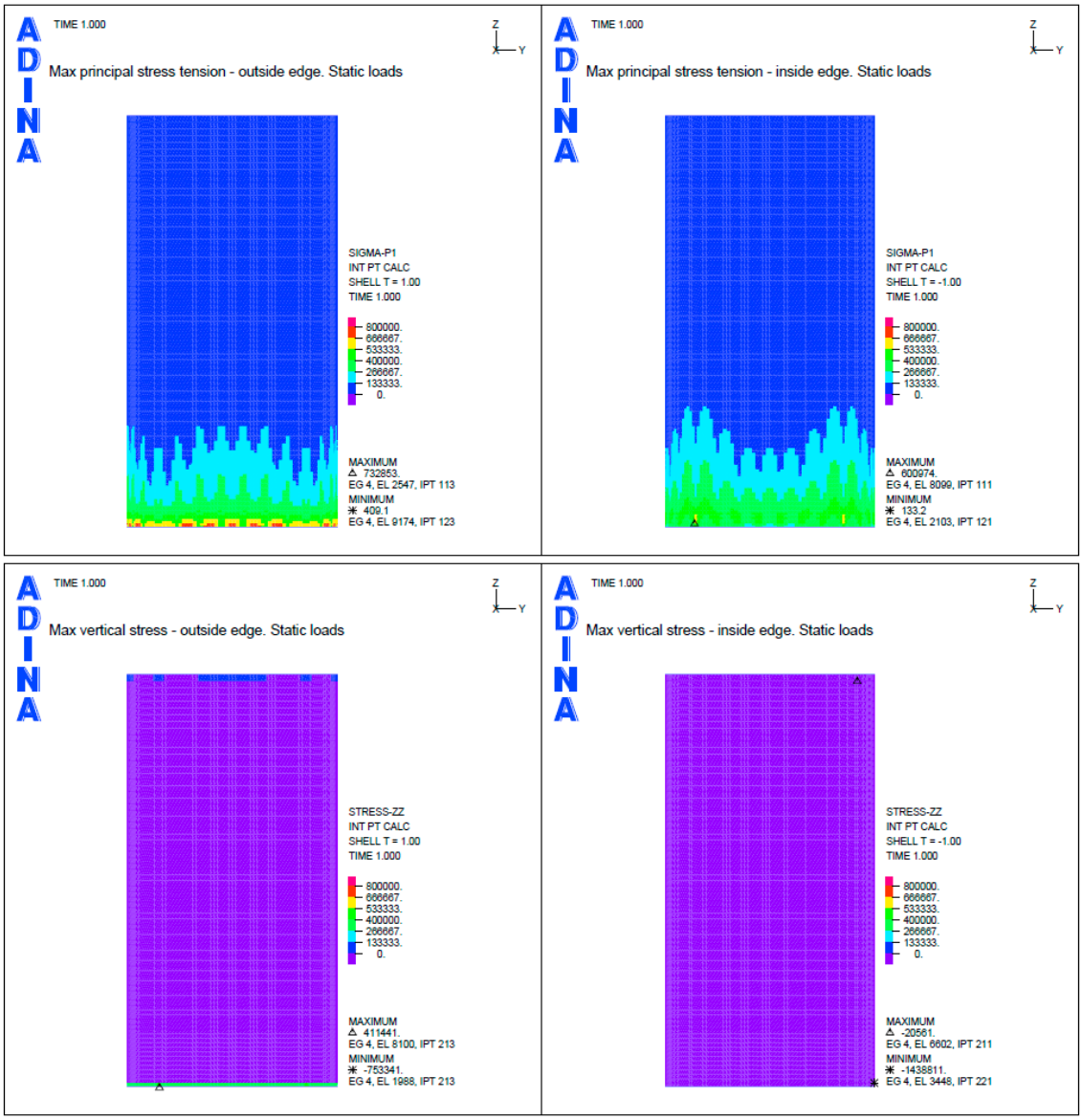

Figure B-13. *Case 1a. Static load cases (permanent loads). Max principal tensile stresses and max vertical stresses.*

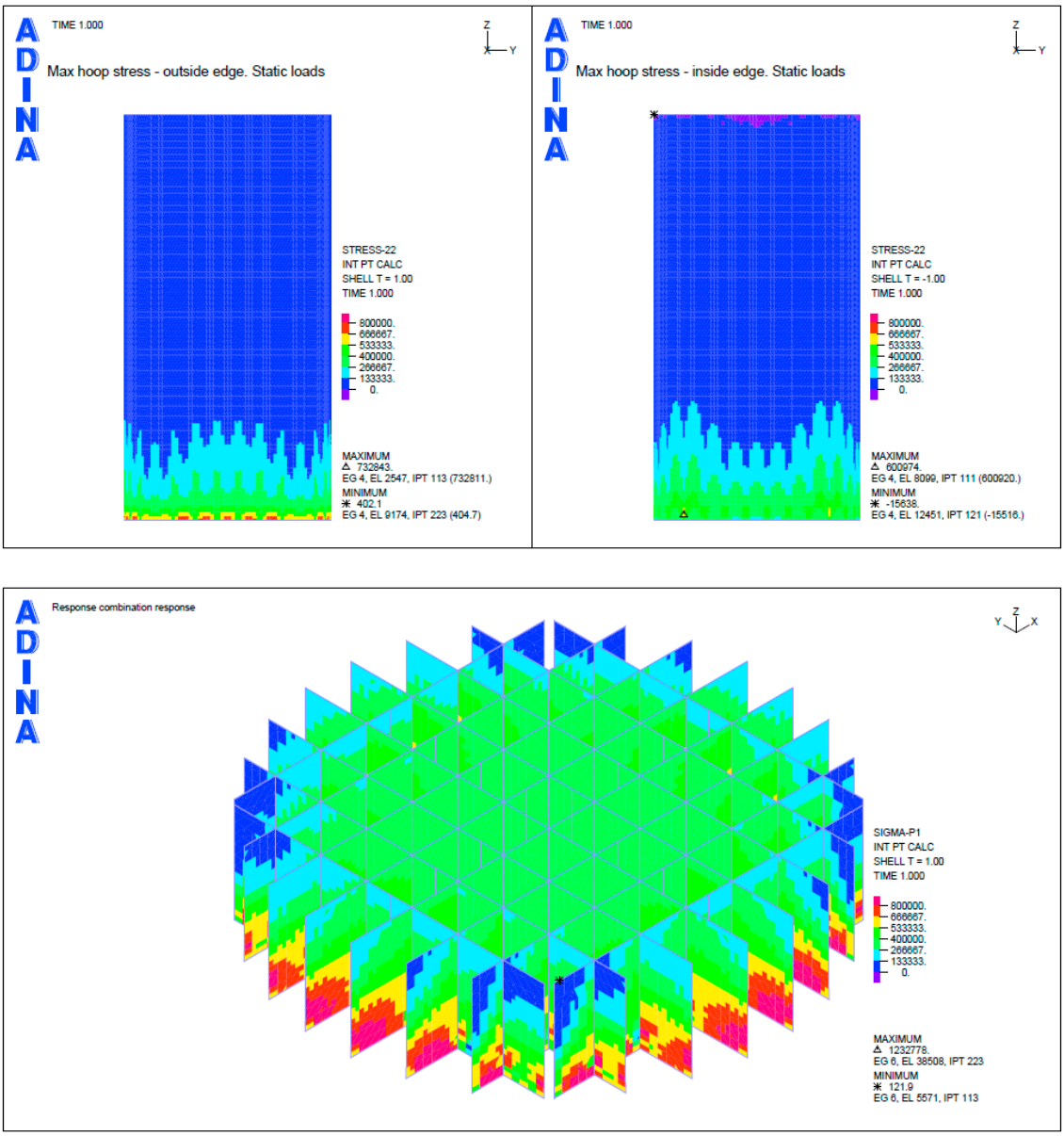

Figure B-14. *Case 1a. Static load cases (permanent loads). Max hoop stresses and max principal tensile stresses for the inner wall.*

SSE 10^{-5} case

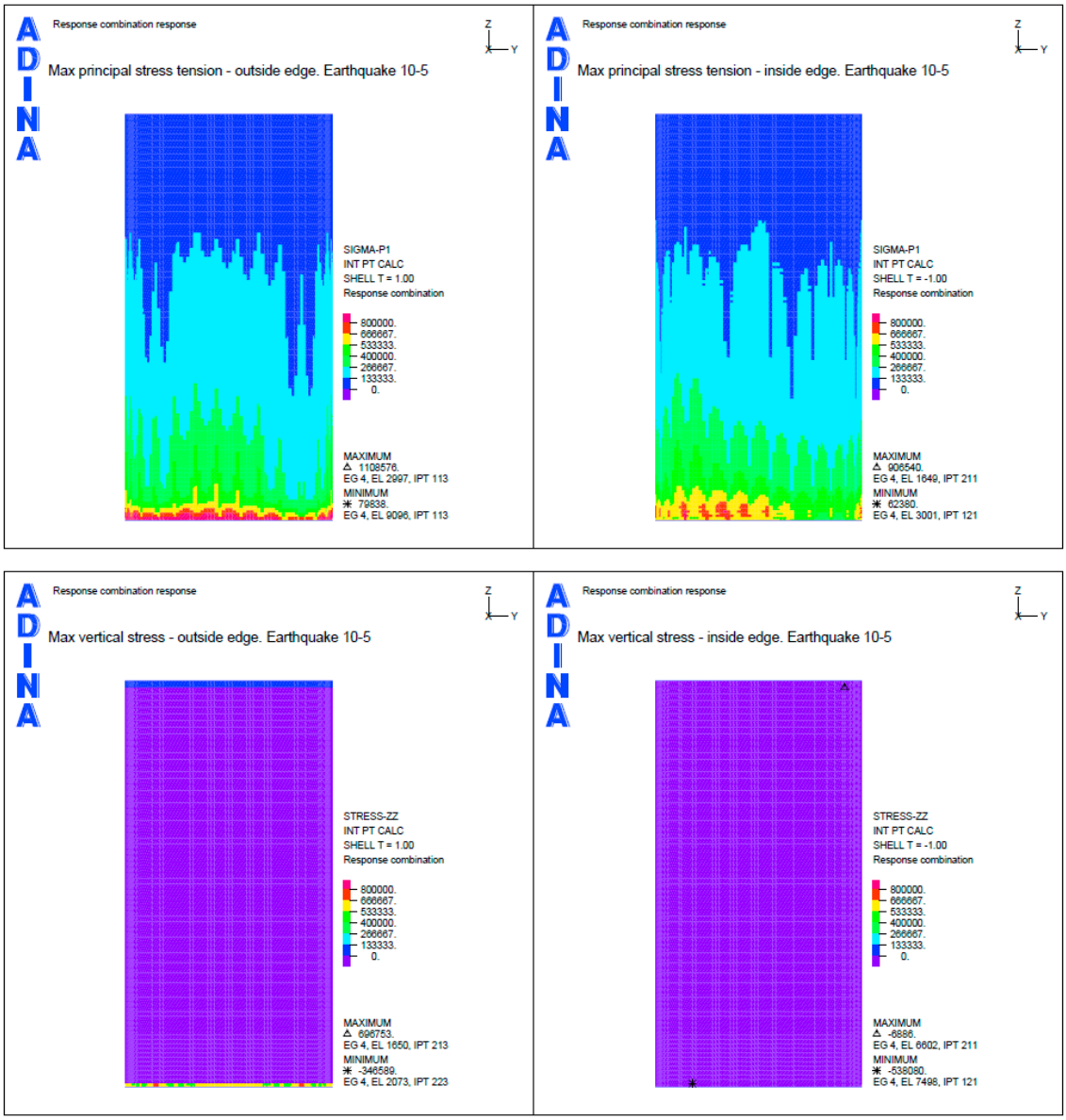

Figure B-15. *Case 1a. Earthquake load combination with SSE 10^{-5}. Max principal tensile stresses and max vertical stresses.*

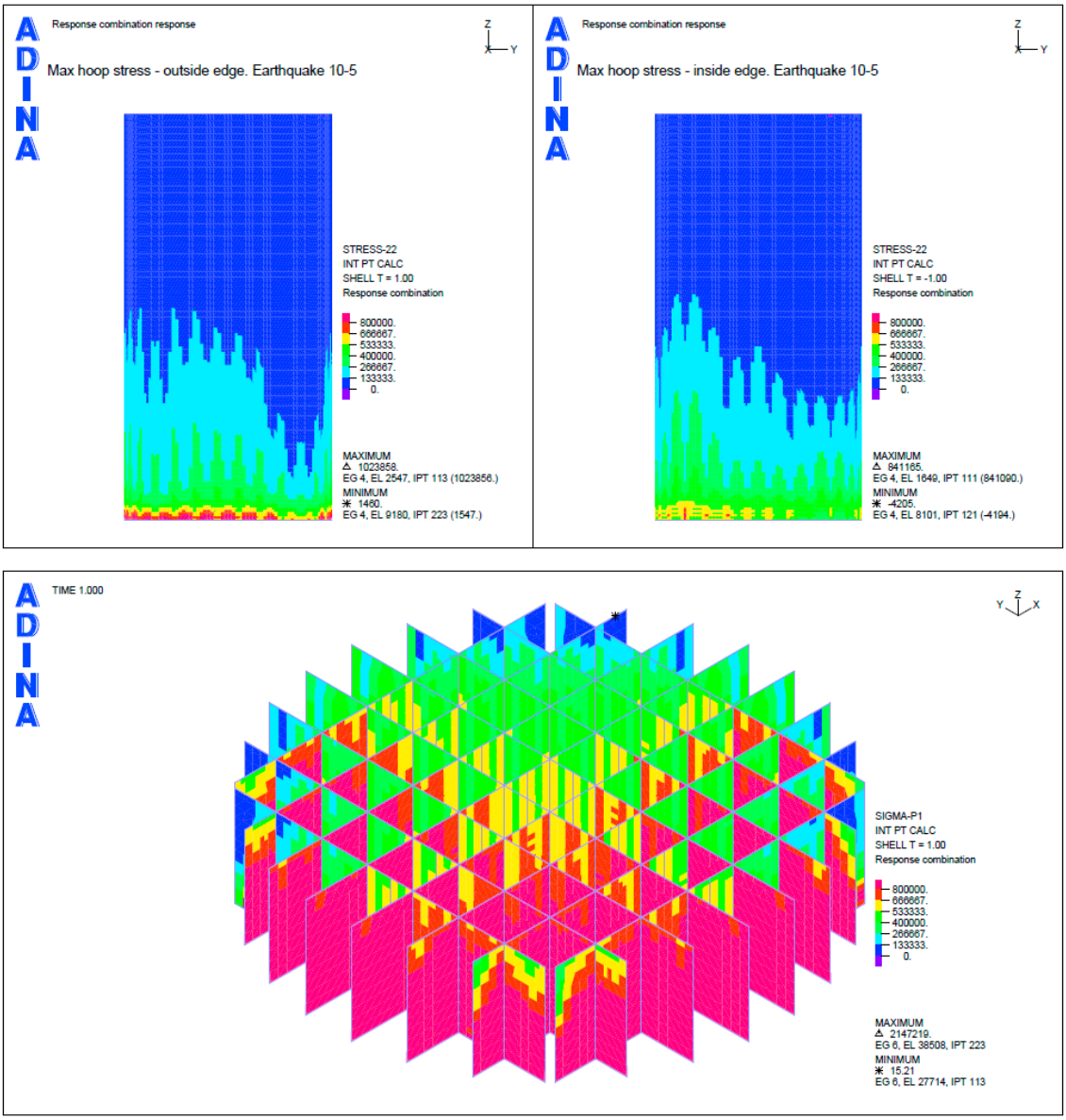

Figure B-16. *Case 1a. Earthquake load combination with SSE 10^{-5}. Max hoop stresses and max principal tensile stresses for the inner wall.*

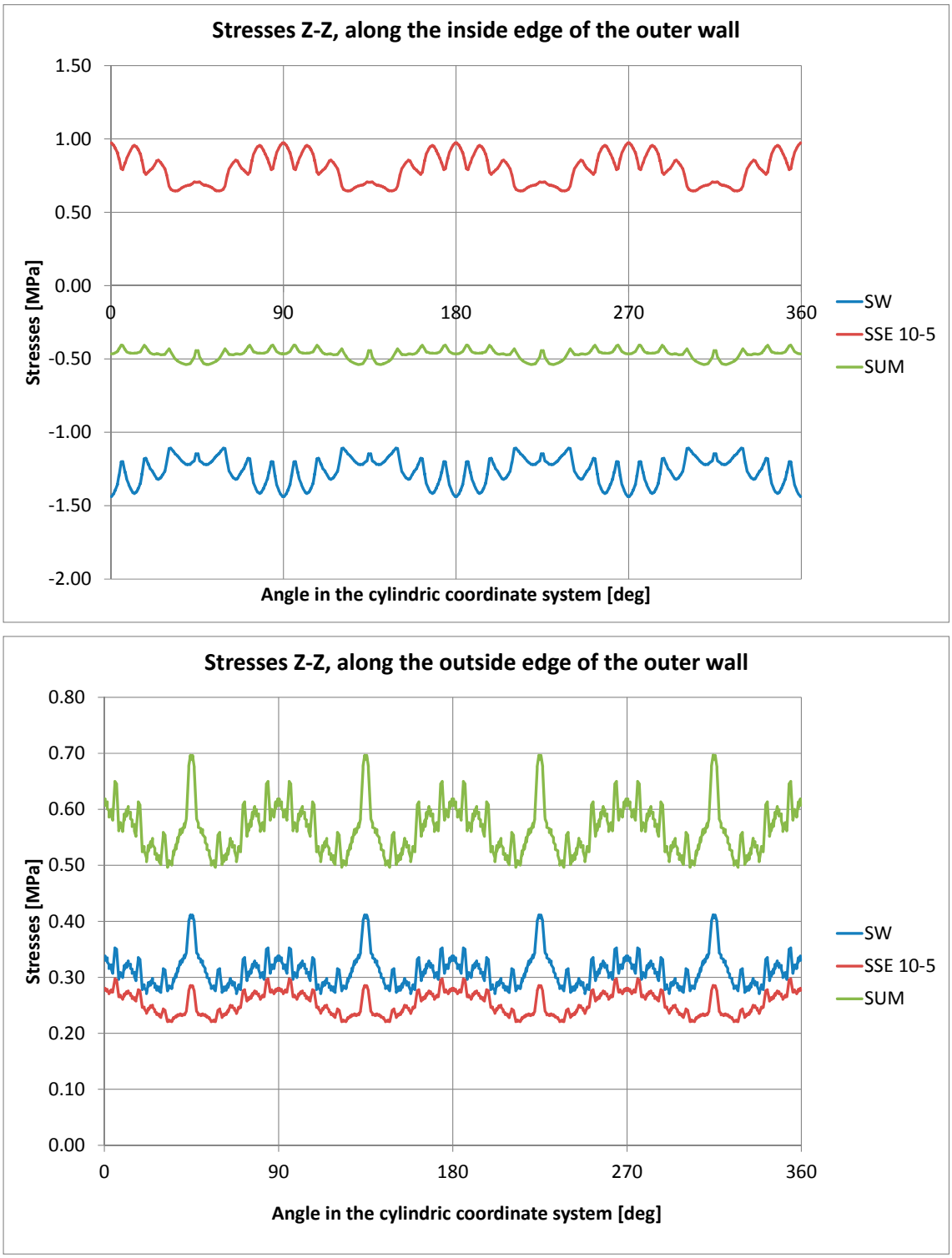

Figure B-17. *Case 1a. Earthquake load combination with SSE 10^{-5}. Vertical stress along the casting joint.*

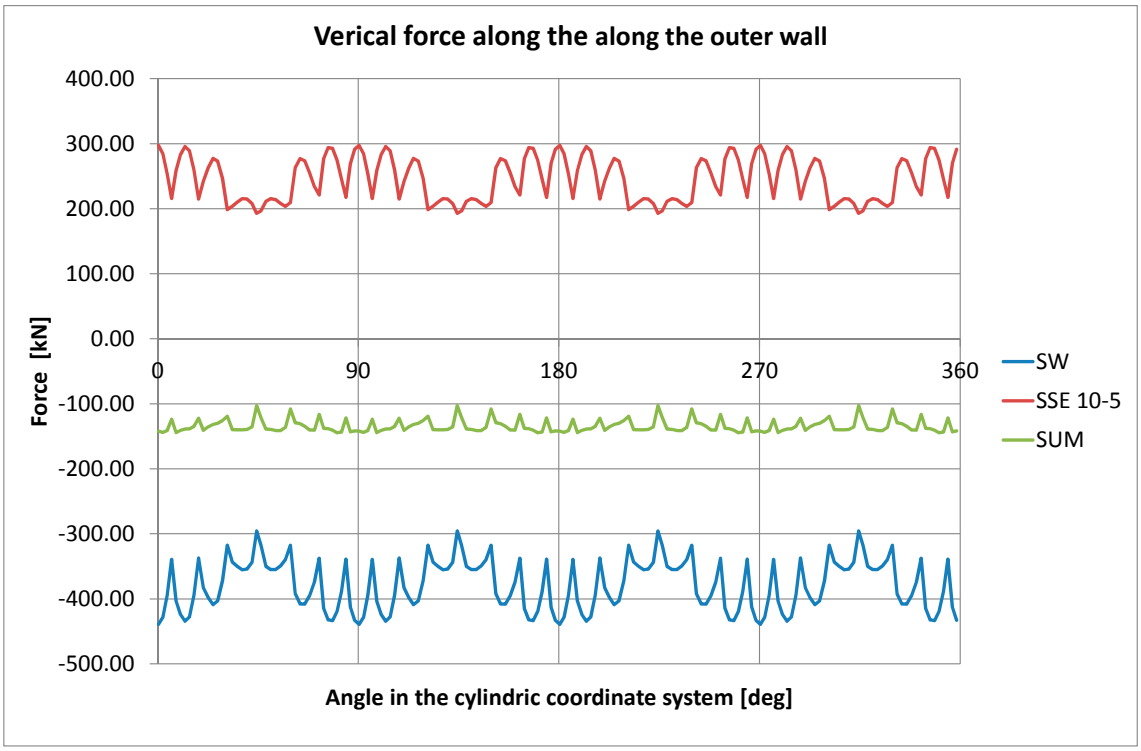

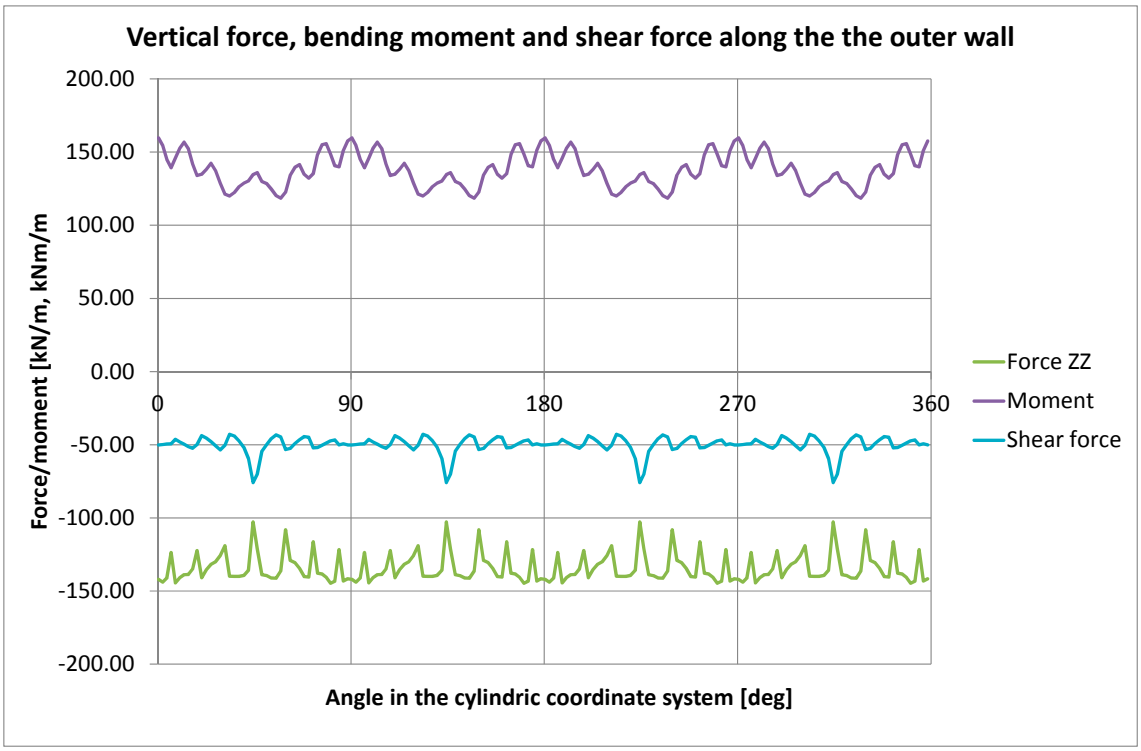

Figure B-18. *Case 1a. Earthquake load combination with SSE 10^{-5}. Forces along the casting joint.*

SSE 10^{-6} case

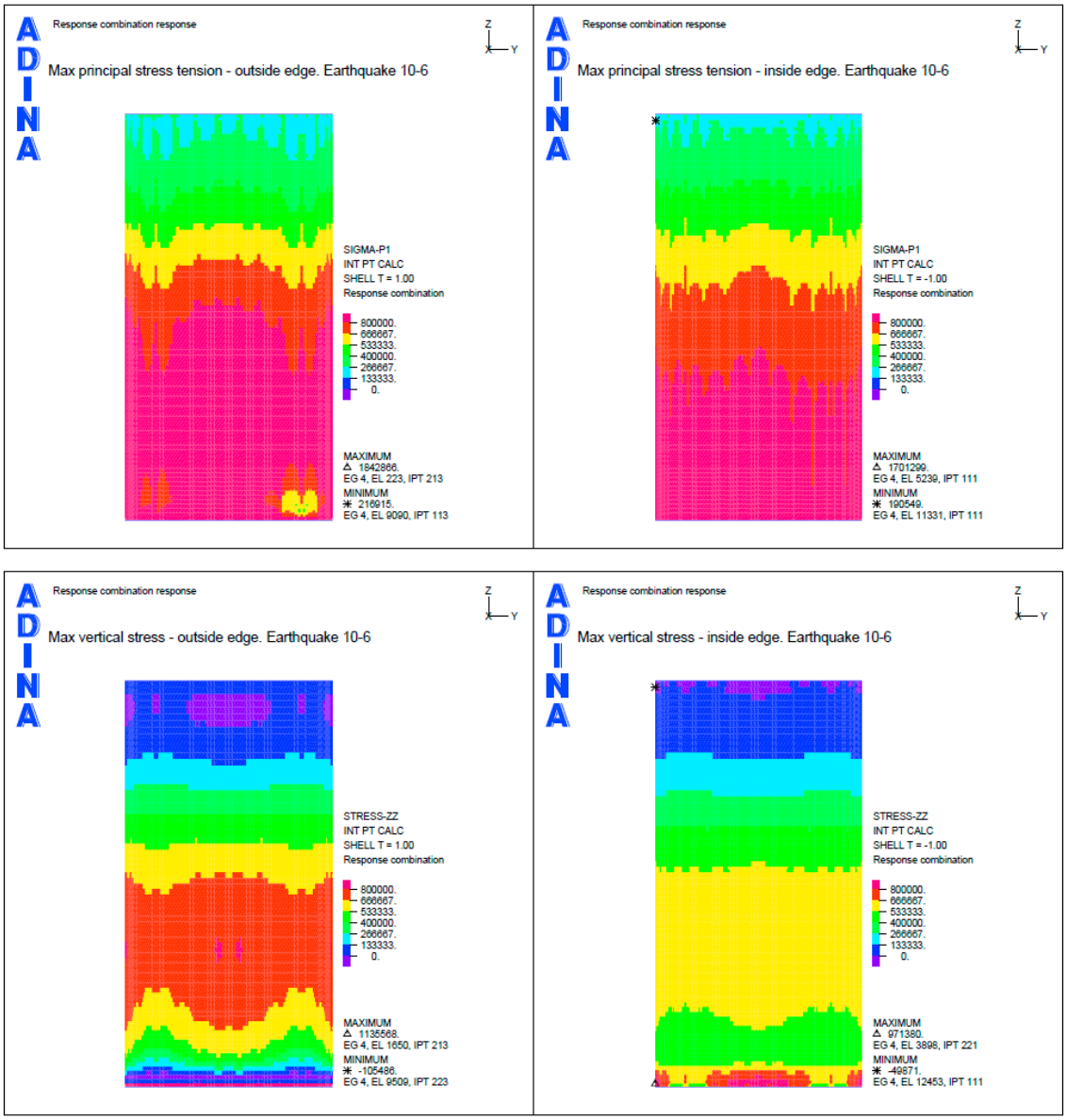

Figure B-19. *Case 1a. Earthquake load combination with SSE 10^{-6}. Max principal tensile stresses and max vertical stresses.*

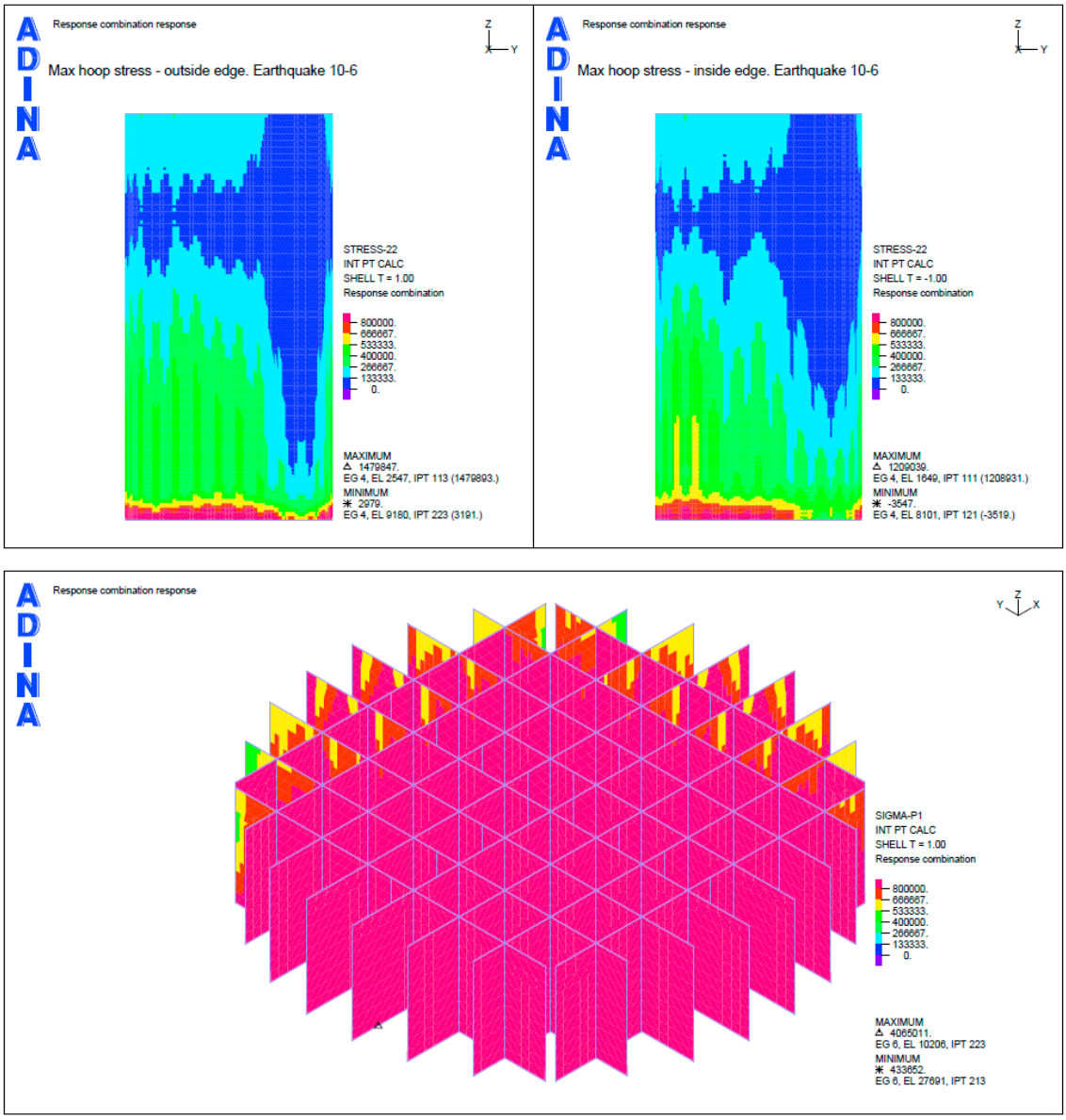

Figure B-20. *Case 1a. Earthquake load combination with SSE 10^{-6}. Max hoop stresses and max principal tensile stresses for the inner wall.*

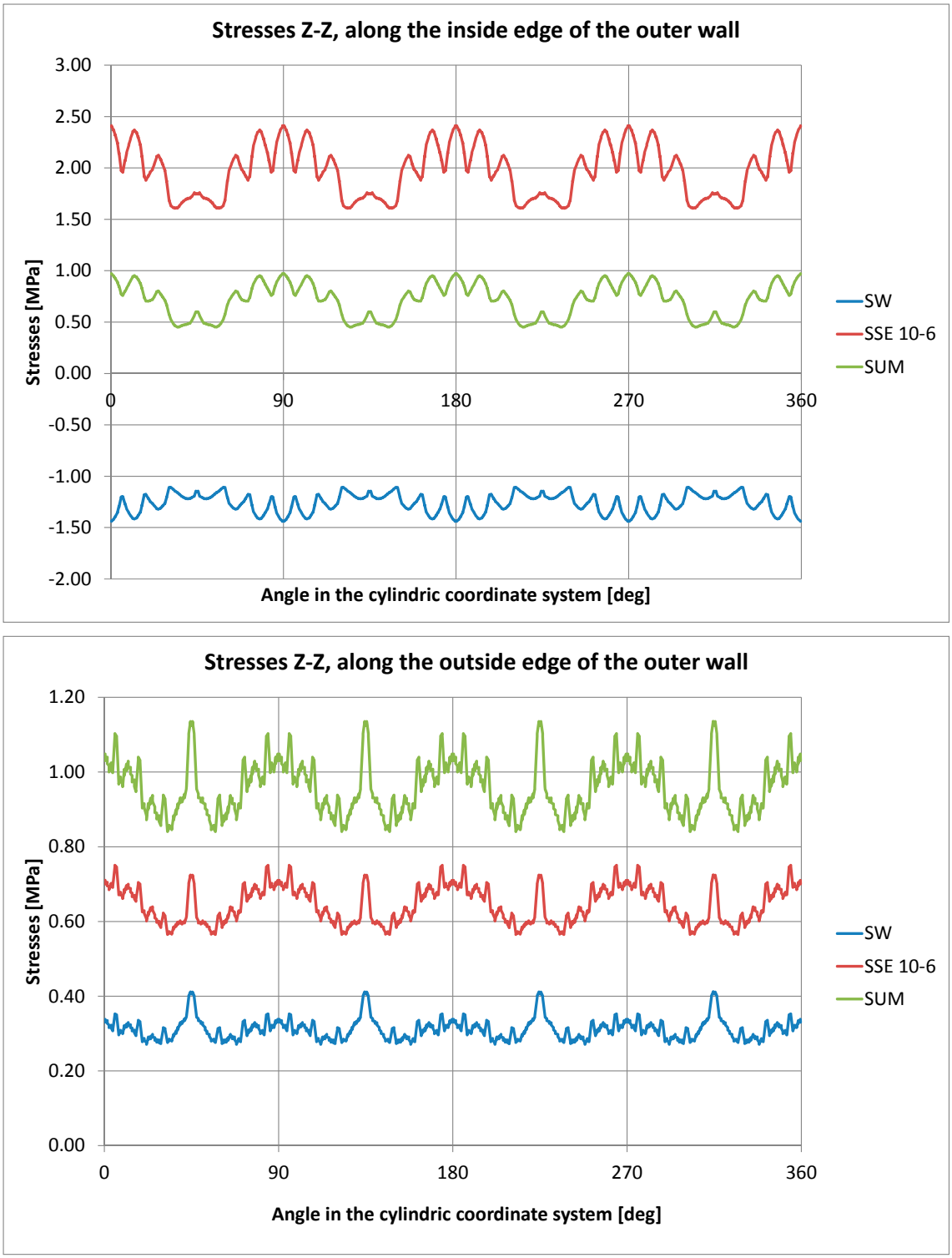

Figure B-21. *Case 1a. Earthquake load combination with SSE 10^{-6}. Vertical stress along the casting joint.*

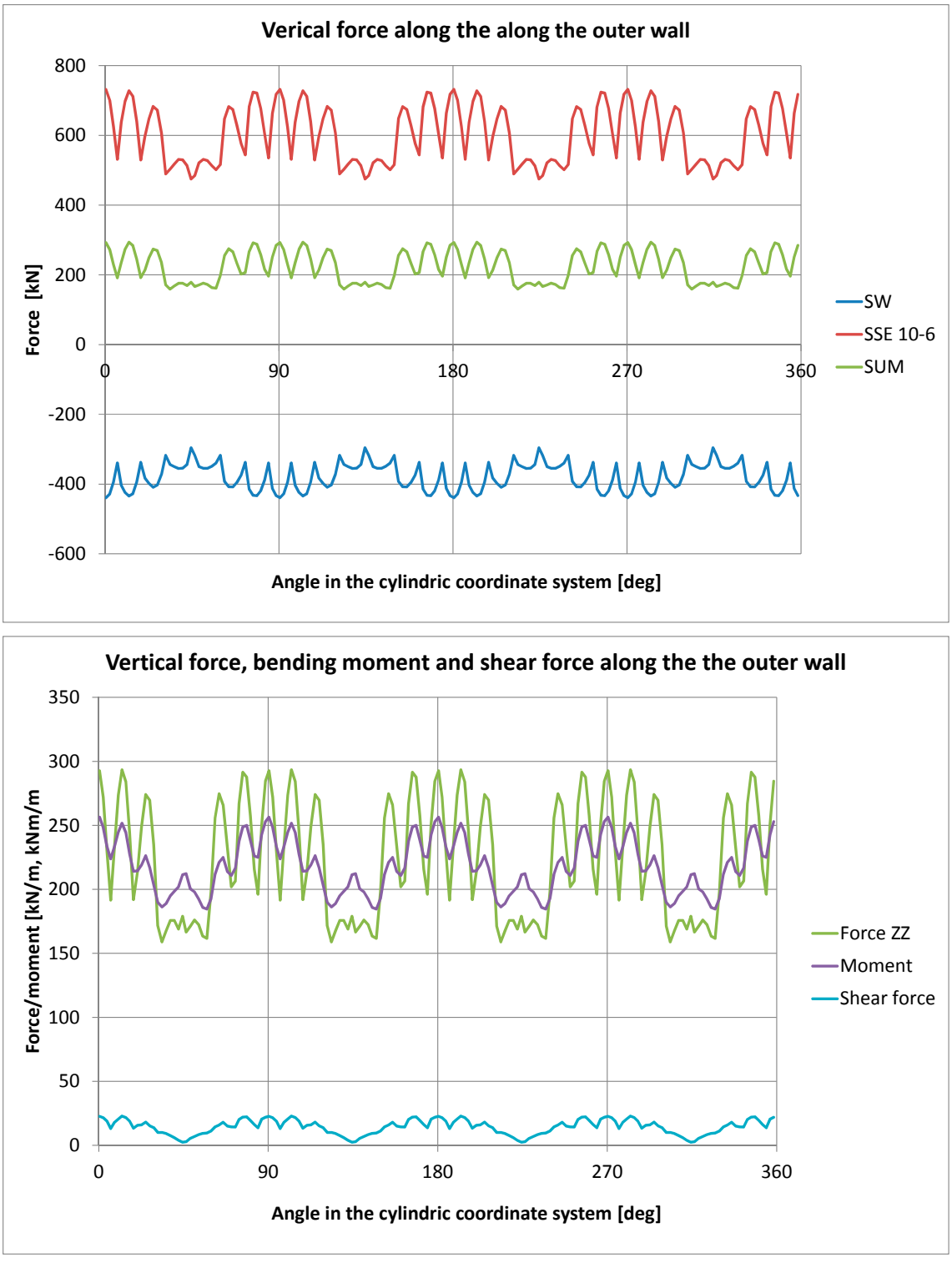

Figure B-22. *Case 1a. Earthquake load combination with SSE 10^{-6}. Forces along the casting joint.*

SSE 10^{-7} case

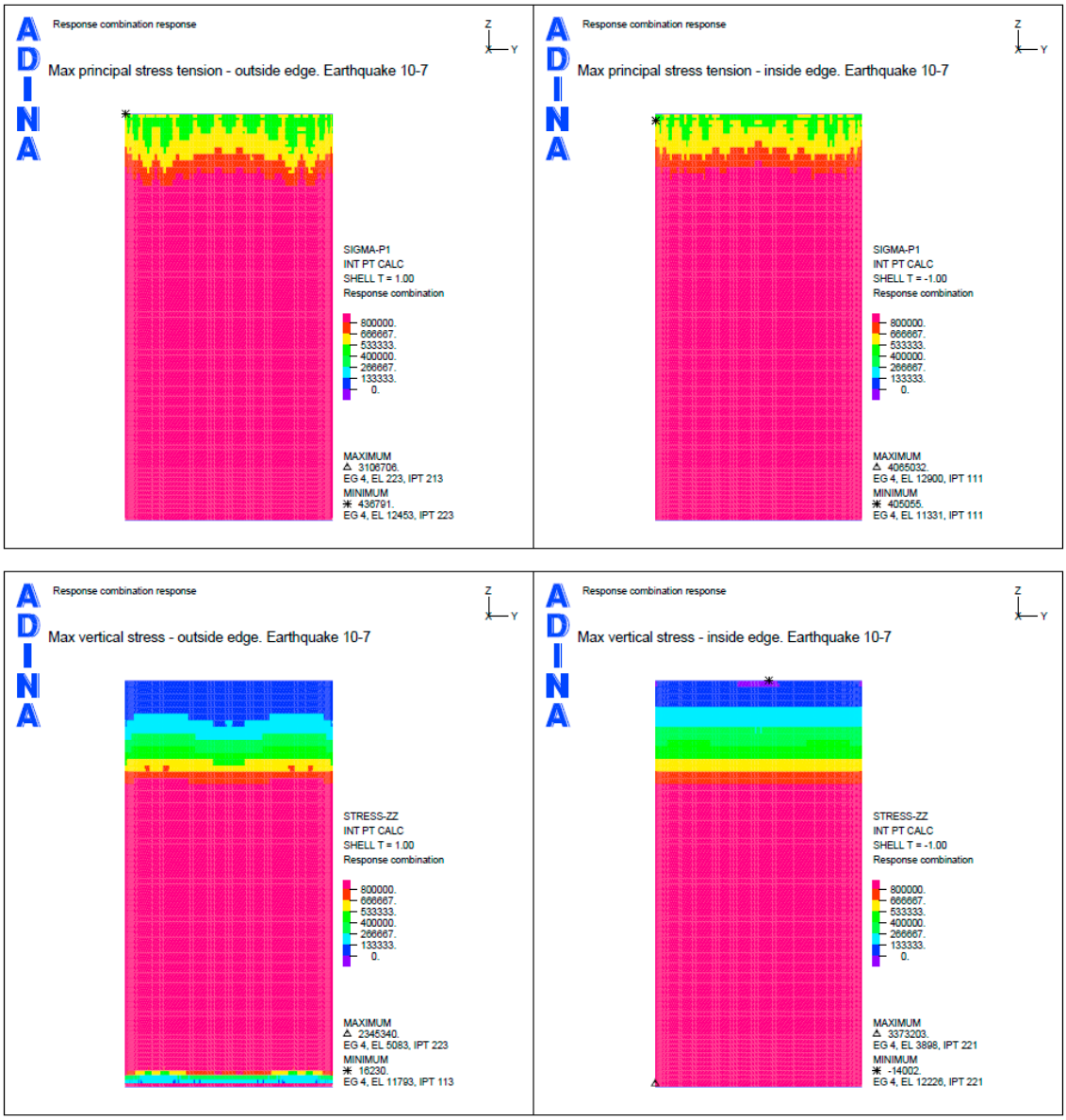

Figure B-23. *Case 1a. Earthquake load combination with SSE 10^{-7}. Max principal tensile stresses and max vertical stresses.*

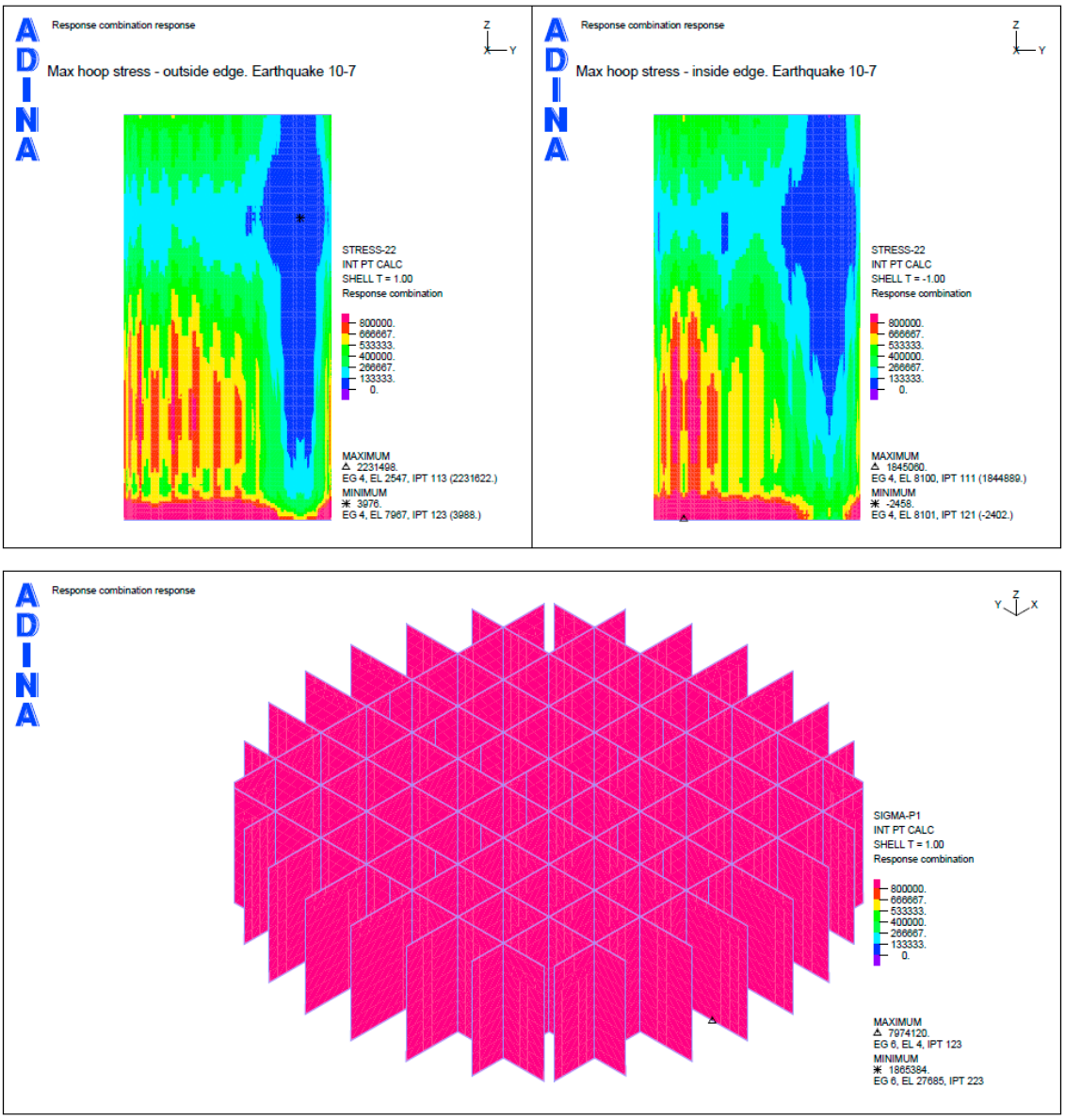

Figure B-24. *Case 1a. Earthquake load combination with SSE 10^{-7}. Max hoop stresses and max principal tensile stresses for the inner wall.*

B4 Case 1b – hinged joint between wall and slab

Static load cases (permanent loads)

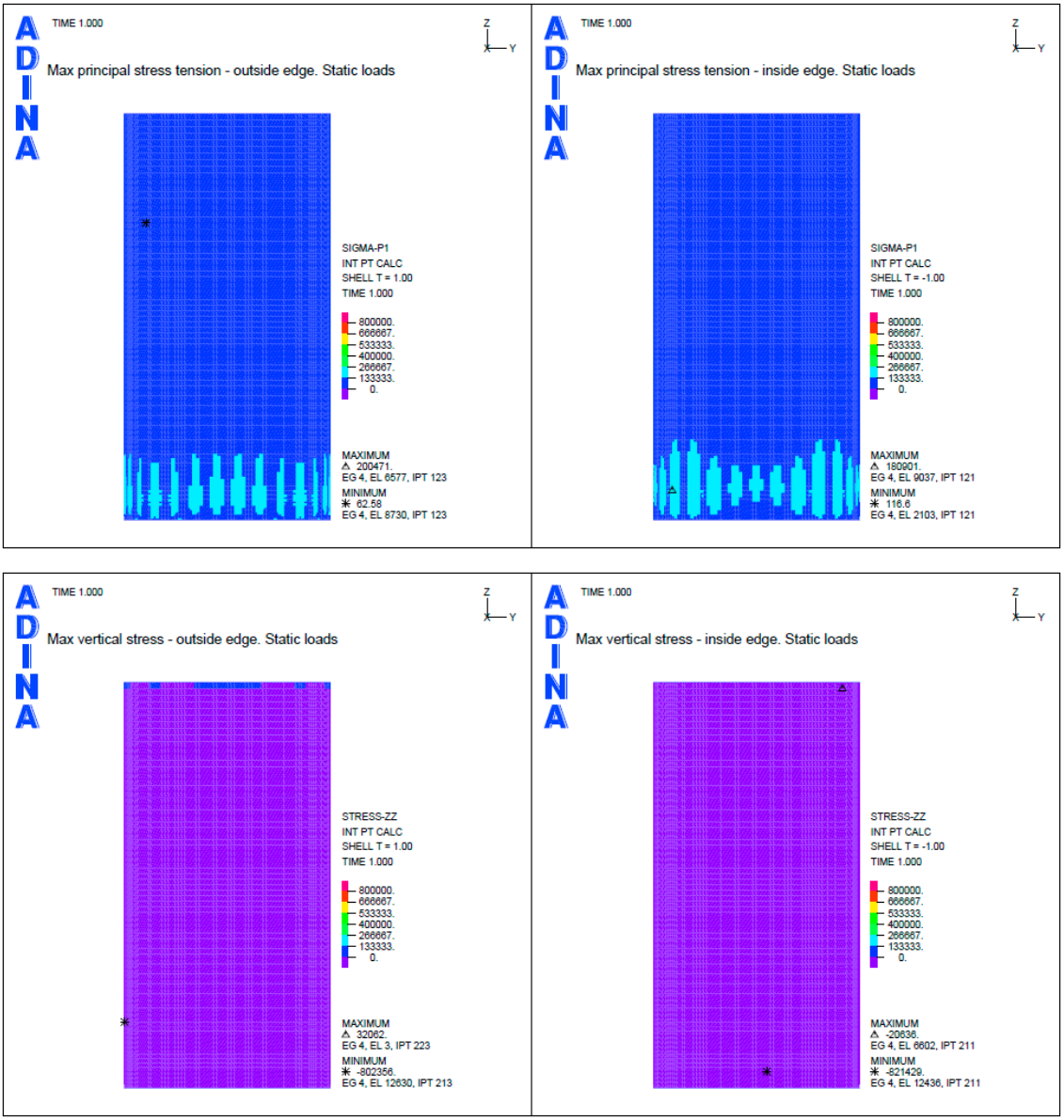

Figure B-25. *Case 1b. Static load cases (permanent loads). Max principal tensile stresses and max vertical stresses.*

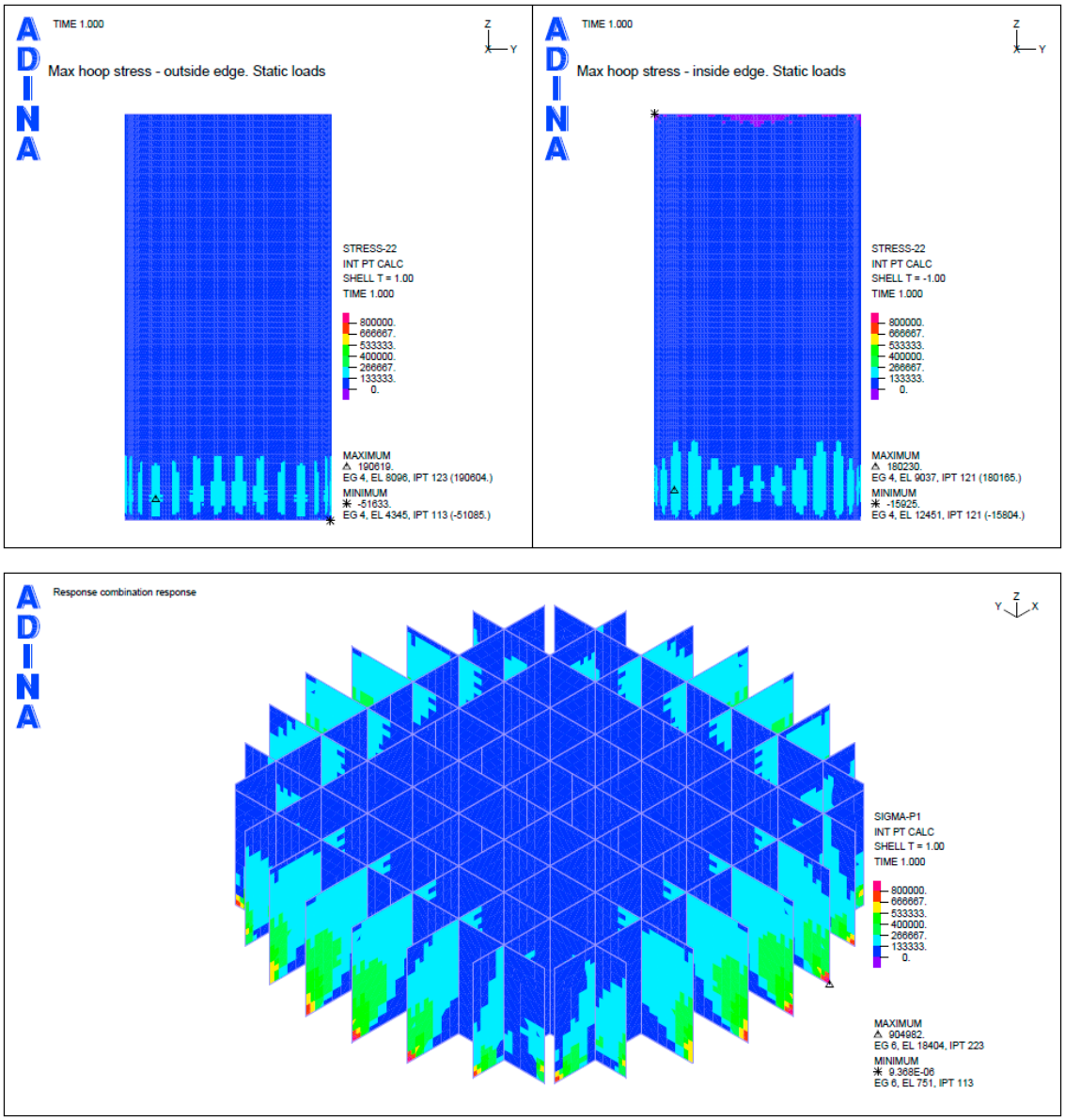

Figure B-26. *Case 1b. Case 1b. Static load cases (permanent loads). Max hoop stresses and max principal tensile stresses for the inner wall.*

SSE 10^{-5} case

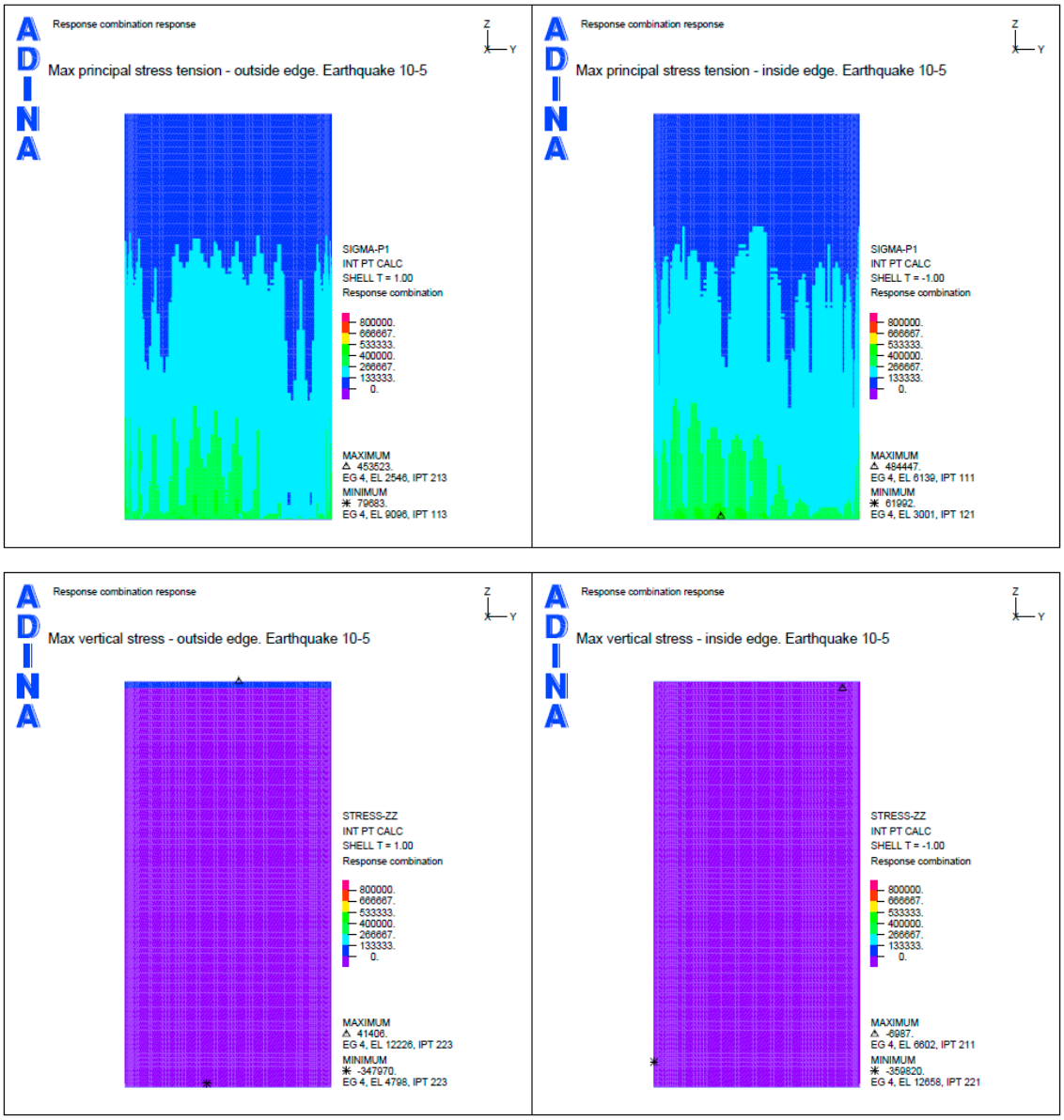

Figure B-27. *Case 1b. Earthquake load combination with SSE 10^{-5}. Max principal tensile stresses and max vertical stresses.*

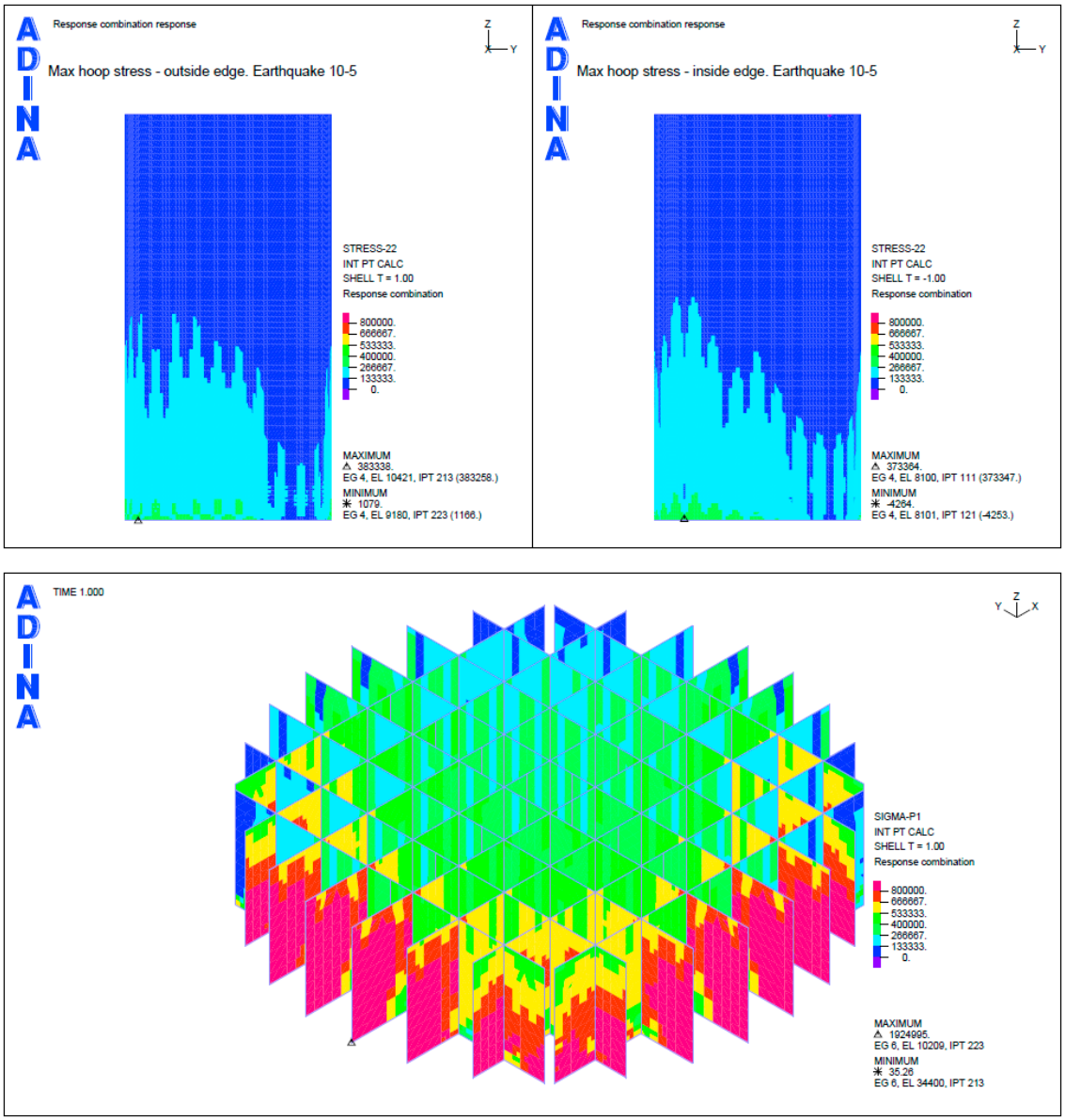

Figure B-28. *Case 1b. Earthquake load combination with SSE 10^{-5}. Max hoop stresses and max principal tensile stresses for the inner wall.*

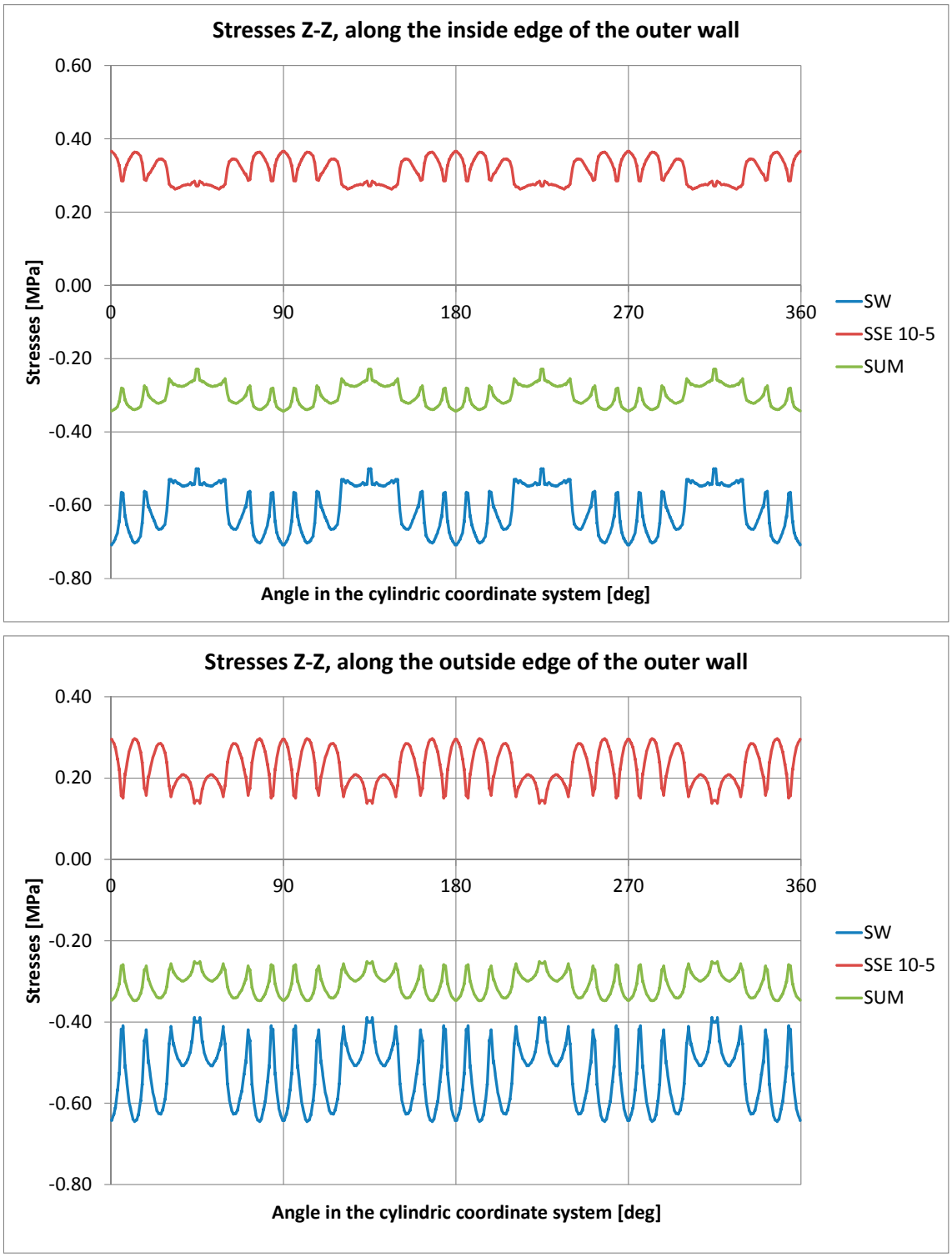

Figure B-29. *Case 1b. Earthquake load combination with SSE 10^{-5}. Vertical stress along the casting joint.*

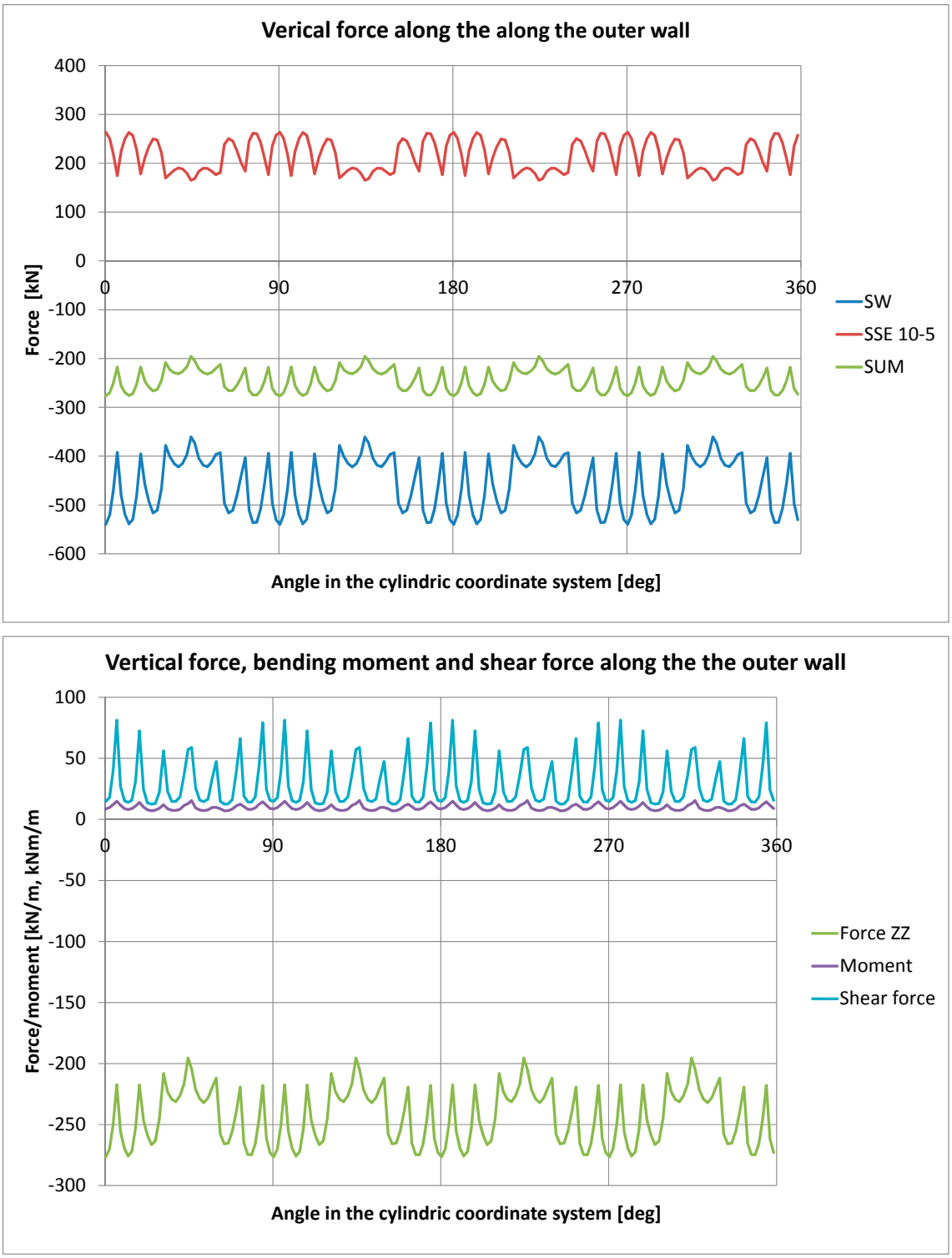

Figure B-30. *Case 1b. Earthquake load combination with SSE 10^{-5}. Forces along the casting joint.*

SSE 10^{-6} case

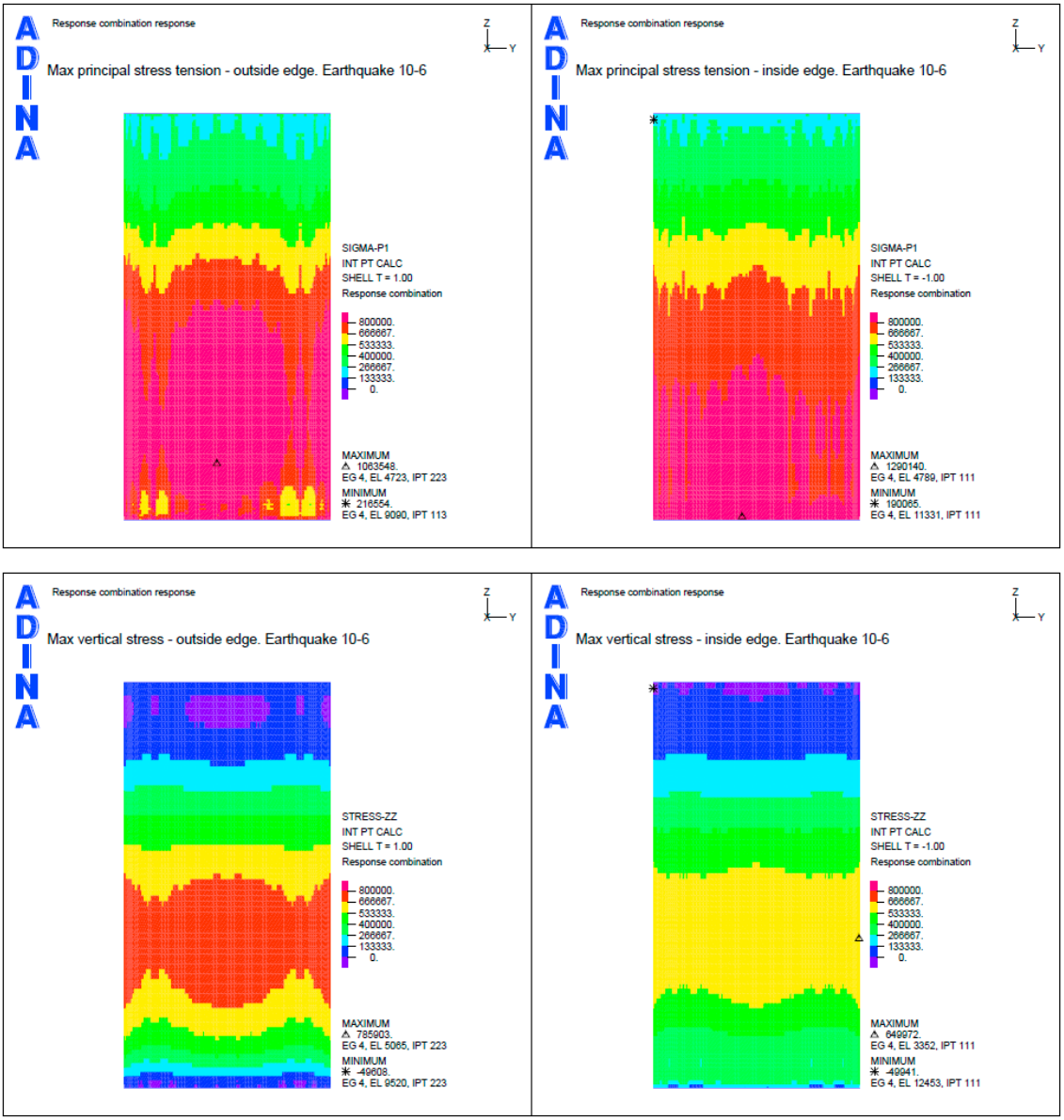

Figure B-31. *Case 1b. Earthquake load combination with SSE 10^{-6}. Max principal tensile stresses and max vertical stresses.*

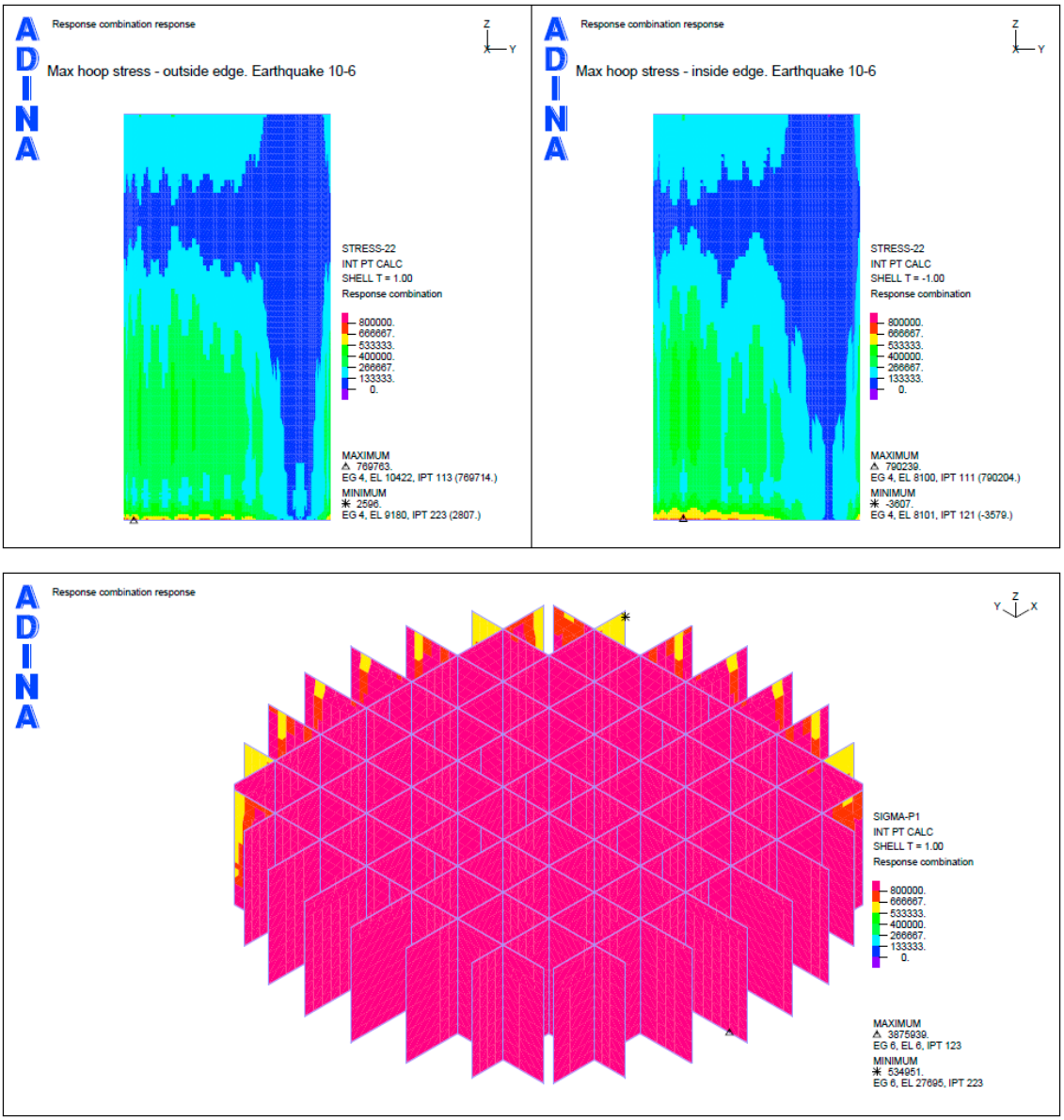

Figure B-32. *Case 1b. Earthquake load combination with SSE 10^{-6}. Max hoop stresses and max principal tensile stresses for the inner wall.*

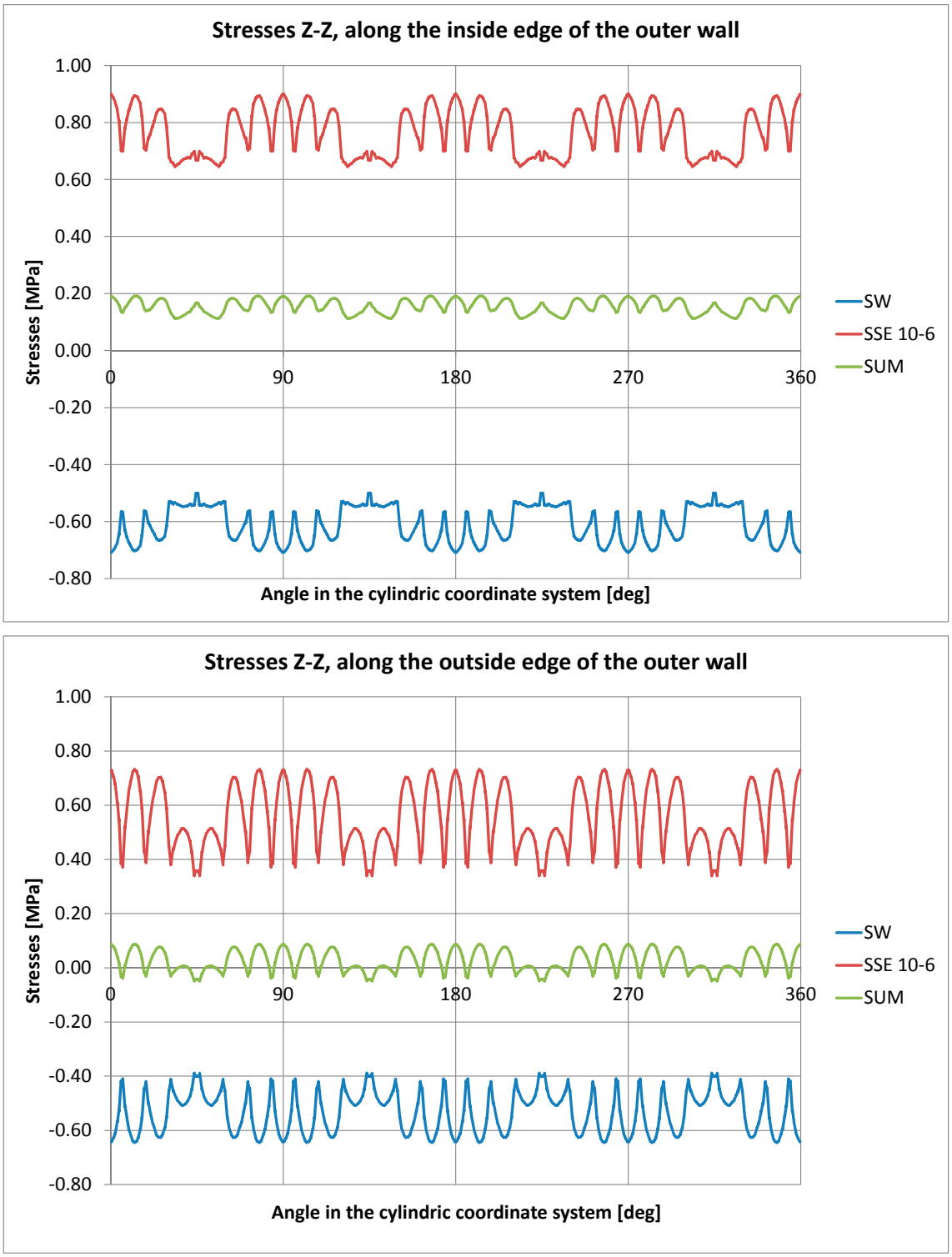

Figure B-33. *Case 1b. Earthquake load combination with SSE 10^{-6}. Vertical stress along the casting joint.*

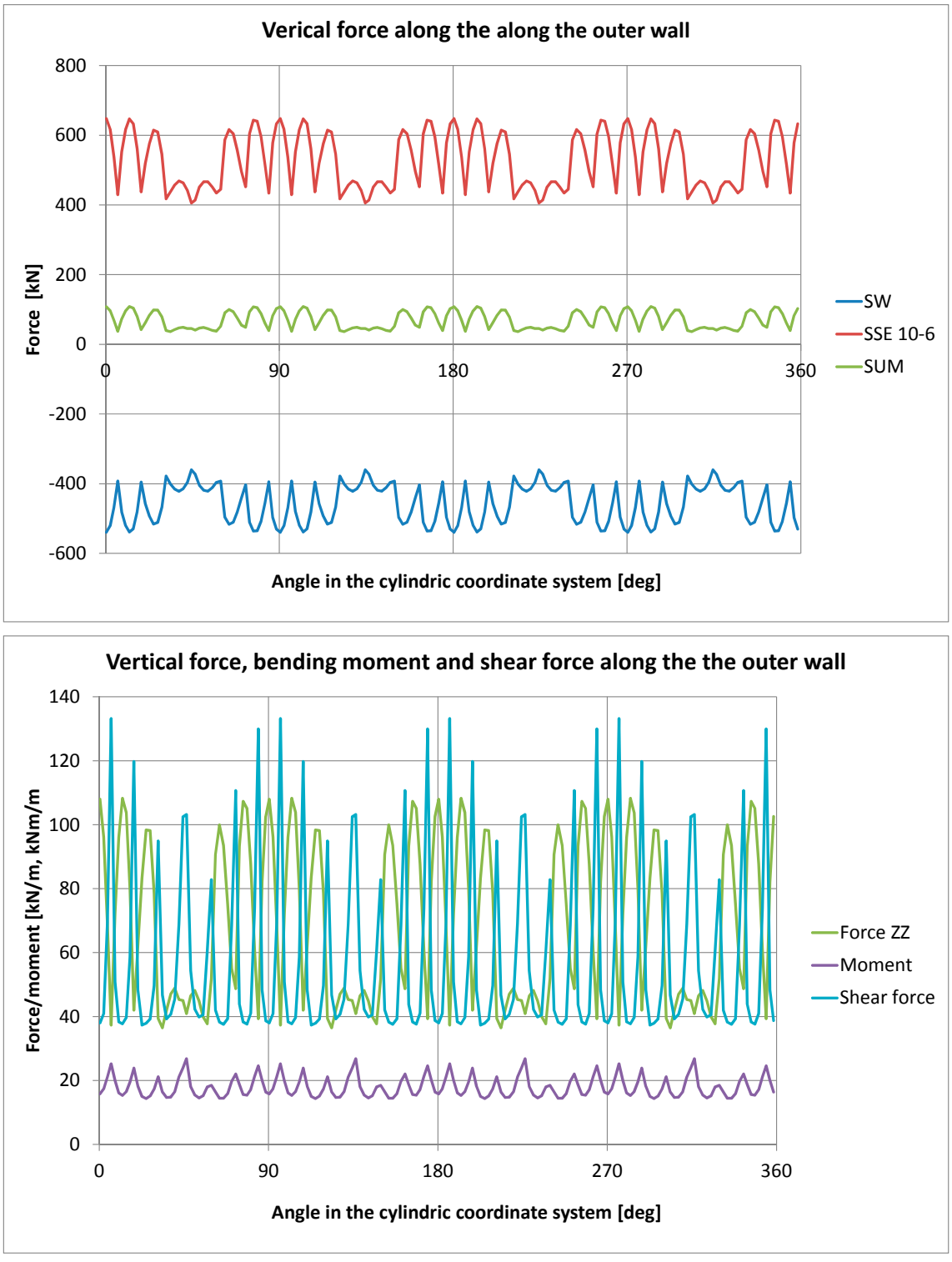

Figure B-34. *Case 1b. Earthquake load combination with SSE 10^{-6}. Forces along the casting joint.*

SSE 10^{-7} case

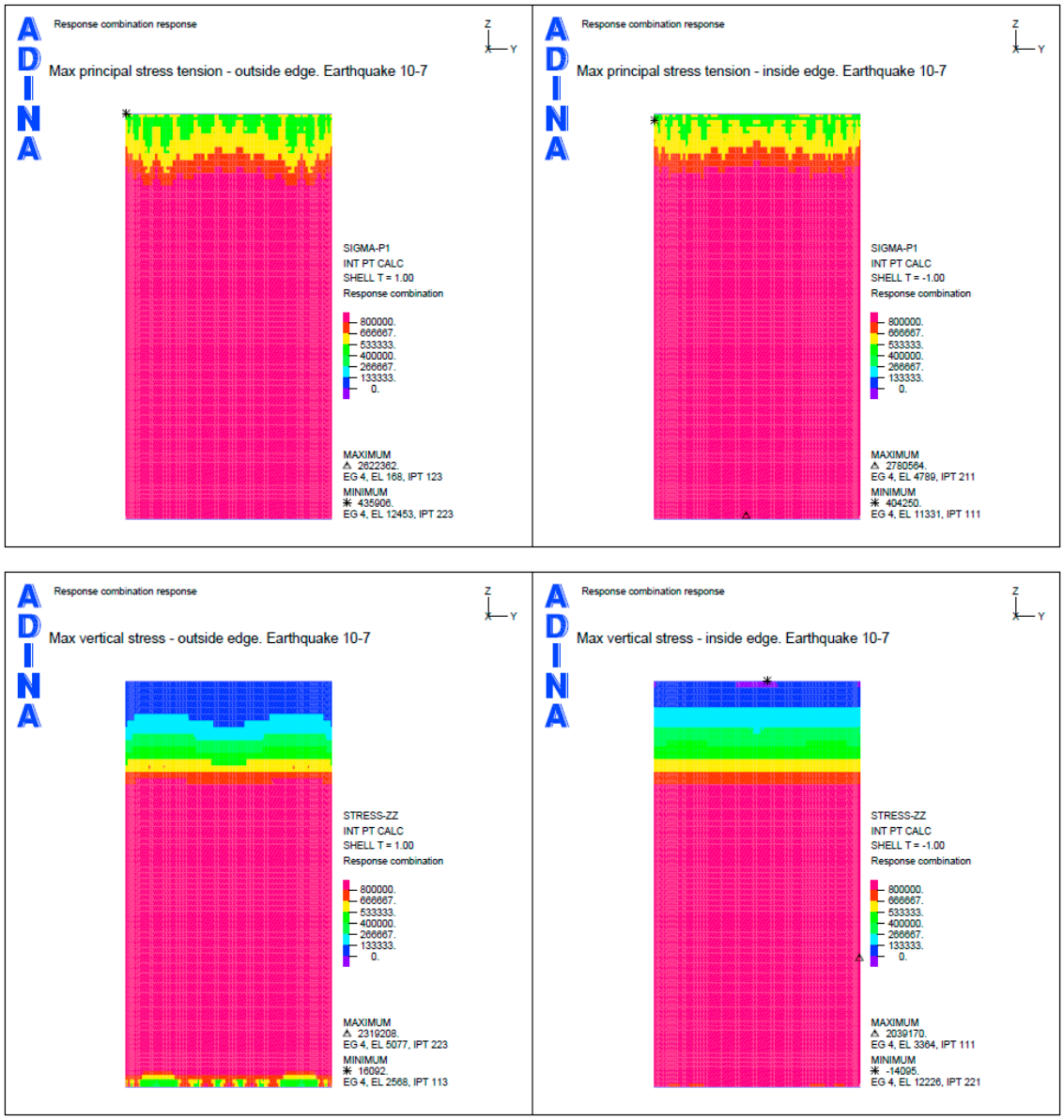

Figure B-35. *Case 1b. Earthquake load combination with SSE 10^{-7}. Max principal tensile stresses and max vertical stresses.*

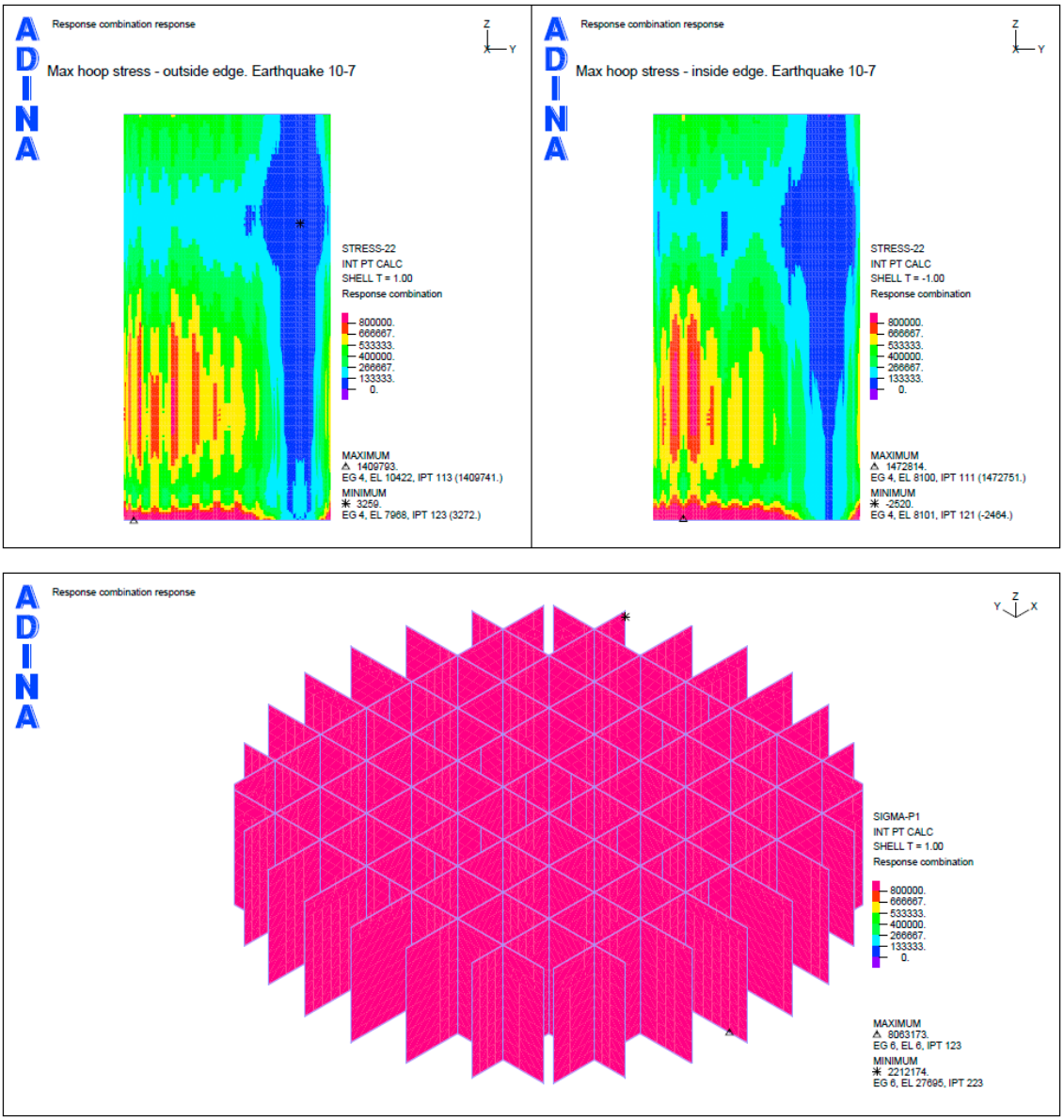

Figure B-36. *Case 1b. Earthquake load combination with SSE 10^{-7}. Max hoop stresses and max principal tensile stresses for the inner wall.*

B5 Case 1b (reduced outer wall thickness) – hinged joint between wall and slab

Static load cases (permanent loads)

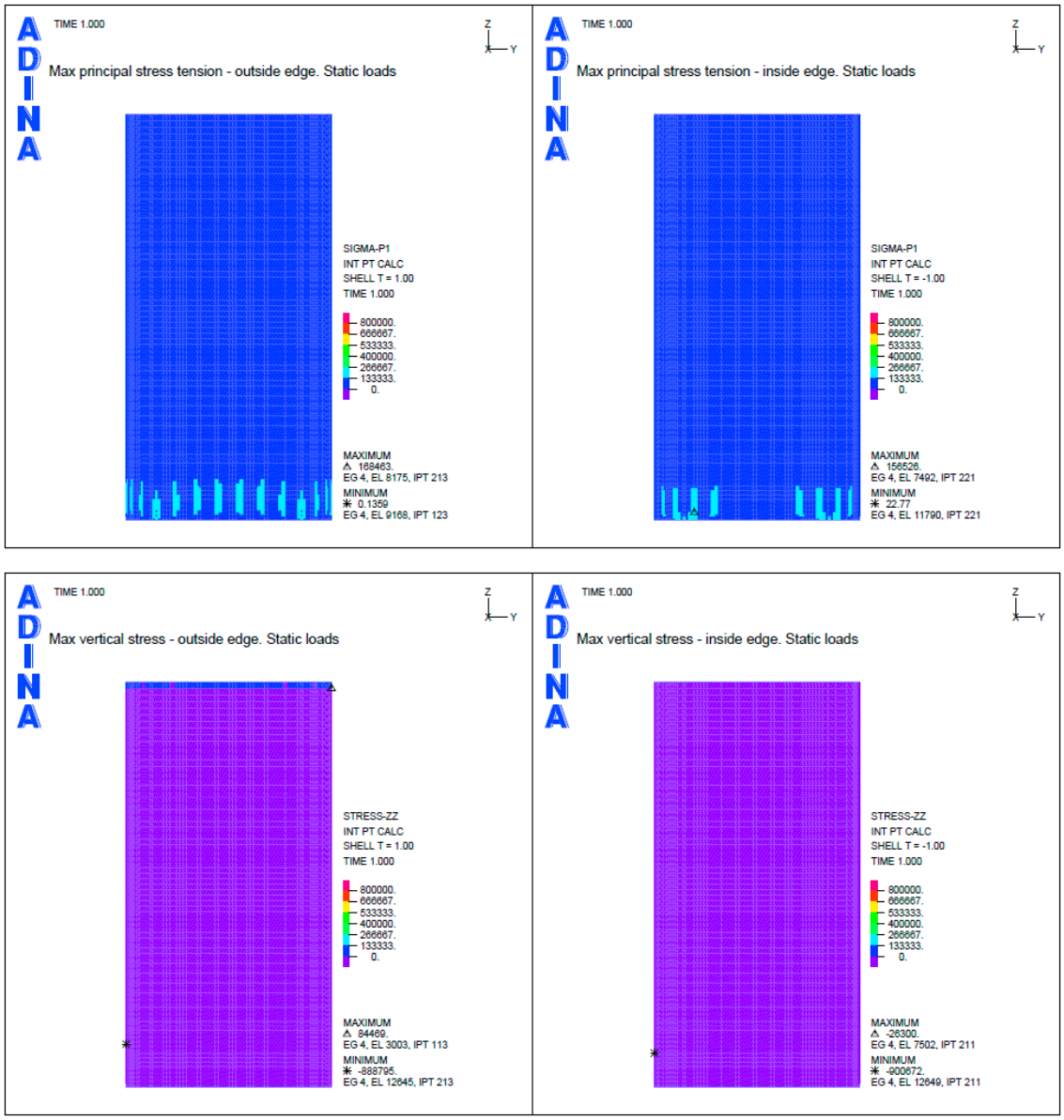

Figure B-37. *Case 1b (reduced wall thickness). Static load cases (permanent loads). Max principal tensile stresses and max vertical stresses.*

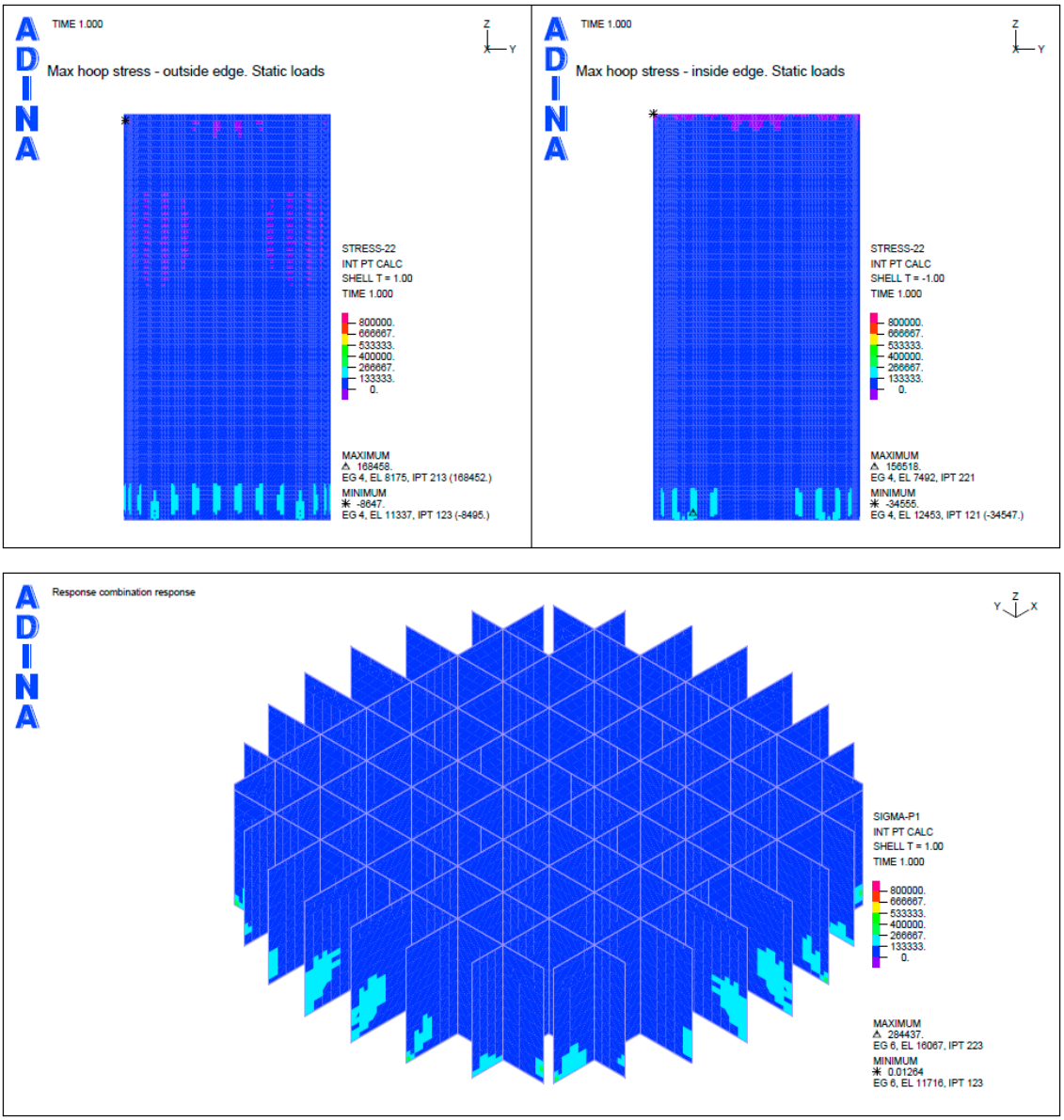

Figure B-38. *Case 1b (reduced wall thickness). Static load cases (permanent loads). Max hoop stresses and max principal tensile stresses for the inner wall.*

SSE 10^{-5} case

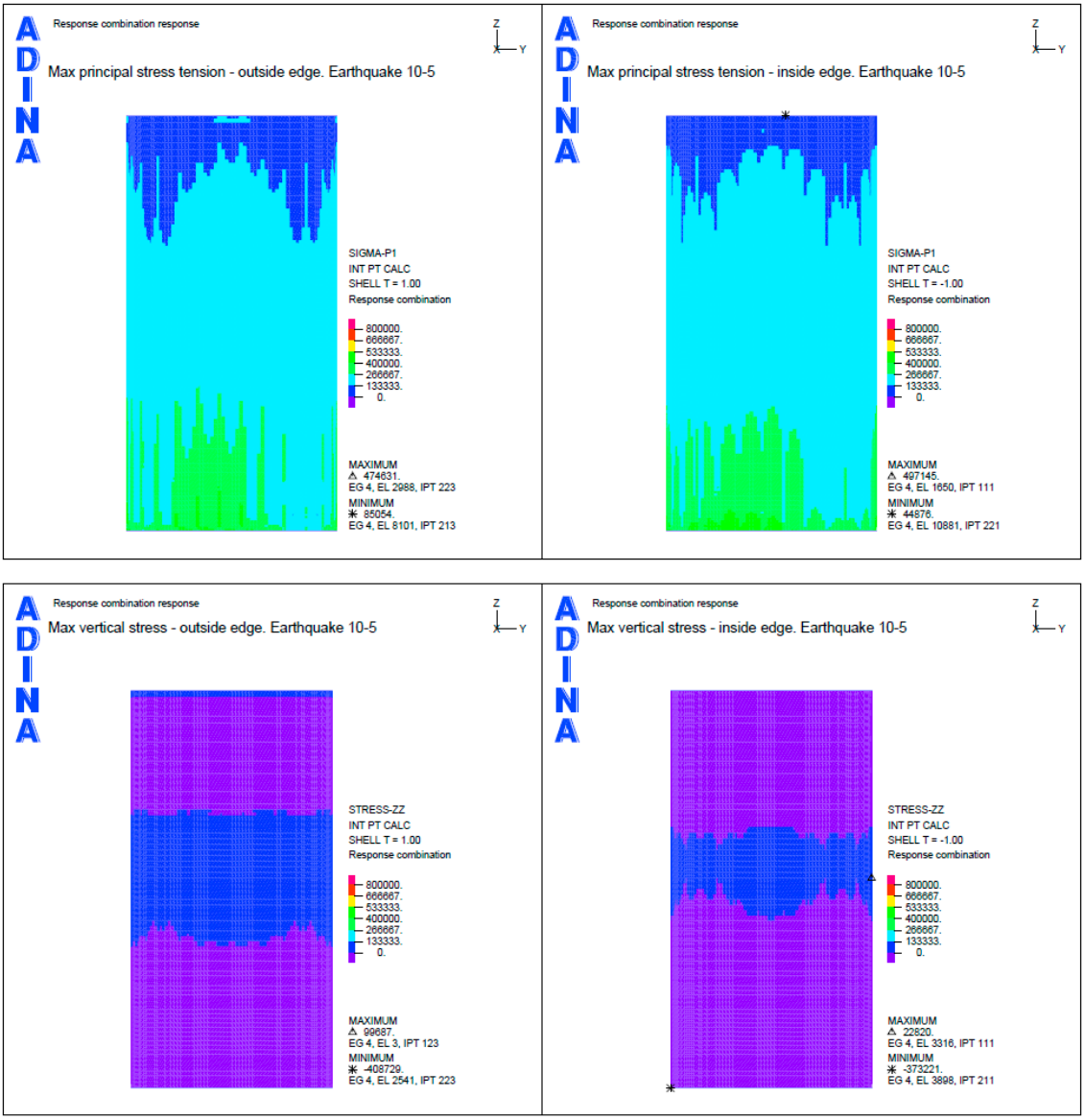

Figure B-39. *Case 1b (reduced wall thickness). Earthquake load combination with SSE 10^{-5}. Max principal tensile stresses and max vertical stresses.*

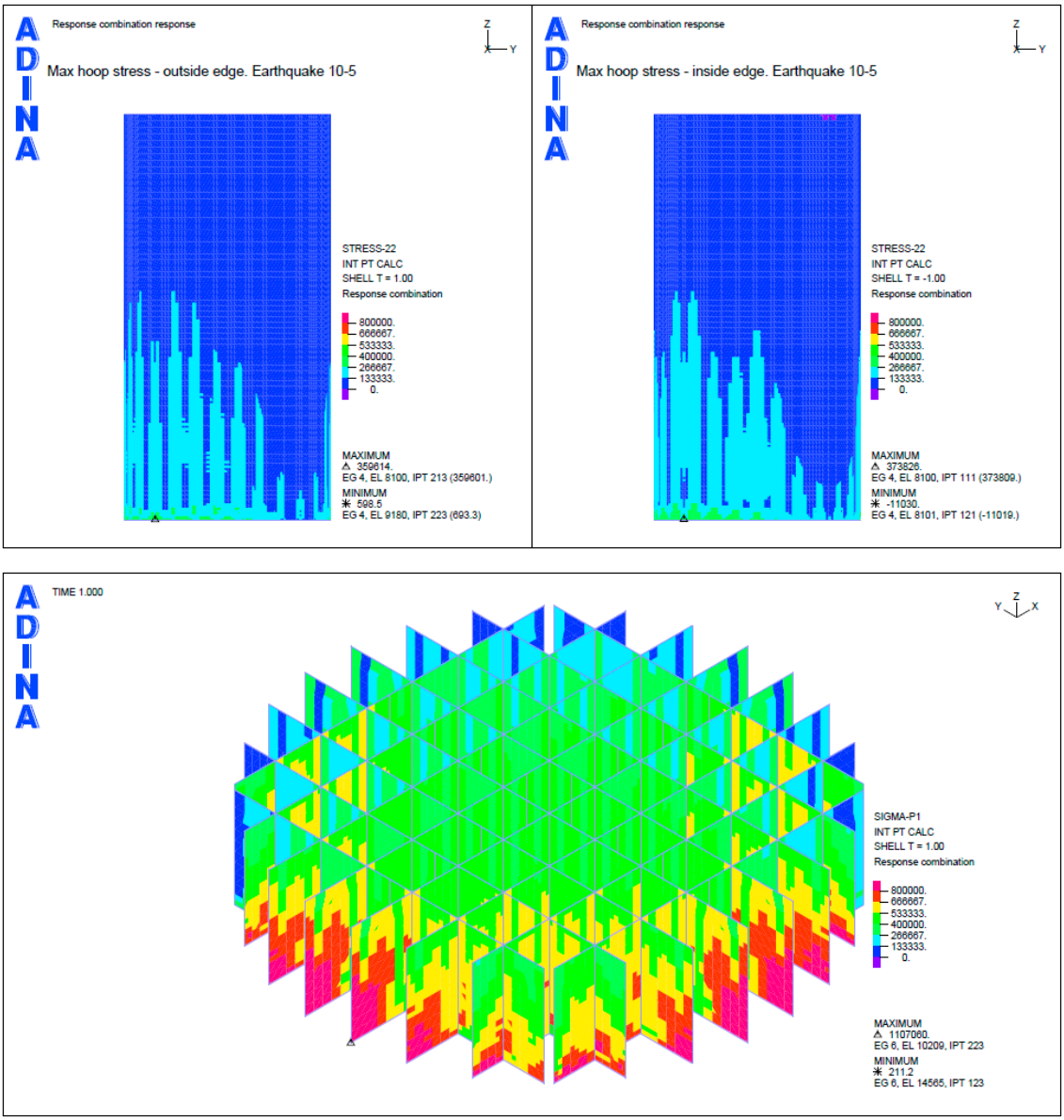

Figure B-40. *Case 1b (reduced wall thickness). Earthquake load combination with SSE 10^{-5}. Max hoop stresses and max principal tensile stresses for the inner wall.*

SSE 10^{-6} case

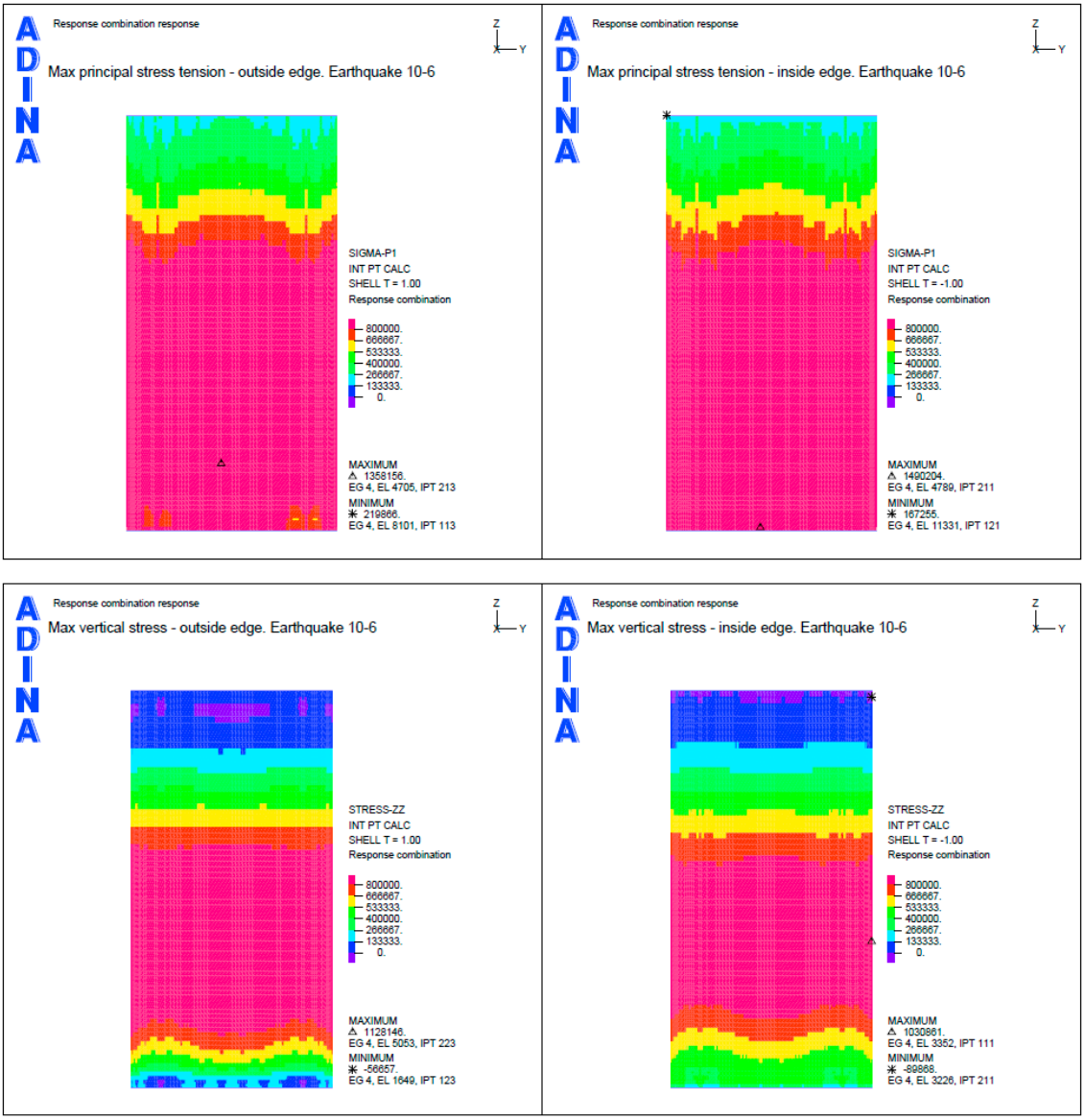

Figure B-41. *Case 1b (reduced wall thickness). Earthquake load combination with SSE 10^{-6}. Max principal tensile stresses and max vertical stresses.*

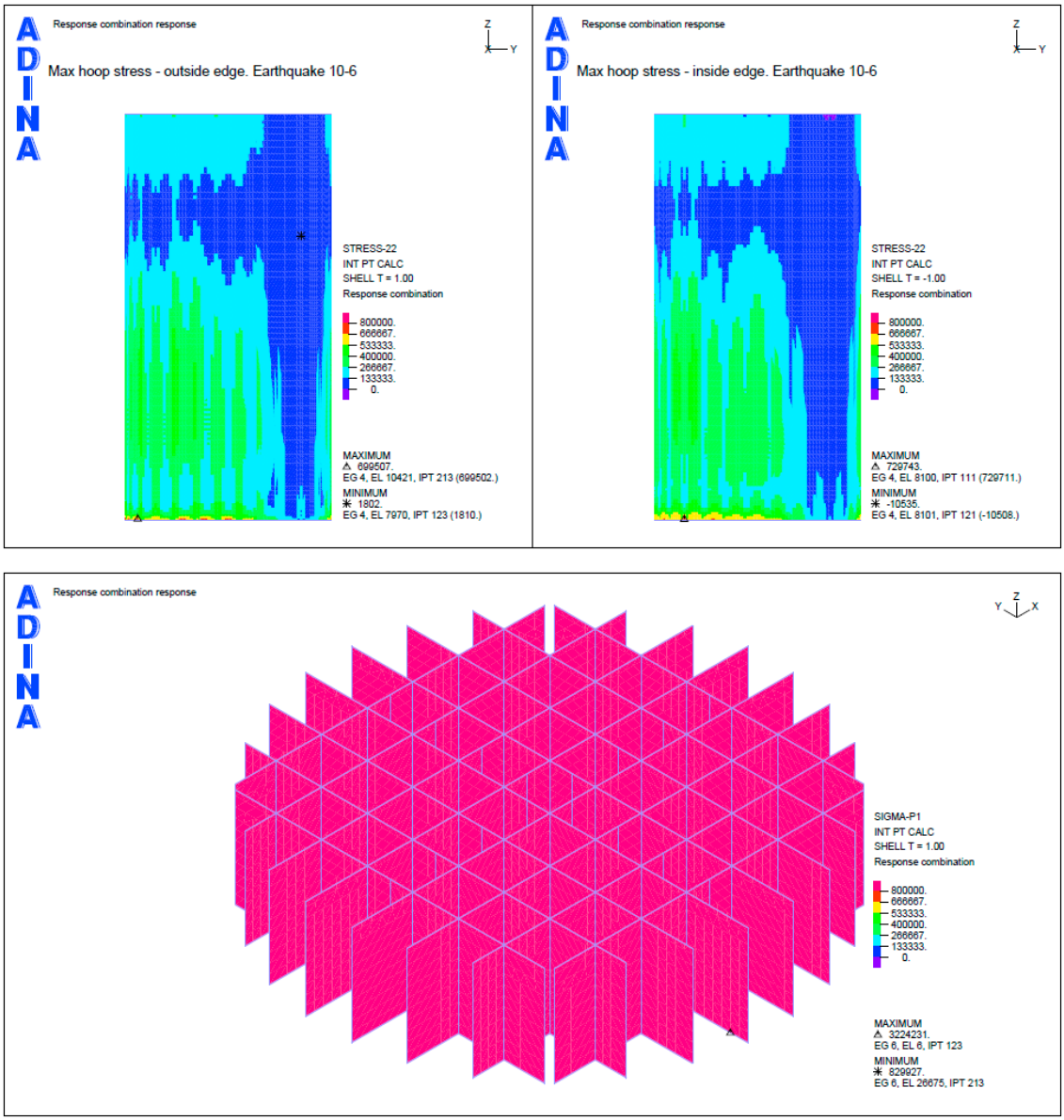

Figure B-42. *Case 1b (reduced wall thickness). Earthquake load combination with SSE 10^{-6}. Max hoop stresses and max principal tensile stresses for the inner wall.*

SSE 10^{-7} case

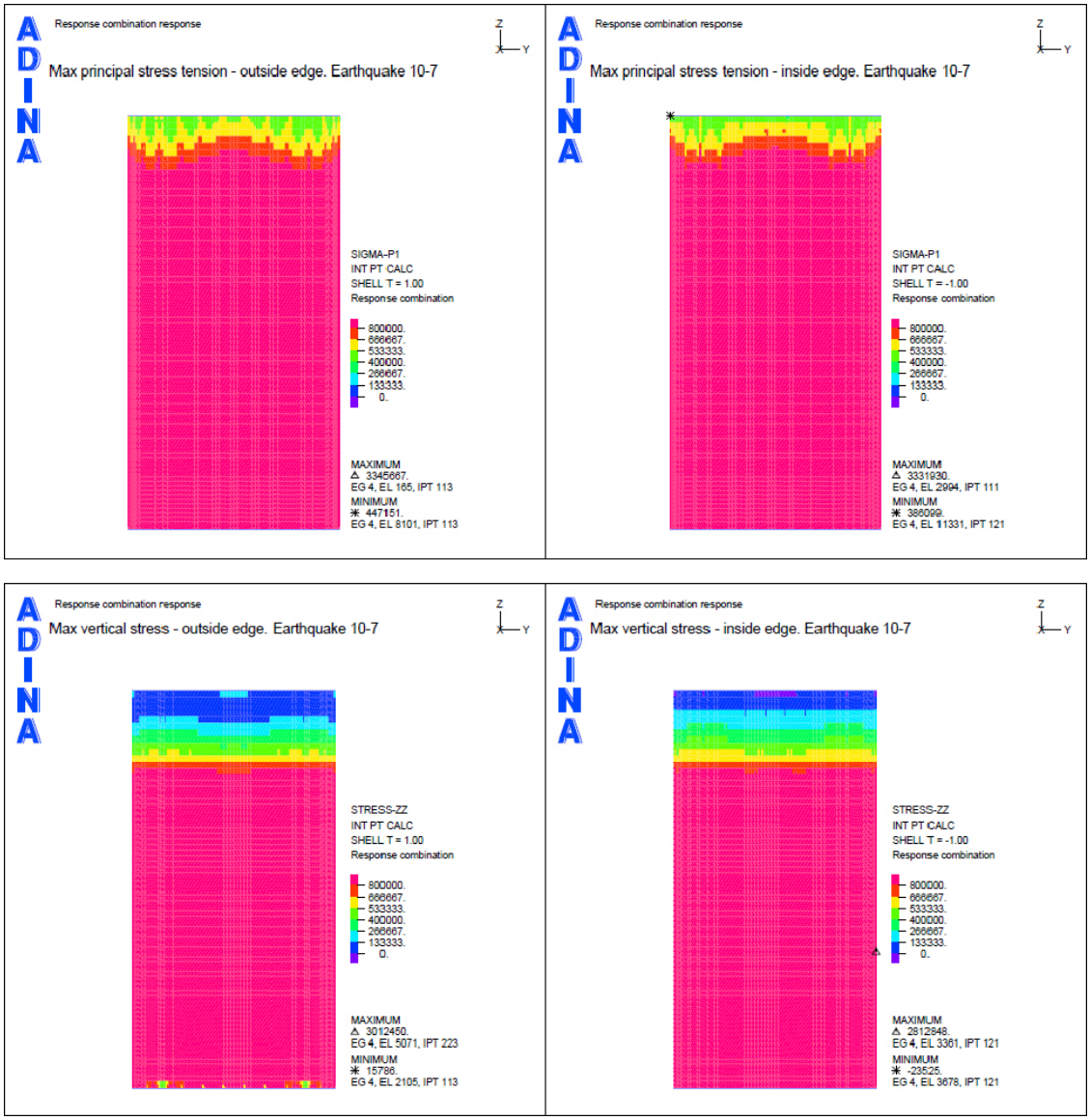

Figure B-43. *Case 1b (reduced wall thickness). Earthquake load combination with SSE 10^{-7}. Max principal tensile stresses and max vertical stresses.*

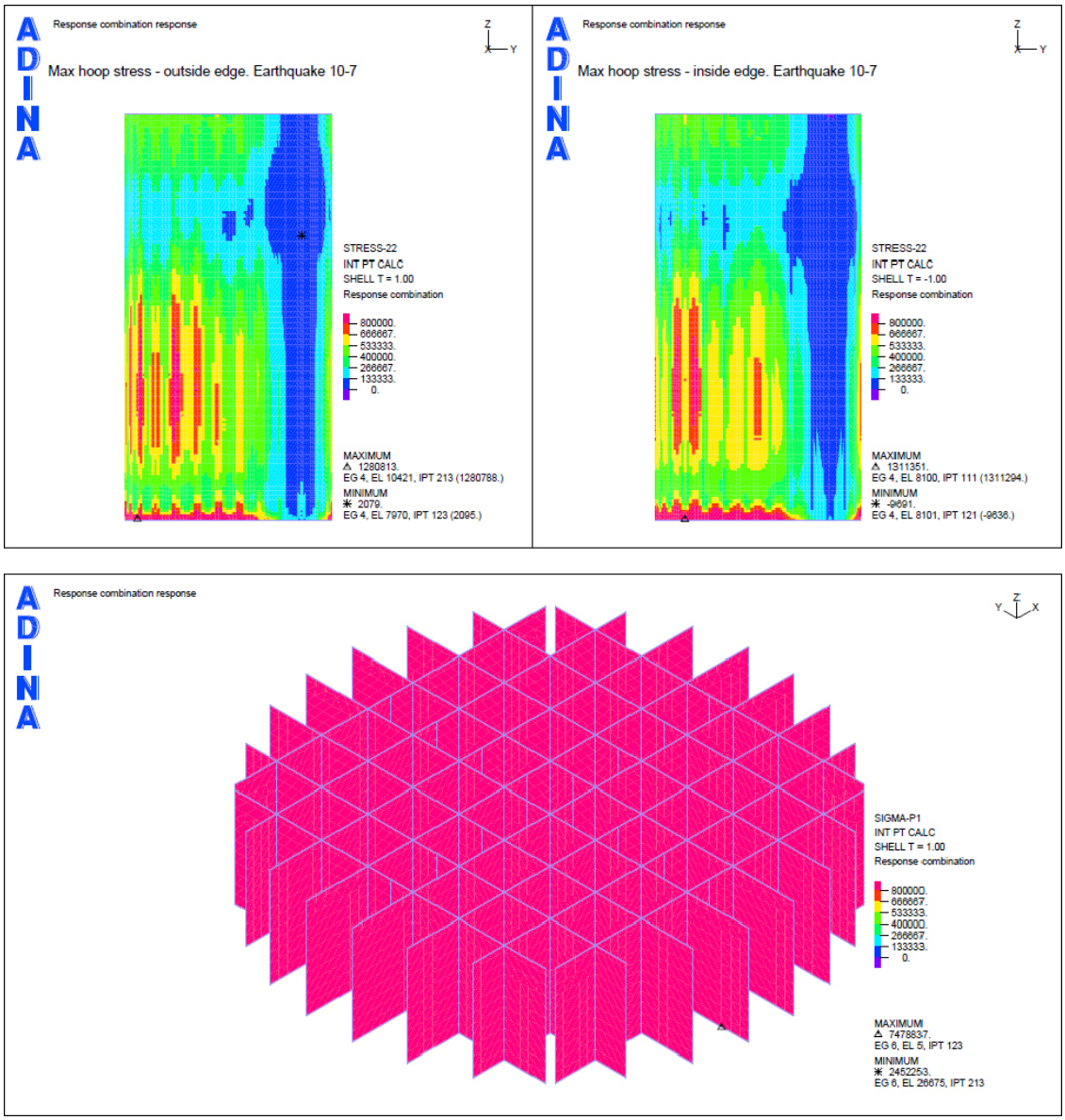

Figure B-44. *Case 1b (reduced wall thickness). Earthquake load combination with SSE 10^{-7}. Max hoop stresses and max principal tensile stresses for the inner wall.*

B6 Case 2a – rigid connection between wall and slab

Static load cases (permanent loads)

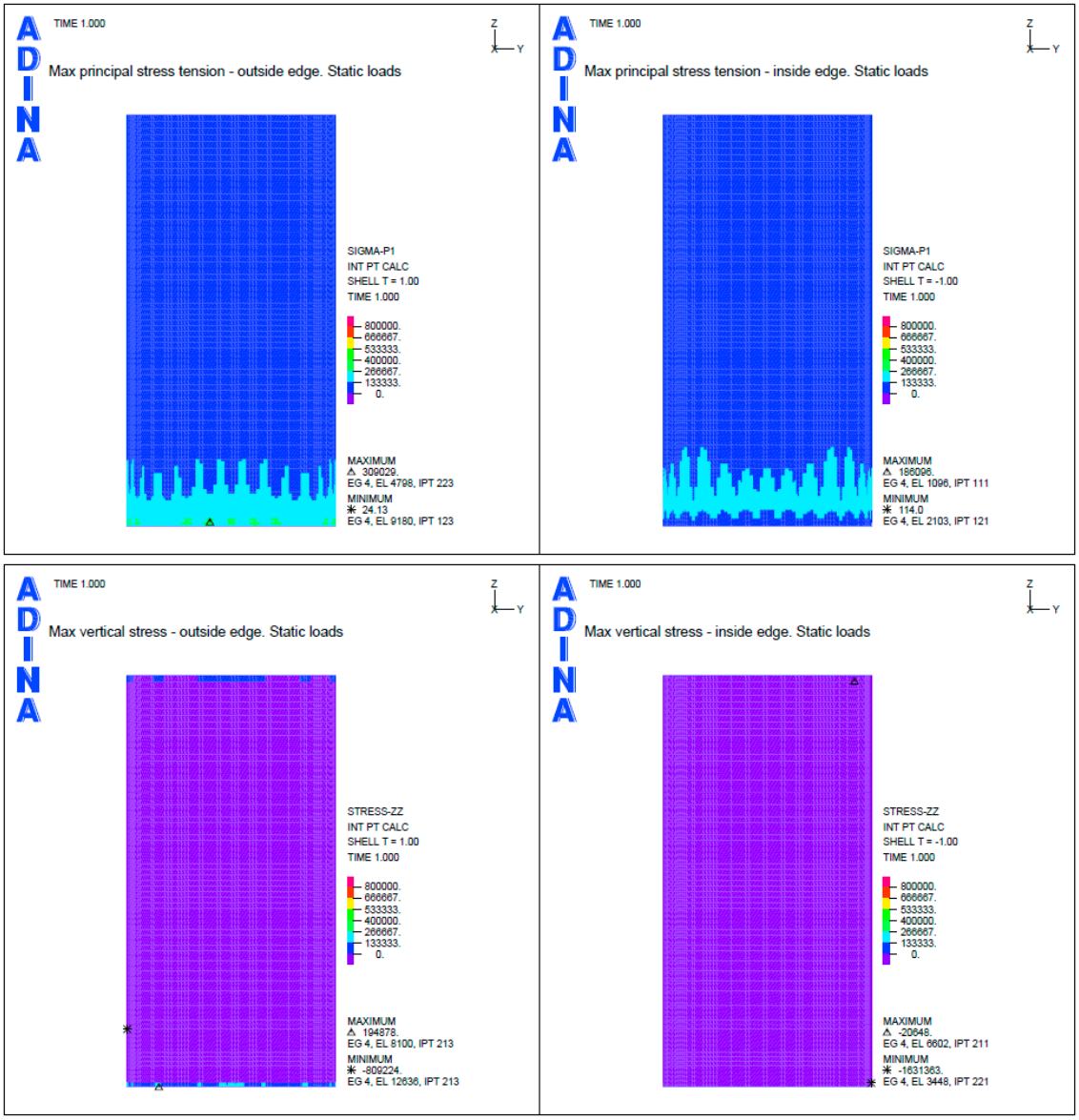

Figure B-45. *Case 2a. Static load cases (permanent loads). Max principal tensile stresses and max vertical stresses.*

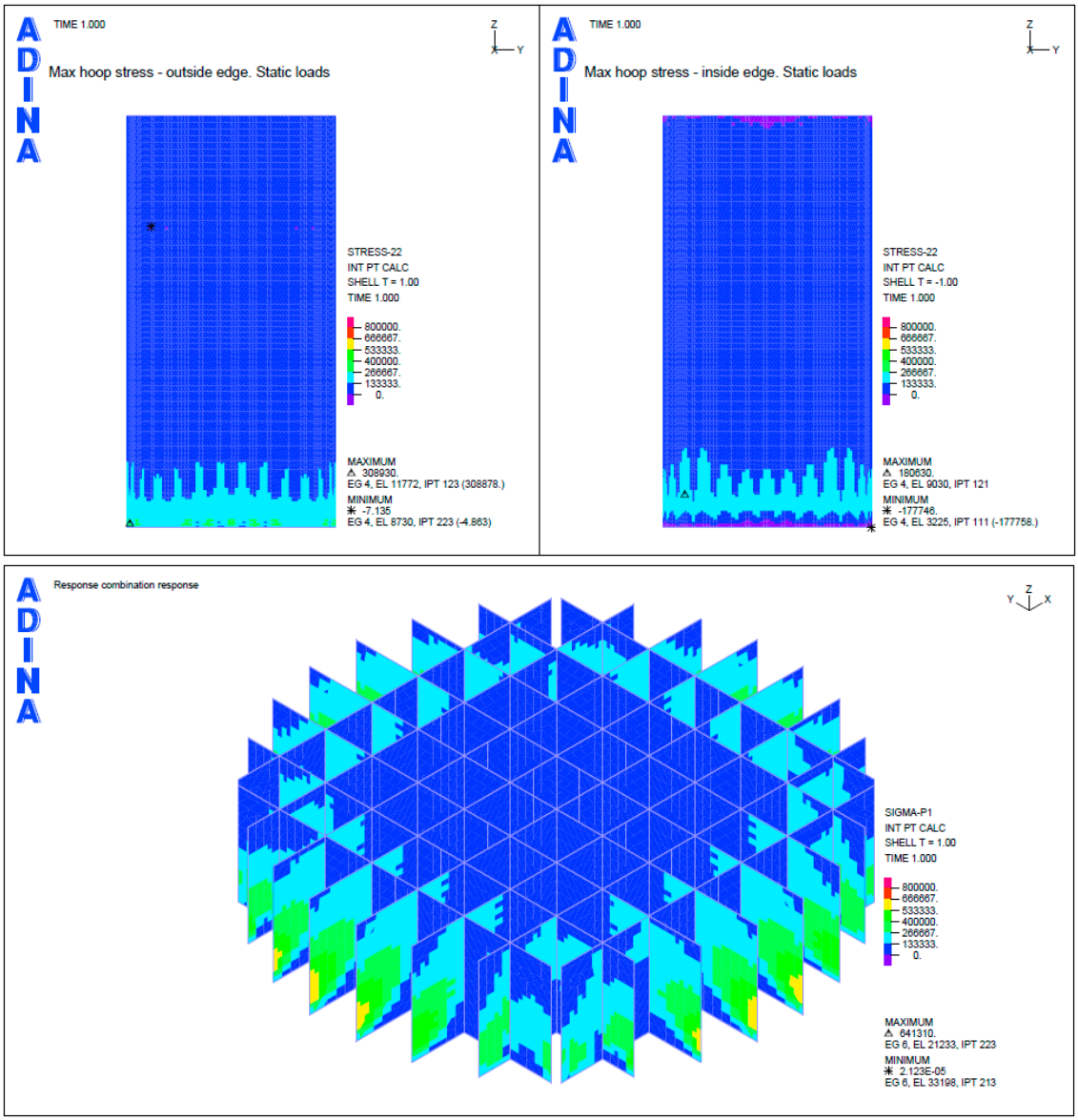

Figure B-46. *Case 2a. Static load cases (permanent loads). Max hoop stresses and max principal tensile stresses for the inner wall.*

SSE 10^{-5} case

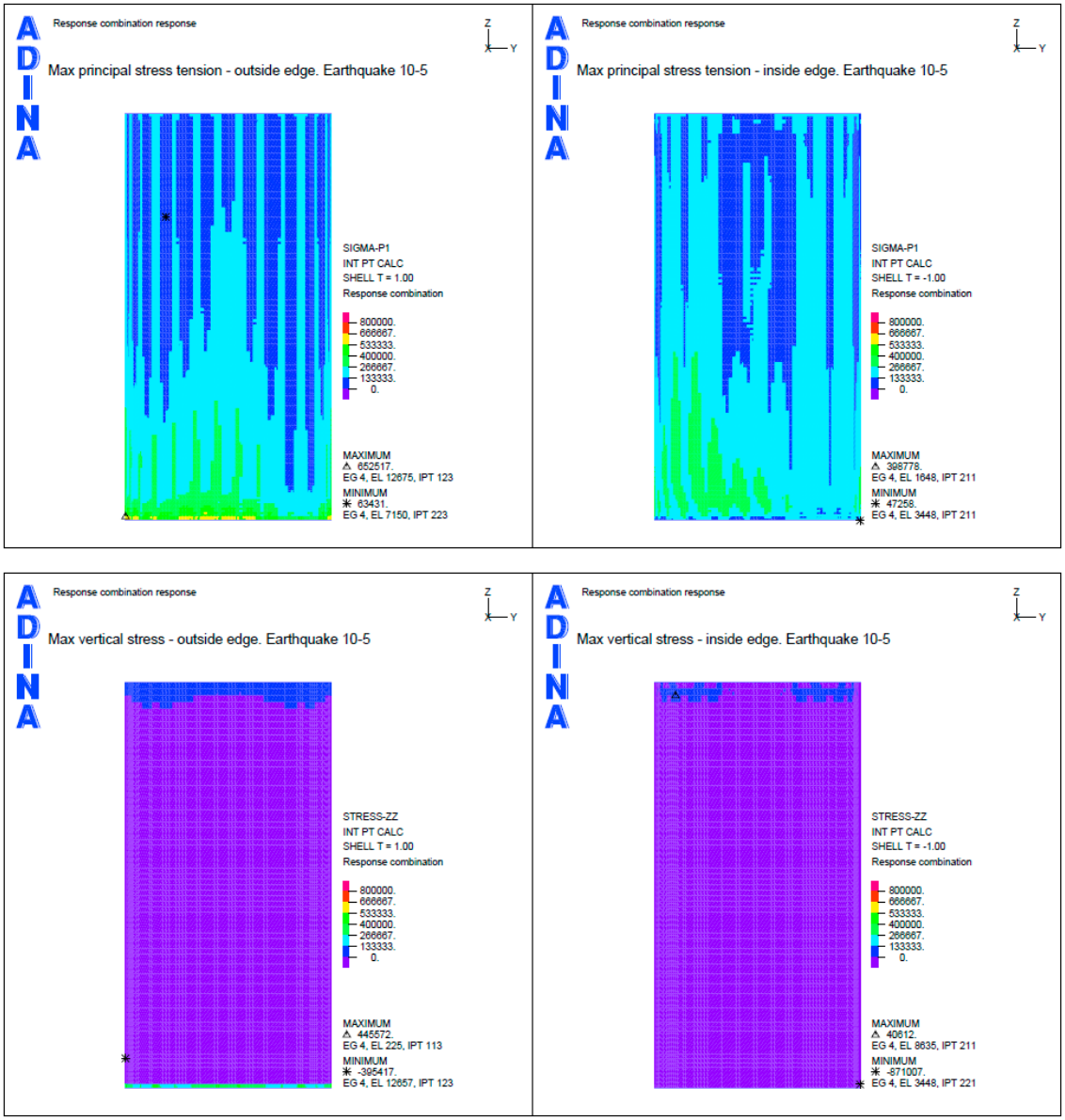

Figure B-47. *Case 2a. Earthquake load combination with SSE 10^{-5}. Max principal tensile stresses and max vertical stresses.*

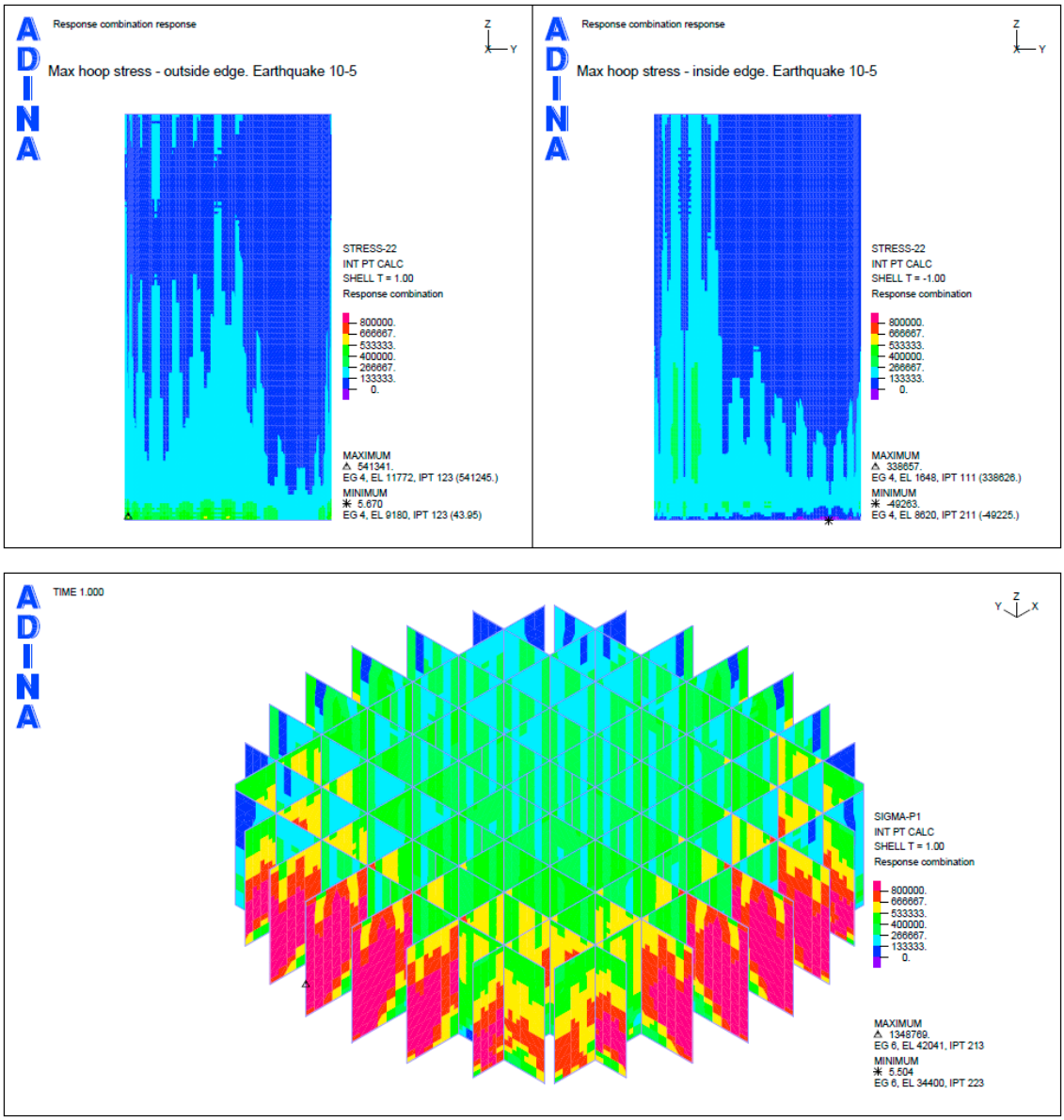

Figure B-48. *Case 2a. Earthquake load combination with SSE 10^{-5}. Max hoop stresses and max principal tensile stresses for the inner wall.*

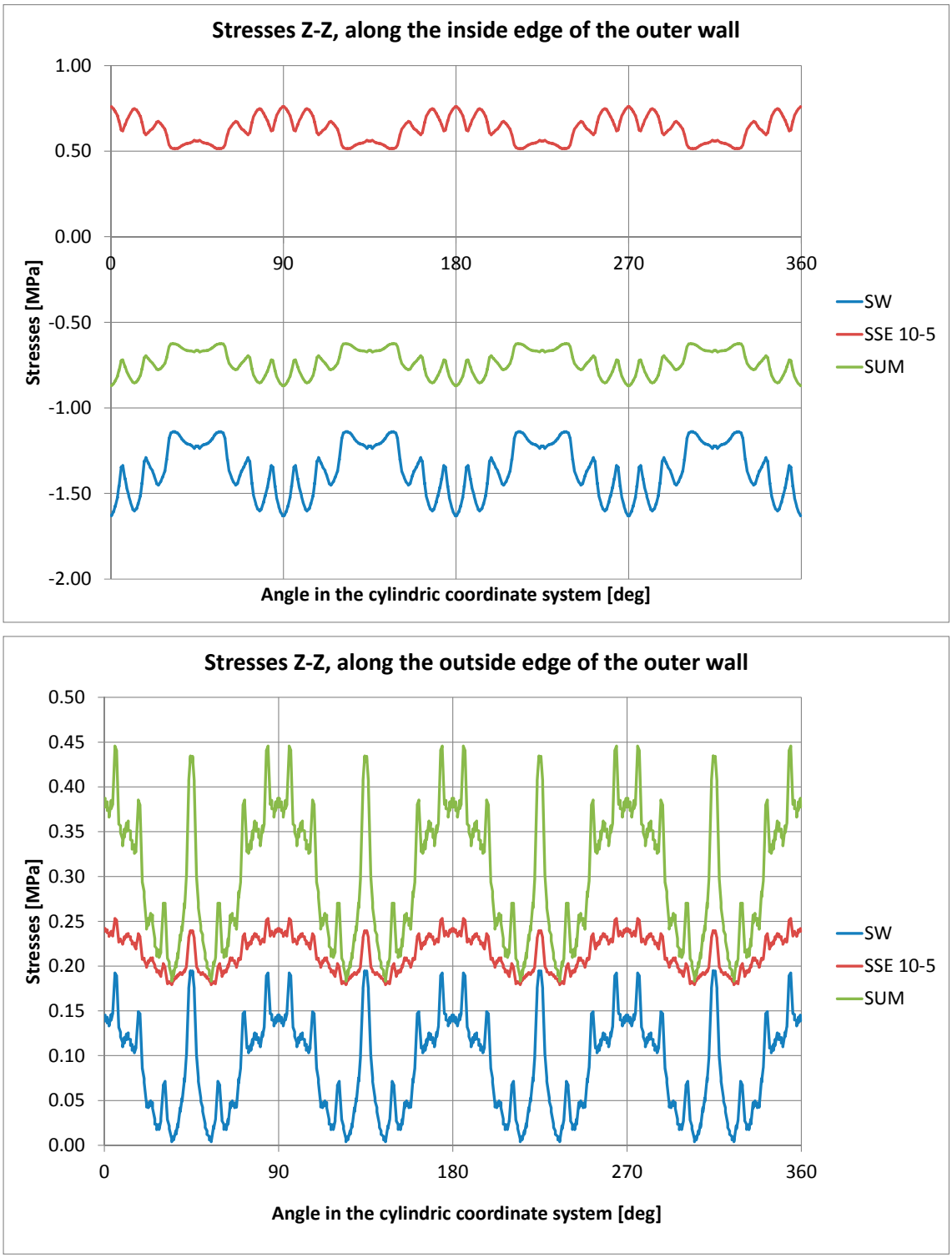

Figure B-49. *Case 2a. Earthquake load combination with SSE 10^{-5}. Vertical stress along the casting joint.*

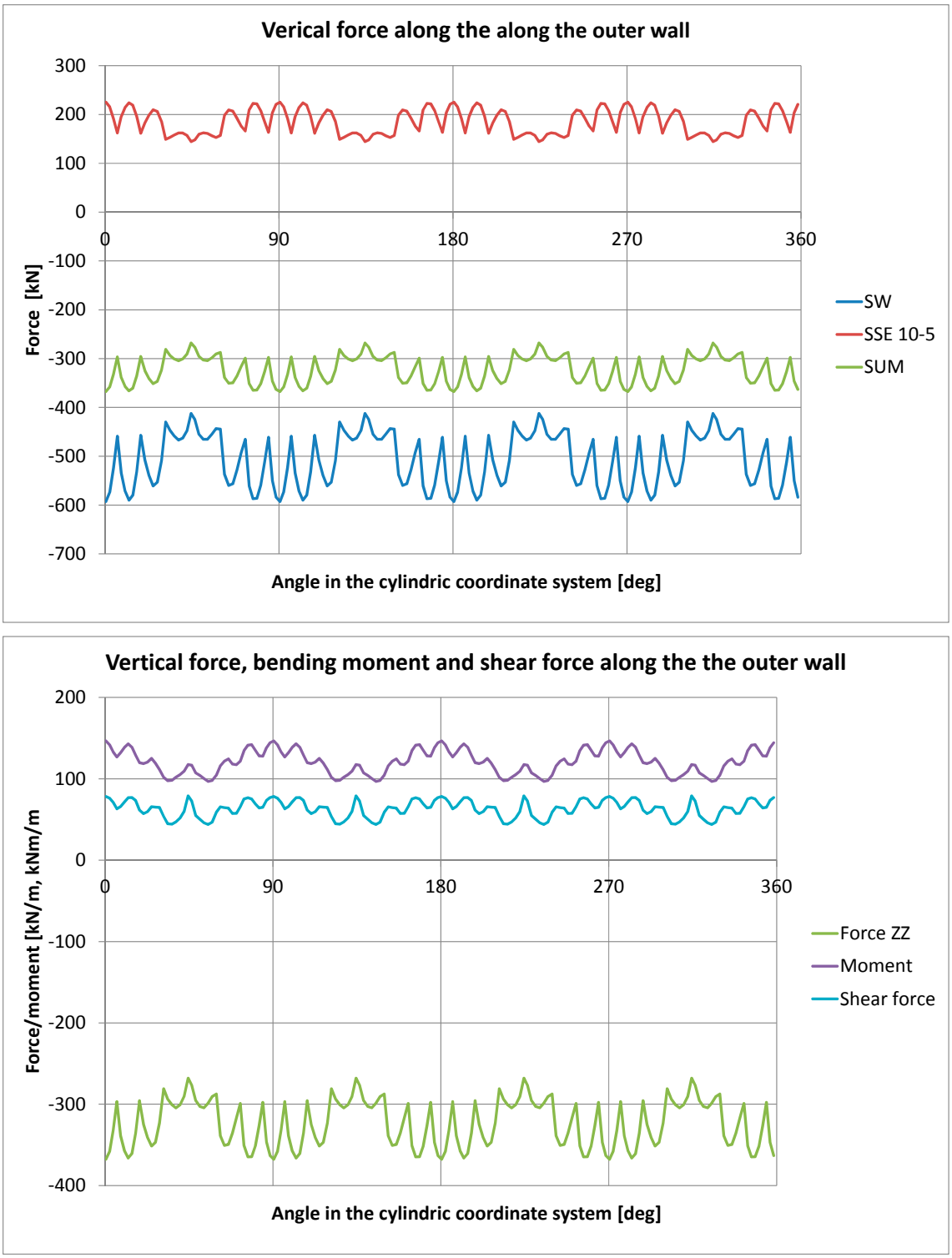

Figure B-50. *Case 2a. Earthquake load combination with SSE 10^{-5}. Forces along the casting joint.*

SSE 10^{-6} case

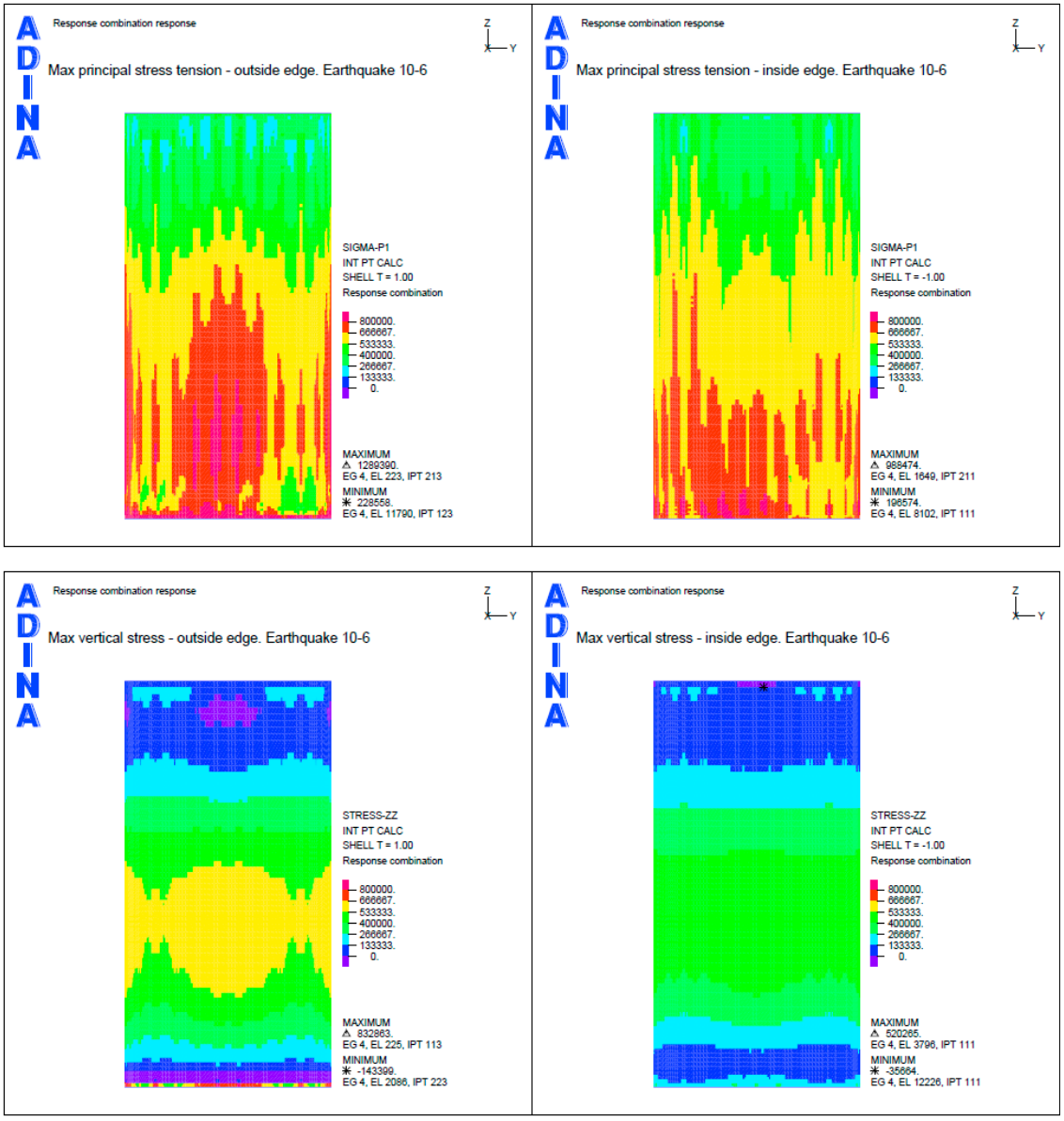

Figure B-51. *Case 2a. Earthquake load combination with SSE 10^{-6}. Max principal tensile stresses and max vertical stresses.*

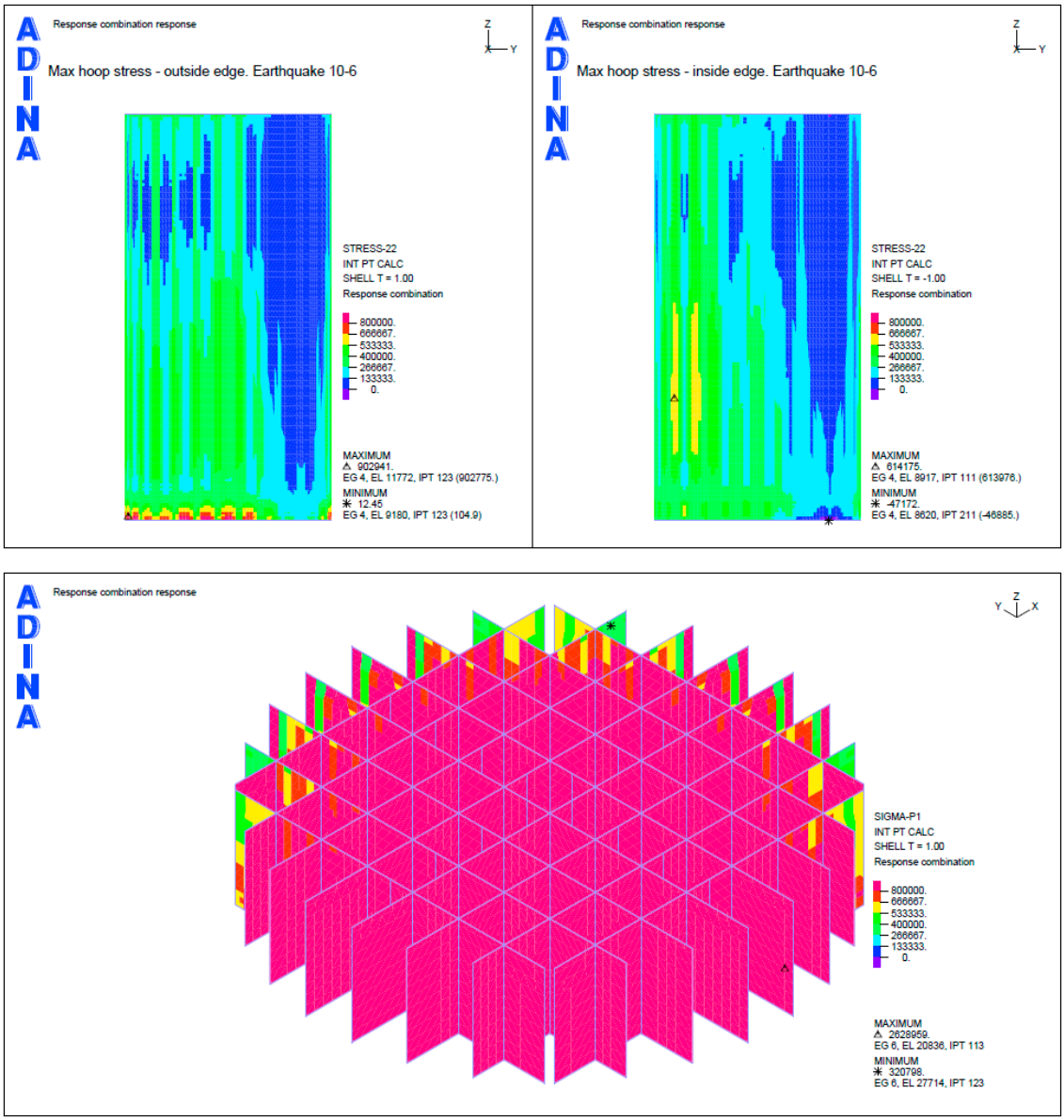

Figure B-52. *Case 2a. Earthquake load combination with SSE 10^{-6}. Max hoop stresses and max principal tensile stresses for the inner wall.*

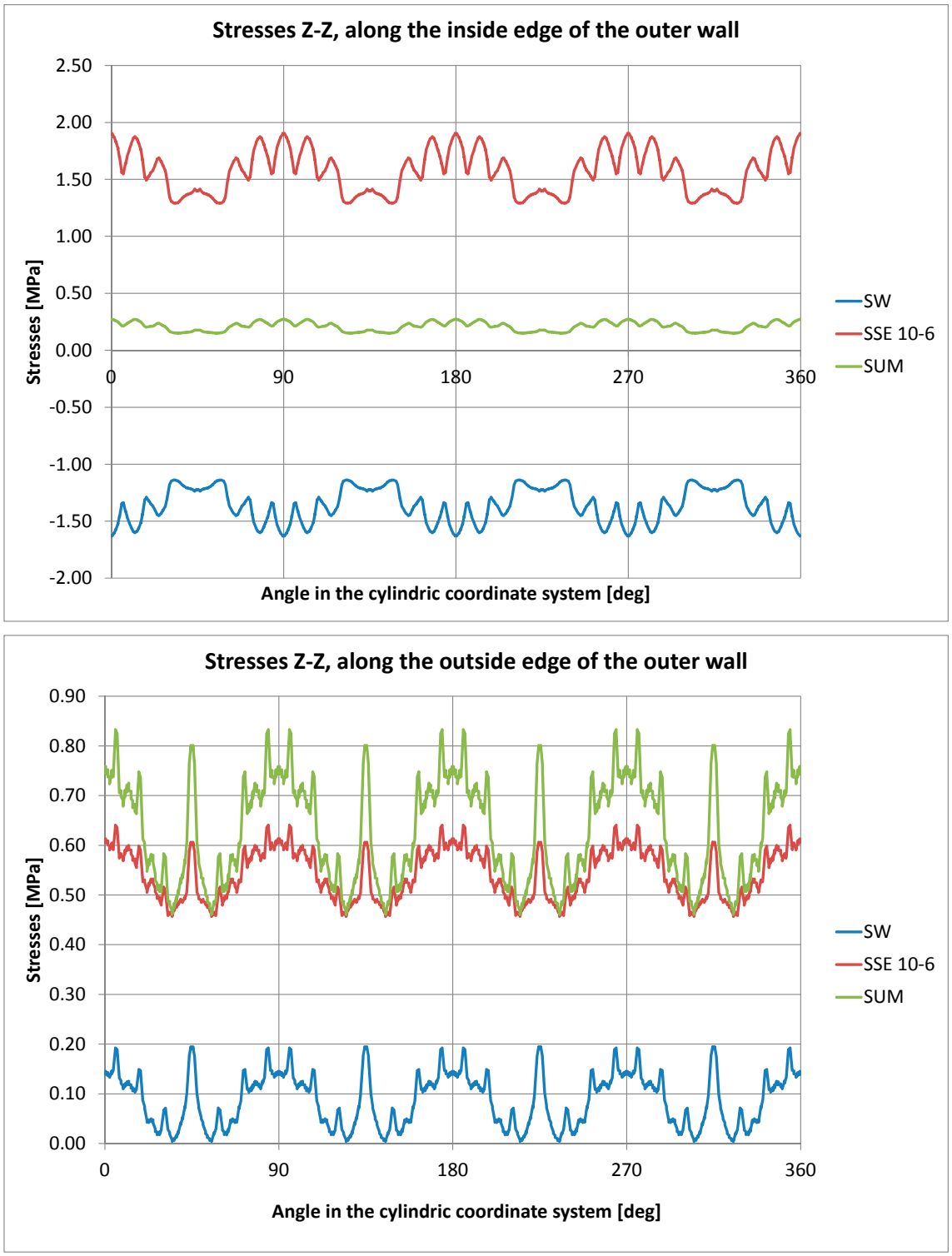

Figure B-53. *Case 2a. Earthquake load combination with SSE 10^{-6}. Vertical stress along the casting joint.*

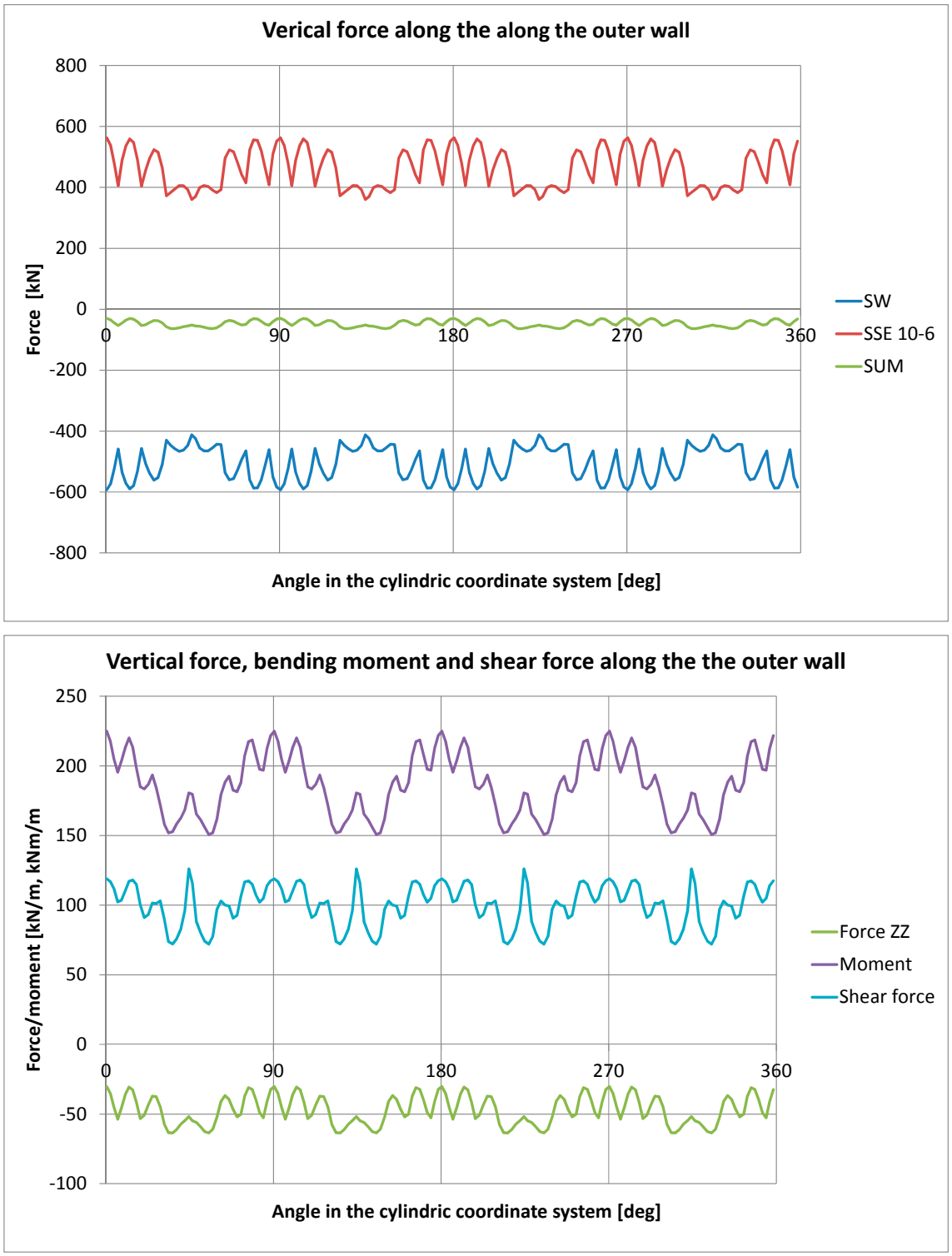

Figure B-54. *Case 2a. Earthquake load combination with SSE 10^{-6}. Forces along the casting joint.*

SSE 10^{-7} case

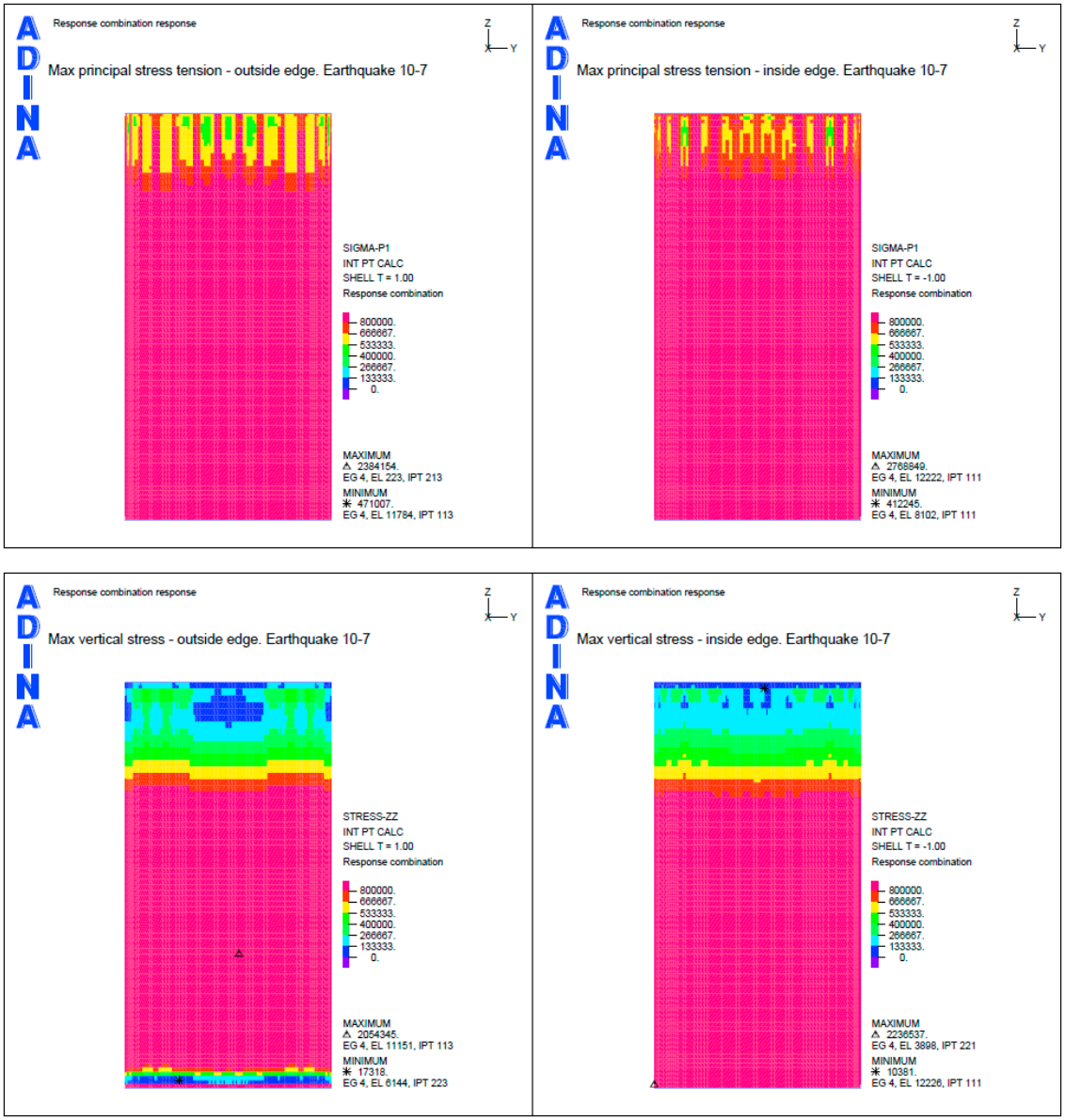

Figure B-55. *Case 1a. Earthquake load combination with SSE 10^{-7}. Max principal tensile stresses and max vertical stresses.*

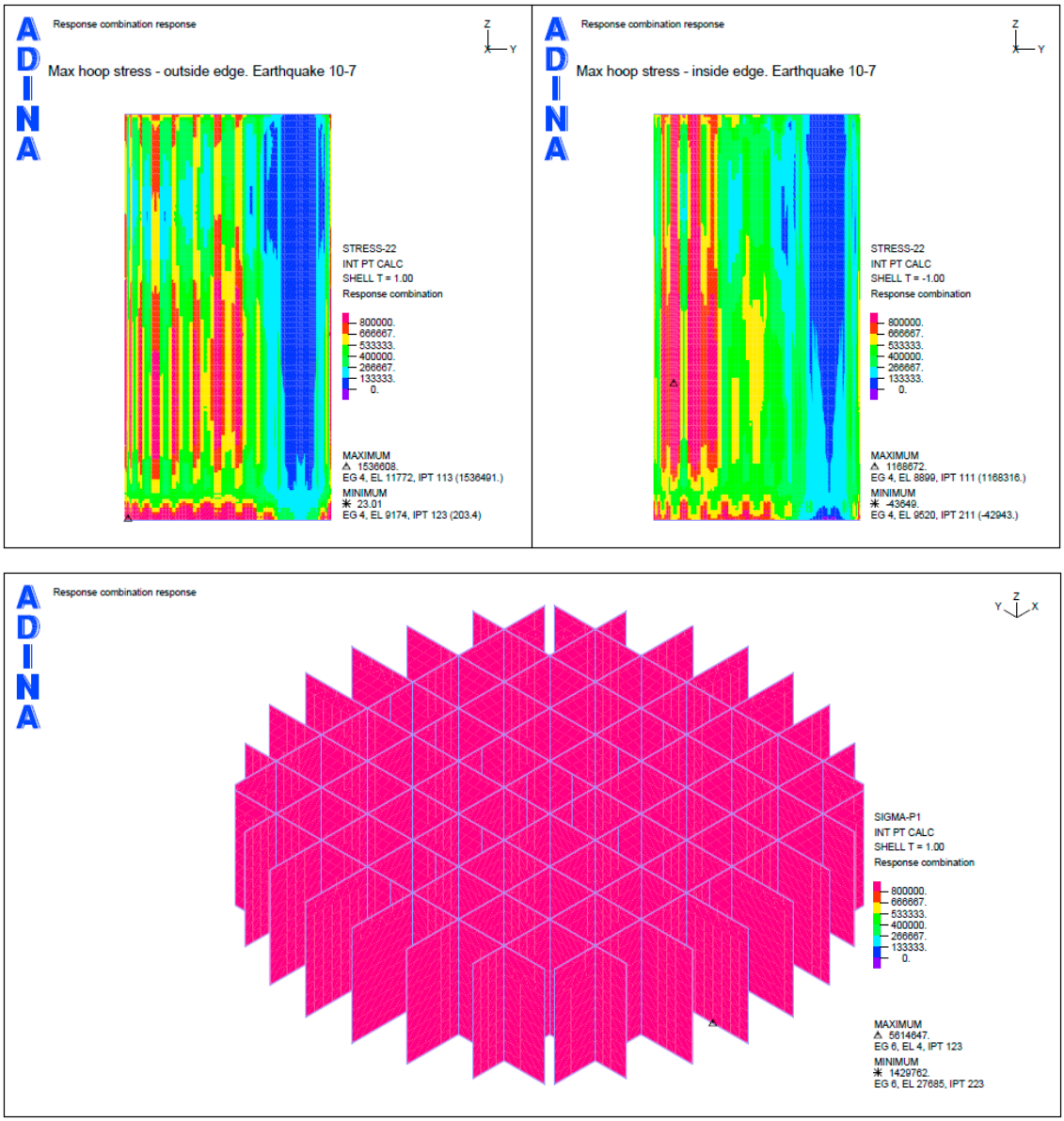

Figure B-56. *Case 1a. Earthquake load combination with SSE 10^{-7}. Max hoop stresses and max principal tensile stresses for the inner wall.*

B7 Case 2b – hinged joint between wall and slab

Static load cases (permanent loads)

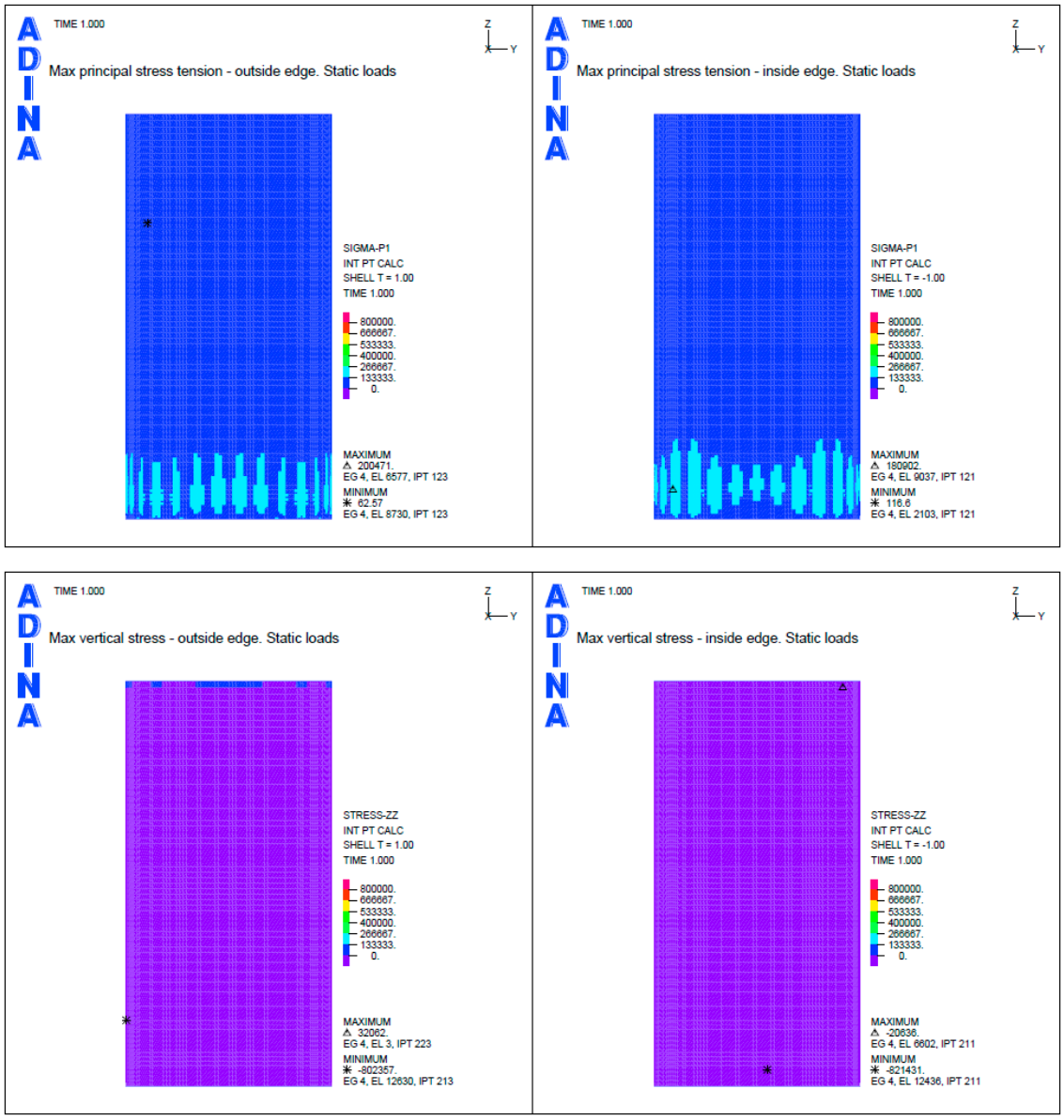

Figure B-57. *Case 2b. Static load cases (permanent loads). Max principal tensile stresses and max vertical stresses.*

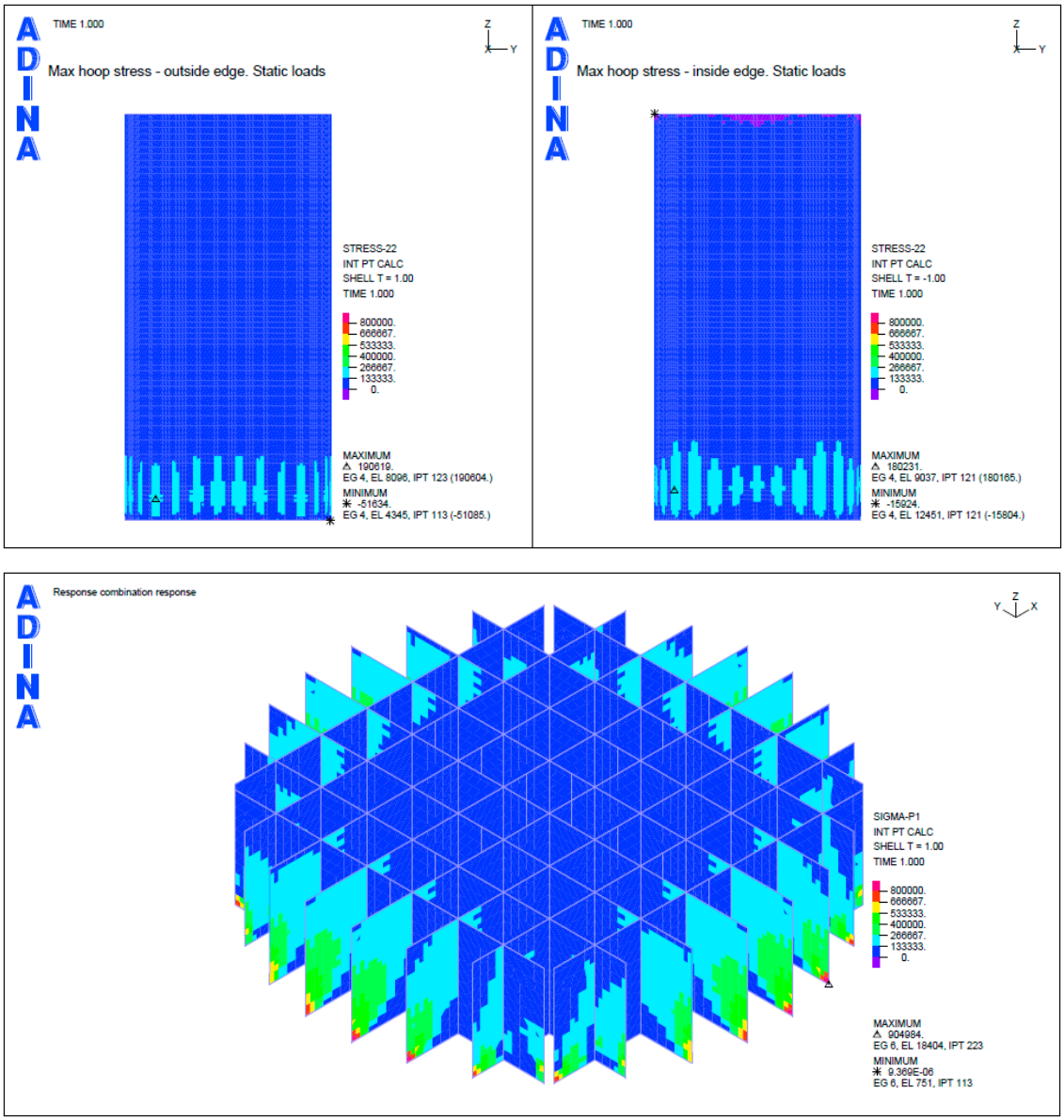

Figure B-58. *Case 2b. Static load cases (permanent loads). Max hoop stresses and max principal tensile stresses for the inner wall.*

SSE 10^{-5} case

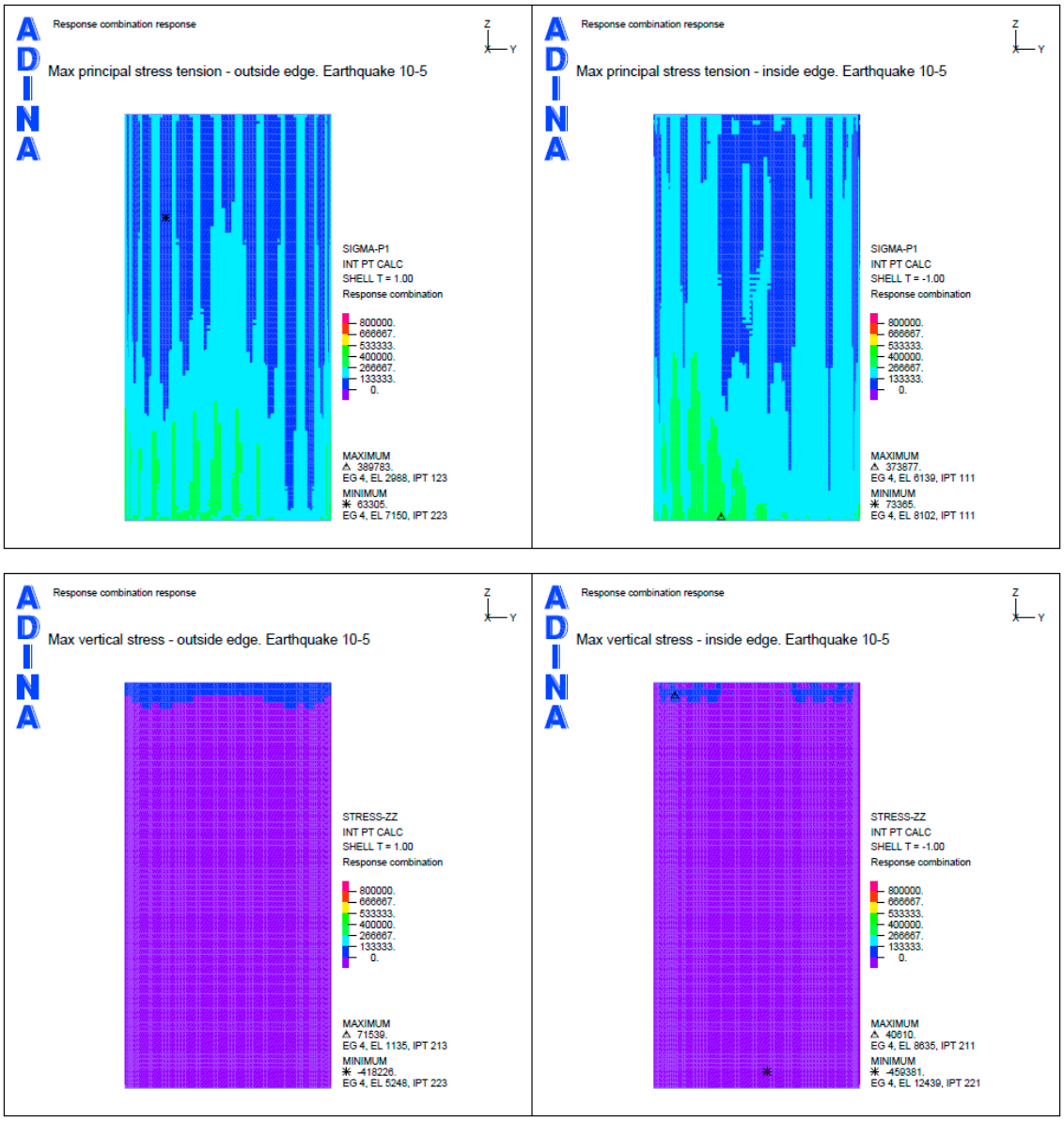

Figure B-59. *Case 2b. Earthquake load combination with SSE 10^{-5}. Max principal tensile stresses and max vertical stresses.*

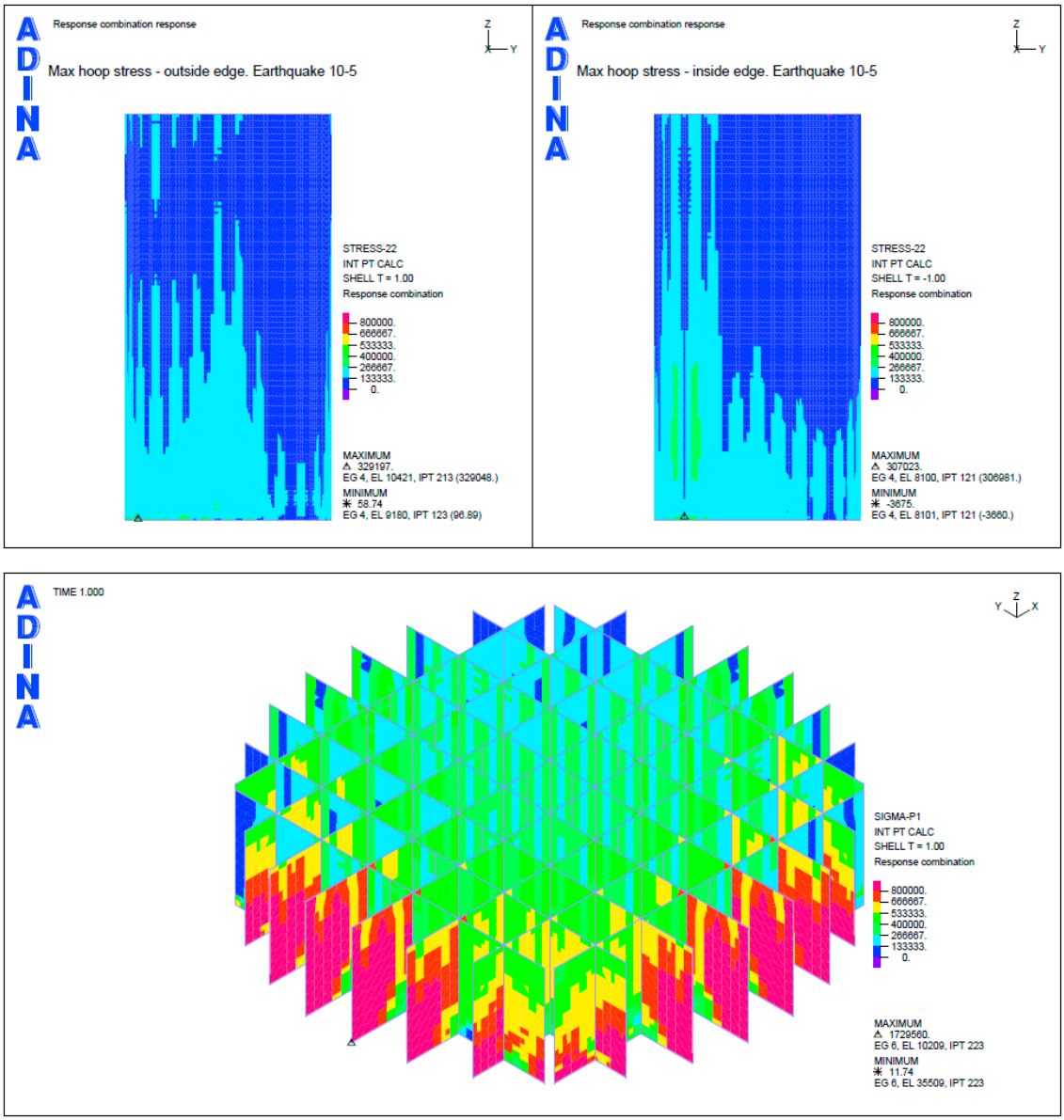

Figure B-60. *Case 2b. Earthquake load combination with SSE 10^{-5}. Max hoop stresses and max principal tensile stresses for the inner wall.*

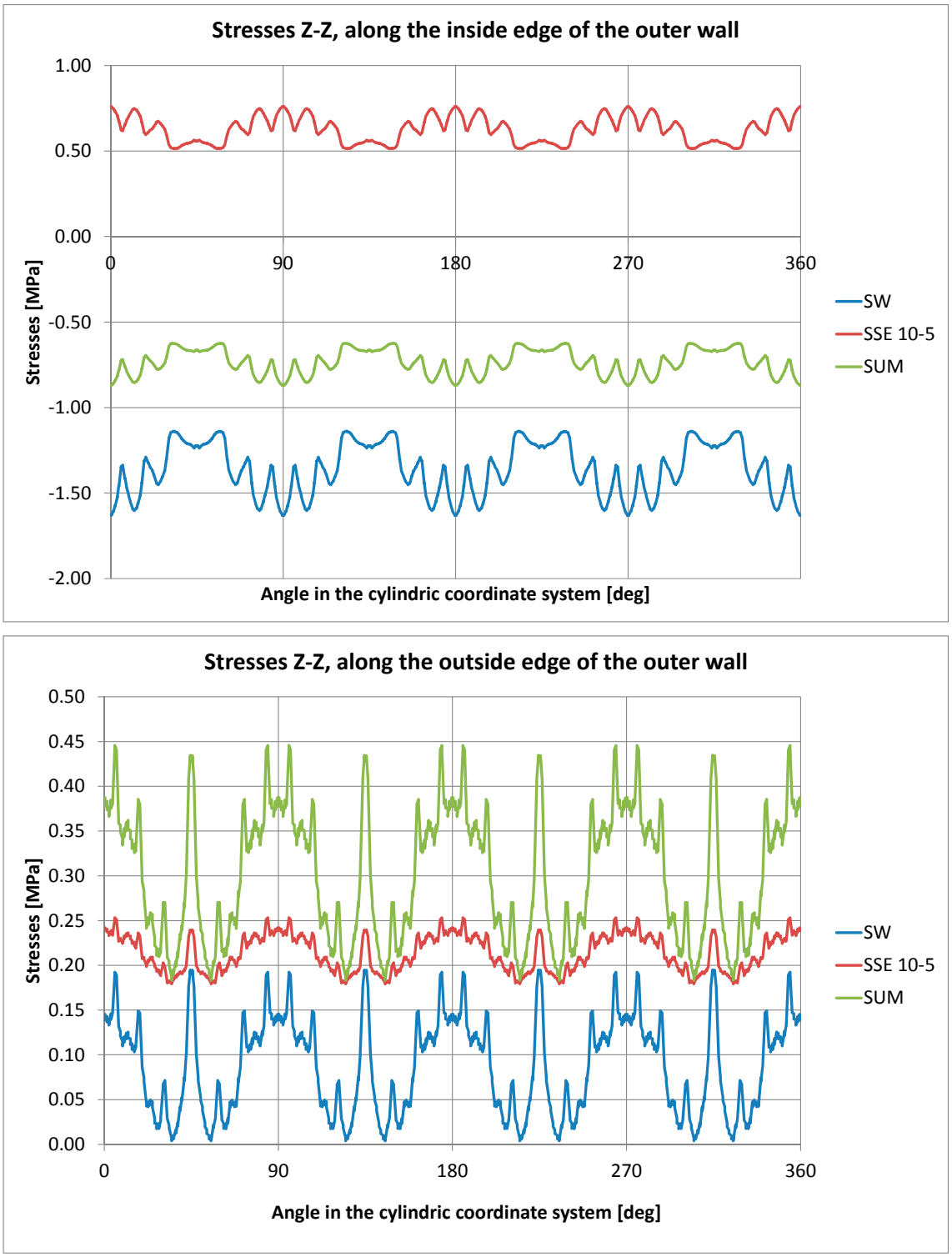

Figure B-61. *Case 2b. Earthquake load combination with SSE 10^{-5}. Vertical stress along the casting joint.*

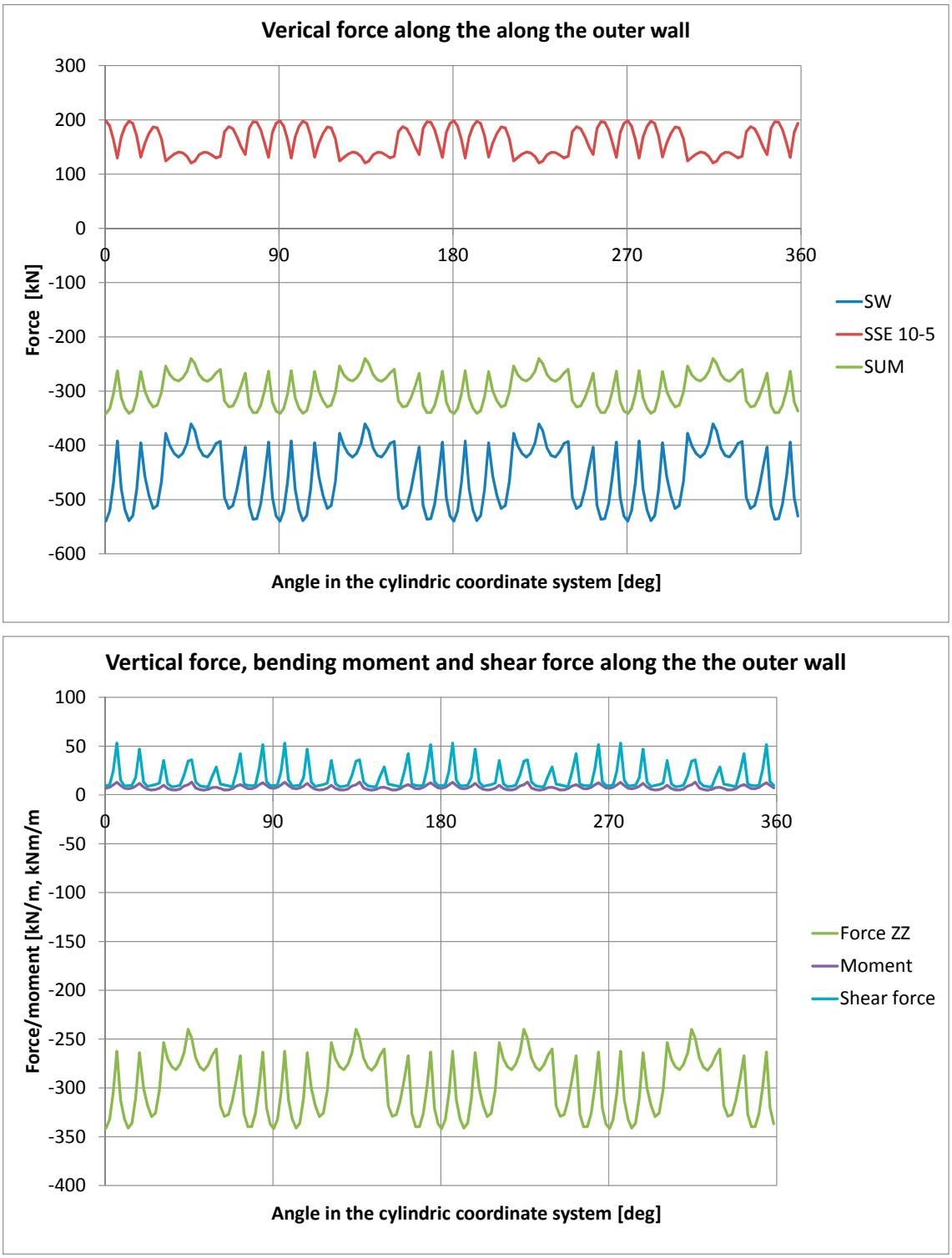

Figure B-62. *Case 2b. Earthquake load combination with SSE 10^{-5}. Forces along the casting joint.*

SSE 10^{-6} case

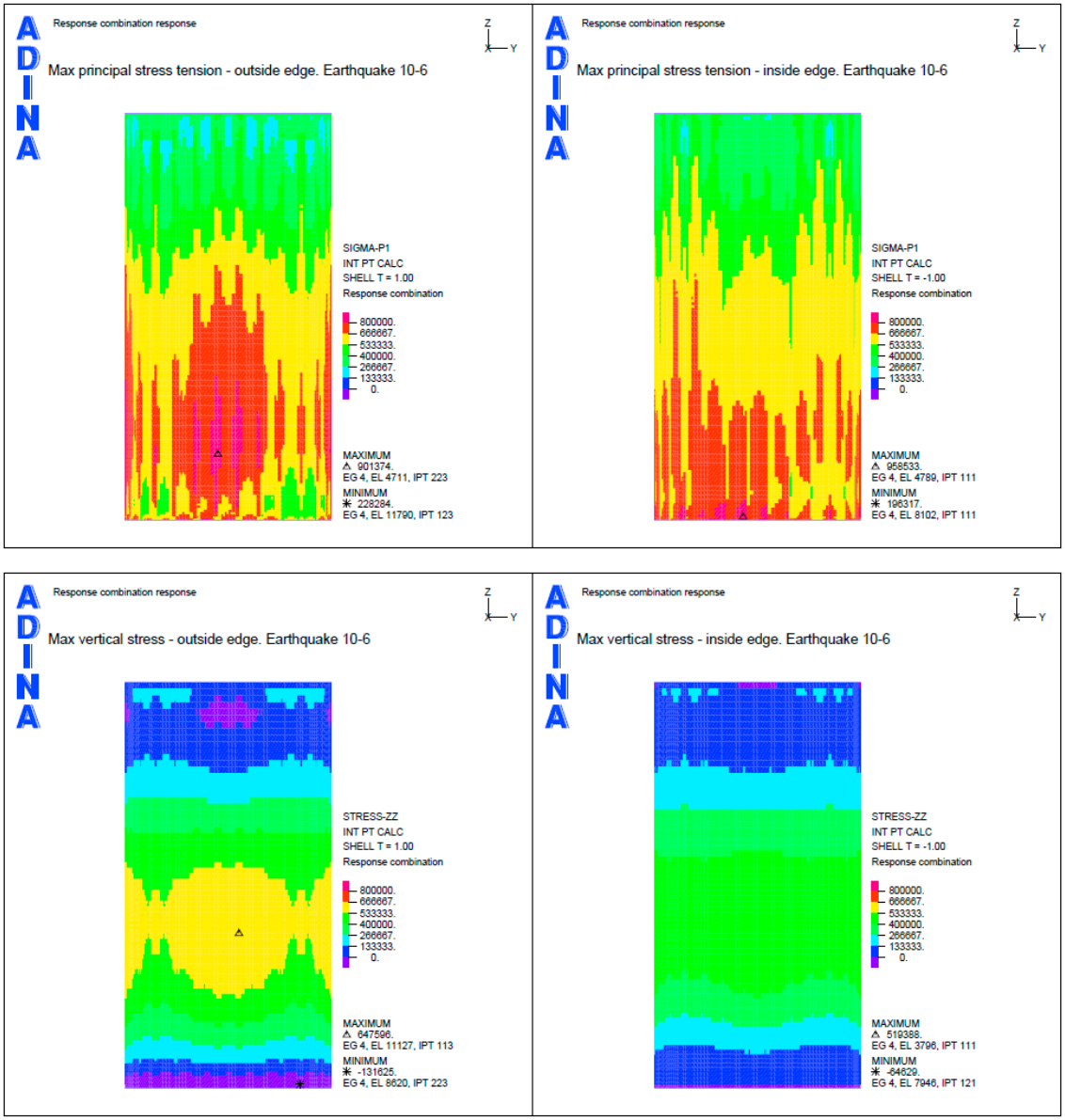

Figure B-63. *Case 2b. Earthquake load combination with SSE 10^{-6}. Max principal tensile stresses and max vertical stresses.*

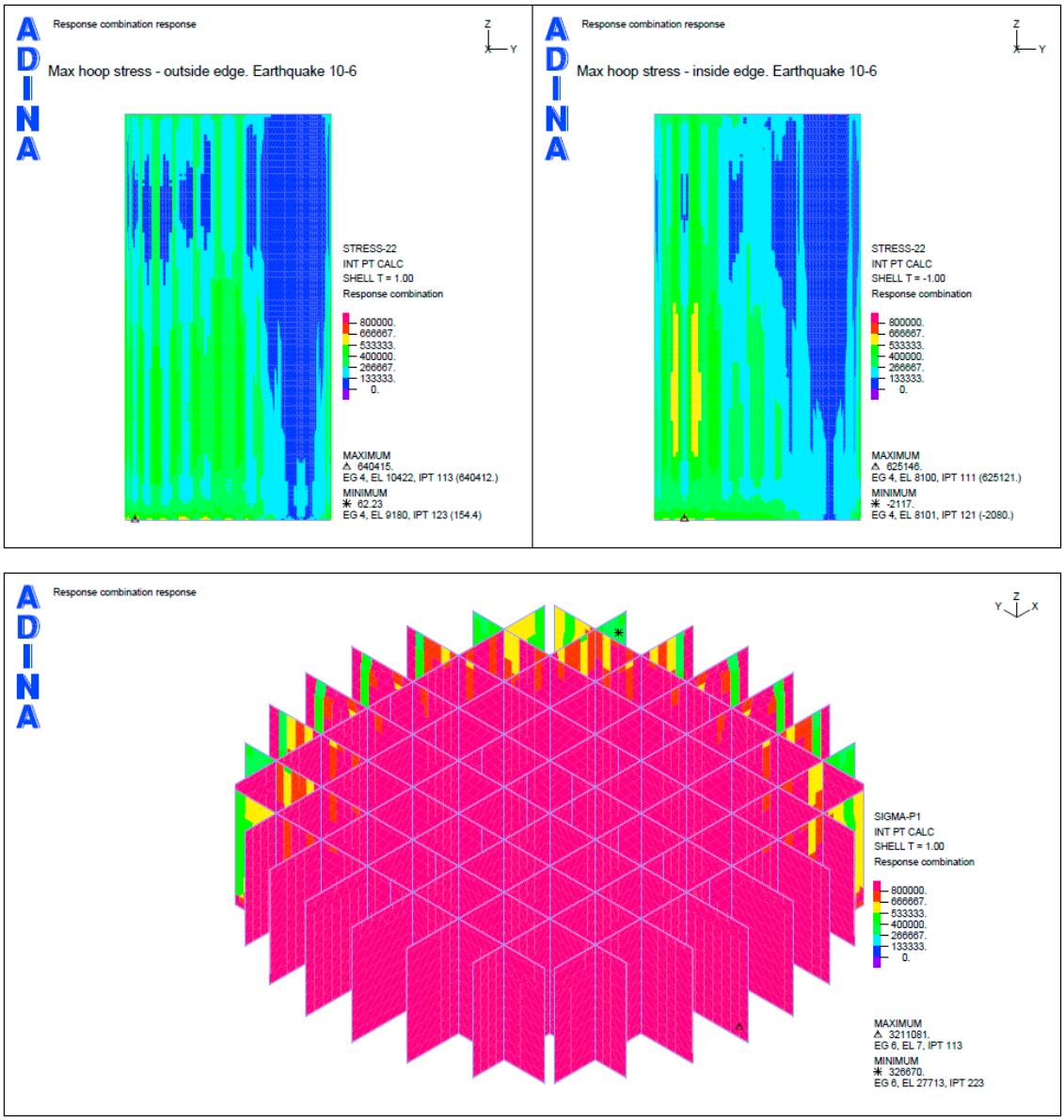

Figure B-64. *Case 2b. Earthquake load combination with SSE 10^{-6}. Max hoop stresses and max principal tensile stresses for the inner wall.*

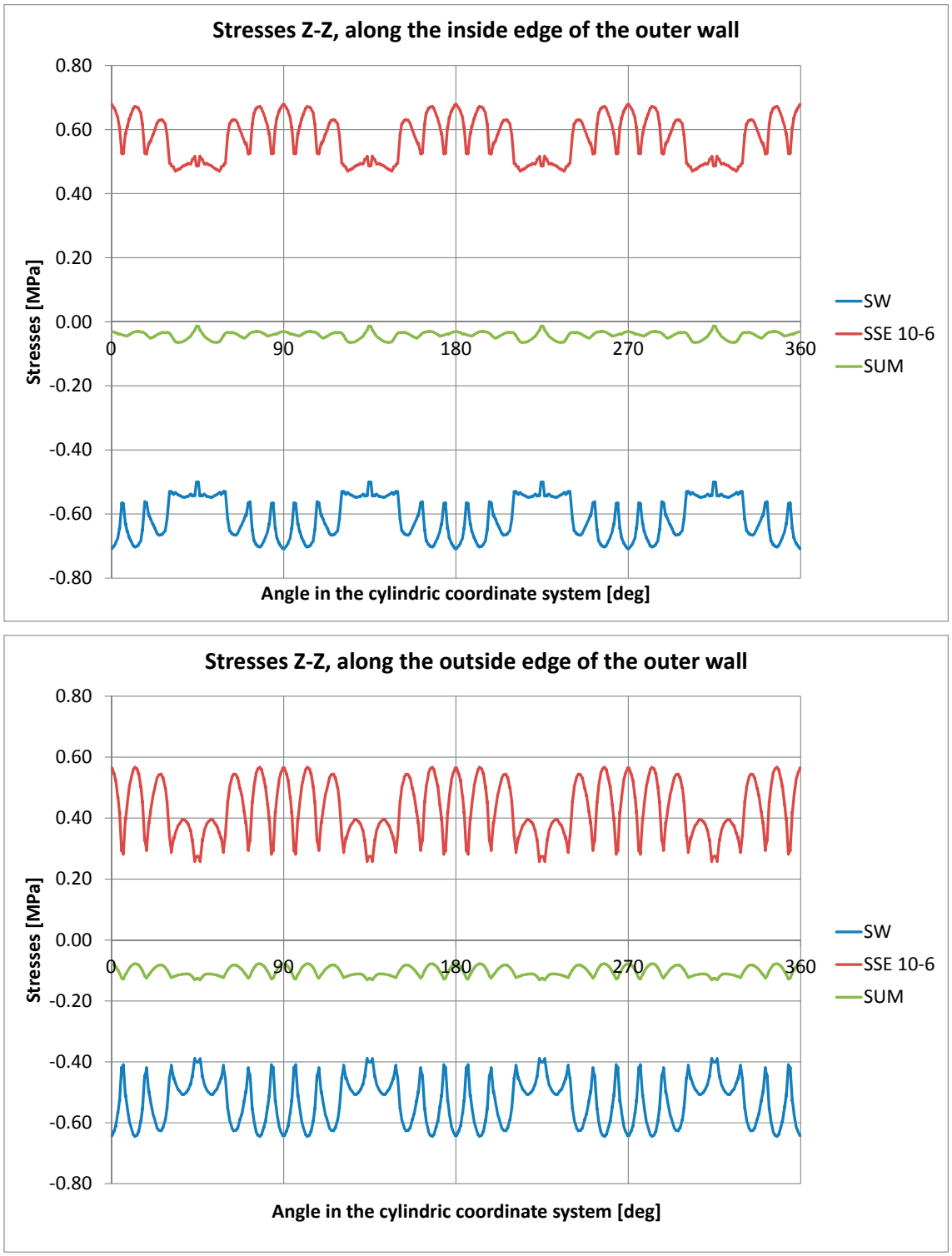

Figure B-65. *Case 2b. Earthquake load combination with SSE 10^{-6}. Vertical stress along the casting joint.*

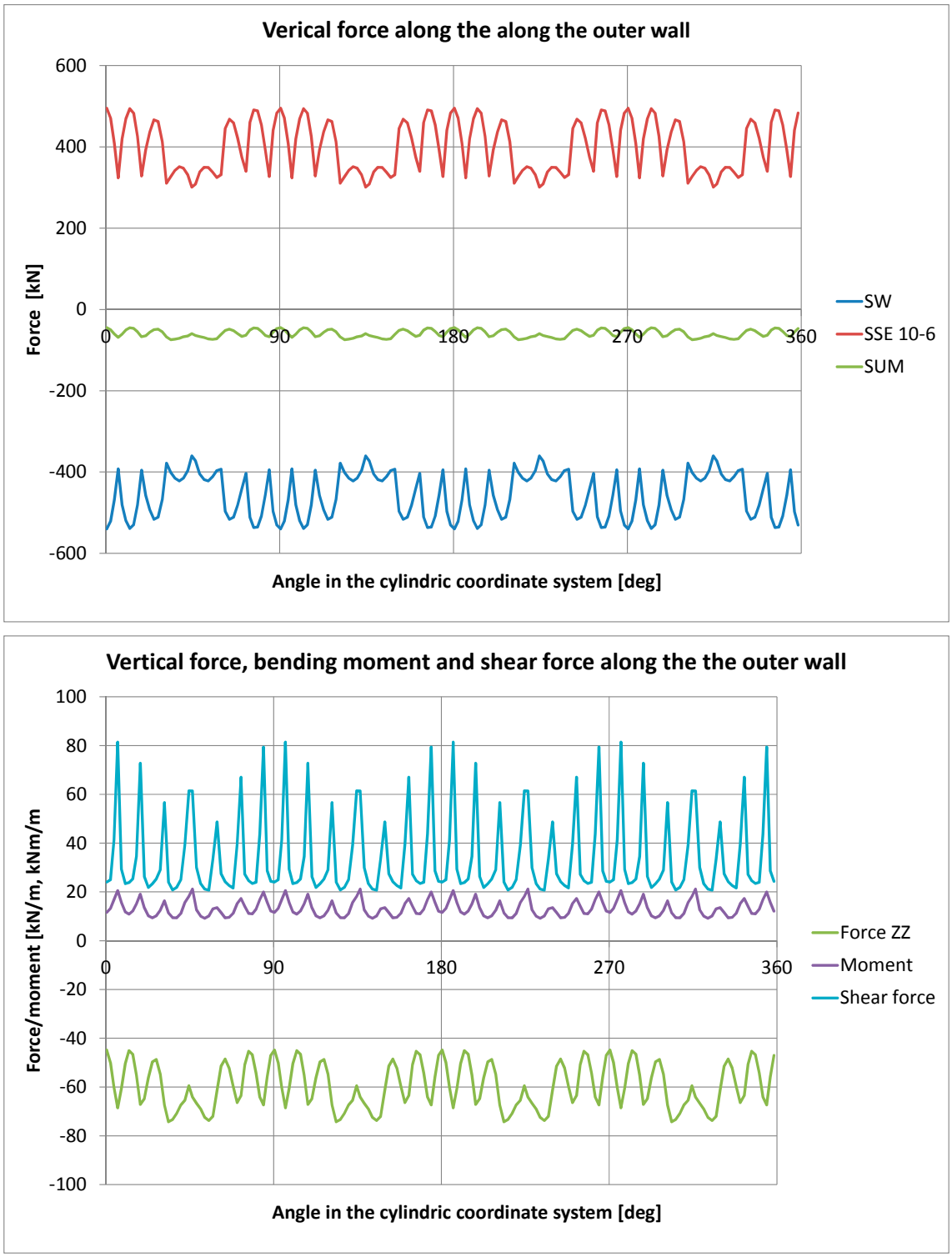

Figure B-66. *Case 2b. Earthquake load combination with SSE 10^{-6}. Forces along the casting joint.*

SSE 10^{-7} case

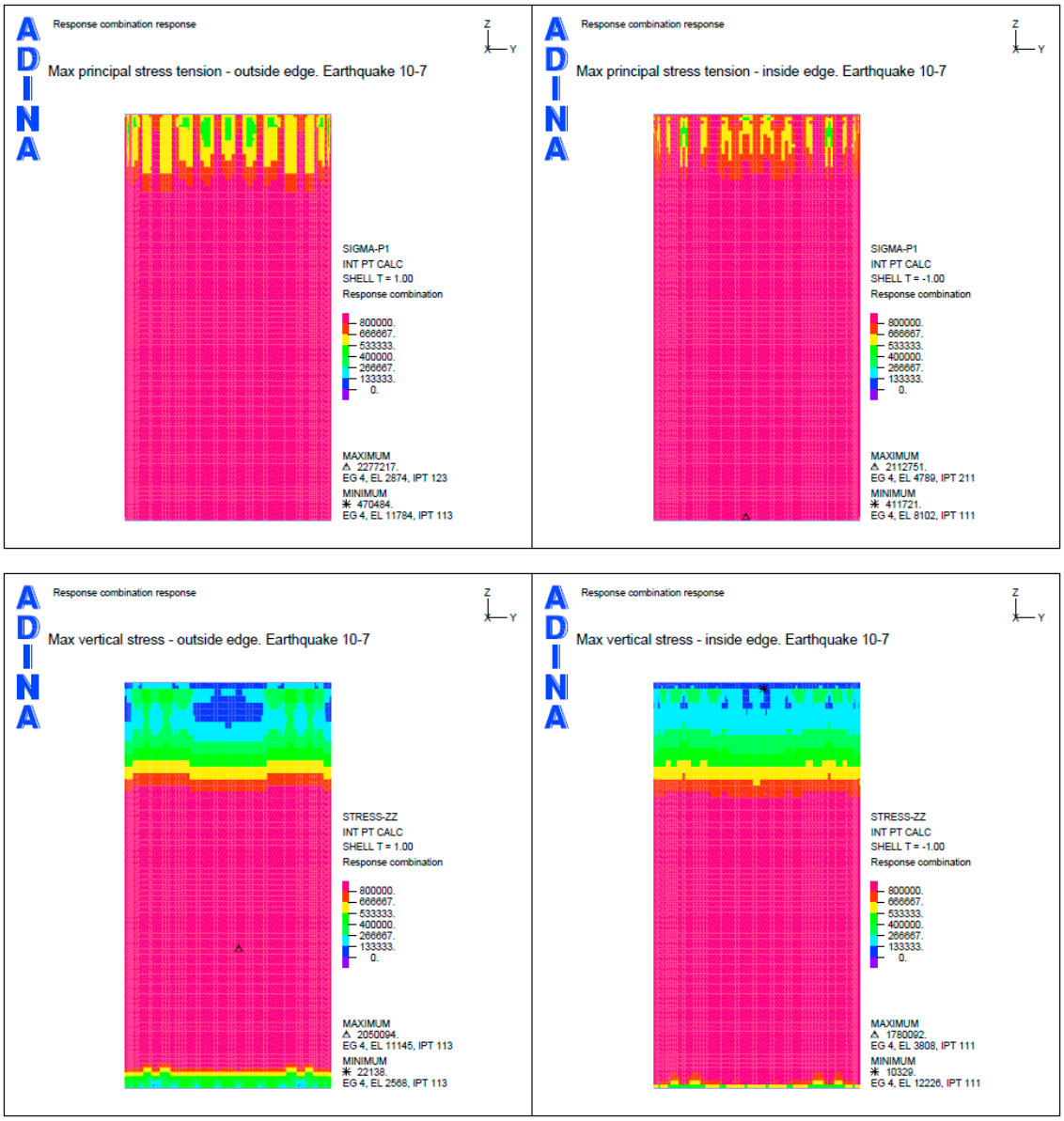

Figure B-67. *Case 2b. Earthquake load combination with SSE 10^{-7}. Max principal tensile stresses and max vertical stresses.*

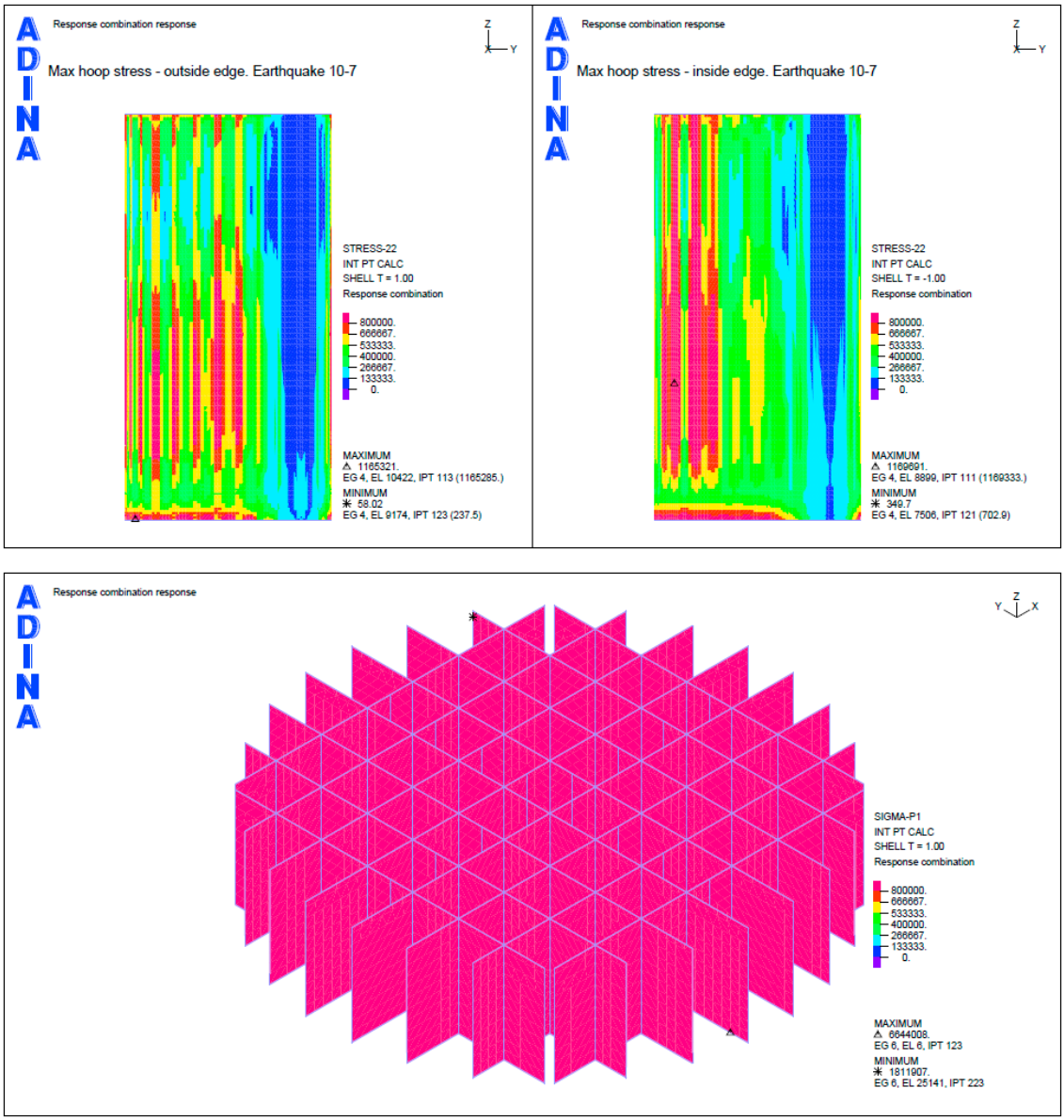

Figure B-68. *Case 2b. Earthquake load combination with SSE 10^{-7}. Max hoop stresses and max principal tensile stresses for the inner wall.*

B8 Case 2b (reduced outer wall thickness) – hinged joint between wall and slab

Static load cases (permanent loads)

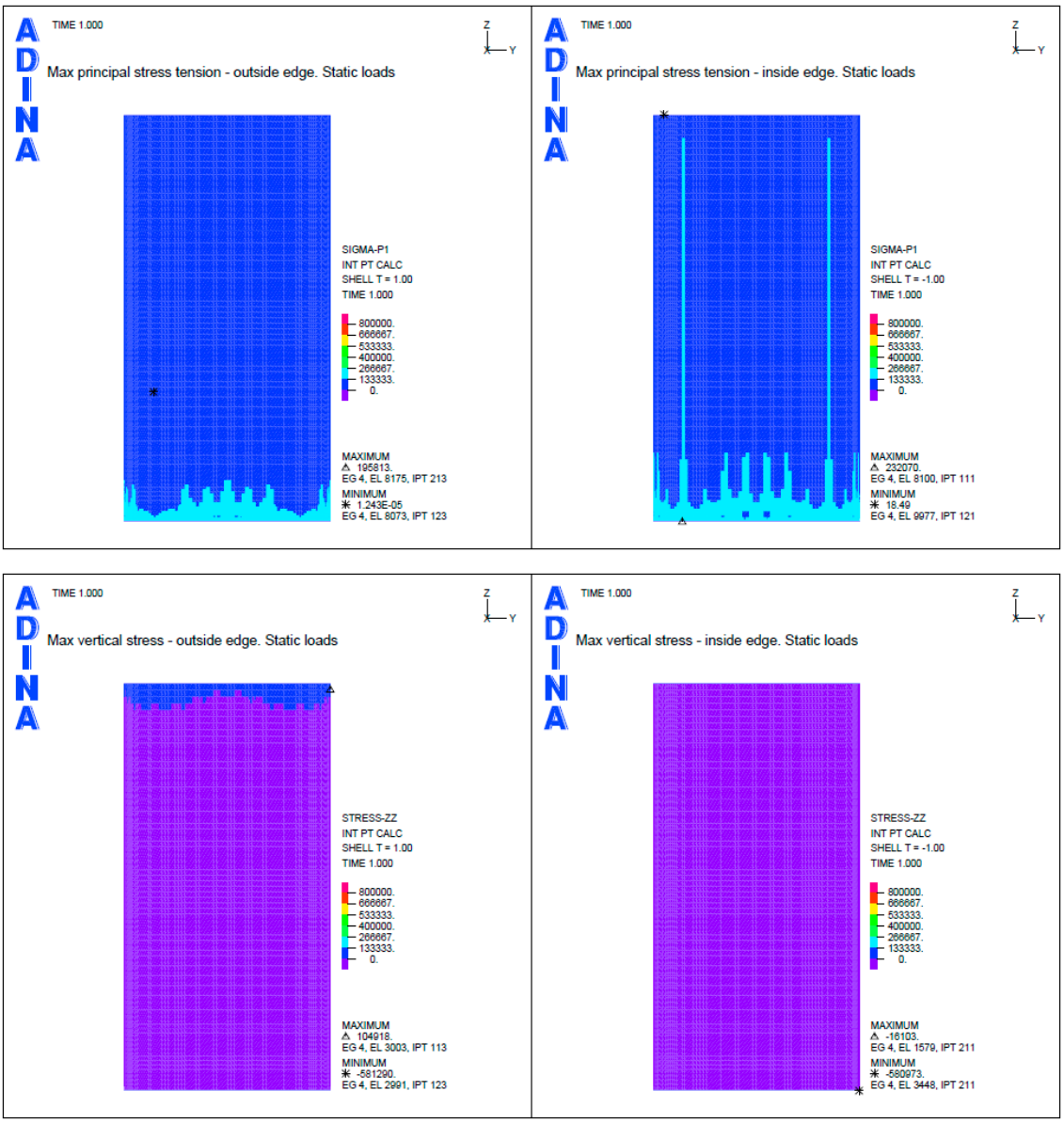

Figure B-69. *Case 2b(reduced wall thickness). Static load cases (permanent loads). Max principal tensile stresses and max vertical stresses.*

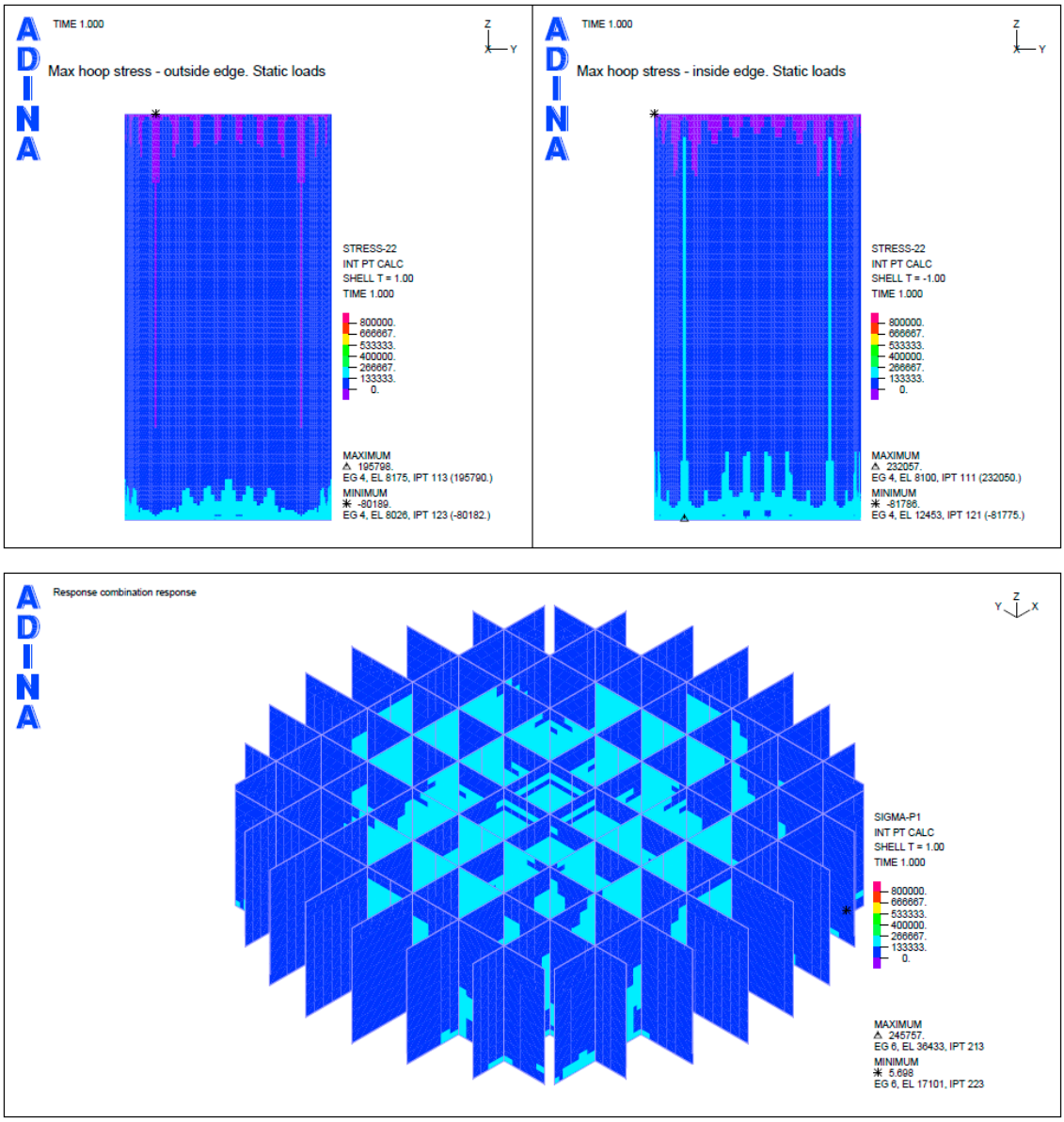

Figure B-70. *Case 2b(reduced wall thickness). Static load cases (permanent loads). Max hoop stresses and max principal tensile stresses for the inner wall.*

SSE 10^{-5} case

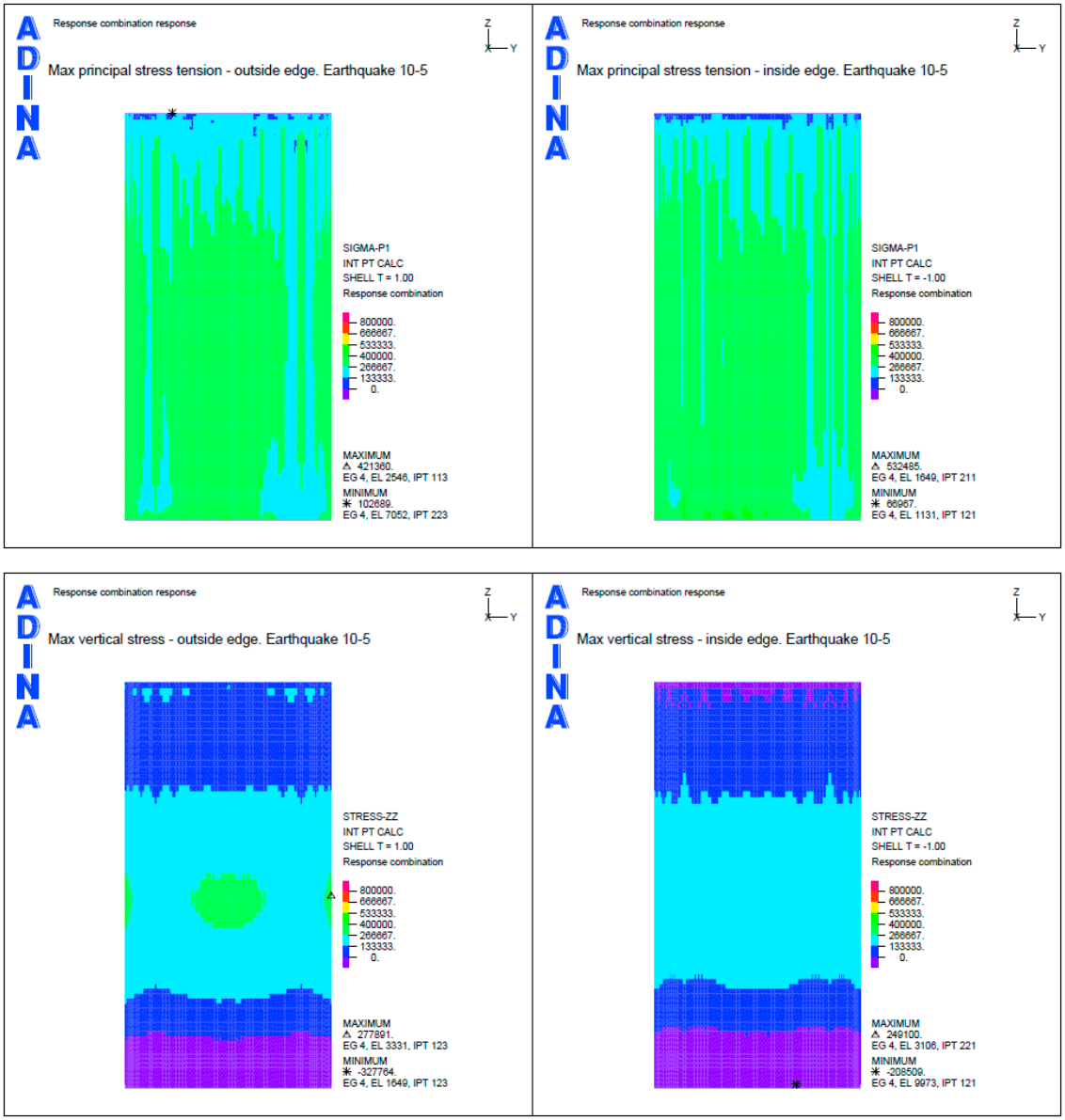

Figure B-71. *Case 2b(reduced wall thickness). Earthquake load combination with SSE 10^{-5}. Max principal tensile stresses and max vertical stresses.*

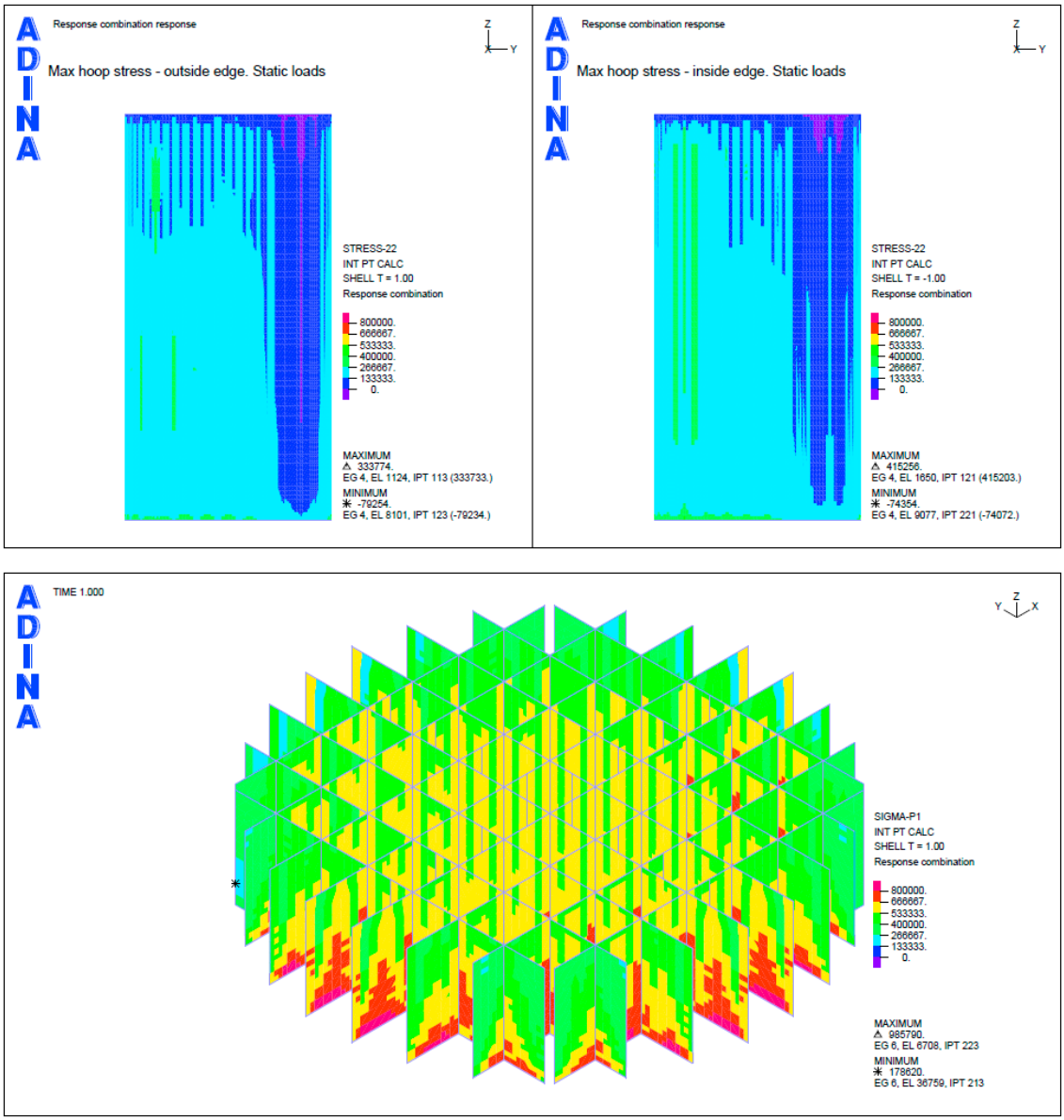

Figure B-72. *Case 2b(reduced wall thickness). Earthquake load combination with SSE 10^{-5}. Max hoop stresses and max principal tensile stresses for the inner wall.*

SSE 10^{-6} case

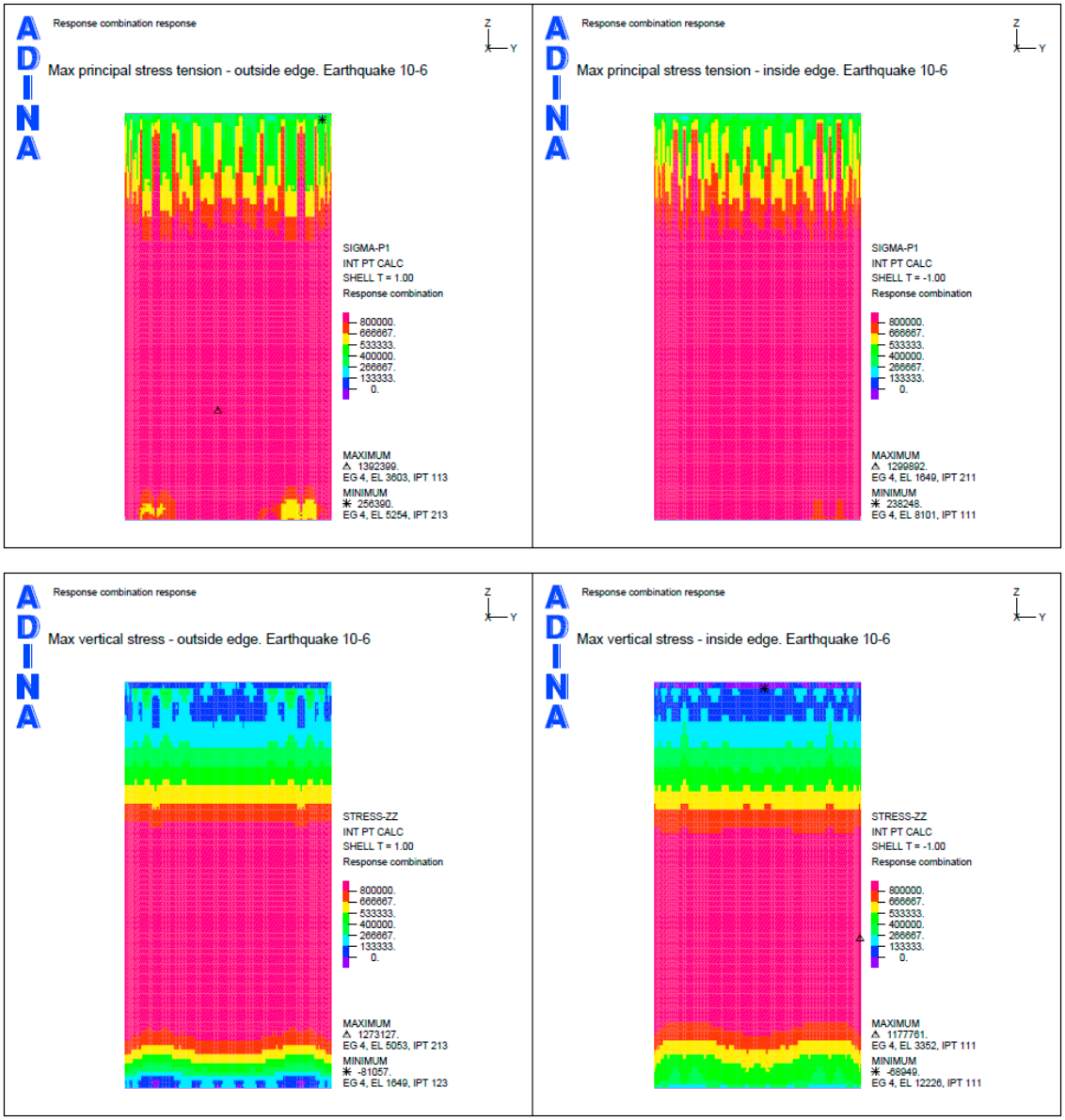

Figure B-73. *Case 2b(reduced wall thickness). Earthquake load combination with SSE 10^{-6}. Max principal tensile stresses and max vertical stresses.*

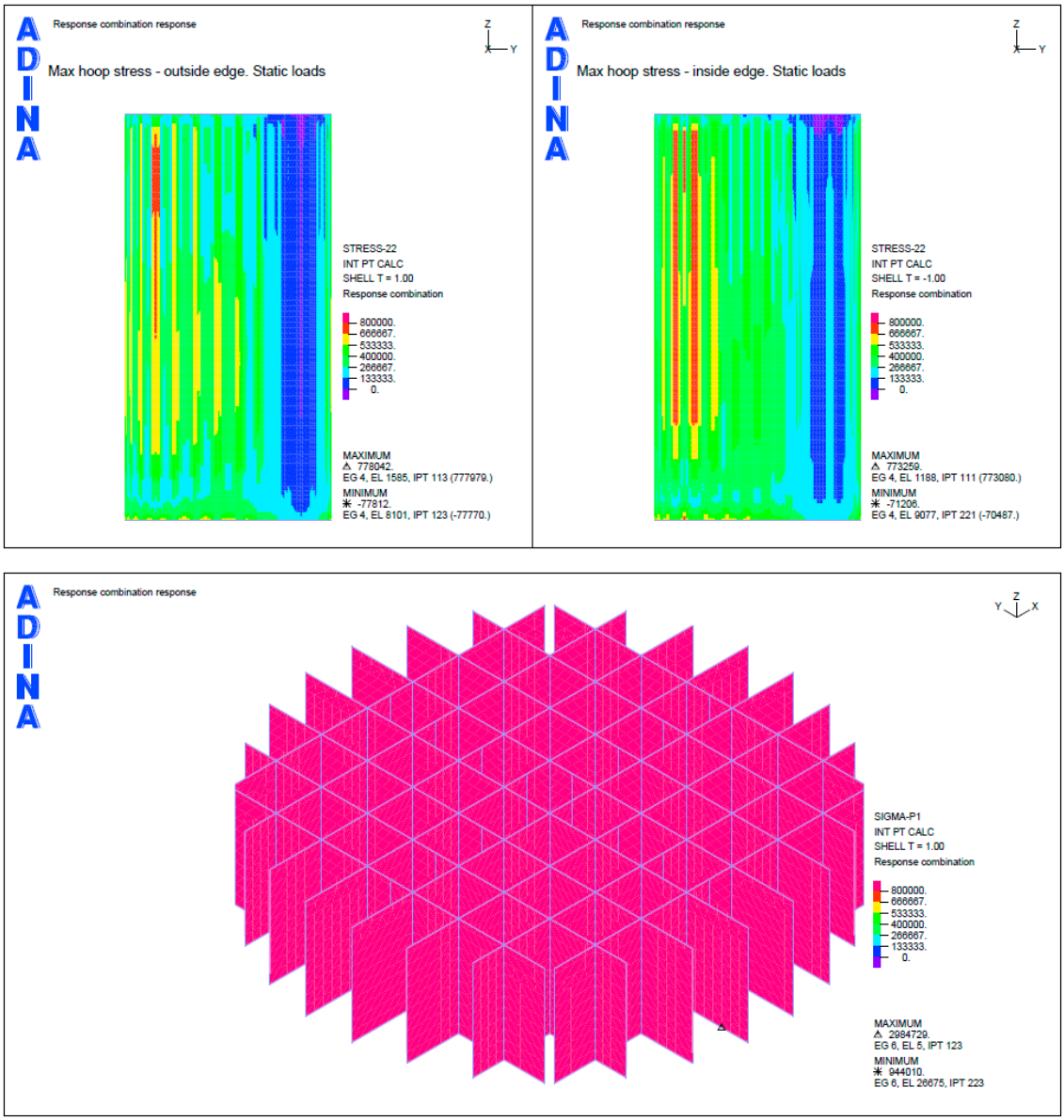

Figure B-74. *Case 2b(reduced wall thickness). Earthquake load combination with SSE 10^{-6}. Max hoop stresses and max principal tensile stresses for the inner wall.*

SSE 10^{-7} case

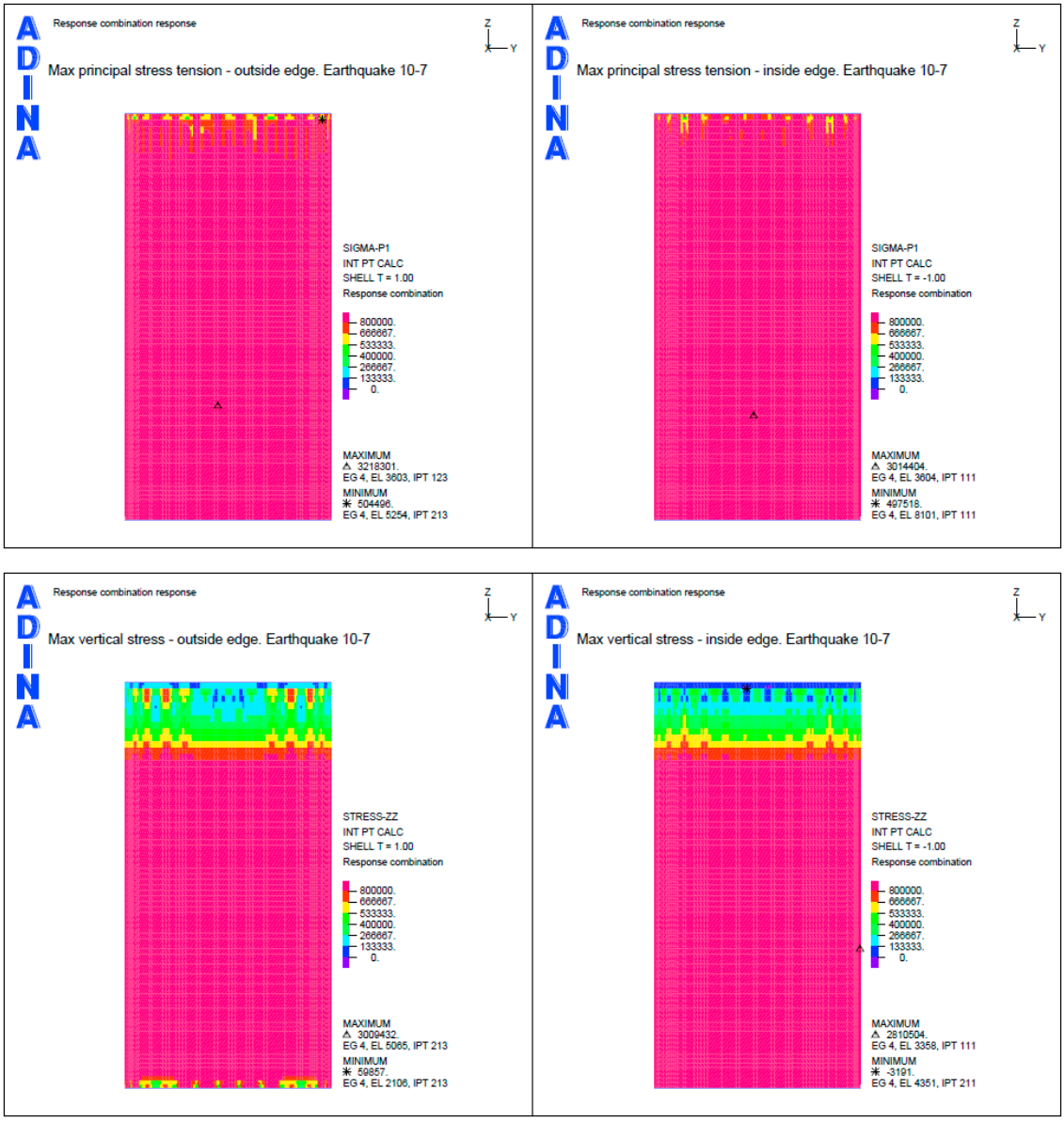

Figure B-75. *Case 2b(reduced wall thickness). Earthquake load combination with SSE 10^{-7}. Max principal tensile stresses and max vertical stresses.*

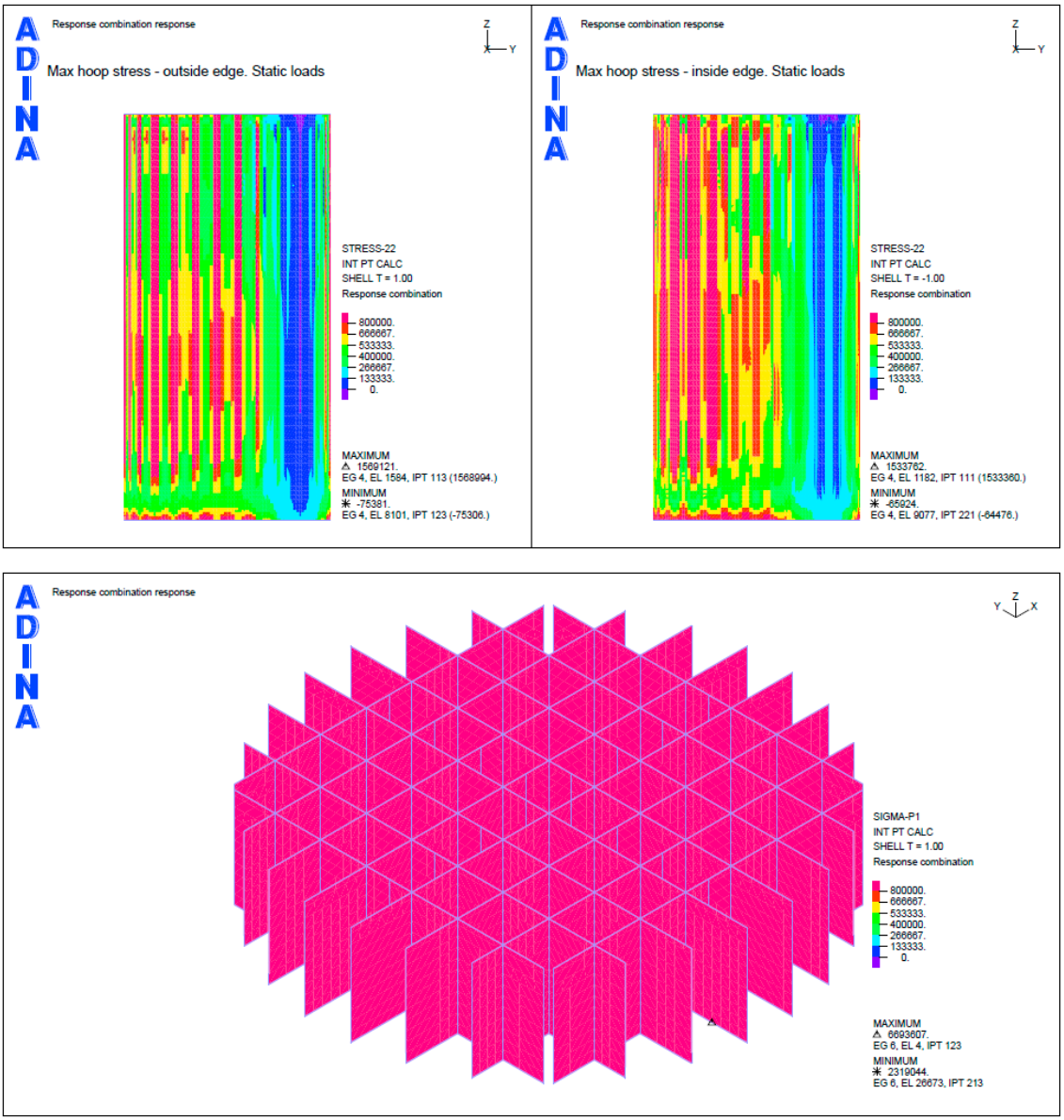

Figure B-76. *Case 2b(reduced wall thickness). Earthquake load combination with SSE 10^{-7}. Max hoop stresses and max principal tensile stresses for the inner wall.*

B9 Shear capacity check for the casting joint

The values for the section forces along the casting joint are taken from diagrams in this appendix. The most unfavorable values are assumed.

For the load combinations for SSE 10^{-6} and 10^{-7} there is tension along the joint which automatically reduces the shear capacity to zero.

The check is performed in accordance with BBK 04 (Boverket 2004) with the provisions for shear keys in the casting joint. However, it can be noted though that even the lowest friction (flat surface, no reinforcement) would show enough capacity for the SSE 10^{-5} load combination.

Case 1 Simple model, load combination for SSE 10^{-5} earthquake:

Capacity in the casting joint, BBK 04, 3.11.3

Accidental load combination $\gamma_n := 1.0$

Wall thickness (joint area) $t_{wall} := 0.8m$

Shear force along the casting joint $F_{v.joint} := 100\frac{kN}{m}$

Vertical compression force along the casting joint $F_{z.joint} := 550\frac{kN}{m}$

Compression stress in the joint $\sigma_{fc} := \frac{1}{1.2\cdot\gamma_n}\frac{F_{z.joint}}{0.8m} = 0.573\cdot MPa$

Modified tensile strength $f_{ct} := \frac{1.625\,MPa}{2} = 8.125\times10^{5}\,Pa$

ratio för the shear keys (approx) $k := 0.4$

joint shear strength $f_f := \min\left(1.5\cdot k\cdot f_{ct} + 0.8\cdot\sigma_{fc}, 2.0\cdot\sigma_{fc}\right) = 0.946\cdot MPa$

Max allowed shear force $F_{v.max} := f_f\cdot t_{wall} = 756.667\cdot\frac{kN}{m}$

Case 1b, load combination for SSE 10^{-5} earthquake

Shear forcealong the casting joint $F_{v.joint} := 80\frac{kN}{m}$

Vertical compression force along the casting joint $F_{z.joint} := 200\frac{kN}{m}$

Compression stress in the joint $\sigma_{fc} := \frac{1}{1.2\cdot\gamma_n}\frac{F_{z.joint}}{0.8\,m} = 0.208\cdot MPa$

joint shear strength $f_f := \min\left(1.5\cdot k\cdot f_{ct} + 0.8\cdot\sigma_{fc}, 2.0\cdot\sigma_{fc}\right) = 0.417\,MPa$

Max allowed shear force $F_{v.max} := f_f\cdot t_{wall} = 333.333\frac{kN}{m}$

Case 2b, load combination for SSE 10^{-5} earthquake

Shear forcealong the casting joint $F_{v.joint} := 50\frac{kN}{m}$

Vertical compression force along the casting joint $F_{z.joint} := 240\frac{kN}{m}$

Compression stress in the joint $\sigma_{fc} := \frac{1}{1.2 \cdot \gamma_n}\frac{F_{z.joint}}{0.8\,m} = 0.25 \cdot MPa$

joint shear strength $f_f := \min\left(1.5 \cdot k \cdot f_{ct} + 0.8 \cdot \sigma_{fc}, 2.0 \cdot \sigma_{fc}\right) = 0.5\,MPa$

Max allowed shear force $F_{v.max} := f_f \cdot t_{wall} = 400\frac{kN}{m}$

Case 2b, load combination for SSE 10^{-6} earthquake

Shear forcealong the casting joint $F_{v.joint} := 80\frac{kN}{m}$

Vertical compression force along the casting joint $F_{z.joint} := 50\frac{kN}{m}$

Compression stress in the joint $\sigma_{fc} := \frac{1}{1.2 \cdot \gamma_n}\frac{F_{z.joint}}{0.8m} = 0.052 \cdot MPa$

joint shear strength $f_f := \min\left(1.5 \cdot k \cdot f_{ct} + 0.8 \cdot \sigma_{fc}, 2.0 \cdot \sigma_{fc}\right) = 0.104\,MPa$

Max allowed shear force $F_{v.max} := f_f \cdot t_{wall} = 83.333\frac{kN}{m}$